Lawrence Berkeley Laboratory
UNIVERSITY OF CALIFORNIA

EARTH SCIENCES DIVISION

Proceedings of the
Symposium on the Long Valley Caldera:
A Pre-Drilling Data Review

Lawrence Berkeley Laboratory
Berkeley, California
March 17–18, 1987

September 1987

Proceedings of the
Symposium on the Long Valley Caldera:
A Pre-Drilling Data Review

Lawrence Berkeley Laboratory
Berkeley, California

March 17–18, 1987

N.E. Goldstein, Editor

Earth Sciences Division
University of California
Lawrence Berkeley Laboratory
Berkeley, California 94720

Cover photo: Mammoth Mountain, a cumulo-volcano viewed from Lake Mary, is the largest of the "rim rhyodacites" that are peripheral to the Long Valley caldera. This volcano is probably no older than 180,000 years and was active over a period of at least 100,000 years.

Preface

This proceedings volume contains papers or abstracts of papers presented at a two-day symposium held at the Lawrence Berkeley Laboratory (LBL) on 17 and 18 March 1987. Speakers presented a large body of new scientific results and geologic-hydrogeologic interpretations for the Long Valley caldera. The talks and the discussions that followed focused on concepts and models for the present-day magmatic-hydrothermal system.

Speakers at the symposium also addressed the topic of where to site future scientific drill holes in the caldera. Deep scientific drilling projects such as those being contemplated by the DOE Division of Geothermal Technology (DGT), under the Magma Energy Program, and by the DOE Office of Energy Research, Division of Engineering and Geosciences (DEG), along with the USGS and NSF, under the Continental Scientific Drilling Program (CSDP), will be major and expensive national undertakings. DOE/DEG is sponsoring a program of relatively shallow coreholes in the caldera, and DOE/DGT is considering the initiation of a multiphase program to drill a deep hole for geophysical observations and sampling of the "near magmatic" environment as early as FY 1988, depending on the DOE budget.

The Long Valley caldera, whose main stage of volcanism was the eruption of the Bishop Tuff (0.73 Ma), is among the candidate areas selected for thermal-regimes scientific drilling on the basis of extensive studies by numerous scientists supported by the CSDP agencies and by geothermal industry explorers and developers over the past 25 or so years. Long Valley is among the better-studied Quaternary ash-flow volcanos in the world and is among those for which there is strong evidence for magma at drillable depths. The caldera is also being investigated and monitored by the USGS because of potential seismic and volcanic hazards to the nearby town of Mammoth Lakes. The arguments that favor the presence of a crustal magma body have been reinforced by the recent unrest within the caldera and in the Sierran block to the south of the caldera. Relatively strong episodes of seismicity, usually initiated by a magnitude 5+ earthquake in the Sierran block to the south or in the Basin and Range Province to the east, have occurred in the caldera at intervals since 1978–1980 along with strong surface deformation in the area of the resurgent dome and sporadic increases in soil gases and steam discharges. The seismic unrest has not, however, led to a volcanic eruption, as was once feared, and has waned since 1983. Nevertheless, there remains strong evidence for partial melt conditions.

One site proposed for drilling a hole "to magma" is near the center of the resurgent dome; the choice of location is based upon proximity to a number of geophysical anomalies that have been inferred to be the result of a shallow magma (Rundle et al., 1985, 1986). Other candidate drill sites are in the western part of the caldera, close to the youngest volcanic eruption centers and within the area of the highest measured subsurface temperatures in the caldera.

Because of the wide interest in selecting a suitable drill site, LBL was authorized and funded by both DEG and DGT to coordinate and expedite the processing and interpretation of outstanding data sets and to integrate geological, geophysical, and hydrogeological data. In addition, LBL organized this symposium to summarize the state of scientific knowledge on the caldera in light of the drilling objectives of all potential participating agencies.

The study began with an attempt to identify research work in progress and data sets needing evaluation. This was done through meetings of three working groups—Seismology, Electrical-Gravity-Magnetics, and Geology-Geohydrology-Geochemistry—composed mostly of people doing research in Long Valley plus some new investigators. Groups met separately once to three times prior to the symposium to review progress, to keep workers informed, and to help plan presentations at the symposium.

LBL supported several critical studies involving the processing, modeling, and interpretation of geophysical data. The USGS continued to support on-going research under their program in Tectonophysics, Geodesy, and Volcanic Hazards. In addition, this project has enjoyed the unprecedented and enthusiastic support of two geothermal developers, Unocal and Chevron, who provided a great deal of previously proprietary downhole and geophysical data. Approximately 100 people attended the symposium to hear 31 papers organized by the three study groups. The symposium concluded with a panel-type discussion in which seven scientists with different areas of expertise summarized their views on deep drilling at Long Valley.

Norman E. Goldstein

Table of Contents

Potential Field and Electromagnetics

Geology, Geohydrology, and Geochemistry

RELATIONSHIP BETWEEN BASEMENT GEOLOGY, FAULTS, AND VOLCANIC VENTS, LONG VALLEY CALDERA, EASTERN CALIFORNIA

Roy A. Bailey
U. S. Geological Survey
Menlo Park, California

Paleozoic and Mesozoic batholithic and roof pendant structures have significantly influenced the location and orientation of Tertiary and Quaternary faulting and volcanism in the Long Valley area. The pre-Tertiary basement consists of two distinct lithologic assemblages (Fig. 1A). In the east, it consists predominantly of large Triassic granodiorite plutons intruded by smaller Jurassic granitic bodies. In the west, it consists mainly of roof-pendant rocks -- Paleozoic metasedimentary and Mesozoic metavolcanic rocks trending generally northwest and dipping nearly vertically -- intruded mainly by Cretaceous plutons. The contact between these two basement assemblages coincides approximately with the Hilton Creek fault, which may be a reactivated pre-Tertiary structure; intracaldera projections of both fault and contact trend north-south just east of the center of Long Valley caldera. Density differences in these eastern and western basement assemblages appear insufficient to affect seismic velocity or gravity, but the metasedimentary roof-pendant rocks, particularly the carbonate-rich formations, are sufficiently nonmagnetic to generate aeromagnetic lows that appear to be traceable even under thick volcanic cover in the western half and north of the caldera.

The elongation of Mesozoic plutons and associated roof pendants is northwesterly in the west and more northerly in the east. Long Valley caldera lies in the general region of this structural divergence. Late Tertiary and early Quaternary faults tend to parallel these pre-Tertiary structural trends, being northwesterly in the west along the Sierran front, and more northerly in the east, sub-parallel to the White Mountain front (Fig. 1B and 2A). In the immediate vicinity of the caldera, the main Sierran frontal faults form a west-stepping en echelon system that suggests the caldera lies in a region of unusual crustal disruption along the front.

Two Sierran frontal faults, the Hilton Creek and Hartley Springs faults, crossed the present site of the caldera in precaldera time, the former dying out northward and the latter southward, forming a north- or northwest-sloping ramp between them, similar to the Coyote Flat ramp between the Big Pine and Round Valley faults southwest of Bishop (Fig. 2A). The Fern Lake-Silver Lake fault also extended into the present western part of the caldera and either converged with or intersected the Hartley Springs fault; if it converged, both faults possibly merged with the Laurel-Convict fault to the south; if it crossed, it probably formed an east-trending, north-downward scarp across the north-sloping precaldera ramp, in about the present site of the south moat of the caldera. Thus, the precaldera terrain consisted of a depressed area east of the Hilton Creek fault, a mountainous Sierran terrain to the south that sloped to the north or northwest forming a ramp betweeen the Hilton Creek and Hartley Springs faults, which was possibly displaced further down to the north by eastward continuation of the Fern Lake fault.

Caldera faulting, as a consequence of eruption of the Bishop Tuff, was superimposed on this terrain (Fig. 2C). Subsidence probably was accommodated mainly along subcircular to elliptical ring faults related to the shape of the subjacent magma chamber, but it may have been accommodated in part along intracaldera Sierran fault segments. Subsequent resurgence probably further modified displacement on many of these faults. Surface geology, gravity, and seismic refraction studies indicate that the intracaldera Hilton Creek fault segment has significant subsurface displacement, dividing the caldera into deeper and shallower parts in the east and west repectively. Surface geology suggests that the intracaldera Hartley Springs fault segment has significant subsurface displacement, but this is not evident in seismic refraction profiles and appears unresolvable by gravity studies. Drillhole data confirm the presence of a ring fault with 1500 m displacement near the western margin of the caldera, but elsewhere ring-fault displacements are best estimated from seismic refraction profiles, which suggest displacements of about 1000 m along the southern margin and as much as 1700 m along the northen margin, giving the cauldron block a northward tilt, particularly in the west. This tilt may be inherited in part from the precaldera Sierran ramp, but chemical studies of the Bishop Tuff suggest that greater subsidence also occured in the north due to deeper withdrawal of magma from the chamber.

Precaldera (Tertiary) volcanic vents are poorly exposed, owing to extensive younger volcanic cover (Fig. 1C). Trachybasaltic-trachyandesitic vents are distributed over 4000-km^2 mainly northeast and southwest of the the caldera, whereas precaldera quartz latite vents occur only around the western half of the caldera. Neither vent type shows strongly preferred alignment, but both northeast and north alignments are evident locally. Vents for the precaldera rhyolites of Glass Mountain are clustered on the northeast caldera rim but do not have a demonstrably arcuate pattern suggestive of eruption from an incipient ring-fracture zone as previously supposed (Figs. 1C and 2B).

In contrast, postcaldera vents show strong preferential alignment (Fig. 1D). Within the caldera, early rhyolite vents on the resurgent dome tend to be localized along northwest-trending faults bounding the medial graben. Moat rhyolite vents, although generally peripheral to the resurgent dome, also are aligned northwest locally, along intracaldera projections of the Hilton Creek and Hartley Springs faults. Similarly, several postcaldera trachyandesite vents are aligned northwest along the intracaldera projection of the Fern Lake fault. Clearly, intracaldera Sierran fault segments were important magma conduits in postcaldera time.

Vents associated with the younger Mono-Inyo Craters volcanic chain are aligned generally north to slightly east of north, forming a 45-km-long zone no more than 7 km wide (Figs. 1D and 2D). As with the precaldera vents, trachybasalts are more widely distributed than quartz latites. The rhyolites (Mono-Inyo domes) are confined to a half-km-wide, 25-km-long chain, suggesting eruption from dike. This northerly Mono-Inyo trend parallels a prominent, regionally extensive, Sierran joint set, as well as the trend of recent seismic epicentral zones in the Sierran block south of the caldera -- all of which reflect the currently active east-west direction of extention in the region.

In summary, pre-Tertiary batholithic and roof-pendant structures have had a significant influence on the orientation of late Tertiary and early Quaternary faults in the Long Valley region, which trend north in the east and northwest in the west. Long Valley caldera lies within this zone of structural

2

divergence, and its subjacent magma chamber formed in a region of unusual
crustal disruption, expressed by local en echelon offset of the Sierran
frontal faults. Precaldera volcanic vents show only weak and local alignment
parallel to early-formed Sierran and Basin and Range faults. Postcaldera
volcanic vents within the caldera show strong preferential northwest alignment
along active Sierran frontal faults, which were apparently important magma
conduits. The younger Mono-Inyo Craters volcanic chain trends more northerly,
possibly reflecting a recent change in the local direction of extention from
northeast-southwest to east-west.

Figure 1. Maps showing distribution of pre-Tertiary basement rock and
interrelation of faults and pre- and post-caldera volcanic vents.
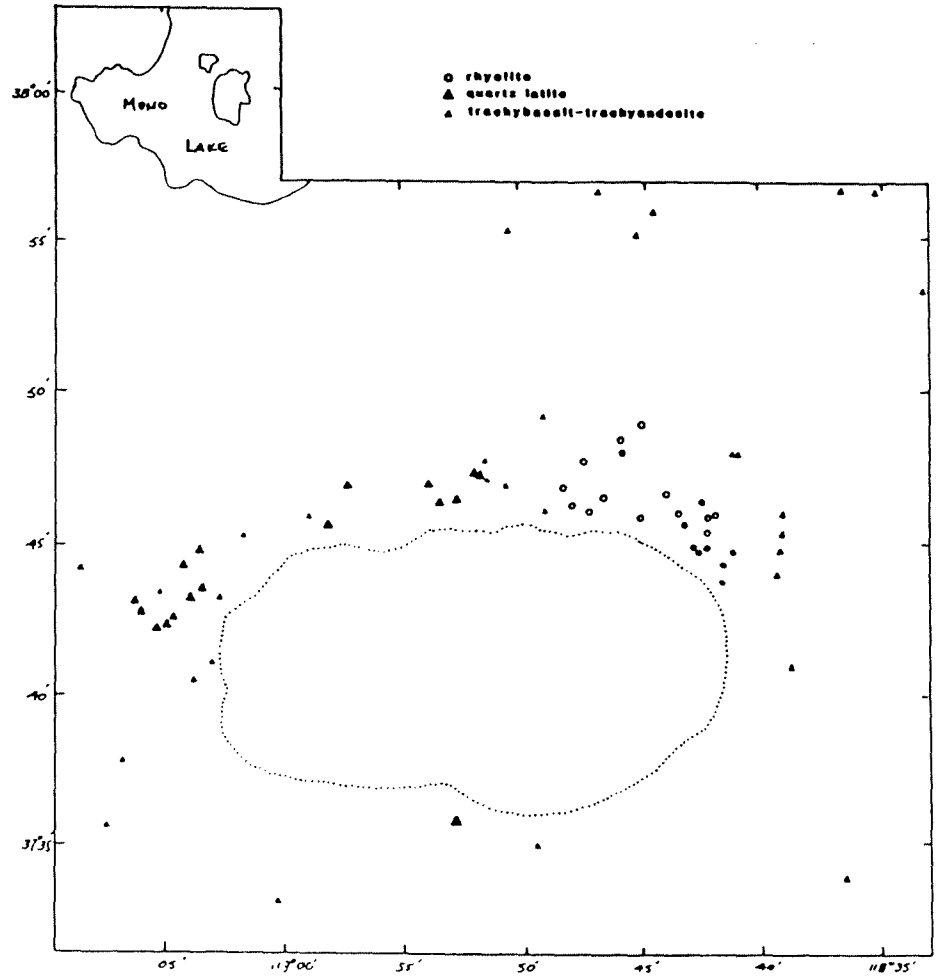
Figure 1. (Continued).
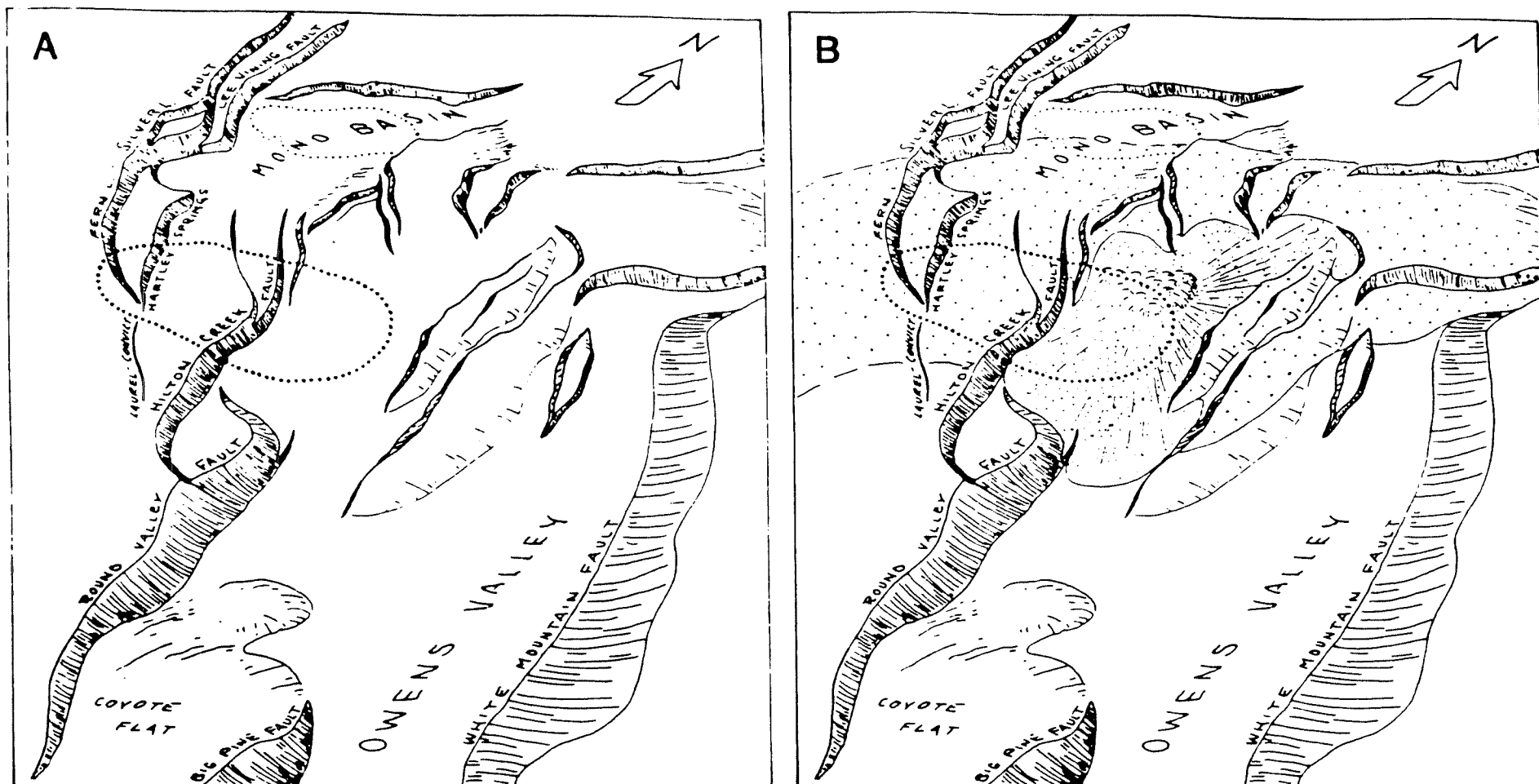
Figure 2. Physiographic sketches showing the structural evolution of the Long Valley region.

   A. Main Tertiary fault scarps about 3.6 Ma.
   B. General distribution of precaldera volcanic rocks: discontinuous mafic
      and intermediate rocks, 3.6 to 2.5 Ma (coarse, open stipple);
      rhyolite domes and pyroclastic flows of Glass Mountain complex, 2.1
      to 0.8 Ma (fine stipple).
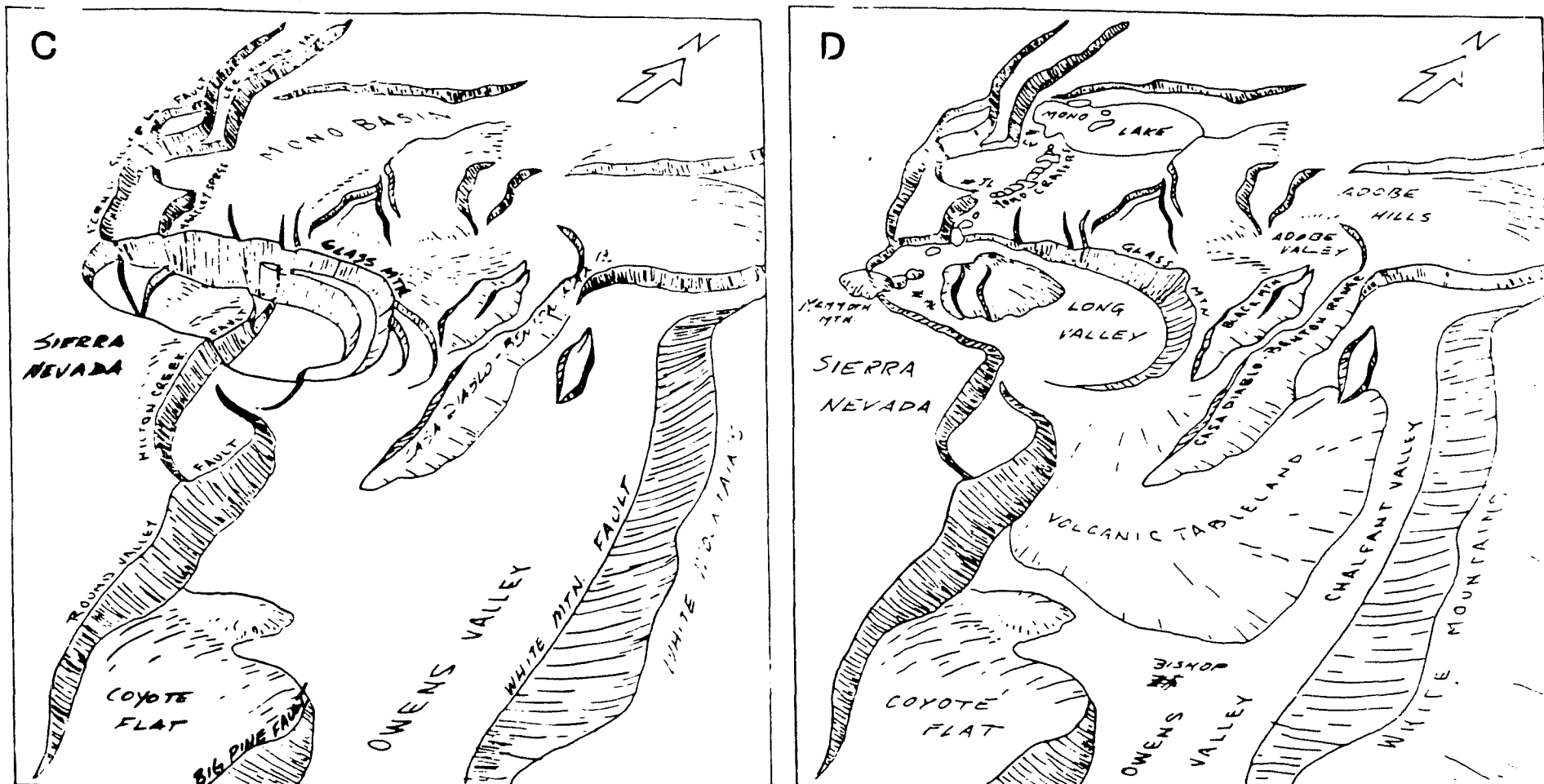
Figure 2. (Continued)

    C. Inferred subsurface structural configuration of Long Valley caldera, showing displacement of intracaldera basement surface (with intracaldera Bishop Tuff and postcaldera volcanic and sedimentary fill removed).

    D. Present configuration of Long Valley caldera and vicinity, showing postcaldera volcanic and sedimentary fill, eroded caldera walls, and resurgent dome (RD).

OVERVIEW OF THE LONG VALLEY HYDROTHERMAL SYSTEM

Michael L. Sorey
U.S. Geological Survey
Menlo Park, California

The hydrothermal system in Long Valley caldera is character-
ised by hot springs and fumaroles that discharge approximately
250 L/s of thermal water from vents located primarily around the
south and east sides of the resurgent dome and in Hot Creek gorge
(fig. 1). Although fluid discharge from some vents has increased
since 1980 in response to increased levels of seismic activity,
the total thermal water discharge has remained relatively con-
stant (Farrar and others, 1985). The most concentrated thermal
fluids encountered to date contain 1000-1500 mg/L dissolved
solids, with chloride concentrations of 250-280 mg/L. Nearly
constant ratios of Cl/B (22) and Cl/Li (85) in hot springs and
shallow aquifers throughout the caldera are indicatve of a common
reservoir source. The relatively low values of these ratios
imply that the source reservoir may occur in marine sedimentary
rocks of the Mt. Morrison roof pendant, as suggested by Shigeno
(see Sorey and others, 1987).

Prior to 1985, scientific investigations and well drilling
activities to delineate the characteristics of the hydrothermal
system were focused on the central and eastern parts of the
caldera. The results of these efforts were summarized and syn-
thesized into conceptual models by Sorey (1985) and Blackwell
(1985). The common assumptions of these models were that thermal
fluids encountered at Casa Diablo Hot Springs and eastward to
Lake Crowley were derived from deeper, higher temperature reser-
voirs located west of Casa Diablo, and that zones of relatively
deep thermal fluid circulation no longer exist beneath the resur-
gent dome. Deep circulation beneath the resurgent dome may have
occured during previous stages in the evolution of the
hydrothermal system.

Data recently aquired from hydrologic and geochemical moni-
toring and test drilling by government and industry groups con-
firms the existence of high-temperature reservoirs beneath the
western moat within volcanic fill and underlying basement rocks
(Suemnicht, 1987; Sorey and others, 1986; Wollenberg and others,
1987). Additional information from geologic and geophysical
investigations in the west moat by Unocal Geothermal (Suemnicht
and Varga, this volume; Nordquist, this volume) have been used to
infer that the principal zone of upflow of hot water occurs
through basement rocks in the vicinity of the 100,000 year-old
moat rhyolite of Bailey and others (1976) (fig. 2). Estimates of
the temperature of this upflowing fluid, based on recent geother-
mometer calculations, range from 220 to 230 C.

Assuming that deep fluid circulation in the west moat has
been active for at least 10,000 years (Sorey, 1985), the primary

heat source for the system could not be recently crystallized intrusives associated with the latest eruptions along the Inyo volcanic chain. A larger, longer-lived magma body is required. Evidence for magma at relatively shallow depths beneath the west moat comes from seismic refraction experiments (Hill and others, 1985), teleseismic P-wave delay studies (Dawson, and others, this volume), and high conductive heat flow measured near Devils Postpile (Lachenbruch and others, 1976). Thermal springs and steam vents on the flanks of Mammoth Mountain also indicate that magma may exist at relatively shallow depths beneath the mountain. Further details on thermal fluid flow and heat input from magmatic sources within the western and southwestern moat areas could come from future test drilling in this part of the caldera.

REFERENCES

Bailey, R.A., Dalrymple, G.B., and Lanphere, M.A., 1976, Volcanism, structure, and geochronology of Long Valley caldera, Mono County, California: Journal of Geophysical Research, v. 81, No. 5, p. 725-744.

Blackwell, D.D., 1985, A transient model of the geothermal system of the Long Valley caldera: Journal of Geophysical Research, v. 90, No. B13, p. 11,229-11,242.

Farrar, C.D., Sorey, M.L., Rojstaczer, S.A., Janik, C.J., Mariner, R.H., Winnett, T.L., and Clark, M.D., 1985, Hydrologic and geochemical monitoring in Long Valley caldera, Mono County, California, 1982-1984: U.S. Geological Survey Water-Resources Investigations Report 85-4183, 127 p.

Hill, D.P., Kissling, E., Luetgert, J.H., and Kradolfer, U., 1985, Constraints on the upper crustal structure of the Long Valley-Mono Craters volcanic complex, Eastern California, from seismic refraction measurements: Journal of Geophysical Research, v. 90, No. B13, p. 11,135-11,150.

Lachenbruch, A.H., Sass, J.H., Munroe, R.J., and Moses, T.H., 1976, Geothermal setting and simple heat conduction models for the Long Valley caldera: Journal of Geophysical Research, v. 81, No. 5, p. 769-784.

Sorey, M.L., 1985, Evolution and present state of the hydrothermal system in Long Valley caldera: Journal of Geophysical Research, v. 90, No. B13, p. 11,219-11,228.

Sorey, M.L., Farrar, C.D., and Wollenberg, H.A., eds., 1986, Proceedings of the second workshop on hydrologic and geochemical monitoring in the Long Valley caldera: Lawrence Berkeley Laboratory Report LBL-22852.
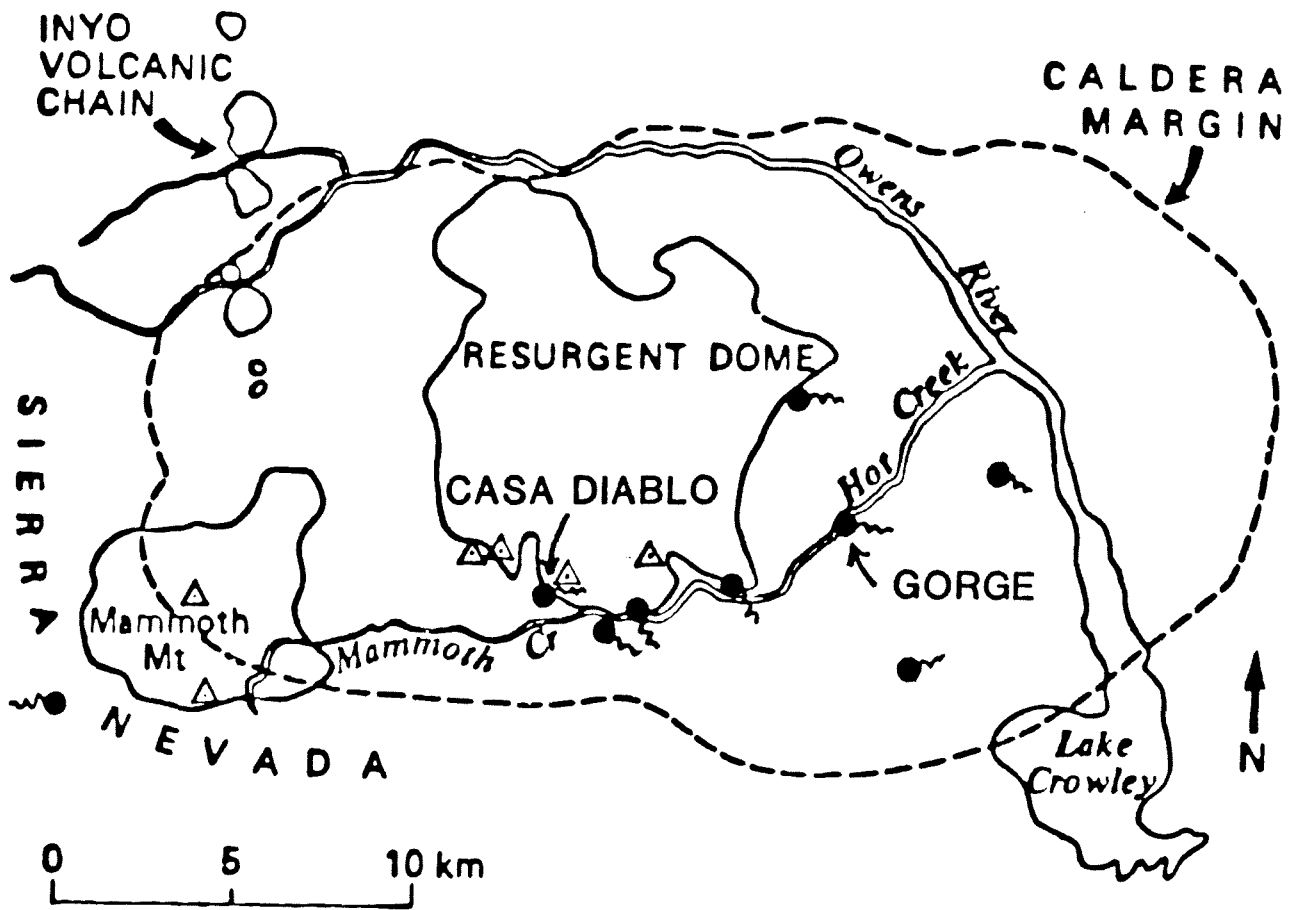
Figure 1. Locations of hot springs (filled circles with tails) and fumaroles (open triangles) in the vicinity of Long Valley caldera, and geographic locals referred to in text.
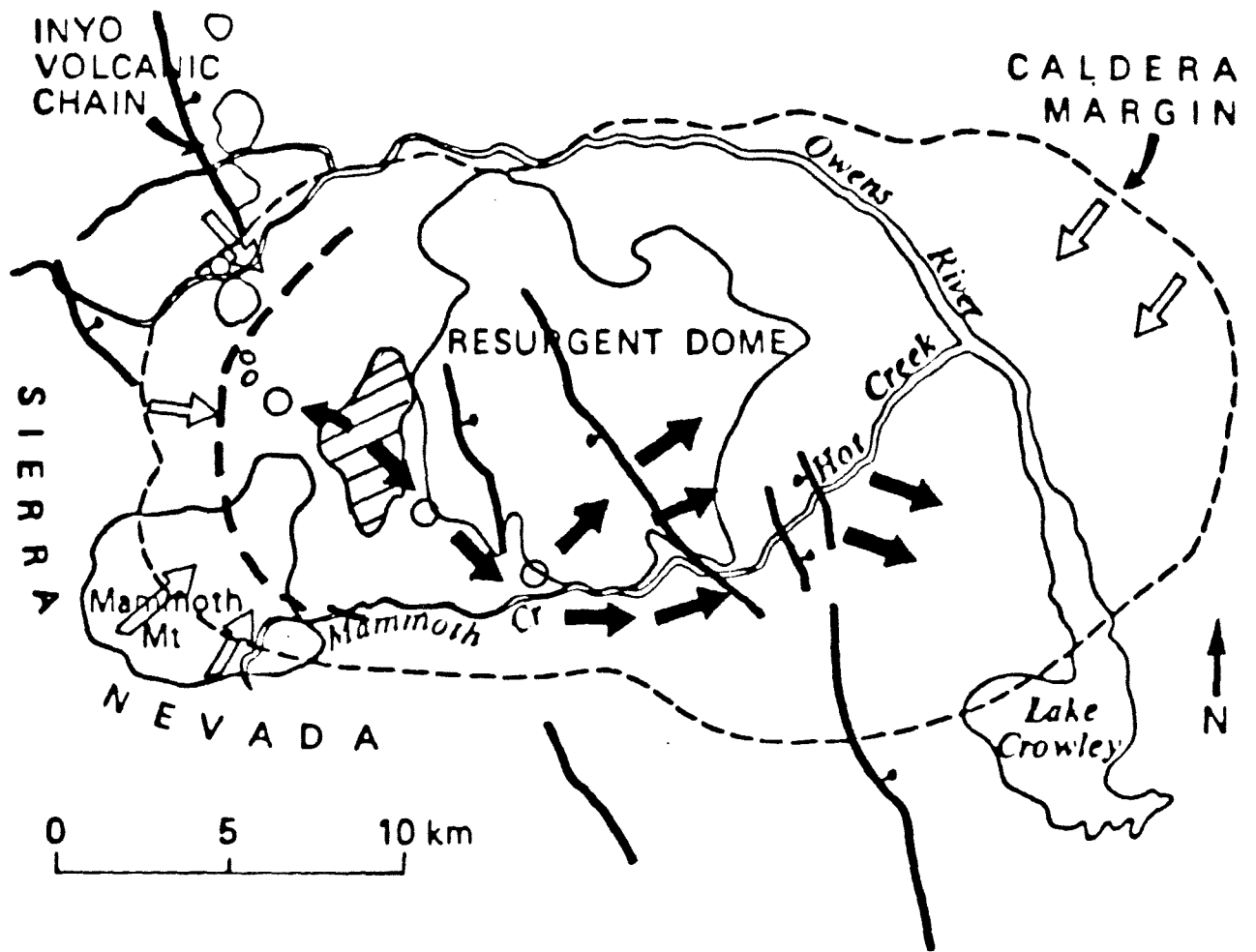
Figure 2. Postulated directions of fluid flow in present-day hydrothermal system, based on recent drilling and geologic and geophysical studies in the west moat of Long Valley caldera. Open arrows signify cold-water recharge; solid arrows signify thermal fluid flow within post-caldera volcanic and sedimentary rocks. Locations of drill holes in the west moat and at Casa Diablo shown as open circles. Principal faults shown with bar and ball on downthrown side; possible position of the caldera ring fracture beneath the west moat shown by heavy dashed line. 100,000 year-old moat rhyolite of Bailey and others (1976) shown by cross-hatch pattern.

11

HYDROLOGIC AND GEOCHEMICAL MONITORING IN
LONG VALLEY CALDERA, CALIFORNIA

by

C.D. Farrar[1], M.L. Sorey[2], S.A. Rojstaczer[2]
U.S. Geological Survey
[1]Santa Rosa, California
[2]Menlo Park, California

Hydrologic and geochemical data are being collected and interpreted by the U.S. Geological Survey and scientists from other organizations to provide a more complete understanding of flow within the hydrothermal system, to locate the present day heat source for the system, to aid in determining the geologic structure of the caldera, and to detect and explain hydrologic and geochemical responses to strain events (Farrar and others, 1985; Sorey and others, 1985 and 1986).

The youngest volcanic features in the caldera are located in the western moat. The western half of the caldera and particularly the western moat are also the areas with steam vents, geochemical anomalies, deformation, and the highest borehole temperatures.

Water-level measurements in a network of 40 wells collected three times per year show hydraulic head decreases from west to east. The western moat is underlain by a thick (50-300 M) unsaturated zone. The depth to water decreases eastward, except under the resurgent dome, as ground water flows to discharge areas near and in Lake Crowley. A network of four wells, each instrumented with a submersible strain-bridge pressure transducer and barometric pressure sensor, provide continuous record of water-level and atmospheric pressure changes. These data and frequency analysis are used to produce a record of crustal strain. Sensitivity of the four wells varies relative to degree of aquifer confinement, compressibility, porosity, and permeability. The LKT site, located near the northwest margin of the resurgent dome, shows the greatest sensitivity (10^{-9} strain units). The instrumentation at this site detected cumulative dilatational deformation of 0.30 microstrain following the July 21, 1986 Chalfant $M_L6.4$ earthquake.

Continuous flow measurements of seven springs have been recorded over periods of 6 months to several years. Coseismic changes in flow volumes have been recorded indicating springs are sensitive to strain events. However springs are probably orders of magnitude less sensitive to strain than water levels in some wells. In an analogous way, continuous vent-temperature record of a sub-boiling temperature steam vent shows that the vapor volume may vary with local crustal strain, assuming a direct correlation of vent-temperature with vapor-flow volume. Steam vents in the caldera all have temperatures $\leq$ ambient boiling temperature ($93°C$). The vents are few in number and are confined to parts of the western moat and the south western part of the resurgent dome, generally topographically higher than thermal spring vents.

Chemical and isotopic data on the compositions of subsurface waters and gases show the detailed ground-water flow regime is more complex than the simple pattern of west to east ground-water flow as derived from hydraulic head data. Vertical flow, mixing of non-thermal and thermal waters, and possibly local boiling occur and are related to the stratigraphy of the caldera fill and geologic structures. Recent chemical and isotopic data from geothermal production wells at Casa Diablo and from exploration holes in the western moat provide the most reliable data on reservoir-fluid composition. Chemical geothermometers estimate reservoir temperatures of about 210-220 °C.

$3/4$He ratios in gases from steam vents and springs increase from west to east across the caldera. The increase may be related to magmatic contributions of ^{3}He (Hilton and others, 1986 and B.M. Kennedy, written communication, 1985) or may relate to water/rock interaction. Hilton and others (1986) also note an increase in $3/4$He in a spring vent in the central part of the caldera, from 1978-83 with subsequent decrease following the 1983 seismicity.

Several other investigative teams have conducted discrete time, regional, soil or soil-gas surveys (Hg°, Rn, He) and also have collected continuous records of ^{222}Rn, H, and He at specific sites for periods of a few months to years. Anomalously high concentrations of Hg° in soil-gas have been identified in the western moat, on the resurgent dome, and on Mammoth Mountain. Anomalously low Hg° concentration in soil-gas was found over the 1983 epicentral area in the south moat (Varekamp and Busek, 1984, and Williams, 1985). Williams also detected anomalously high concentrations of Rn in soil-gas overlying the 1983 epicentral area, however, overall background Rn values declined from 1983-84. High helium anomalies occur in the western moat and locally around hot springs; no He anomaly is associated with the 1983 epicentral area (Reimer, 1986). Hydrogen and to a lesser degree radon spikes in continuous long-term records correlate with seismicity in the caldera (McGee and Sutton, 1986; and Flexer and Wollenberg 1986).

REFERENCES

Farrar, C.D., Sorey, M.L., Rojstaczer, S.A. Janik, C.A., Mariner, R.H., Winnett, T.L., and Clark, M.D., 1985, Hydrologic and Geochemical monitoring in Long Valley Caldera, Mono County, California, 1982-1984: U.S. Geological Survey WRI 85-4183, 137p.

Flexser, S. and Wollenberg, H, 1986, Radon monitoring at Long Valley Fish Hatchery (Abstr): in Sorey, M.L., Farrar, C.D., and Wollenberg, H., 1986) Proceedings of the second workshop on Hydrologic and Geochemical monitoring in the Long Valley Caldera, July 1986: Lawrence Berkeley Laboratory Rpt. (in press).

Hilton, D.R., Poreda, R.J., Rison, W., and Craig, H. 1986, Helium Isotope Variations and Seismicity at Long Valley Caldera (Abstr.): in Sorey, M.L., Farrar, C.D., and Wollenberg, H., 1986) Proceedings of the second workshop on Hydrologic and Geochemical monitoring in the Long Valley Caldera, July 1986: Lawrence Berkeley Laboratory Rpt. (in press).

McGee, K.A. and Sutton, A.J., 1986, Gas monitoring at Long Valley- status report (Abstr): in Sorey, M.L., Farrar, C.D., and Wollenberg, H., 1986) Proceedings of the second workshop on Hydrologic and Geochemical monitoring in the Long Valley Caldera, July 1986: Lawrence Berkeley Laboratory Rpt. (in press).

Reimer,, G.M., Friedman, I., Been, J.M., Szarzi, S.L., 1986, Helium-4 measurements in Long Valley (Abstr): in Sorey, M.L., Farrar, C.D., and Wollenberg, H., 1986) Proceedings of the second workshop on Hydrologic and Geochemical monitoring in the Long Valley Caldera, July 1986: Lawrence Berkeley Laboaratory Rpt. (in press).

Sorey, M.L., Farrar, C.D., and Wollenberg, H., 1985 eds, Proceedings of the workshop on Hydrologic and Geochemical monitoring in the long Valley Caldera, October 1984: Lawrence Berkeley Laboratory report LBL-20020, 82p.

Sorey, M.L., Farrar, C.D., and Wollenberg, H., 1986, eds., Proceedings of the second workshop on Hydrologic and Geochemical Monitoring in the Long Valley Caldera, July 1986: Lawrence Berkeley Laboratory Report (in Press).

Varekamp, J.C. and Busek, P.R., 1984, Changing mercury anomalies in Long Valley, California: Geology, V. 12., p. 283-286.

Williams, S.N., 1985, Soil radon and elemental mercury distribution and relation to the magmatic resurgence at Long Valley Caldera: Science, V. 229, p 551-553.

MIXING AND BOILING OF THERMAL FLUIDS IN LONG VALLEY CALDERA, CALIFORNIA

by

Lisa Shevenell, C. O. Grigsby, Fraser Goff,
Earth and Space Sciences Division
Alamos National Laboratory
Los Alamos, New Mexico 87545

and

Nancy O. Jannik, and F. Phillips
New Mexico Institute of Mining and Technology
Socorro, New Mexico 87801

Recharge to the Long Valley geothermal system occurs in the western part of the caldera along the Sierra Nevada front with the water being heated at depth and flowing laterally eastward into the caldera (Farrar et al., 1985). As the Na-K-HCO$_3$-Cl fluids flow eastward they are increasingly mixed with meteoric water to form the more diluted fluids found within the caldera. Evidence for mixing is illustrated in plots of B and Li versus Cl and δ^{18}O versus δD. Clear mixing trends exist between fluids similar in composition to thermal waters in the Casa Diablo area and cold, dilute groundwaters, with the more concentrated fluids emerging in the western part of the caldera. Oxygen-18 versus deuterium and chloride plots indicate that the dilute end-member which mixes with thermal fluids is isotopically very depleted, similar to cold waters east of Lake Crowley (Mariner and Willey, 1979; Sorey, 1985). However, the dilute end-member on these plots could also represent the isotopically depleted composition of steam, because the chloride versus deuterium plot suggests the possibility that some thermal fluids east of Casa Diablo are mixtures of thermal fluid and steam.

Boiling is an important mechanism controlling the chemical compositions of thermal fluids in the Casa Diablo area. While boiling trends are coincident with mixing trends on the Li and B versus Cl plots, a plot of NH_4 versus Cl more clearly identifies the end-member, boiled, and mixed components of the thermal fluids. Assuming that the Casa Diablo well fluid is conductively cooled end-member geothermal water, we calculate steam fractions with Cl mass balance for Colton Hot Spring and Casa Diablo Hot Spring. Using these steam fractions and the gas distribution coefficient for NH_3 for single-stage boiling at $100^{\circ}C$ (Henley et al., 1984), we can show that near surface boiling of Casa Diablo well fluids at $100^{\circ}C$ can form waters with the compositions of Colton Hot Spring and Casa Diablo Hot Spring. A 9% loss of steam during boiling of Casa Diablo well fluids produces a fluid with the composition of Colton Hot Spring, while a 19% steam loss would result in a fluid with the composition of Casa Diablo Hot Spring. Waters to the east of the Casa Diablo area are mixtures of meteoric water and boiled thermal fluids with a composition close to that of Colton Hot Spring. However, Colton Hot Spring appears to be slightly mixed with dilute groundwater.

One would expect an increase of ^3H and ^{36}Cl from west to east as fluids are progressively mixed because ^{36}Cl increases with increasing ^3H in cold waters of the region between Bishop and Long Valley. However, no correlation exists between ^3H and ^{36}Cl in thermal fluids or between these components and conservative species. Except for the hot spring north of Whitmore and Meadow hot spring, it appears that cold end-member fluids involved in mixing in Long Valley caldera must be relatively old fluids low in both meteoric ^3H and ^{36}Cl. The ^{36}Cl of the mixed thermal fluids may also be controlled by the ^{36}Cl in the rocks through which the water flows.

References

Farrar, C. D., Sorey, M. L., Rojstaczer, S. A., Janik, C. J., Mariner, R. H., Winnett, T. L., and Clark, M. D., 1985, Hydrologic and Geochemical Monitoring in Long Valley Caldera, Mono County, California, 1982-1984, U.S. Geol. Surv. Water-Resources Invest. Report 85-4183, 137 pp.

Henley, R. N., Truesdell, A. H., Barton, Jr., R. B., and Whitney, J. A., 1984, Fluid-Mineral Equilibria in Hydrothermal Systems, Reviews in Economic Geology, Volume 1, Society of Economic Geologists, El Paso, Texas, 267 pp.

Mariner, R. H., and L. M. Willey, 1979, Geochemistry of Thermal Waters in Long Valley, Mono County, California, J. Geophys. Res., 81(5), 792-800.

Sorey, M. L., 1985, Evolution and Present State of the Hydrothermal System in Long Valley Caldera, J. Geophys. Res., 90(B13), 11,219-11,228.

A CORE HOLE INTO THE HYDROTHERMAL SYSTEM OF THE LONG VALLEY CALDERA

Harold Wollenberg, Art White, Steve Flexser; Lawrence Berkeley Laboratory

Mike Sorey, Chris Farrar; U.S. Geological Survey

To investigate the present-day hydrothermal system, the "Shady Rest" hole was continuously cored 715m into the southwestern moat of the Long Valley caldera (Figure 1). The hole intersected 100m of glacial till and 300m of postcaldera rhyolite before entering the welded Bishop Tuff and bottoming in that unit (Figure 2). A sharp temperature rise over the upper 350m, and near-isothermal conditions below reflect the presence of ~ 200°C water moving through open, calcite-lined fractures in silicified Early Rhyolite and the Bishop Tuff. The depth to the Bishop is the shallowest encountered in holes in the caldera, and the temperatures measured are among the hottest observed in wells drilled within the caldera.

Difficulties were encountered in completing the hole; sloughing, squeezing, and lost circulation prevented installation of casing over the full 715 m depth. Attempts to redrill and recover the portion of the hole below 245 m resulted in a "new" hole, diverging from the original at 241 m (Figure 3). The "new" hole was cored to a depth of 426 m, where N-sized casing (6 cm I.D.) was cemented in and filled with water; temporarily configured as a thermal gradient hole.

Following repeated temperature surveys to determine an equilibrium profile, a portion of the casing in the high temperature zone was perforated, the fluids were sampled. Preliminary chemical analyses and calculated geothermometer temperatures are compared with analyses of a Casa Diablo geothermal well fluid in Table 1. The similarities in most of the chemical concentrations and in ionic ratios suggest that the Shady Rest fluids are the predominant constituents of fluid flowing through the Casa Diablo geothermal field. The higher Ca concentration at Shady Rest is probably due to the abundant calcite that lines the open fractures of the high temperature zone. Calculated Na/K/Ca chemical geothermometer temperatures for the Shady Rest and Casa Diablo well samples are higher than those measured down-hole, but are similar

to the temperature measured at Unocal's 44-16 hole (218°C), ~ 6 km northwest of Shady Rest.

Planned investigations of Shady Rest core include alteration mineralogy, $^{87/86}$Sr and $^{12/13}$C measurements on fracture calcite, and $^{18/16}$O and H/D determinations on fracture minerals and whole-rock specimens. Uranium-series disequilibrium will be investigated in intervals indicated by gamma-ray logs. Major- and trace chemical constituents of fluid and gases will be analyzed, and measurements of fluid inclusion temperature will be attempted.

The hole serves the multiple purposes of identifying a potential geothermal resource for Mammoth Lakes, as a point for monitoring changes in hydrologic and fluid chemical parameters, and as an indicator of a principal heat source for the caldera's hydrothermal system. It was the consensus of participants at recent Long Valley hydrothermal workshops that a 1 to 2 km-deep hole should be drilled to resolve the critical question of the flow paths in the hydrothermal system of the western moat area and the location of the associated heat source. In this respect, the Shady Rest hole can be considered a "stepout" west of Casa Diablo, to test the rationale for the deeper hole. Though the Shady Rest hole does not penetrate deeply enough to fully delineate the characteristics of the hydrothermal system in the western moat, it does confirm the presence of 200° + water, and provides access to hydrologic and geochemical information otherwise unobtainable until a deeper hole is drilled. Such information will prove invaluable in siting and determining the depth of the deeper hole.

The Shady Rest hole was drilled under the joint auspices of the USDOE's Office of Basic Energy Sciences, the California Energy Commission, and Mono County.

Table 1. Preliminary chemical analyses[a] and geothermometer temperatures of Shady Rest fluid, compared with fluids from a Casa Diablo well.

	Shady Rest[b]	Casa Diablo[c]
Na	369	350
K	43	36
Ca	7.4	1.2
Li	2.8	2.6
Cl	280	270
SO_4	159	120
B	12	11
SiO_2	250	250
$\delta^{18}O$	-14.3	-14.8
Na/K/Ca geothermometer temperature (°C)	214	224

[a] In milligrams per liter.

[b] Bailed sample, analysis by USGS.

[c] Well MBP-3, sampled 7/12/85, analysis by USGS.
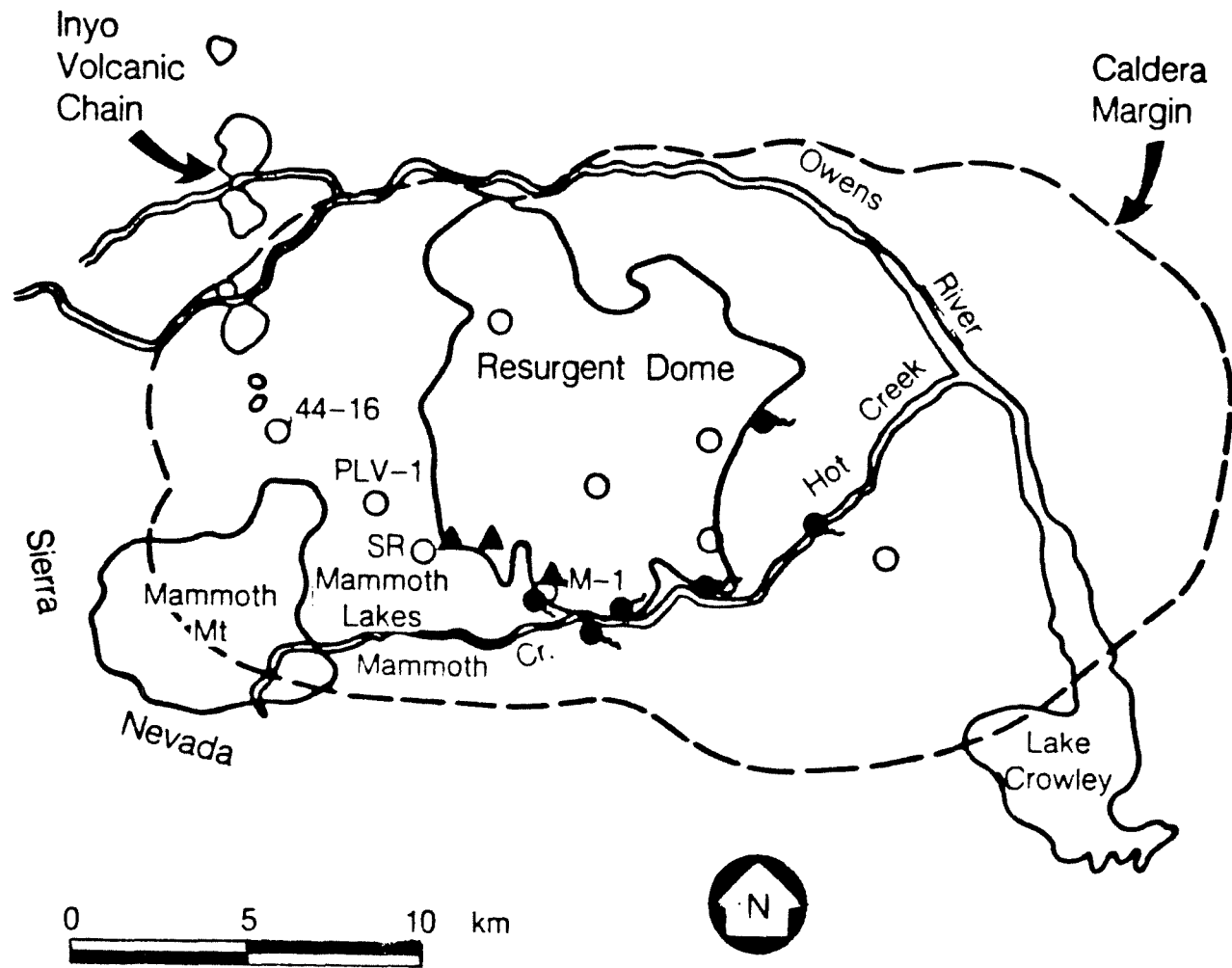
Figure 1. Map of Long Valley caldera showing locations of deep test wells
(open circles) and active thermal features (hot springs are filled
circles with tails, fumaroles are filled triangles). SR designates
the Shady Rest hole, M-1 locates Casa Diablo Hot Springs.
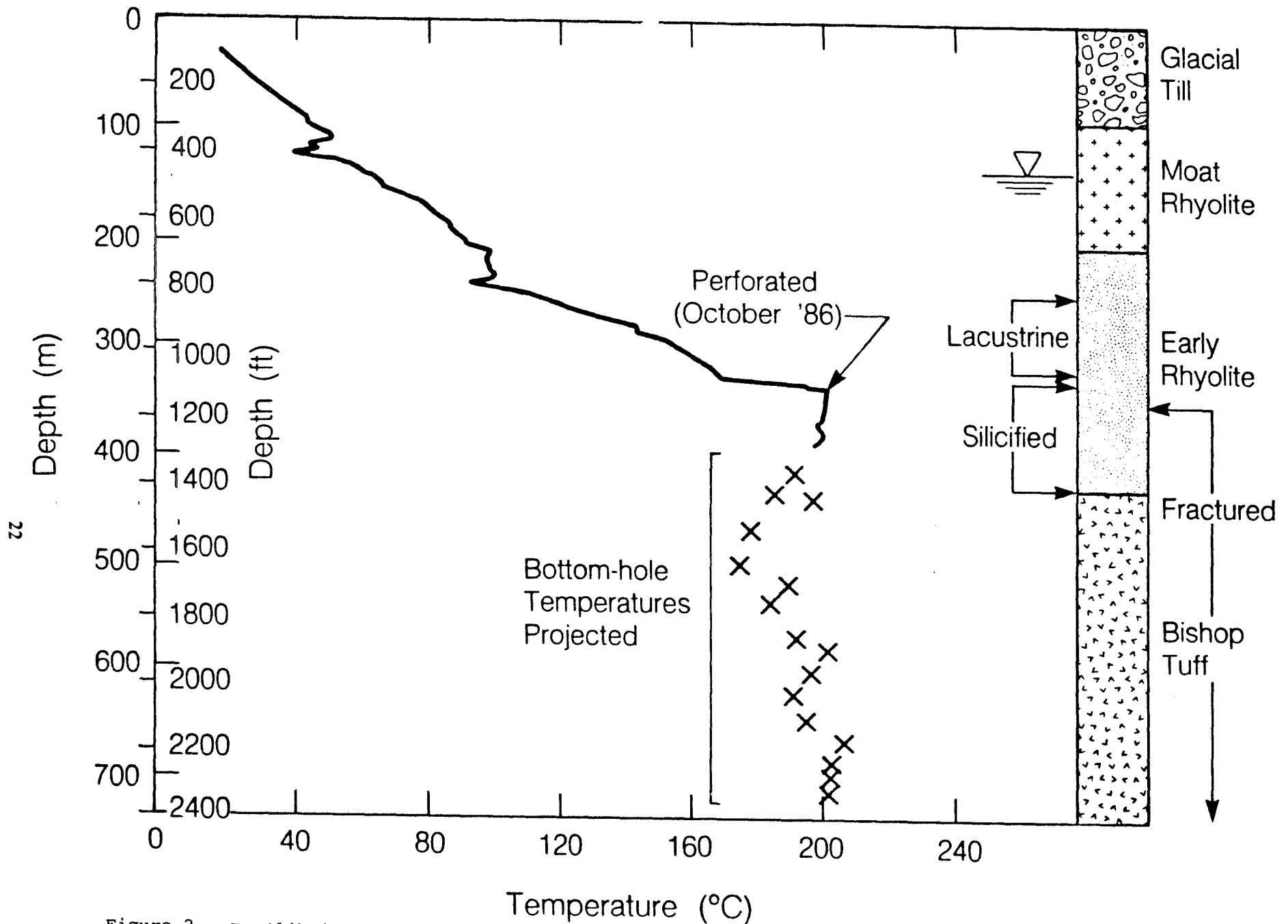
Figure 2. Equilibrium temperature profile (7/7/86) with projected temperatures from bottom-hole measurements during coring, together with a lithologic diagram of the Shady Rest hole.

XBL 868-10961
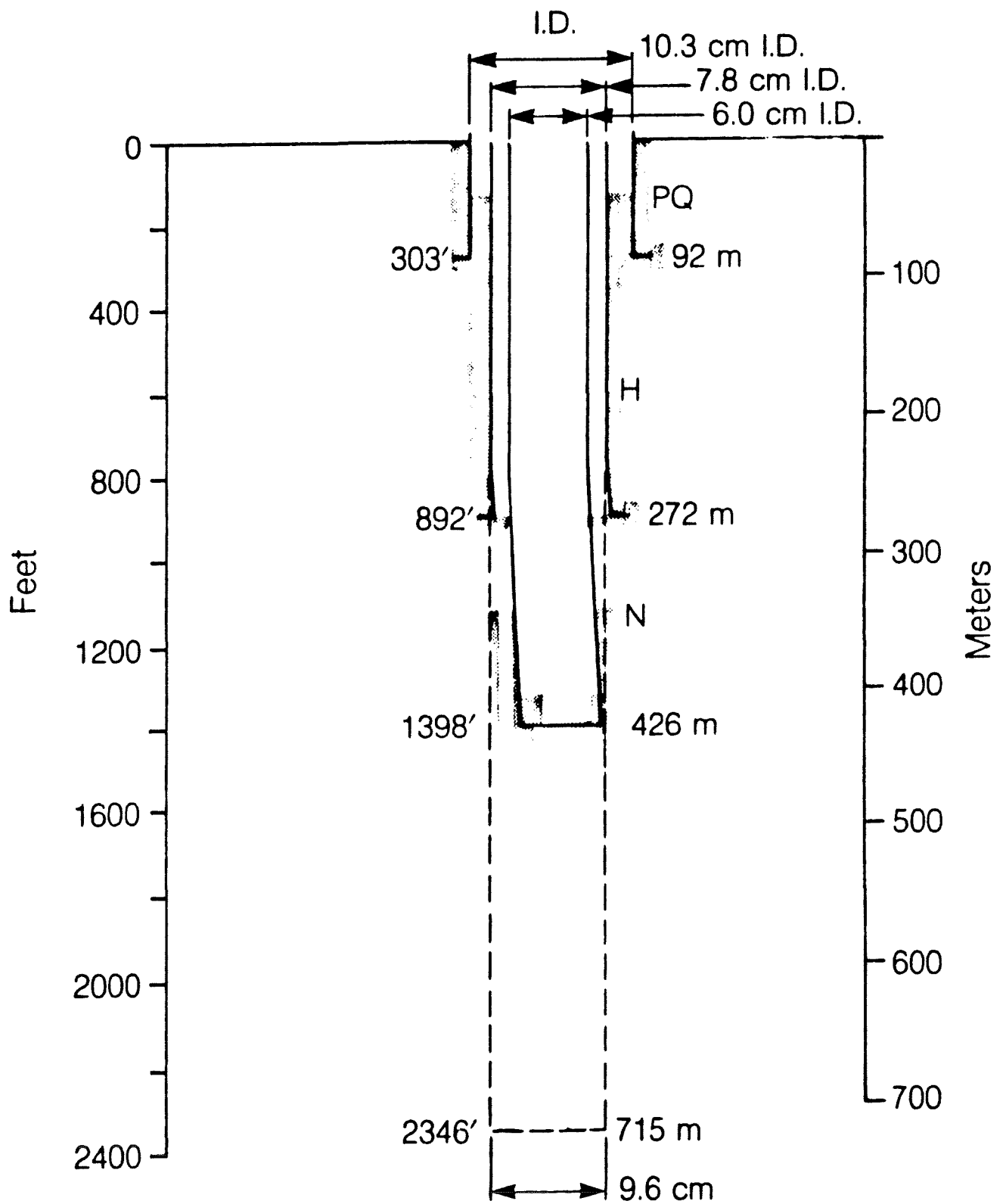
Figure 3. Completion diagram of the Shady Rest hole.

MAPPING THE HYDROTHERMAL SYSTEM BENEATH THE WESTERN MOAT OF THE LONG VALLEY CALDERA USING MAGNETOTELLURIC AND TIME-DOMAIN ELECTROMAGNETIC MEASUREMENTS

Gregg Nordquist
Unocal Geothermal Division
P.O. Box 6854
Santa Rosa, CA 95406

Geophysical surveys conducted by Unocal in the western Long Valley caldera have been designed to assess the hydrothermal system and to locate possible deep geothermal drilling targets. Interpretations based on magnetotelluric (MT) and time-domain electromagnetic (TDEM) measurements with constraints from structural mapping and well data have located a possible source area for the hydrothermal system. This region of potential upflow occurs at the intersection of major crustal structures in the western moat of the caldera.

Figure 1 shows a plan view of the caldera's resistivity structure defined by Unocal's MT data at 1 Hz. Data from shallow drill holes show that the large 20 ohm-m anomaly located northeast of MAM-1 is associated with clay mineralization (Sorey et al., 1978). The other areas of less than 20 ohm-m are found in the western caldera northwest of MAM-1. Two-dimensional (2-D) MT resistivity models were constructed across these anomalous regions to determine the depth and areal extent of the low resistivity zone.

The interpretation of MT and TDEM data show depths to low resistivities that correlate with an increase in clay mineralization in the wells IDFU 44-16 and PLV-1 (Figures 2 and 3). Beneath both wells the MT resistivity models have an approximately 400 meter thick 10 ohm-m layer. In IDFU 44-16 this layer extends into the Bishop Tuff and contains a temperature reversal interpreted as outflow in a lateral hot water aquifer. Similarly, a lateral aquifer may be present beneath PLV-1 suggesting that a similar reversal in the temperature profile would have been encountered had the well been drilled deeper.

A 2-D MT model along line A-A' (Figure 4) shows that east of IDFU 44-16 the 10 ohm-m layer thickens to 1800 meters and extends into the basement as defined by seismic refraction data (Hill et al., 1985). This zone of unusually deep low resistivities continues to the southeast and wraps around the resurgent dome (Figure 5). Temperature data from MAM-1 and CP-1 show that there is no active upflow associated with the southern and eastern lobes of the deep low resistivities. However, east of IDFU 44-16 active upflow may be associated with increased permeabilities at the intersection of major northeast and northwest trending structures (Suemnicht and Varga, this volume).

Figure 6 shows a model for the hydrothermal system based on an interpretation of a 2-D MT resistivity model along B-B'. In this model the hot water aquifer is inferred to be within the 10 ohm-m layer and beneath an impermeable clay layer similar to IDFU 44-16. Upflow is located in the area of unusually deep low resistivities and is the source for the lateral hot water aquifer which flows to the west beneath PLV-1 and IDFU 44-16. The extension of the unusually deep low resistivities to the southeast, may delineate a preferred path for the hot water system as it flows around the resurgent dome towards MAM-1.

Although these interpretations are consistent with the available structural and well data they cannot be considered unique. The area of unusually thick low resistivities may be due to a localized change in the metamorphic basement rocks or they could be caused by alteration along an extinct upflow zone. In either case the source for the system would have to be somewhere else, possibly related to Mammoth Mountain or to the young extrusives in the Inyo Domes.

References:

Hill, D.P., Kissling, E., Luetgert, J.H. and Kradolfer, U., Constraints on the upper crustal structure of the Long Valley-Mono Craters volcanic complex, eastern California, from seismic refraction measurements, J. Geophys. Res., 90 (B13), 11135-11150, 1985.

Sorey, M.L., Lewis, R.E. and Olmsted, F.H., The hydrothermal system of the Long Valley caldera, California, USGS Prof. Paper, 1044-A, 60 pp., 1978.

Suemnicht, G.A. and Varga, R.J., Constraints on models of structure and hydrothermal circulation in the Long Valley caldera, this publication.
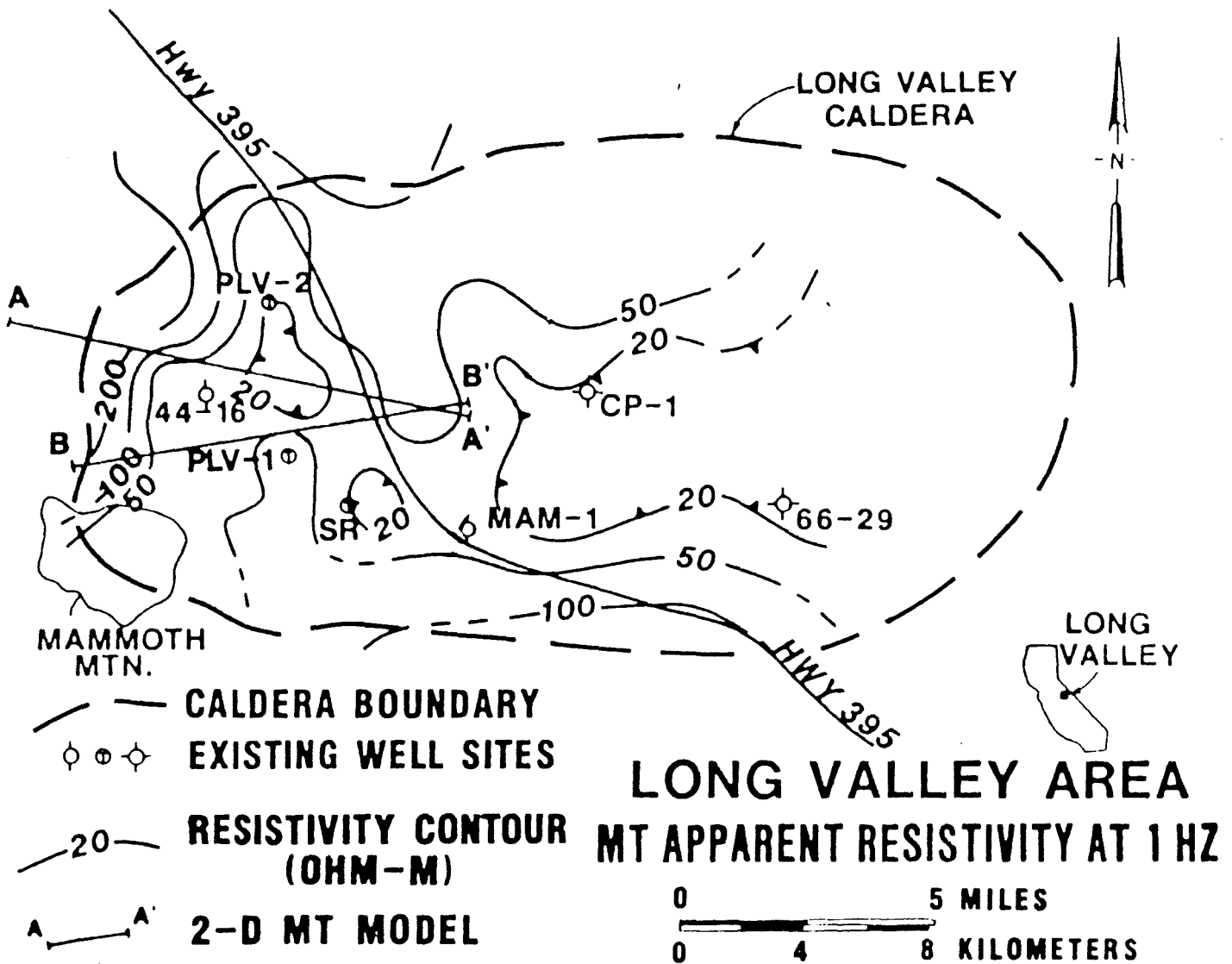
Figure 1   Invarient apparent resistivity at 1 Hz for Unocal's MT data. Also shown are the locations for the 2-D models.

LONG VALLEY AREA
44-16

RESISTIVITY
MODELS
(OHM-M)
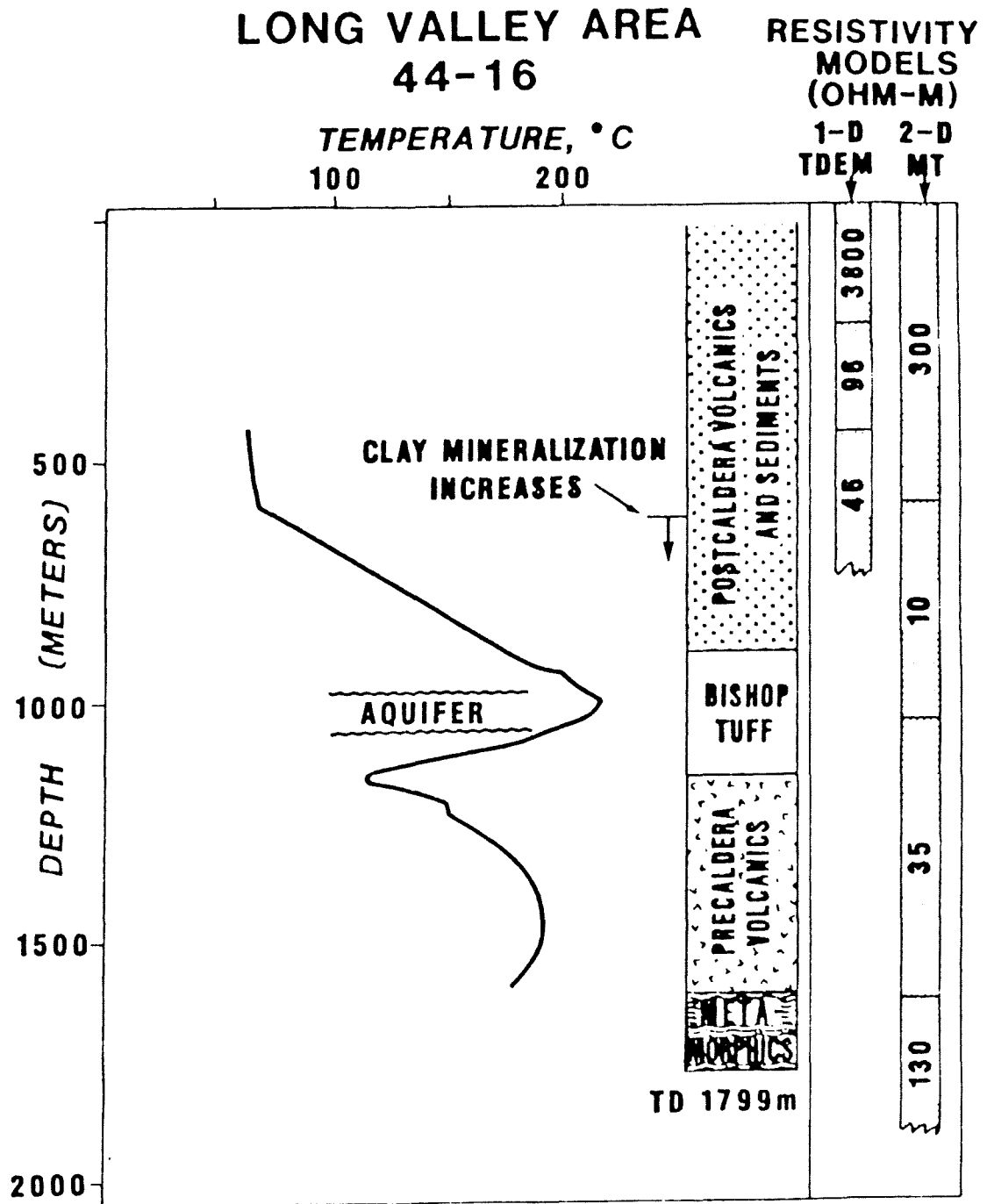
TEMPERATURE, °C

Figure 2 A comparison of the temperature and generalized stratigraphy
from well IDFU 44-16 with 1-D TDEM and 2-D MT resistivity
models. The 1-D TDEM model is from Unocal's 1985 survey;
line 3, site 15 (Earth Technology, 1985). The 2-D MT model
is from line A-A', Figure 4. Note the correspondence of the
low resistivity layer for both models with an observed in-
crease in clay mineralization and the interpreted aquifer
within the 10 ohm-m MT model.

LONG VALLEY AREA
PLV-1
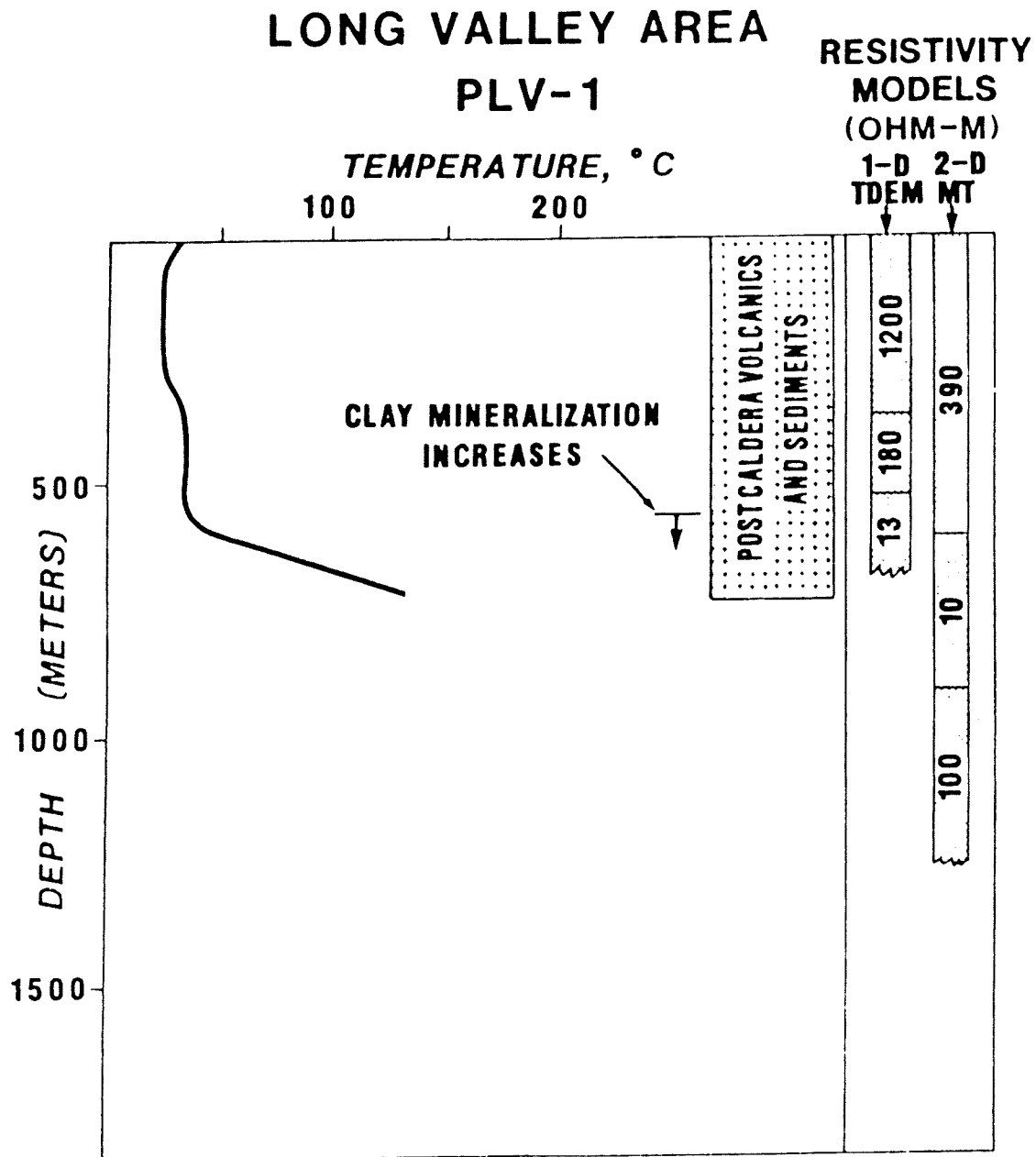
Figure 3   A comparison of the temperature and generalized stratigraphy
from PLV-1 with 1-D TDEM and 2-D MT resistivity models.   The
1-D TDEM model is from Unocal's 1985 survey; Line 4, site
23 (Earth Technology, 1985).   The 2-D MT model is from
Line B-B', Figure 6.   Note the correspondence of the low
resistivity layer for both models with an observed increase
in the clay mineralization.

LONG VALLEY CALDERA
TWO-DIMENSIONAL MT RESISTIVITY
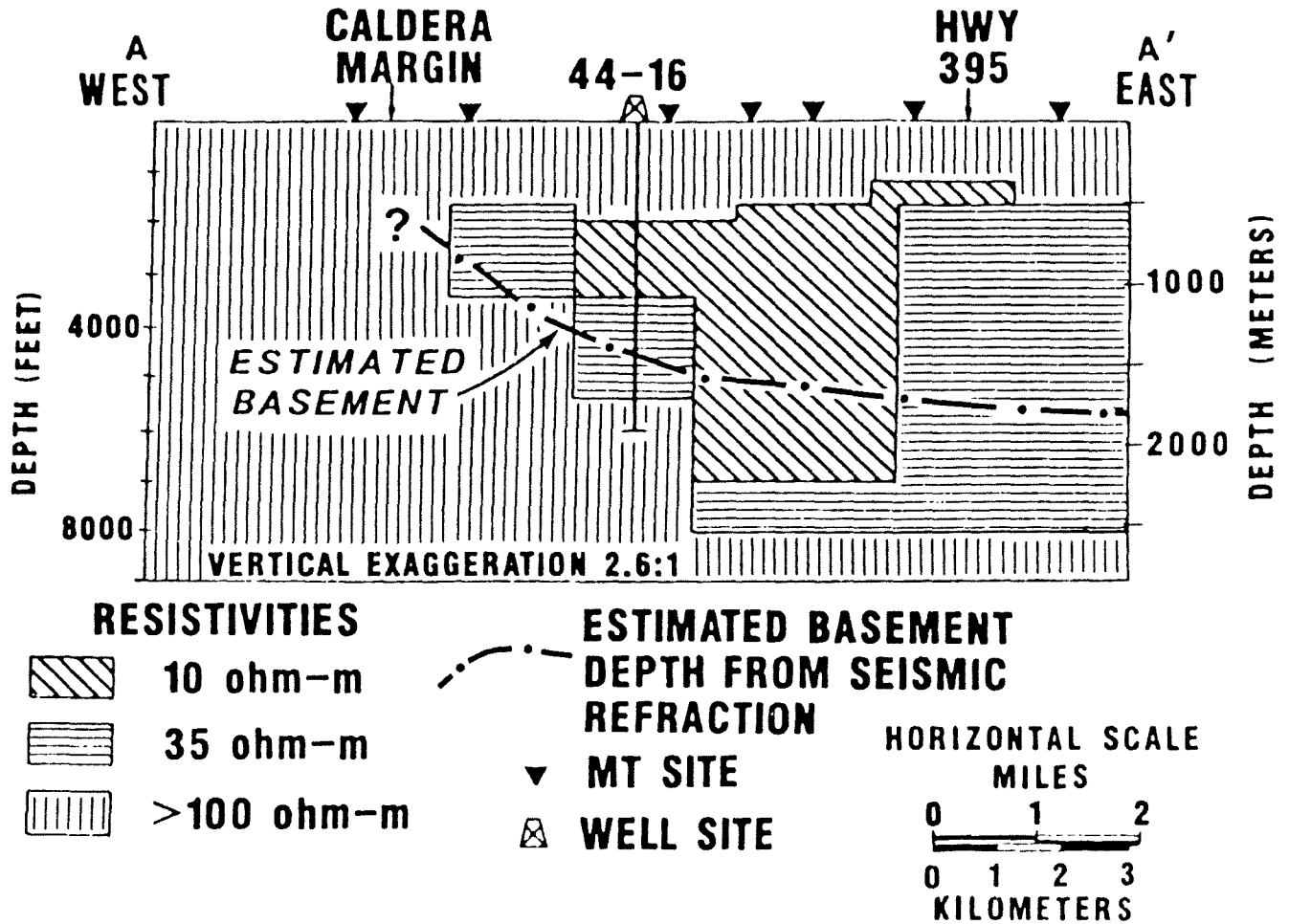
Figure 4   This figure shows the generalized results from a 2-D MT
resistivity model along the line A-A', Figure 1. The
area of unusually deep low resistivities is located
beneath the 20 ohm-m MT anomaly observed at a frequency
of 1 Hz.

AREA OF UNUSUALLY DEEP LOW RESISTIVITIES

LONG VALLEY CALDERA

- N -

MAMMOTH MTN.

LONG VALLEY

⌒ — CALDERA BOUNDARY

◇ ⊕ ◇ EXISTING WELL SITES

⌒20⌒ RESISTIVITY CONTOUR (OHM-M)

A——A' 2-D MT MODEL

LONG VALLEY AREA
MT APPARENT RESISTIVITY AT 1 HZ

```
0                    5 MILES
0        4          8 KILOMETERS
```
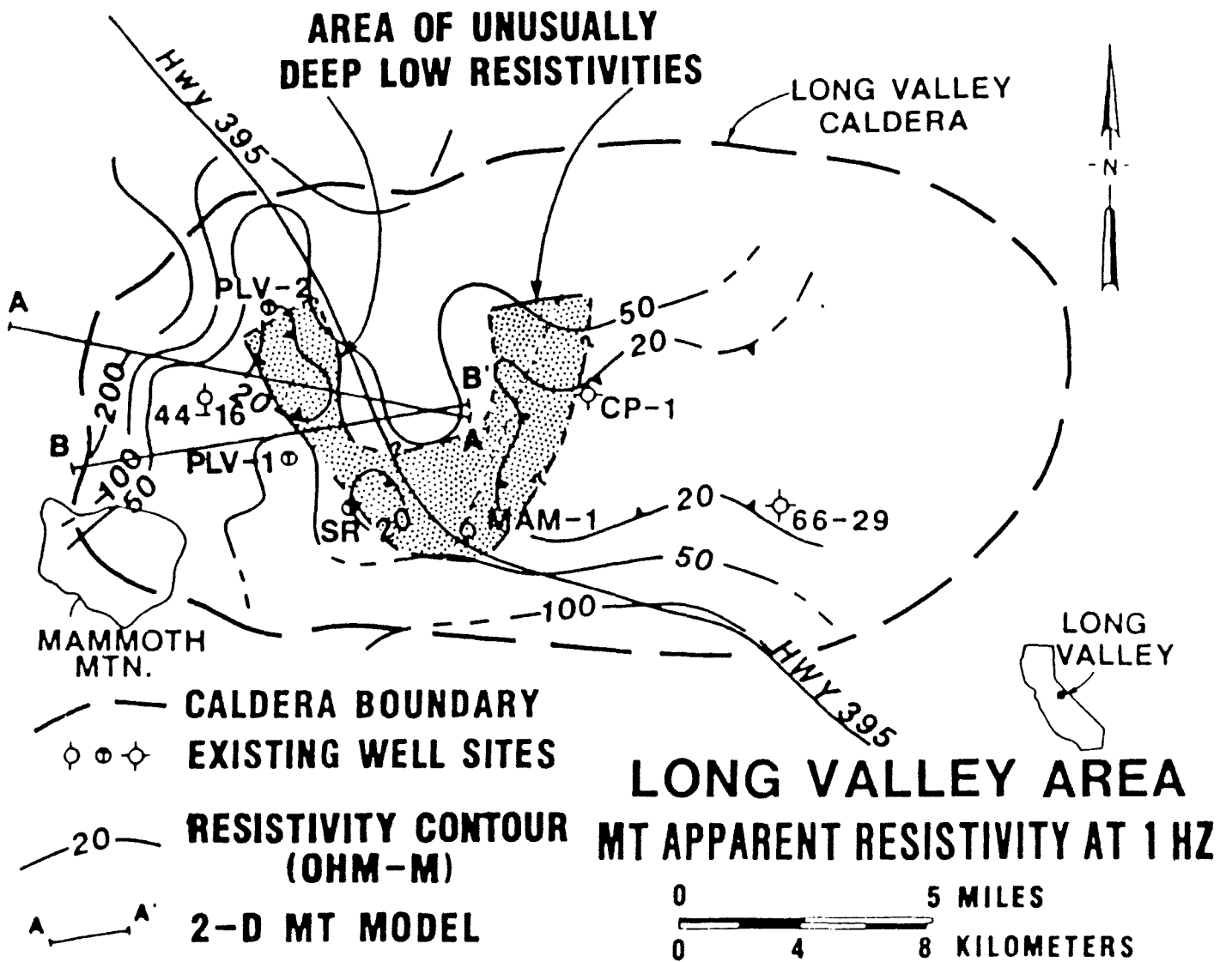
Figure 5   Location of an area of unusually deep low resistivities as interpreted from 2-D and 1-D MT interpretations. The boundaries for the zone are well constrained in the vicinity of the 2-D models and less well determined elsewhere. This zone may act as a preferred pathway for the hot water aquifer within the Bishop Tuff.

LONG VALLEY CALDERA
INTERPRETATIVE CROSS-SECTION
ALONG TWO-DIMENSIONAL MT MODEL B-B'
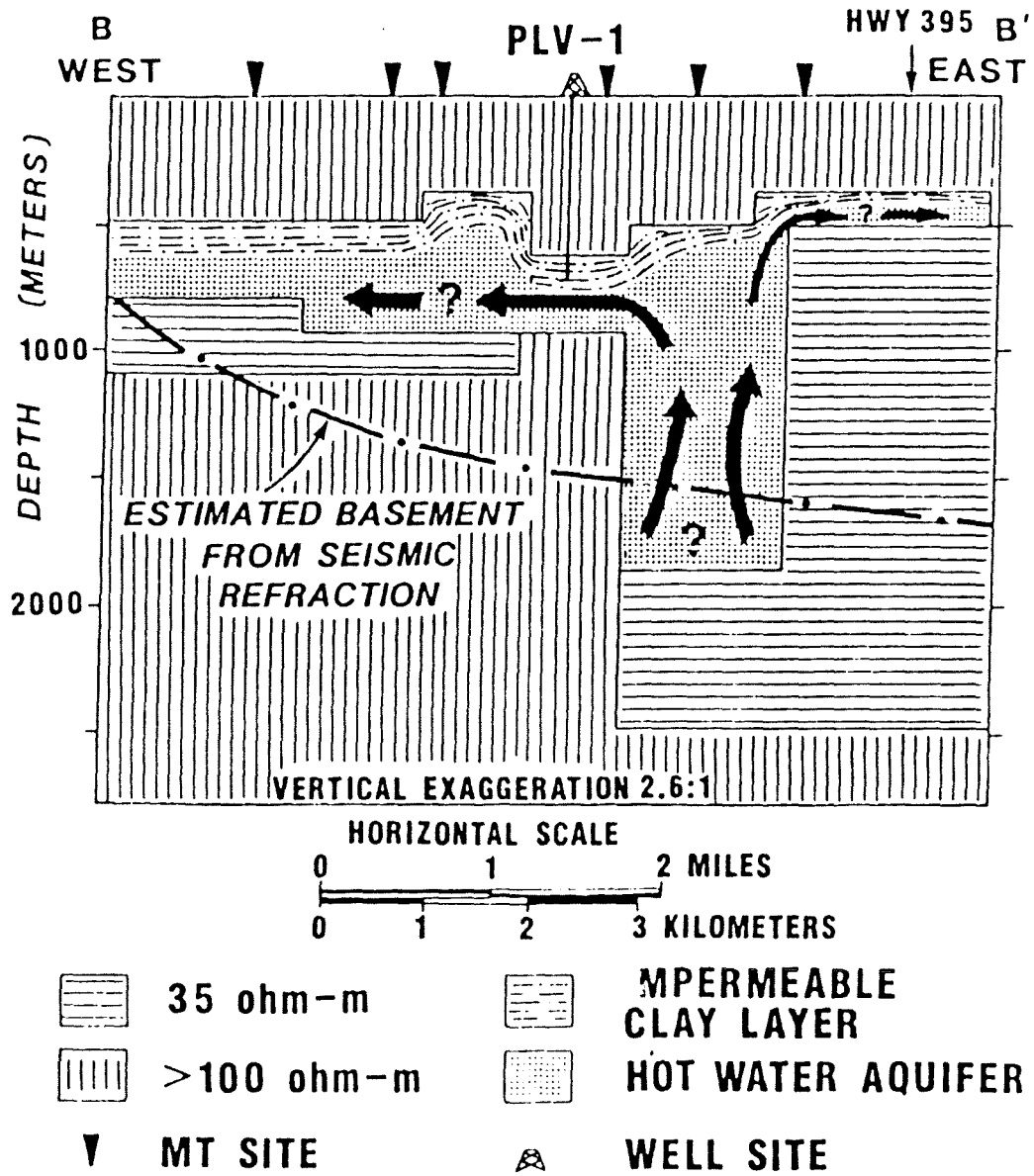
Figure 6   Interpretative model of the Long Valley hydrothermal
            system superimposed on the MT model along B-B'. In this
            model upflow is located within the zone of unusually deep
            low resistivities and act as a source for the aquifer
            observed beneath IDFU 44-16 and inferred beneath PLV-1.
            The aquifer is sealed from the surface by an impermeable
            clay layer.

CONSTRAINTS ON MODELS OF STRUCTURE AND HYDROTHERMAL

CIRCULATION IN LONG VALLEY CALDERA, CALIFORNIA

by

GENE A. SUEMNICHT
Unocal Geothermal Division
P.O. Box 6584
Santa Rosa, CA 95496

ROBERT J. VARGA
Unocal Science and Technology Division
P.O. Box 76
Brea, CA 92621

Long Valley caldera has been studied extensively by a number of agencies to evaluate models of caldera magmatism and the caldera's current eruptive potential. The data presented here are part of Unocal's exploration and assessment of the area's geothermal potential. We derive a model for the caldera based on surface mapping, structural and geophysical interpretation, and data from deep wells.

Since 1976 four deep geothermal tests have been drilled within the caldera (Fig. 1). Data from three of those wells was released by 1981. Unocal's most recent deep well, designated IDFU 44-16, was drilled to a depth of 1.8 km in the western moat, approximately 1km from the Inyo Craters. The geologic data from this well are summarized in Figure 2. The rock units in this well are different in both thickness and type from those encountered in wells drilled around the resurgent dome. IDFU 44-16 drilled 915 m of post collapse caldera fill which is at least 450 m more than the two wells on the resurgent dome. The Bishop Tuff is only 250 m thick in this part of the western moat in contrast with 860 to 1085 m encountered on the resurgent dome. Andesites and dacites occur in the lower portion of the well at a depth of 1183 m and calc-silicate metamorphic rocks at a depth of 1615 m. The volcanic rocks yield a radiometric age of 1.98 + 0.1 my and are tentatively correlated with the Tertiary volcanics of San Joaquin Ridge (Bailey and Koeppen, 1977) on the caldera's western wall. The occurrence of pre-caldera volcanics in this well is consistent with a location of the caldera ring fracture system, or pre-caldera faults, as far east as the Inyo Craters.

The temperature regime in IDFU 44-16 is as complex as in the Mammoth 1 well drilled near Casa Diablo. Temperature reversals in the hottest portion of the wellbore are interpreted as lateral outflow of hot water floating over cold, as suggested for other wells drilled near the caldera's margin (Blackwell, 1985). Data from cores cut in the pre-caldera volcanics and calc-silicate metamorphic rocks show the caldera's basement is virtually impermeable. However, temperature data and whole rock stable isotopic analyses show some evidence of hydrothermal circulation in the pre-caldera volcanics. The hottest basement section encountered in the caldera is found in this well despite a temperature reversal at 1.8 km. There is no evidence in the temperature profile for a deep, upwelling hydrothermal system beneath the Bishop Tuff in this part of the western caldera moat. We interpret the deep temperature reversals in IDFU 44-16 as evidence for deep, penetrative fractures in the western caldera and suggest that pre-caldera fractures or the caldera's ring fracture system provide permeable conduits for cold recharge to circulate deep in the impermeable caldera basement.

The stratigraphy of the intra-caldera fill is critical to understanding the structure of the caldera. In IDFU 44-16 the top of the Bishop Tuff occurs at an elevation of 1537 m approximately 200 m deeper than at Casa Diablo. Further, drilling at Shady Rest (Wollenberg and others, 1986; this volume) and detailed TDEM modelling (Nordquist, this volume) confirm at least 400 m of elevation difference in the top of the Bishop Tuff between this well and the western margin of the resurgent dome. Our detailed mapping in the western moat has revealed a complex of NE-trending, transcurrent faults cutting 100,000 yr-old moat rhyolites and forming a structural boundary to a paleohighland in the western moat. The offset of the top of the Bishop Tuff occurs across this fault system which appears to be a major crustal flaw in the western moat.

A schematic cross section summarizes our interpretation of the data from the western moat (Fig. 3). The principal constraints to this cross section are well data, interpreted seismic refraction data (Hill and others, 1985) and 2d gravity interpretations (Nordquist, personal communication, 1987). The offset along the Discovery fault system is evident as is a pattern of block displacements across the caldera. We offer a model (Fig. 4) wherein the NE-trending Discovery system connects the buried extensions of the Hartley Springs and Hilton Creek faults. Together, these faults and possible extensions of the Laurel-Convict fault define a major left-stepping jog in the Sierran escarpment that was captured by collapse of Long Valley caldera. We see little evidence for significant resurgent doming in the caldera. Based on

interpreted geophysical and drilling evidence we suggest that
the general pattern of deformation within the caldera is one of
Basin and Range style block faulting controlled by pre-caldera
faults. These structures apparently control permeability in the
caldera fill and have localized recent eruptive centers in the
western moat.

References

Bailey, R. A. and Koeppen, R. P., 1977, Preliminary Geologic
     Map of Long Valley Caldera, Mono County, CA: USGS Open
     File Map.

Blackwell, D. D., 1984, A Transient Model of The Geothermal
     System of Long Valley Caldera, California: J. Geophys. Res.
     81 n 5.

Hill. D. P., Kissling, E., Luetgert, J. H., and Kradolfer, U.,
     1985, Constraints on the upper crustal structure of the
     Long Valley - Mono Craters volcanic complex, eastern
     California, from seismic refraction measurements: J.
     Geophys. Res., 90 (B13).

Wollenburg, H. A., White, A., Flexser, S., Sorey, M., Farrar,
     C., Bartel, L., 1986, A Core Hole in Southwestern Moat of
     the Long Valley Caldera: Early Returns.   EOS v 67 n 44.
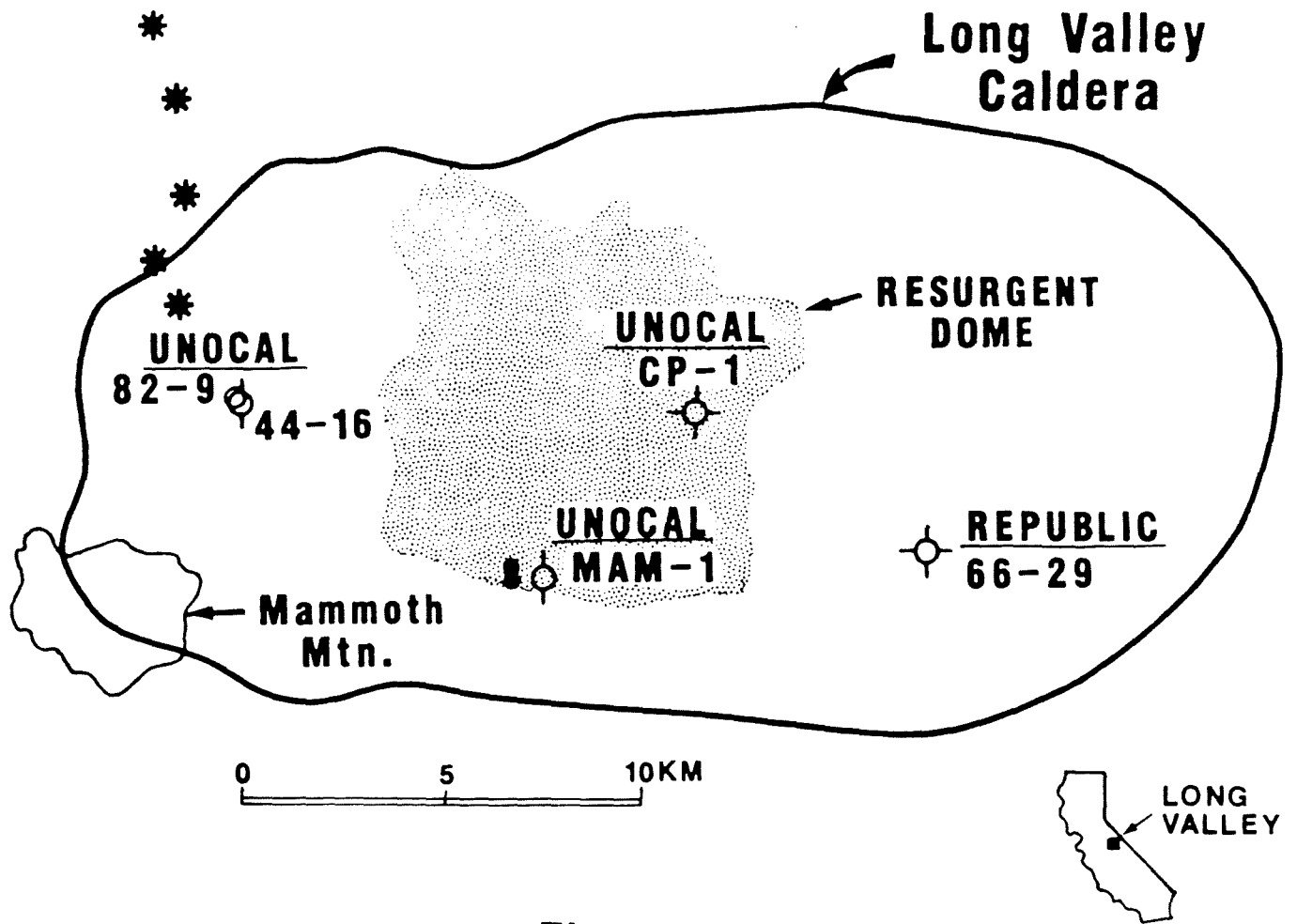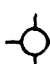
Figure 1

GENERALIZED GEOLOGY OF LONG VALLEY CALDERA

EXPLANATION

⌒ CALDERA BOUNDARY

φ ⌀ DEEP WELLS

✳ RECENT ERUPTIVES

● SHALLOW PRODUCTIVE WELLS

Figure 2

IDFU 44-16

Temperature, °Celsius

Depth, Meters

Moat Basalts

378m

Early Rhyolites & Tuff

915m

Bishop Tuff

1168m

Tertiary Dacites & Andesites

1634m

Metamorphic Basement

TD 1799m
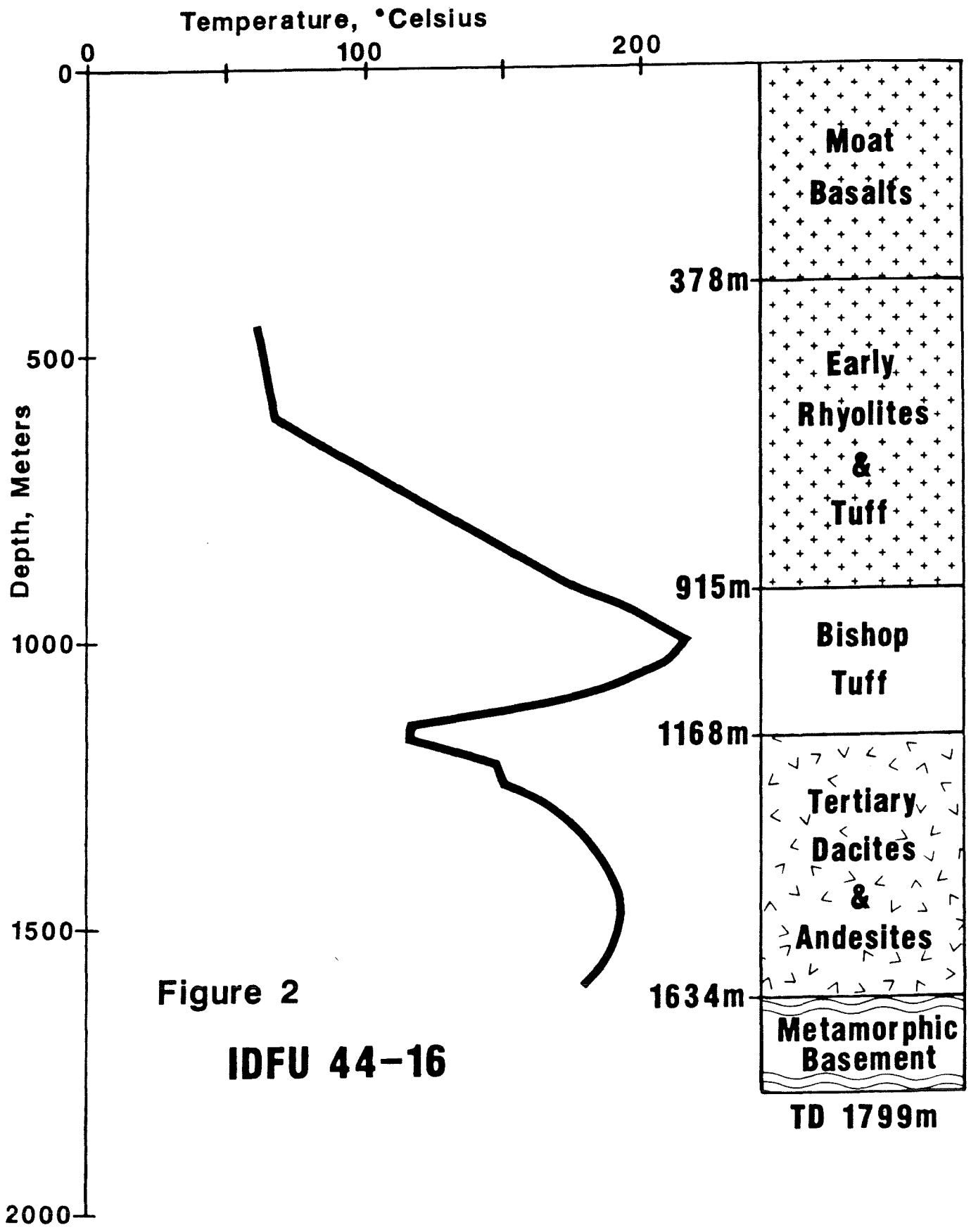
Figure 3. Generalized cross section A-A' through deep wells drilled in Long Valley (based on data through 9-86.)
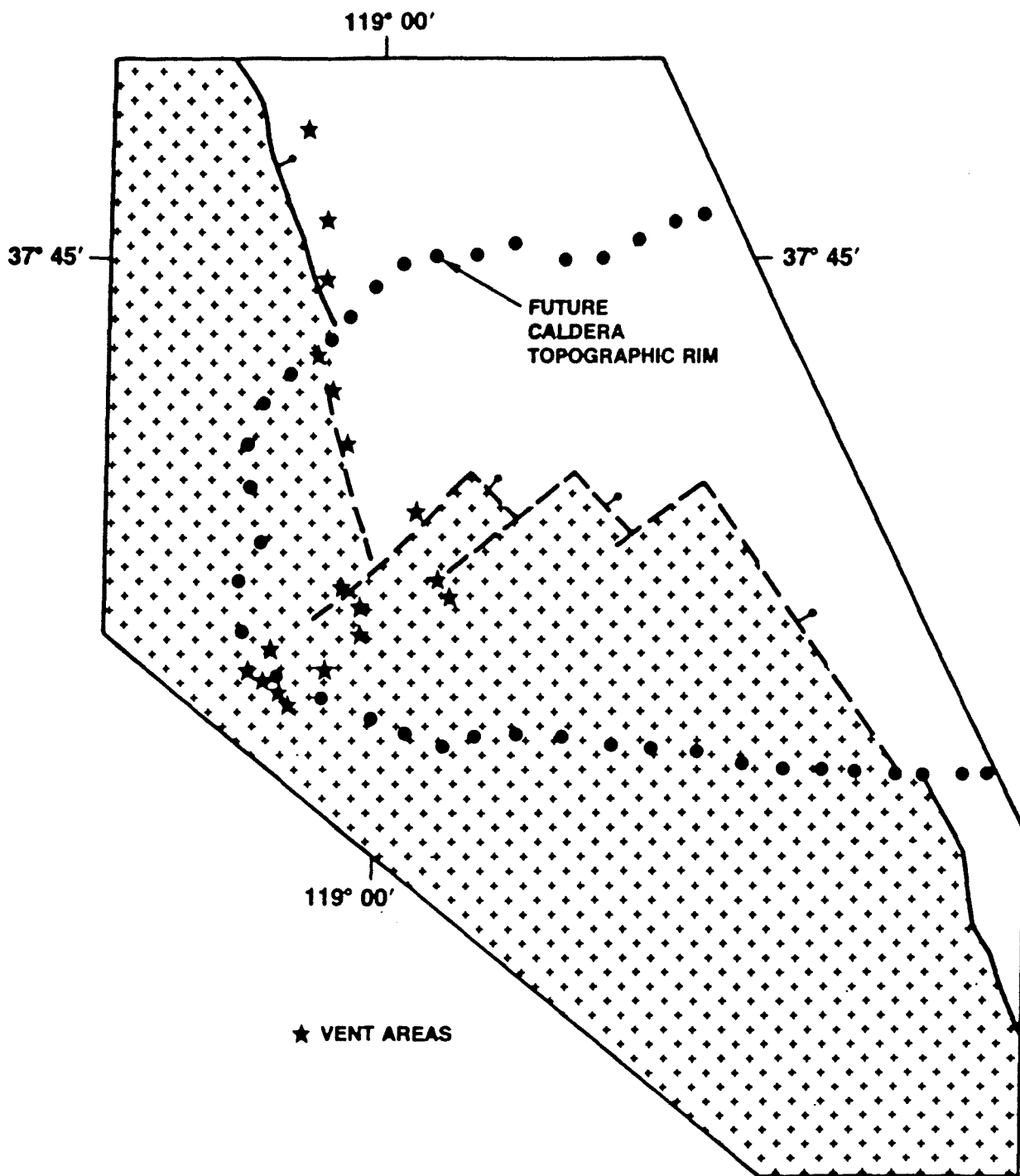
FIGURE 4

HYPOTHETICAL MODEL OF CONFIGURATION OF EASTERN SIERRAN
MARGIN PRIOR TO CALDERA COLLAPSE. NOTE THAT COLLAPSE OF
THE CALDERA "CAPTURES" SOME OF THE SIERRAN TOPOGRAPHY
THAT NOW DEFINES RHYOLITE PLATEAU AND REGION WEST OF
INYO VOLCANIC TREND.

TARGETS FOR FUTURE SCIENTIFIC DRILLING

Michael L.Sorey
U.S. Geological Survey
Menlo Park, California

ABSTRACT

Information presented at the sysmposium by members of the Geology, Geohydrology, and Geochemistry Study Group leads to the conclusion that the roots of the present-day hydrothermal system and its primary heat source lie beneath the caldera's western moat. Particularly significant in this regard are data from Unocal's 44-16 well, DOE's Shady Rest well, and Unocal's studies of geologic structure and electrical geophysics. When combined with hydrologic, geochemical, and thermal data from wells and thermal features in other parts of the caldera, a conceptual model emerges of a source reservoir in Sierran basement rocks from which fluid at temperatures of 220-230 C flows upward along fault conduits and then moves laterally through volcanic rocks filling the western moat. Several intersecting fault systems could control the locations of zones of upflow and directions of lateral flow of thermal water. Favorable indications of magmatic heat sources in this region are provided by seismic refraction and teleseismic studies, regional heat flow measurements, and the occurrence of surficial hydrothermal features on the flanks of Mammoth Mountain.

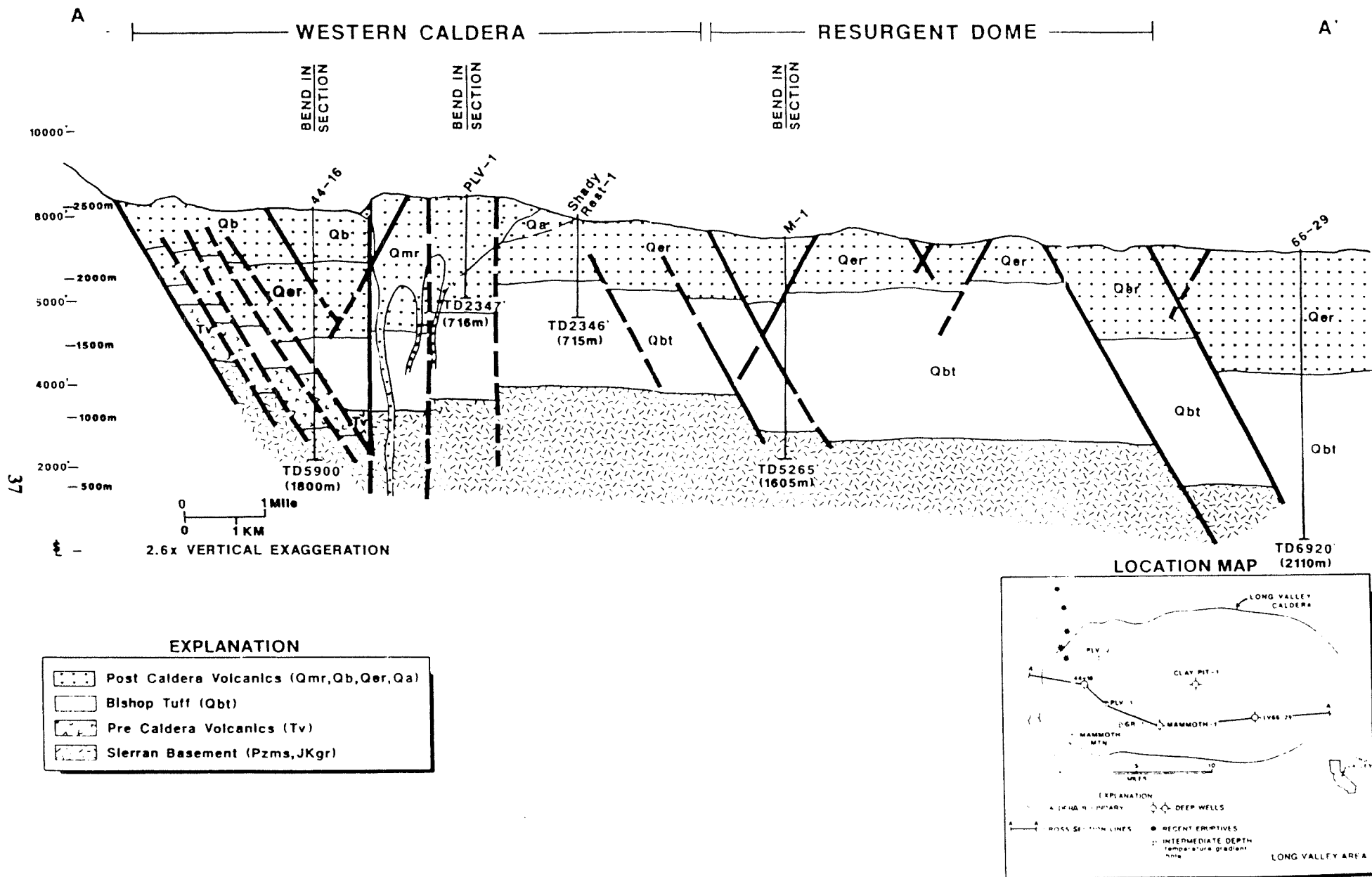The results from the two recent drill holes in the west moat provide useful stratigraphic and lithologic information and evidence of high temperature reservoirs in the Bishop Tuff and adjacent formations. However, the measured temperature profiles in these wells suggest that neither drill site is situated above the principal zone of thermal fluid upflow. Additional scientific drilling in this region is needed to adequately delineate the hydrothermal system and its heat source. Such drilling could also elucidate the magnitude of displacements on the various fault systems crossing the west moat. Three target areas are considered favorable for these purposes (c.f. Sorey and others, 1987, and figure 1).

Target area (1) is near the existing Shady Rest drill site, where projected temperatures within the 1,000-ft section of Bishop Tuff penetrated by the core hole are near 200 C and show little evidence of cooling with depth. This suggests that a zone of upflow of hotter water may exist nearby. Alternatively, a high conductive gradient may occur at depths below 2,400 feet at this site, indicative of a shallow magmatic heat source. Completion of a second well in this vicinity that reaches Sierran basement would allow these possibilites to be investigated.

Target area (2) is on the northern flank of Mammoth Mountain, near the base of Chair 21 and the road to Mineret Summit. This site is within the area of intersection of extensional faults of the Inyo volcanic chain, the caldera ring frac-

ture, and Unocal's postulated northeast-trending Discovery fault system. Although a drill hole in this area may be outside the ring fracture and would involve approximately 600 to 1,000 feet of elevation penalty relative to the other two sites, it could provide indications of a magmatic heat source and thermal fluid upflow beneath Mammoth Mountain. Drilling in this target area would also permit evaluation of the possibility that water in the 218 C reservoir encountered in well 44-16 actually flows northward from Mammoth Mountain to the Inyo Craters area rather than eastward from an upflow zone associated with the ring fracture.

Target area (3) is on the rhyolite plateau formed by the 100,000-year old moat rhyolite in the area between wells 44-16 and SR. As discussed by Suemnicht and Varga (this volume) and Nordquist (this volume), favorable indications for drilling on the rhyolite plateau include a pronounced and apparantly deep-rooted resistivity low, and intersections of the Discovery fault zone with pre-caldera basement faults aligned with the Hartly Springs and Laurel-Convict faults and with northwest-trending faults along the western side of the resurgent dome. In addition, the high temperature gradient in the lower section of well PLV-1 (fig.1), drilled by Phillips Petroleum to a depth of 2340 feet (Benoit, 1984), indicates that a high-temperature reservoir may exist beneath this area. Core drilling in target area (3) could also provide useful stratigraphic control on pre-caldera basement topography and post-caldera fault displacements

It is anticipated that core drilling to depths of about 6,000 feet would be required to meet the stated objectives. Ideally, drill-hole information from each of the target areas combined with other sources of data would yield a reasonably complete picture of the present-day hydrothermal system and its magmatic heat source. Toward this end a detailed drilling proposal should be prepared that would set priorities for drilling in different areas and summarize results from previous drilling in the western moat.

REFERENCES

Benoit, W.R., 1984, Initial results from drillholes PLV-1 and PLV-2 in the western moat of the Long Valley caldera: Geothermal Resources Council TRANSACTIONS, v. 8, p. 397-402.

Sorey, M.L., Farrar, C.D., and Wollenberg, H.A., eds., 1986, Proceedings of the second workshop on hydrologic and geochemical monitoring in the Long Valley caldera: Lawrence Berkeley Laboratory Report LBL-22852.
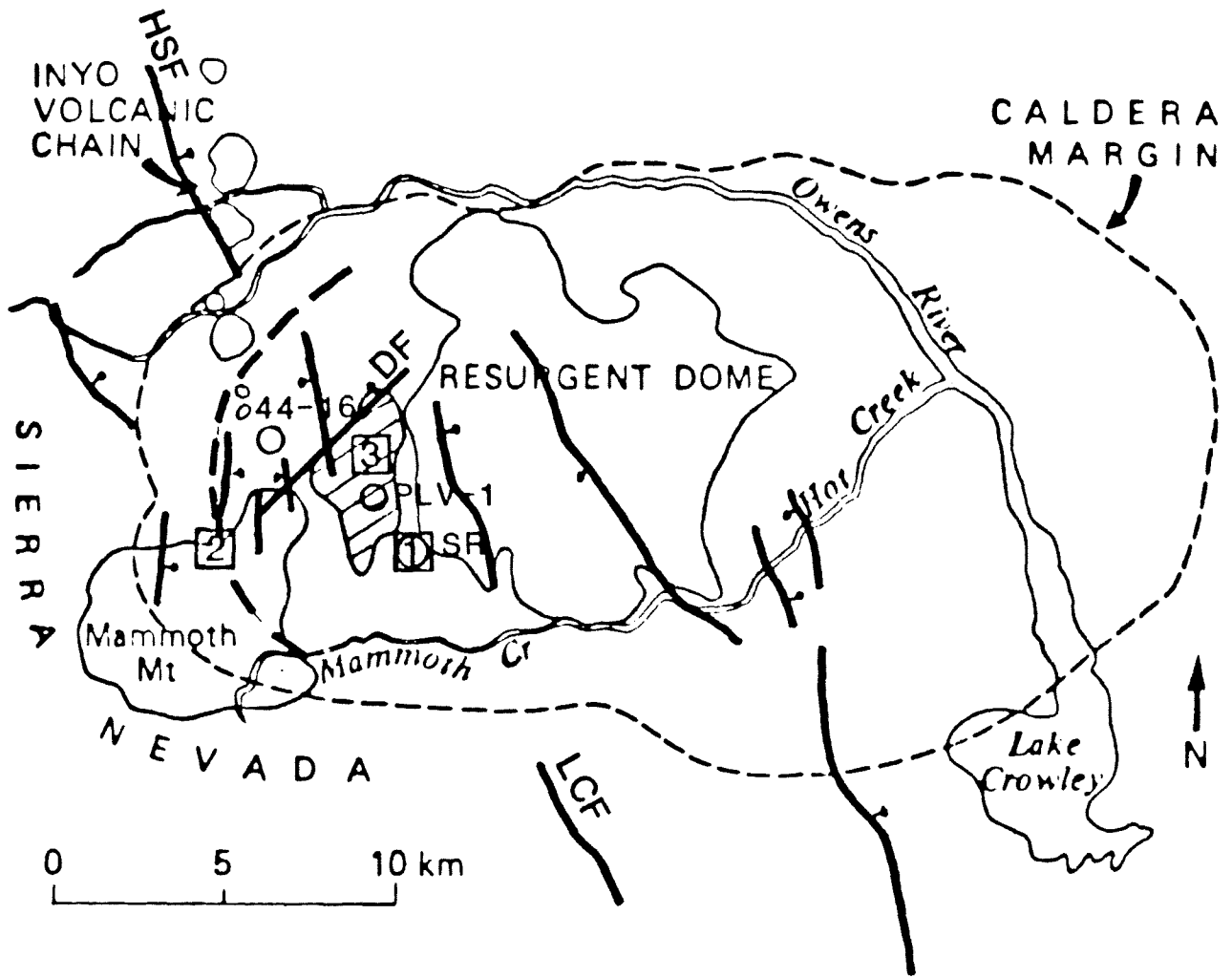
Figure 1. Target areas 1-3 for future scientific drilling in the west moat
of Long Valley caldera. Open circles with labels denote drill
hole locations referred to in text; principal faults shown with
bar and ball on downthrown side - HSF = Hartley Springs Fault,
LCF = Laurel Convict Fault, DF = Discovery Fault (postulated).
100,000 year-old moat rhyolite shown by crosshatched pattern.
Possible position of caldera ring fracture at the edge of the
west moat shown by heavy dashed line.

Seismological Studies

UPPER CRUSTAL STRUCTURE AND SEISMICITY IN LONG VALLEY CALDERA AND VICINITY

by

David P. Hill, Edy Kissling*, Urs Kradolfer*,
and Robert S. Cockerham

U.S. Geological Survey, Menlo Park CA
*Institut fur Geophysik, ETH, Zurich, Switzerland

STRUCTURE

We have completed an interpretation of the seismic refraction profiles shot in 1982-1983 across Long Valley caldera and the Inyo-Mono craters region (Figure 1) and used the resulting velocity structure to develop a three-dimensional density model of the caldera consistent with the observed gravity field. Combined, these velocity-density models further improve our image of the distinctly three-dimensional structure of the caldera and the upper 5 to 6 km of the surrounding crust.

Hill et al. (1985) presented an interpretation of the four refraction profiles that span the Inyo-Mono craters region and the western part of the caldera. Figures 2 summarizes our interpretation of the remaining two profiles in terms of major rock units. The upper section represents the northeast-trending profile that crosses the caldera from Mammoth Lakes through Casa Diablo to Glass Mountain and beyond; the lower section represents the east-trending profile that parallels the southern margin of the caldera (see Figure 1). The relation between major rock units and P-wave velocities is the same as that used in Hill et al. (1985). In particular:

    1.2-1.8 km/s: sediments, pumice, & brecciated flows
    2.8-3.2 km/s: buried lava flows and non-welded tuff
    3.9-4.4 km/s: welded Bishop tuff
    4.9-5.6 km/s: crystalline basement beneath caldera fill
    3.0-5.6 km/s: crystalline basement outside the caldera
                  (velocity gradients reflect crack closure
                  with depth)

Both profiles re-enforce gross structural relations within the caldera found by Hill et al. (1985); the caldera fill is roughly 2 km thick with the welded Bishop tuff forming the lower half of the fill. The two profiles in Figure 2 emphasize that the depth to crystalline basement generally increases eastward and northward within the caldera. It appears, in particular, that the greatest subsidence of the crystalline basement may have occurred along the northern and eastern sections of the ring fracture system, although we cannot rule out the possibility that much of this relative depression in the crystalline basement beneath the moat along the eastern and northern margins of the caldera predates caldera collapse. The step-like increase in basement depth just east of the resurgent dome (distance = 23 km) in the lower section of Figure 2 is on trend with the Hilton Creek fault, and the nearly flat surface of the overlying Bishop tuff suggests little

43

if any vertical offset along the extension of the Hilton Creek fault within the caldera since the caldera-forming eruption 700,000 years ago.

Figure 3 shows the complete Bouguer gravity field over Long Valley caldera and vicinity compiled from Pakiser (1961), Kane et al. (1976), and Oliver and Robbins (1978). The lower section of Figure 3 shows the residual anomaly associated with the caldera obtained by subtracting a plane through the regional trend of the complete Bouguer field. Using the velocity-density relation developed for the caldera fill by Abers (1985), the two-dimensional velocity structure developed for the seismic-refraction profiles in Figure 1, and a forward, three-dimensional modeling technique developed by Kissling (1980), we developed the three-dimensional density model of the caldera illustrated in Figures 4, 5, 6, and 7. Figure 4 shows the gravitational contribution of the topography above the arbitrary elevation of 2057 m above sea level assuming the resurgent dome and Mammoth Mountain have a density of 2.37 g/cm^3 and the sedimentary fill of the eastern caldera has a density of 1.90 g/cm^3. Figure 5 shows the elevation the upper surface of the welded Bishop tuff (upper diagram) and the contribution of the caldera fill above this surface to the gravity field (lower diagram). Figure 6 shows the elevation of the crystalline basement (upper diagram) and the contribution of the welded Bishop tuff to the gravity field (lower diagram). The density with the welded Bishop tuff in this model increases with depth from 2.27 to 2.47 g/cm^3. The total contribution of the caldera fill to the gravity field is shown in the upper two diagrams in Figure 7, and the difference between this computed field and the observed, residual field (lower diagram of Figure 4) is shown in the lower two diagrams. The undulations in this difference field over the caldera are less than 5 milligals and thus less than the undulation in the observed field over the crystalline basement away from the caldera.

The following aspects of the density model are noteworthy:

1) The topographic expression of the resurgent dome is not simply reflected in the subsurface elevation of either the upper surface of the welded Bishop tuff or the crystalline basement.
2) A ridge in the crystalline basement extending northward from the southern margin of the caldera separates pronounced depressions in the southeastern and northwestern sections of the caldera. The eastern, more sharply defined margin of this ridge is in line with the northward extension of the Hilton Creek fault into the caldera.
3) Density structure of the caldera fill accounts for most of the the observed low in the local gravity field over Long Valley caldera; the gravity data thus do not require the presence of a large, low-density magma chamber at shallow depths within the crystalline basement beneath the caldera.
4) A regional, trough-like low in the residual gravity field (bottom diagram in Figures 4 and 7) roughly coincides with the topographic low along the base of the Sierra Nevada escarpment. Although we have not modeled this low, we suspect that it

reflects, at least in part, a density difference between the relatively resistant, unfractured crystalline basement beneath the uplands and a more highly fractured basement beneath the lowland along the base of the escarpment. Because this trough also coincides with the axis of the Long Valley caldera-Inyo-Mono craters volcanic system, however, the possibility also remains that it may reflect a distributed magmatic system within the underlying upper crust.

SEISMICITY

Major episodes of earthquake activity in the Long Valley region have occurred at roughly 18 month intervals beginning with the M=5.8 event beneath Wheeler Crest on October 4, 1978 (Savage and Cockerham, 1987). The largest and most recent of these major episodes involved the M=6.4 Chalfant Valley earthquake of July 21, 1986. With the exception of the September 1981 M=5.5 event in the Sierra Nevada block south of the caldera, each of these episodes has occurred in a different location defining a broad, irregular swath of seismicity south and east of the caldera (see Figure 8). These earthquake sequences are dominated by strike-slip focal mechanisms along fault planes that, for the most part, show no correlation to the major range-bounding normal faults in the region. The 1986 Chalfant event is an exception in this regard; it appears to have involved slip on the west-dipping White Mountains frontal fault. Even in this case, however, the slip was dominantly strike-slip (right-lateral) with only a small normal component along a fault plane that is associated with one of the highest and steepest range fronts in the Basin and Range province (see Cockerham and Corbett, 1987).

Earthquake activity within Long Valley caldera has gradually decreased since the elevated 1980-1983 level, which included one of the four M=6 events of May 25-27, 1980, a recurring series of M=4 south-moat swarms from 1981 through 1982, and the intense south-moat swarm of January 1983. Intracaldera seismicity is confined almost entirely to the south moat extending from Mammoth Mountain on the west to the point where the Hilton Creek fault enters the caldera on the east, although several small swarms occurred beneath the eastern margin of the resurgent dome in 1981 and again in 1986. Maximum focal depths of earthquakes within the caldera are 7 to 8 km in contrast to maximum depths of 15 to 18 km in the Sierran block south of the caldera. Focal mechanism of south moat earthquakes are dominantly strike-slip with T-axes showing a NE-SW orientation. Clusters of small (M<3) earthquakes began occurring around the base of Mammoth Mountain in 1982 and have subsequently defined a doughnut pattern that surrounds the mountain. These earthquakes are limited to depths less than 5 km and have predominantly normal slip focal mechanism with the T-axes oriented in an E-W direction. A number of these Mammoth Mountain clusters have occurred as rapid-fire sequences of small (M<2) events all of comparable magnitude. The durations of such sequences varies from between 5 minutes to as long as 20 minutes.

REFERENCES

Abers, G., 1985, The subsurface structure of Long Valley caldera, Mono County, California: a preliminary synthesis of gravity, seismic, and drilling information, J. Geophys. Res., v.90, pp.3627-3648.

Cockerham, R.S. and E.J. Corbett, 1987, The July 1986 Chalfant Valley, California, earthquake sequence: preliminary results, Bull. Seismol. Soc. Am., v.77, pp. 280-289.

Hill, D.P., E. Kissling, J.H. Luetgert, and U. Kradolfer, 1985, Constraints on the upper crustal structure of the Long Valley-Mono Craters volcanic complex, eastern California, from seismic refraction measurements, J. Geophys. Res., v.90, pp. 11,135-11,150.

Kane, M.F., Mabey, D.R., and Brace, R.L., 1976, A gravity and magnetic investigation of Long Valley caldera, Mono County, California, J. Geophys. Res., v.81, pp.754-762.

Kissling, E., 1980, Krustenaufbau and Isostasie in der Schweiz, PhD Thesis, ETH Zurich, Switzerland, 165 p.

Oliver, H.W., and S.L. Robbins, 1978, Bouguer gravity map of California, Mariposa Sheet, Calif. Div. Mines and Geology, Sacramento CA.

Pakiser, L.C., 1961, Gravity, volcanism, and crustal deformation in Long Valley, California, U.S. Geol. Surv. Prof. Pap. 424B, pp. B250-B253.

Savage, J.C. and R.S. Cockerham, 1987, Quasiperiodic occurrence of earthquakes in the 1978-1986 Bishop-Mammoth Lakes sequence, eastern California, Bull. Seismol. Soc. Am. (in press).
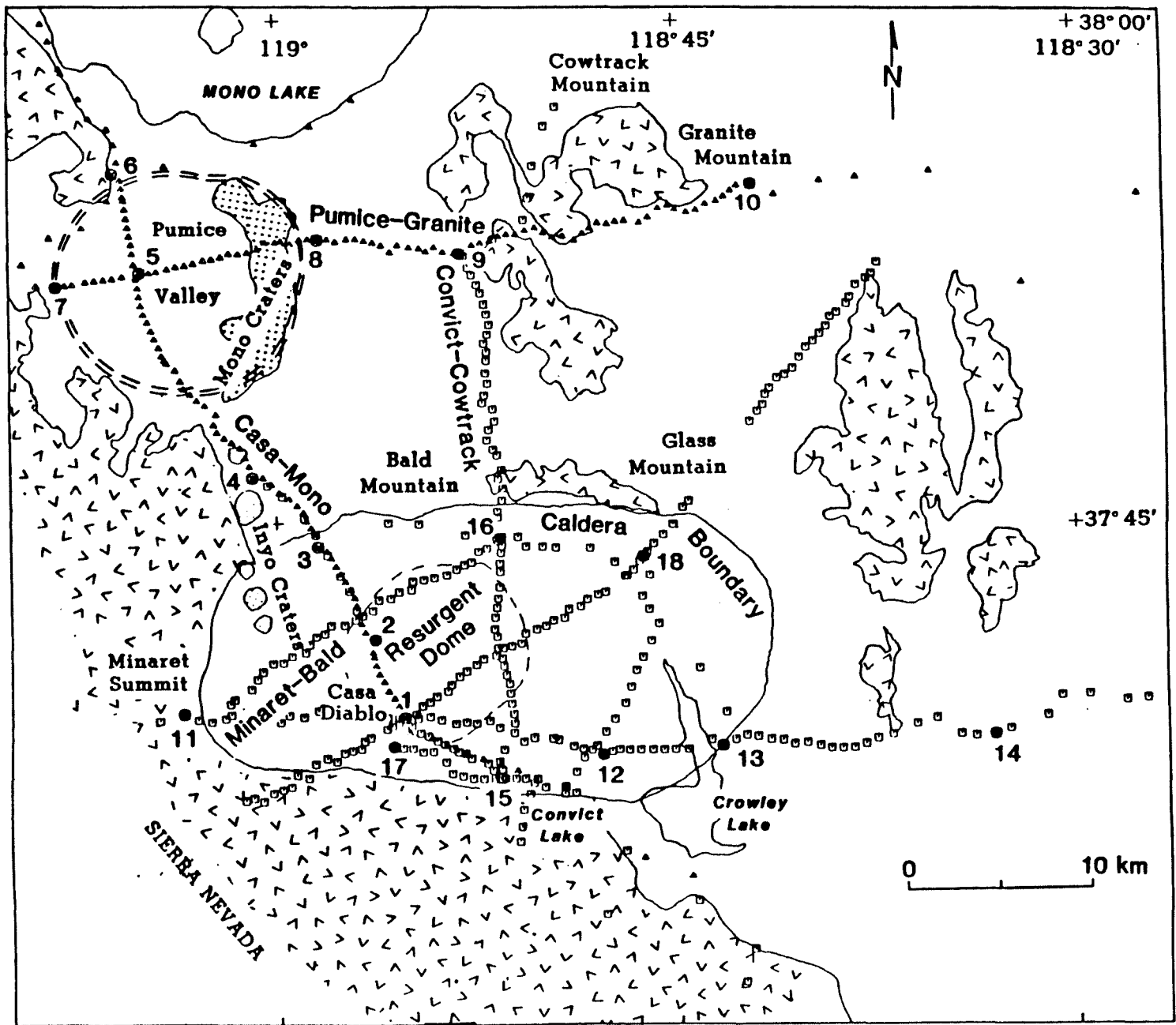
Figure 1. Map showing seismic refraction profiles shot in the
Long Valley caldera region of eastern California in 1982 and
1983. Triangles = recording sites in 1982; squares =
recording sites in 1983. Numbered circles are shot points.
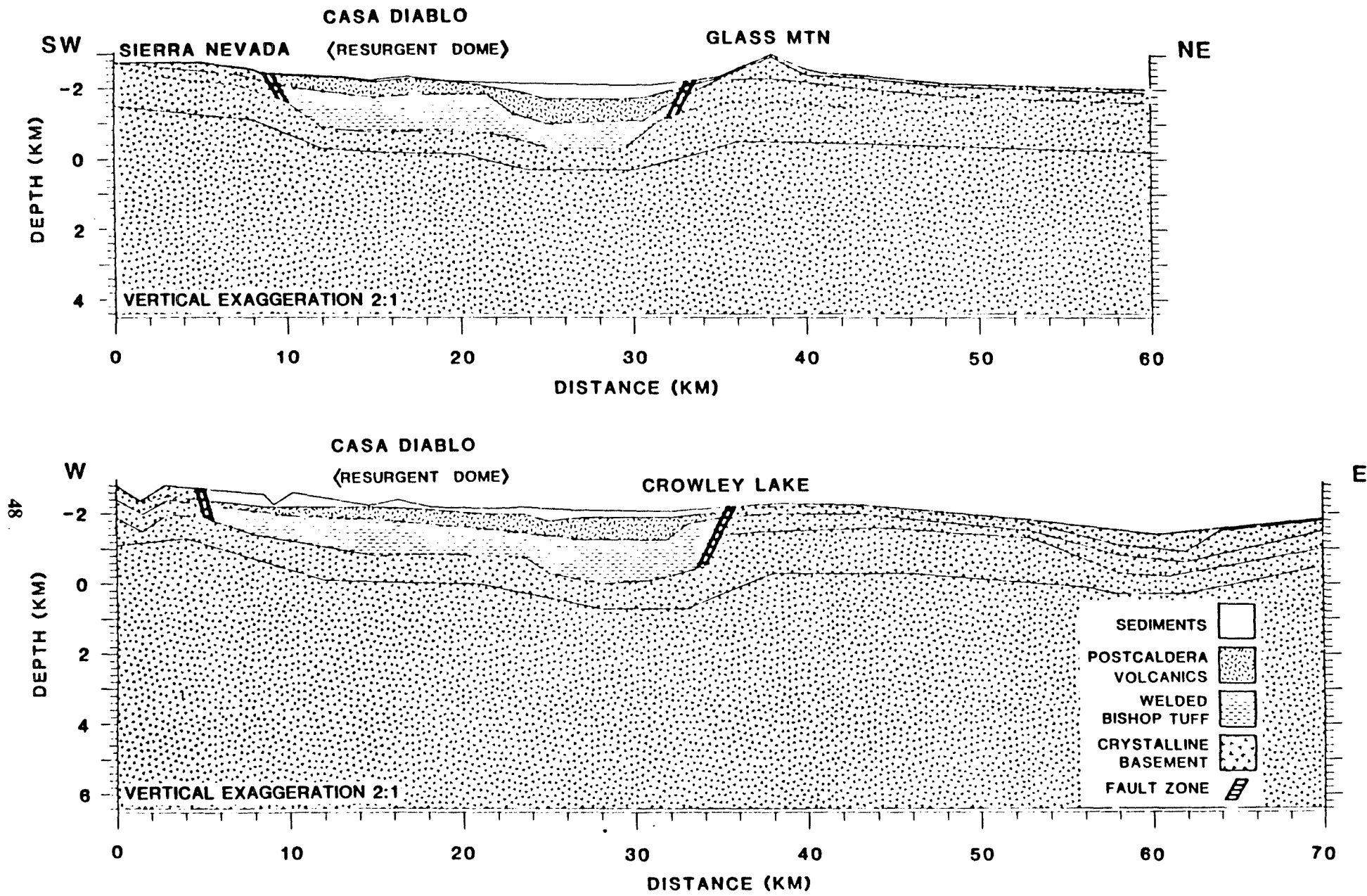
Figure 2. Interperative cross-sections for the NE-SE profile that
includes shotpoints 1 and 18 (top) and the E-W profile
between shotpoints 11 and 14 (bottom).
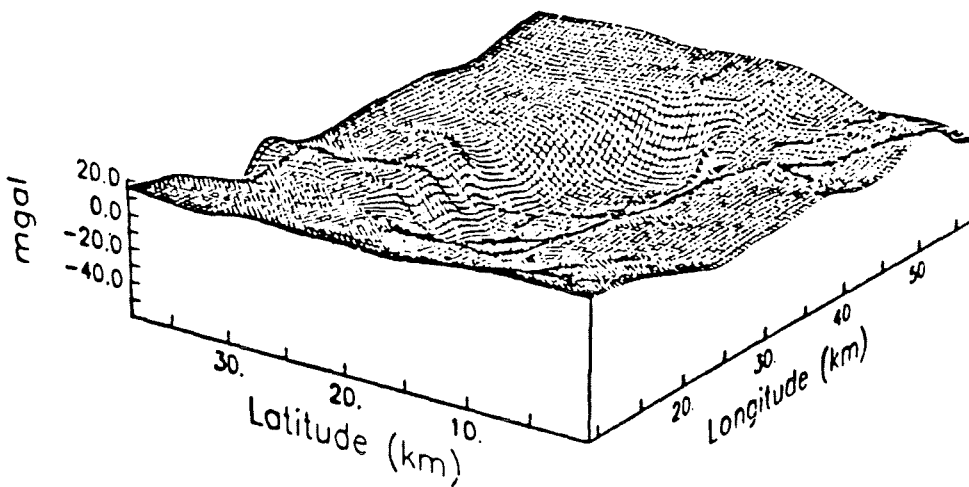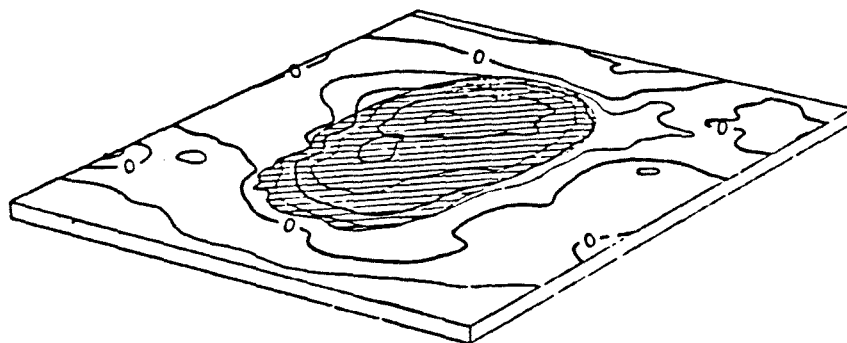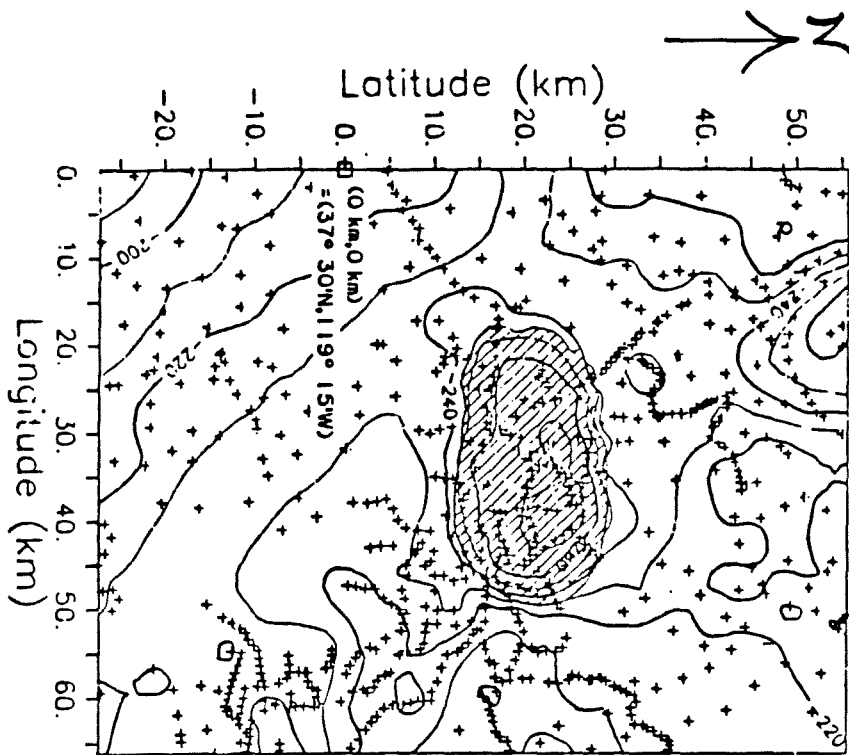
Figure 3. Bouguer gravity field over Long Valley caldera and vicinity (top). Residual gravity field after removing a plane through the regional trend (middle and bottom).

49
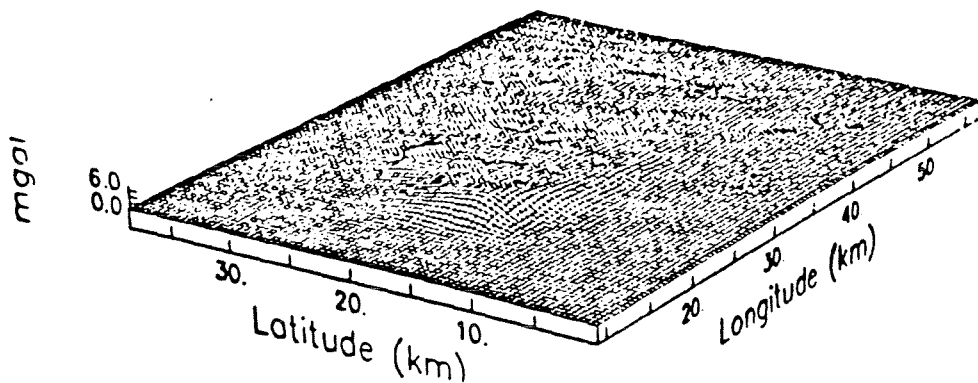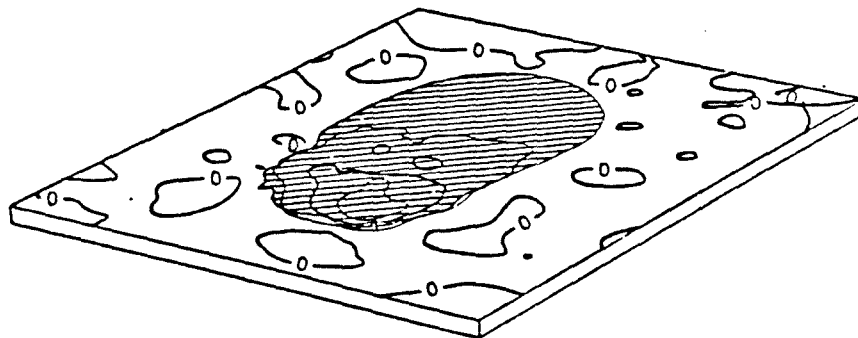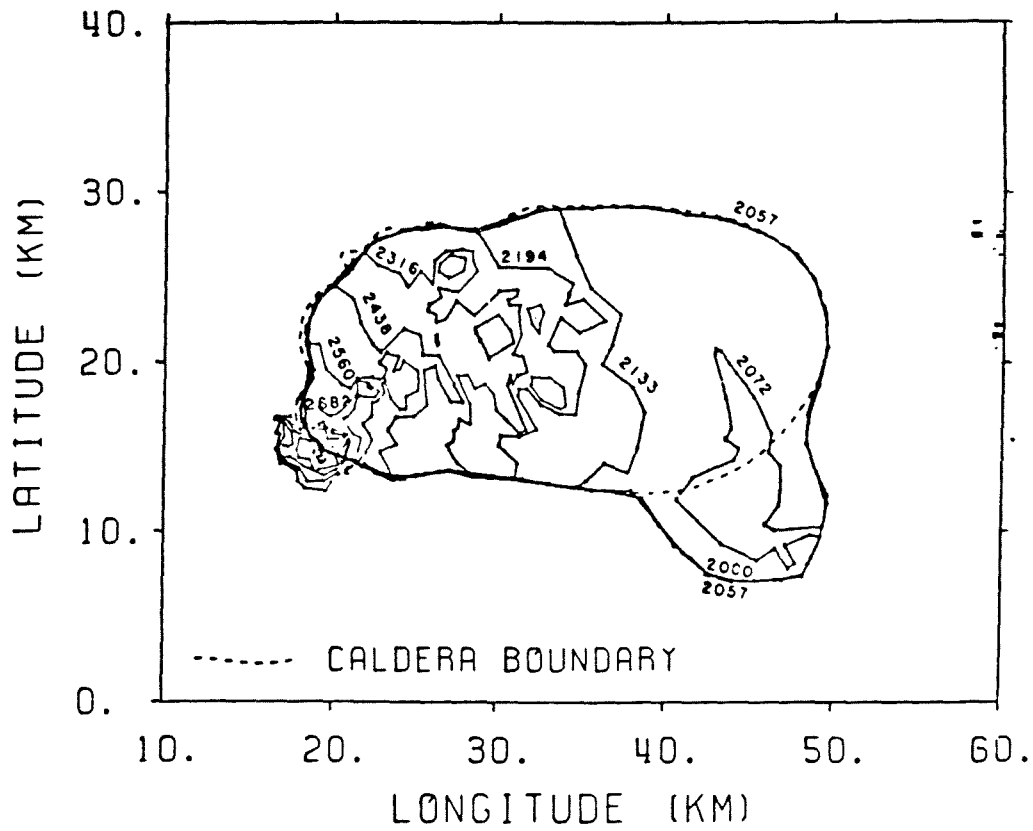
Figure 4. Topographic elevation within the caldera (top).
    Computed contribution to the gravity field from the
    topography above 2057 m (middle and bottom).
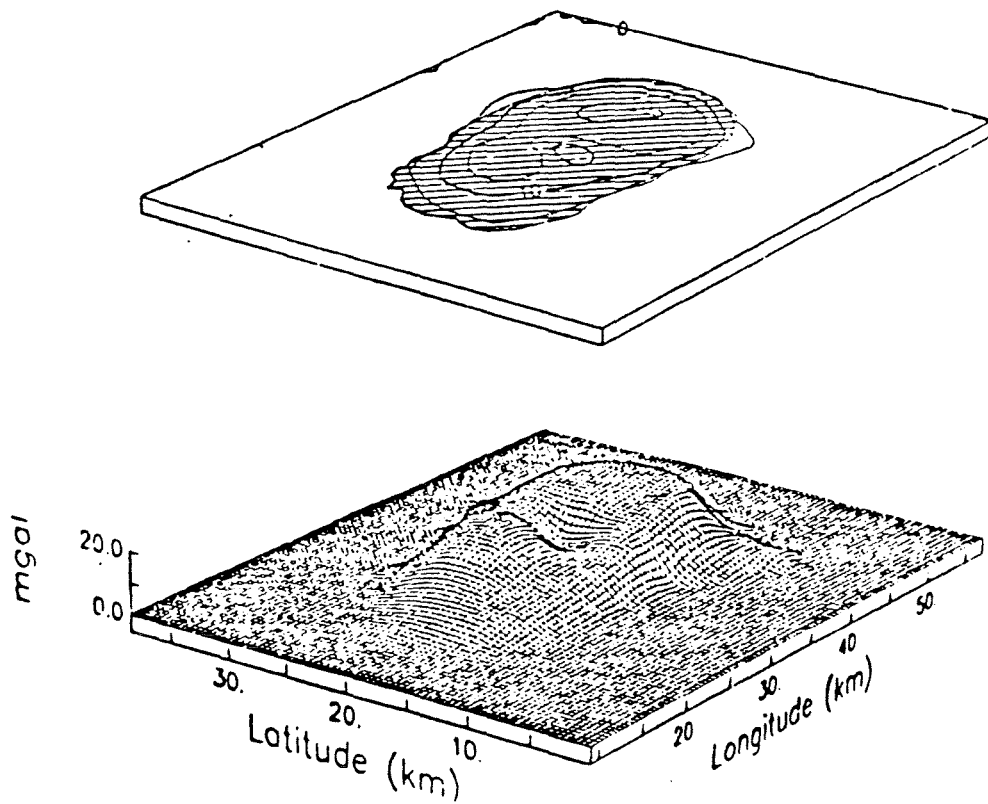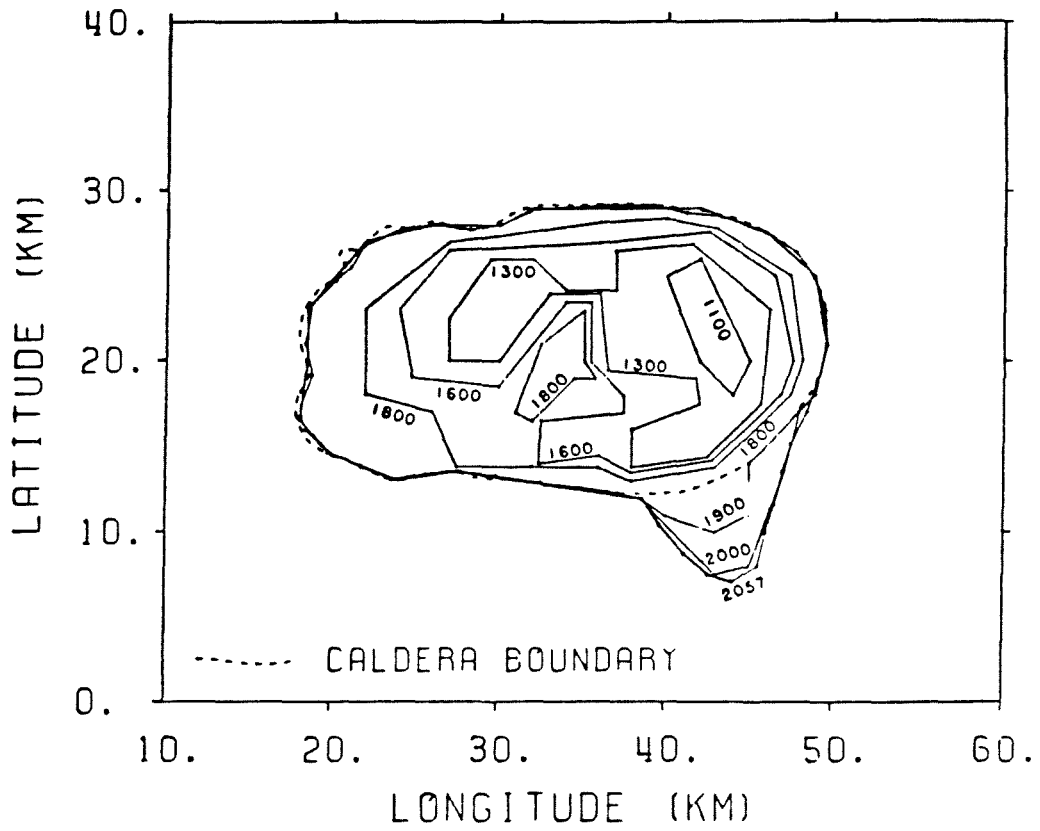
Figure 5. Elevation to the upper surface of the welded Bishop
   tuff (top). Contribution to the gravity field from the
   caldera fill (post-caldera volcanics and sediments) between
   2057 m and the top of the Bishop tuff (middle and bottom).

51
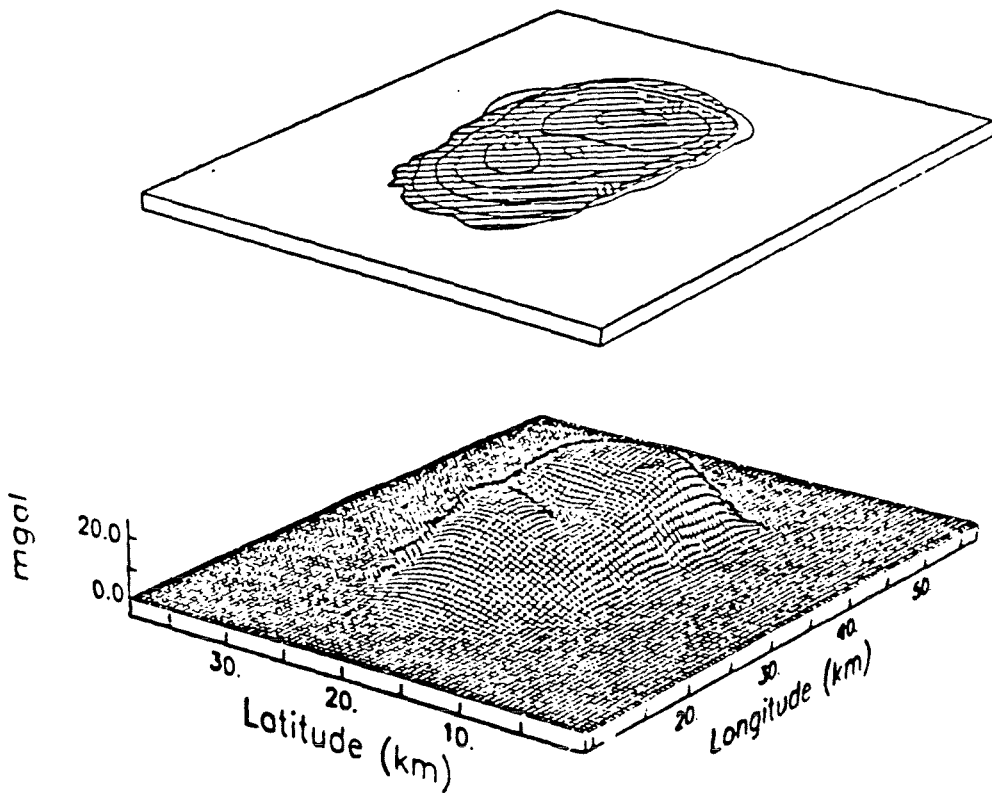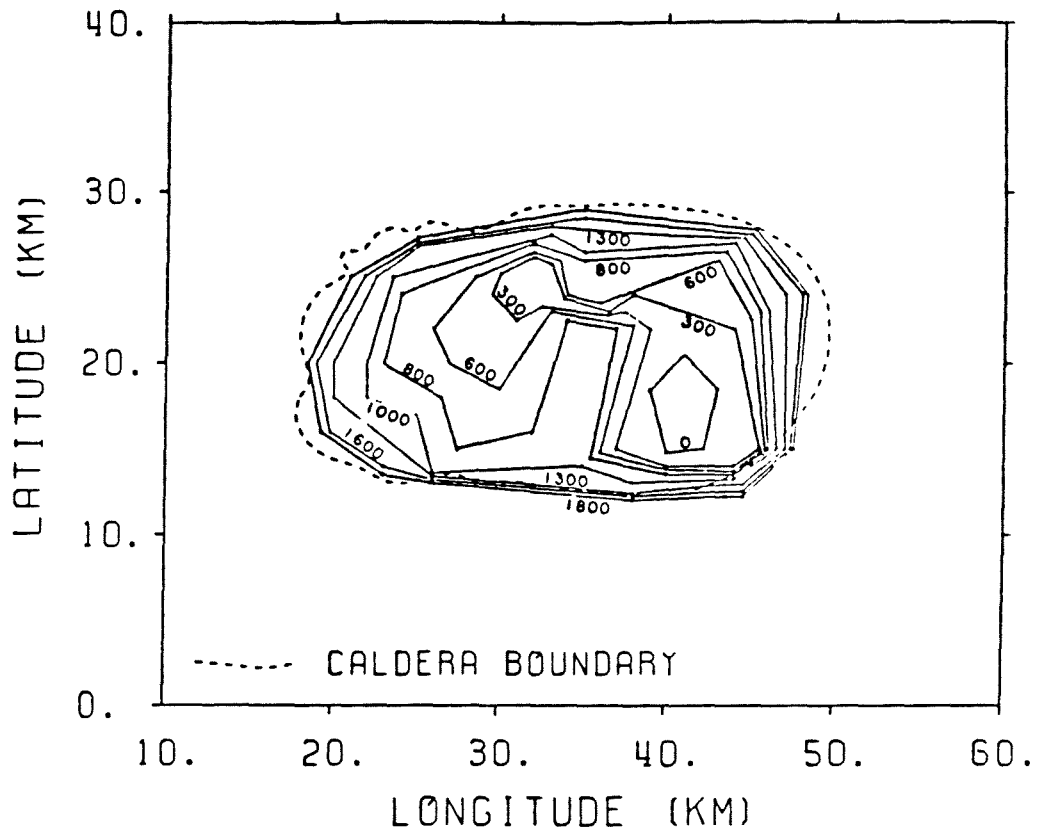
Figure 6. Elevation of the surface of the crystalline basement beneath the caldera (top). Contibution to the gravity field from the welded Bishop tuff (middle and bottom).
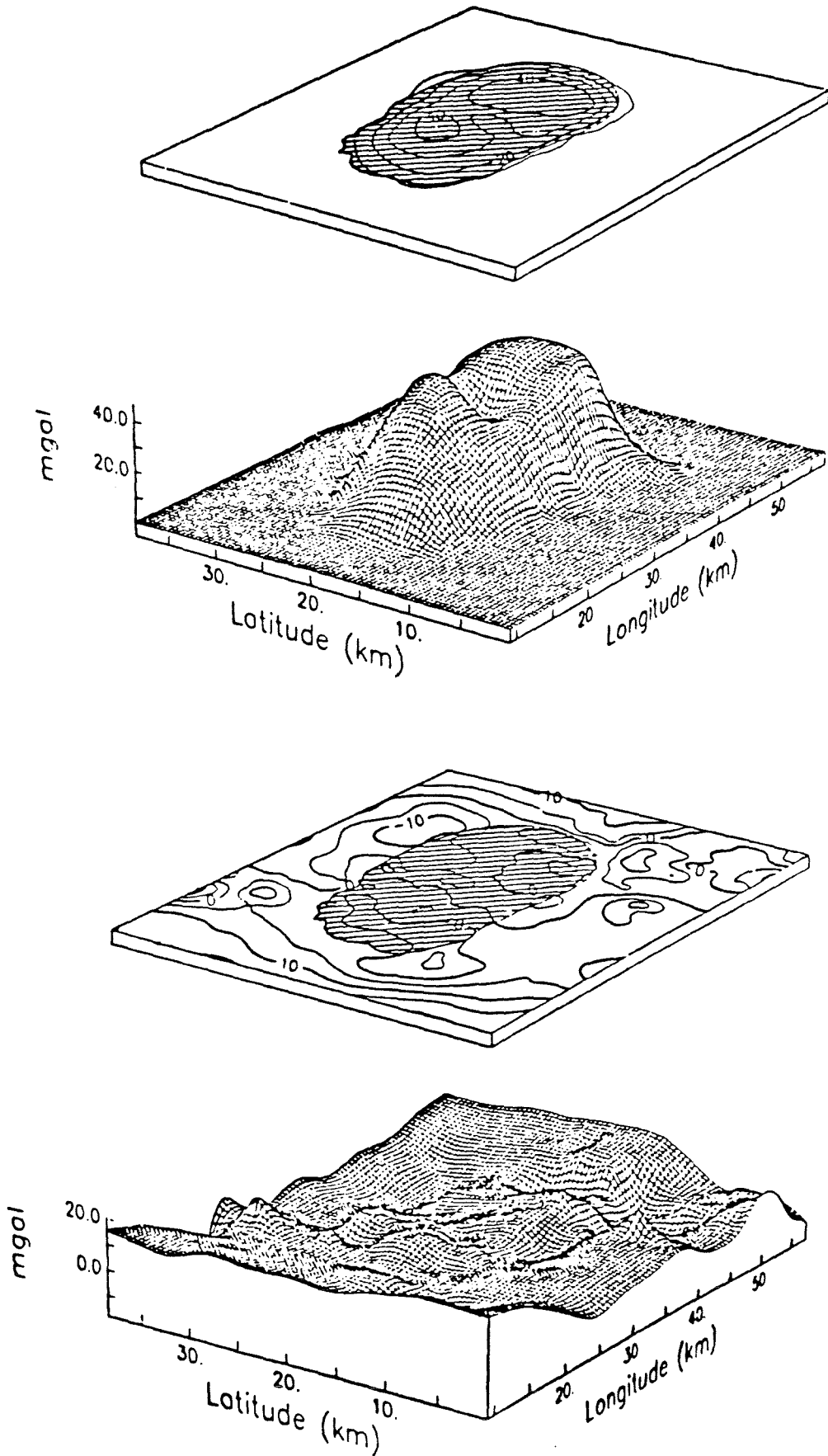
Figure 7. Total contribution of the caldera fill to the gravity
field for the model illustrated in Figures 3, 4, and 5
(upper two diagrams). Difference between computed (above)
and observed (Figure 3, bottom) gravity fields.

STRUCTURE OF THE CRUST AND UPPER MANTLE IN THE LONG VALLEY, CALIFORNIA REGION AS DETERMINED FROM TELESEISMIC TRAVEL TIME RESIDUALS

P.B. Dawson, H.M. Iyer, and J.R. Evans
United States Geological Survey
Menlo Park, California

Long Valley, California has been the site of extensive volcanism over the last 3.0 m.y. Several past geophysical studies (Hill (1976), Steeples and Iyer (1976), and Sanders and Ryall (1983)) and ongoing studies leave little doubt that a substantial volume of magma is present beneath the resurgent dome in Long Valley Caldera. Vertical uplift (Savage and Clark, 1982), and earthquake mechanisms (Julian, 1983) suggest that magma has recently been intruded into this low P-velocity zone and possibly into the shallow crust to the south of the resurgent dome. Thermal calculations by Lachenbruch et al. (1976) demonstrate that a continued resupply of heat is required to have maintained a mid-crustal magma chamber since the eruption of the Bishop Tuff. The intensive seismic activity since 1978 in and near Long Valley caldera also suggests ongoing magmatic processes.

The analysis of teleseismic compressional waves has been developed in recent years to the point where it has been used to detect small anomalous velocity bodies in many volcanic areas (Iyer, 1984). The experiment described here is designed to examine the deeper portion of the anomalous region seen by several investigators beneath the resurgent dome of Long Valley caldera. This study is similar to that done by Steeples and Iyer (1976) but is much broader in scope. Steeples and Iyer were limited by a small data set and partial station coverage, but were able to put general limits on the low-velocity anomaly beneath the resurgent dome of Long Valley caldera. With the new data we are able to investigate the position of the postulated current magmatic

system beneath the resurgent dome and to image the upper mantle and lower crust where, presumably, the source of mafic magmas supplying the magmatic system and the zone of interaction between the mafic magmas and crustal rhyolites occurs. The minimum size of resolvable structures is determined by the wavelength of the seismic waves and the spacing of sensors and is about 6 km.

EXPERIMENT

Sixtyone stations with a mean spacing of 6 km in a 45 x 70 km grid centered on the Long Valley caldera were used for this experiment (Figure 1a). Seventyfive teleseismic events have been digitized and timed using correlative methods similar to those of Steeples and Iyer (1976). Theoretical travel times were calculated from the "Preliminary Determinations of Epicenters" bulletin and the Herrin et al. (1968) travel time tables. Absolute residuals then were calculated by subtracting the theoretical travel times from the observed travel time. To isolate the effects of local structure beneath the array, the parts of the residuals from source and path errors and anomalies were removed by calculating relative residuals. Relative residuals are derived by subtracting the weighted mean residual for each event from the residuals of every station for that event. Figure 1a is a map of the mean relative residuals for each station with teleseisms arriving from all azimuths averaged together. These average residuals are independant of azimuth and incidence angle and reflect velocity heterogeneities at shallow depth. This is called the "invariant" part of the residual.

To show the effects of deeper structures, the teleseisms were divided into 3 groups according to ray orientation beneath the array. The invariant part

of the residuals then was subtracted from these ray groups to isolate the effects of deeper structures. The changes in relative residual patterns between these different ray directions are due to anomalous velocity regions at depth beneath the array. The relative residual patterns can be thought of as the shadows of deep objects projected to the surface along "beams" of rays.

The invariant part of the delay pattern (Figure 1a) shows that nearly all of the stations within the caldera are delayed relative to the surrounding stations. These delays are largely due to the several kilometers of Bishop Tuff and low-velocity sediments and flows filling the caldera. The invariant part of the residuals has been subtracted from the ray groups in Figures 1b-d so that the affects of this caldera fill and other shallow structure is removed. The remaining part reveals a deeper low-velocity anomaly beneath the resurgent dome as seen from the shifting of the delayed pattern with event azimuth. In Figures 1b-d a small region of delays is seen on the opposite side of the resurgent dome from the source events. The observed delays are about 0.2 seconds.

This migrating pattern of delays is a classic pattern and can be explained by a small mid-crustal low-velocity region beneath the western portion of the resurgent dome. The horizontal dimensions of this pattern are about 5 to 8 km. The depth to the center of this feature can be estimated at 11 km from the distances the pattern moves, and it is centered just west of the resurgent dome. A similar pattern is observed around the Mono Craters and has been imaged in a seperate study (Achauer et al. 1986) as a mid-crustal magma chamber centered beneath the southern portion of Mono Craters.

SIMULTANEOUS INVERSION OF THE MONO CRATERS AND

LONG VALLEY TELESEISMIC DATA

The travel time residuals derived from this experiment were combined with the data from the Mono Craters experiment and inverted using the method of Aki et al. (1977). This method is described in detail by Aki et al. (1977), Ellsworth (1977), and Iyer et al. (1981). The region below the seismic array is parameterized by dividing it into plane layers and dividing each layer in a grid of rectangular blocks. Block sizes are governed by the station spacing and the wavelength of the compressional waves (about 6 km). Velocity perturbations derived from the inversion are relative, rather than absolute, because relative residuals are used.

The three-dimensional velocity structure of the Long Valley region obtained from the inversion reveals several significant features. The most significant features are low-velocity bodies beneath Mono Craters (discussed by Achauer et al. (1986)) and the resurgent dome of the Long Valley caldera, and a high velocity body east of Mono Craters in the mid-crust. The low velocity body in the Long Valley caldera is restricted to the upper 20 km of the crust, and is centered in the depth range of 6-15 km and 2-3 km west of the resurgent dome. Beneath this low-velocity anomaly is a zone of normal velocity extending through the crust and underlain by a large but weak high velocity zone into the upper mantle. The low-velocity body beneath Mono Craters appears to extend from the middle crust all the way to the Moho. The high velocity anomaly to the east of Mono Craters may correspond to shallowing of the crystalline basement to within a few hundred meters of the surface, as shown by seismic refraction profiling performed by Hill et al. (1986). Figure 2 is a depth cross-section along line A-A' of Figure 1a. It shows in percent, the velocity perturbations of the layered model.

CONCLUSIONS

A low-velocity anomaly has been imaged beneath the western portion of the resurgent dome of Long Valley caldera using the teleseismic residual technique. It is interpreted as a body of partial silicic melt with a volume of roughly 200 km^3. There is no evidence that the low velocity anomaly extends through the crust, while there is evidence for high velocity beneath the western portion of Long Valley caldera in the upper mantle. This observation suggests that the upper mantle and lower crust are in the process of "healing" beneath the caldera. The greater apparent size of the magmatic system beneath Mono Craters may indicate the focus of magmatism is moving or has moved to beneath this very young system.

REFERENCES

Achauer, U., L. Greene, J.R. Evans, and H.M. Iyer, Nature of the magma camber underlying the Mono Craters area, eastern California, as determined from teleseismic traveltime residuals, J. Geophy. Res., v. 91, p. No. B14, 13873-13891, 1986.

Aki, K., A. Christoffersson, and E.S. Husebye, Determination of the three-dimensional seismic structure of the lithosphere, J. Geophys. Res., 82, 237-296, 1977.

Ellsworth, W.L., Three-dimensional structure of the crust and mantle beneath the Island of Hawaii, Ph.D. thesis, Mass. Inst. Tech., 337 pp., 1977.

Herrin, E., E.P. Arnold, B.A. Bolt, G.E. Clawson., E.R. Engdahl, H.W. Freedman, D.W. Gordon, A.L. Hales, J.L. Lobdek, O. Nuttli, C. Romney, J. Taggert, and W. Tucker, 1968 Seismological tables for P-phases, Bull. Seis. Soc. Am., 58, 1193-1241, 1968.

Hill, David P., Structure of Long Valley Caldera, California, from a seismic refraction experiment, J. Geophys. Res., 81, 745-753, 1976.

Hill, D.P., E. Kissling, J.H. Luetgert, and U. Kradolfer, Constraints on the upper crustal structure of the Long Valley-Mono Craters volcanic complex, eastern California, from seismic refraction measurements, J. Geophys. Res., 90, No. B13, 11135-11150, 1985

Iyer, H.M., Geophysical evidence for the locations, shapes and sizes, and internal structures of magma chambers beneath regions of Quaternary volcanism, Phil. Trans. R. Soc. Lond., A310, 437-510, 1984

Iyer, H.M., J.R. Evans, G. Zandt, R.M. Stewart, J.M. Coakley, and J.N. Roloff, A deep low velocity body under the Yellowstone caldera, Wyoming: delineation using teleseismic P-wave residuals and tectonic interpretation, Geol. Soc. Am. Bull., 92, Part I: 792-798, Part II: 1471-1646, 1981.

Julian, B.R., Evidence for dyke intrusion earthquake mechanisms near Long Valley caldera, California, Nature, 303, 323-325, 1983.

Lachenbruch, A.H., J.H. Sass, R.J. Munroe, and T.H. Moses, Geothermal setting and simple heat conduction models for the Long Valley caldera, J. Geophys. Res., 81, 769-784, 1976.

Sanders, C.O., and F. Ryall, Geometry of magma bodies beneath Long Valley, California, determined for anomalous earthquake signals, Geophys. Res. Lett., 10, 2597-2609, 1983.

Savage, J.C., and M.M. Clark, Magmatic resurgence in Long Valley caldera, California: possible cause of the 1980 Mammoth Lakes earthquakes, Science, 217, 531-533, 1983.

Steeples, D.W., and H.M. Iyer, Low velocity zone under Long Valley as determined from teleseismic events, J. Geophys. Res., 81, 849-860, 1976.

FIGURES

la. Location map of seismic stations used for the teleseismic
experiment. Dots indicate station locations. The Long Valley caldera caldera
and Mono Craters/Inyo Domes volcanic complexes are shown in outline. The
shaded area shows the area of mean positive travel time residuals for all
teleseisms from all azimuths. The northwest trending line indicates the depth
cross-section for Figure 2.

lb. Plot of traveltime residuals from events to the northwest as
indicated by the arrow. The mean travel time residual for each station has
been subtracted from the travel time residual at each station for these
events. The shaded area indicates late arrivals.

lc-d. Same as for 1b except for azimuth of ray group. 1c is for events
from the southwest and 1d is for events from the southeast.

2. Depth cross-section along line B-B' of Figure la. Original figure is
in color. Starting model velocities are shown in km/s. Dark areas show
blocks with negative velocity perturbations or low velocity . Light areas are
positive velocity perturbations or high velocity. Scale is 1:1. The Long
Valley caldera and Mono Craters are indicated by bars. 0 elevation line is
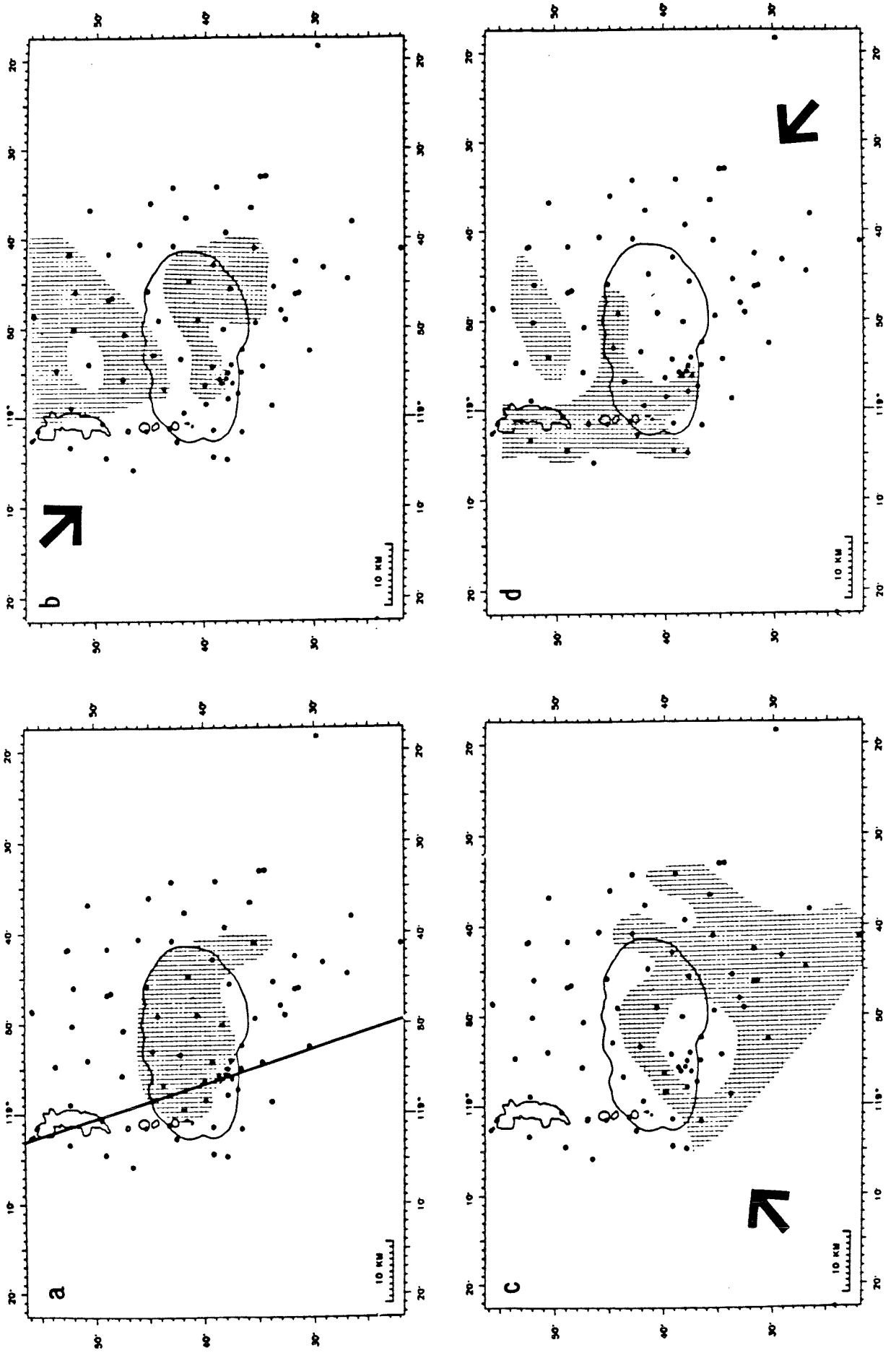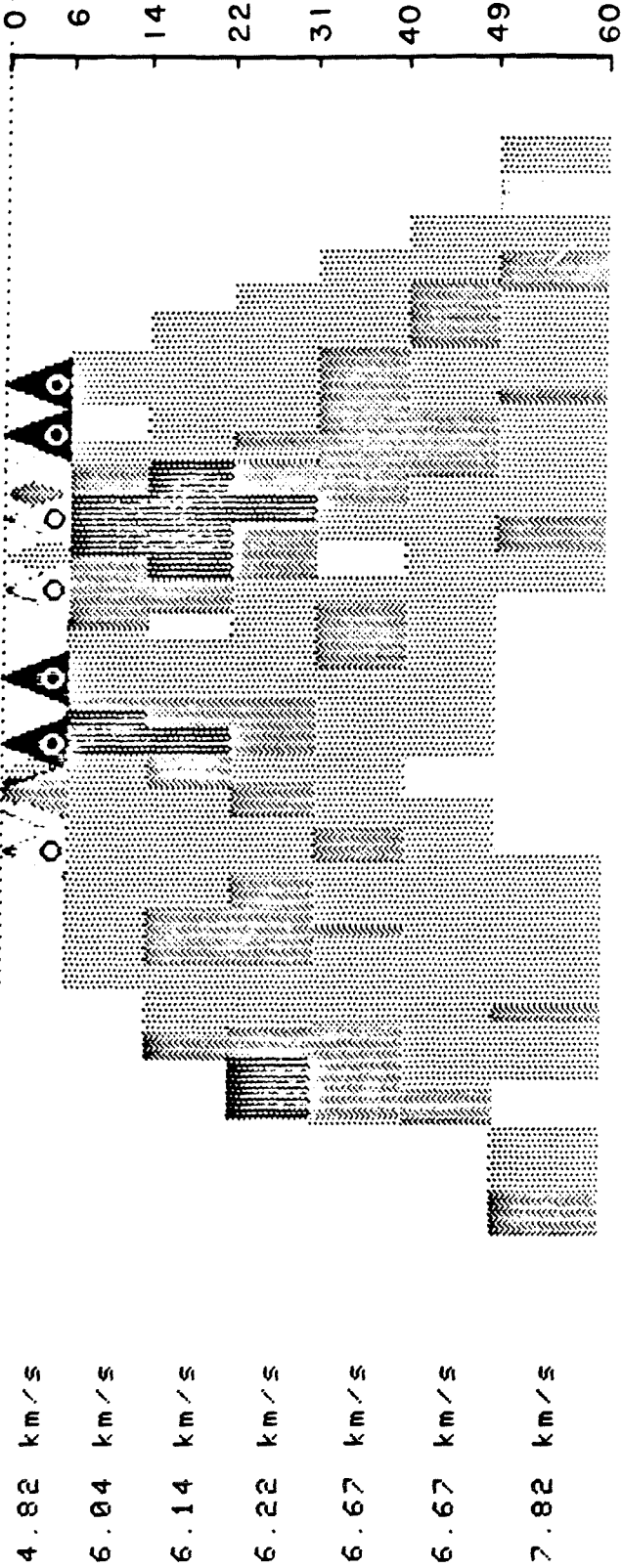the mean station elevation, about 2400 m.

Figure 1

61

Figure 2

62

Three-Dimensional P-wave Velocity Structure of the Long Valley Region

Edi Kissling
Institut fur Geophysik
ETH-Honggerberg
CH-8093 Zurich, Switzerland

William L. Ellsworth and Robert S. Cockerham
U.S. Geological Survey
345 Middlefield Road
Menlo Park, California 94025

Our investigations of the crustal structure of Long Valley caldera and surrounding regions have been updated with an expanded set of travel time observations and revised computational proceedures. The models presented are derived from 3831 well-distributed earthquakes observed by over 100 stations, producing 89,500 observations. The three-dimensional velocity structure is determined by iterative solution of the coupled hypocenter/structure problem using the parameter separation strategy of Pavlis and Booker (1980) as implimented by Thurber (1981). We solve for the velocity perturbations using both approximate methods (commonly referred to as tomography) and full matrix methods (as originally applied in the teleseismic imaging problem by Aki, Christofferson and Husebye (ACH) 1977).

Results obtained after the second iteration for the tomographic and ACH methods are generally similar, with the ACH solution displaying stronger short wave length varations and generally lower-amplitude anomalies. The data variance reduction after two steps was 65% for the tomographic solutions and 40% for the ACH solution. Tests with artificial data and several distributions of random reading errors, including normal and uniform, adequately recover the synthetic structure, which gives us some confidence that our models reflect earth structure rather than noise.

The resulting three-dimensional model for Long Valley caldera is generally similar to preliminary models presented earlier (Kissling, et. al., 1984). The outline of the caldera is clearly defined to a depth of 3 km below the Caldera floor by the sharp contrast between the relatively low velocity caldera fill and the Sierran granite to its south and west. The magnitude of the velocity contrast decreases with depth, having essentially dissapeared at a depth of about 5-6 km. Velocity anomalies within the basement (below the Bishop tuff or at depths greater than 3km) are no stronger than $\pm$ 5% when averaged on a 5 km scale length. This suggests that any zones of intense p-wave velocity reduction must be no larger than 2-3 km in linear dimension. Suggestive, but as yet unconfirmed small-scale low velocity anomalies underly Mammoth Mountain (5-7 km depth interval), the southern and southeastern parts of the moat (5-14 km) and Glass Mountain (3-10 km).

The velocity field to the north and west of the resurgent dome is essentially featureless between 5 and 10km. The relatively low amplitude ($\pm$ 2 to 3%) fluctuations observed beneath Long Valley caldera are of comparable magnitude to the variations reported in many other crustal modelling studies from non-volcanic regions. Collectively, they stand in sharp contrast to the large, intense low velocity zone beneath Yellowstone as determined using the same computer programs. At Yellowstone, the evidence for a large, continuous magma chamber in the upper-middle crust is strong (Kissling, in prep.) At Long Valley, it is questionable, or at least deeper than 14 km.

Several well-defined regions of laterally-varying strcuture were found outside of the caldera and deserve mention. The Sierran block south of the caldera is underlain by an intense low-velocity zone at depths greater than 14 km. The north-south extent of this body cannot be precisely defined, as it lies on the periphery of model. It may lie directly beneath the active earthquake source region south of the Caldera at a depth of 14-18 km or deeper and further to the south or both. Velocities are also significantly below average in Chalfant Valley at depths above the aftershocks of the M 6.4 earthquake. We also find that on a regional scale the area north of the Caldera is slightly slower on average (1-3%) than the surrounding crust. This feature may also be seen in our preliminary results (Kissling, et. al., 1984) and is now on much firmer ground.

Seismic Reflection Studies in Long Valley

R.M. Berg, R.A. Black, and S.B. Smithson

Program for Crustal Studies
Department of Geology and Geophysics
University of Wyoming
Laramie, WY 82071

Two normal-incidence and one wide-angle CDP reflection lines have been recorded in the Long Valley caldera. The first recorded in 1984 is an E-W line along the south side of Lookout Mountain and ending near the Unocal geothermal exploration drill hole on the west. The second line recorded in 1985 runs NW from Casa Diablo hot springs over a postulated domed magma chamber. The wide-angle profile was intended to duplicate the USGS refraction spread that recorded a reflection interpreted to come from a postulated magma chamber. Because of unusually unfavorable recording conditions, processing of this data required particular care.

Processing

Data sets gathered during the 1984 and 1985 experiments were processed through both standard petroleum industry procedures and through specialized routines developed at the University of Wyoming. Both CDP lines were processed through the following procedures.

 1) Demultiplexing
 2) Cross correlation
 3) Trace editing
 4) Vertical stacking (source record summing)
 5) Line geometry redefinition
 6) Refraction statics analysis
 7) Common depth point sorting
 8) Gapped deconvolution
 9) Velocity analysis
10) NMO correction
11) Trace muting
12) Datum static correction
13) Refraction static correction
14) Residual static correction
15) CDP stacking
16) Section display

The order in which these processes were performed and the specific algorithms used varied slightly between lines. The trace muting was performed before NMO correction on the 1984 data set, but was performed after NMO on the 1985 data set. Deconvolution was performed with a 4 millisecond sample rate and a 1001 point operator on the 1984 data set, while the 1985 data set was processed with a 255 point operator after being resampled to an 8 millisecond interval. In addition, the residual statics analysis performed on the 1984 data

was nonsurface-consistent, while the 1985 data set was processed using a surface-consistent algorithm.

The refraction statics analysis routines were developed at the University of Wyoming. These routines utilize the Generalized Reciprocal Method (GRM) of refraction interpretation. A pre-existing industry-standard routine designed to perform the gapped deconvolution was modified at U.W. to allow operators of length greater than 255 points.

In addition to the standard processing steps listed above, several new techniques were applied to the data. A coherency filter was applied to the stacked sections to enhance coherent energy buried in the noise at deeper levels in the section. Also, a covariance based eigenstructure analysis was performed on some of the data to obtain more detailed velocity information and detect hyperbolic events in the presence of a low signal to noise ratio. An additional technique, involving suppression of regions of low signal to noise on traces before correlation, based on an analysis of the traces envelope function, was also applied to some of the 1985 data set.

Results 1984 Line

Two stacked sections have been produced from the 1984 CDP data, a first section, Figure 1, displaying events from 1–2 seconds in time (1 to 3.5 km in depth), and a section, Figure 2, reprocessed by keying on the major shallow reflectors above 1.5 seconds (2.25 km).

In the first section a major reflector is evident at about 1 second. This event probably correlates with a blockfaulted package of breccia, till and flows at the top of the Bishop Tuff observed at about 1 km depth in the UNOCAL well IDFU-44-16. Located about 3 km to the southwest of the southwest end of the CDP line, this well is the main source of subsurface information in this area.

A second event evident on the section is a group of fairly low amplitude, dipping reflectors apparent at about 1.1 to 1.3 seconds. This event may be the complex expression of the paleotopography below the Bishop Tuff.

A package of reflectors is also evident at 1.5 to 2.0 seconds at the northeastern end of the section. Currently no subsurface information is available at these depths, so any interpretation is unconstrained. Various possibilities include a package of metasediments, flows, layered intrusives, or reverberations of energy higher in the section.

On the second, reprocessed section two of the same events seen on the first section are evident. The major reflector from the top of the Bishop Tuff at about one second is now very well imaged, and the structural relief varies from 0.9 to 1.3 seconds in time. The details of the block faulting on this horizon have been cleaned up on this section. The probable paleotopography at the base of the Bishop Tuff is again imaged. The deeper events at 1.5 to 2.0 seconds are not well imaged on this section. However, a shallow event is observed at about 0.5 seconds. This event correlates well with a package of tills, and sand and gravel, above a tuff observed in the UNOCAL well at about 0.3 km. An interpreted section is shown in Figure 2a.

Probably the most important unit imaged within this section is the Bishop Tuff, since this unit was apparently the main geothermal reservoir encountered in the UNOCAL well. The ability of the seismic reflection method to apparently image the reservoir geometry could be significant in the exploitation of this resource.

Results from the 1984 wide-angle experiment of significance include the development of a general velocity function for the area and the imaging of several subtle, tentative events (Deemer, 1985) which may be correlative with a previously postulated magma chamber (Hill et al., 1985).

Results 1985 Line

The most coherent event on the final stacked section (Fig. 3) is between 1.2 and 1.6 seconds and has a high stacking velocity (4.3 km/sec). This event is anticlinal in shape between CDP 130 and CDP 210, and is discontinuous north of CDP 210. The structure and velocity in this area are supported by a refraction model using first breaks. This structure is interpreted as an intrusive dome. The discontinuity suggests faults located at about CDPs 210, 260, 280, 300, 340, 395, and 400 (Fig. 3a). There are hints of events down to about three seconds that are most easily seen on the coherency filtered section (Fig. 4). This section was produced by filtering the stacked section in Figure 3. The near surface static shifts have been corrected well enough that deeper events should stack in judging from the improvement in the shallow event mentioned previously and the improved alignment of first breaks on CDP gathers. The absence of deeper events implies that attenuation of seismic energy has reduced the signal to noise ratio below that at which events may be detected by conventional methods.

CDP

889
879
869
859
849
839
829
819
809
799
789
779
769
759
749
739
729
719
709
699
689
679
669
659
649
639
629
619
609
599
589
579
569
559
549
539
529
519
509
499
489

0.00   1.00   2.00   3.00   4.00   5.00   6.00
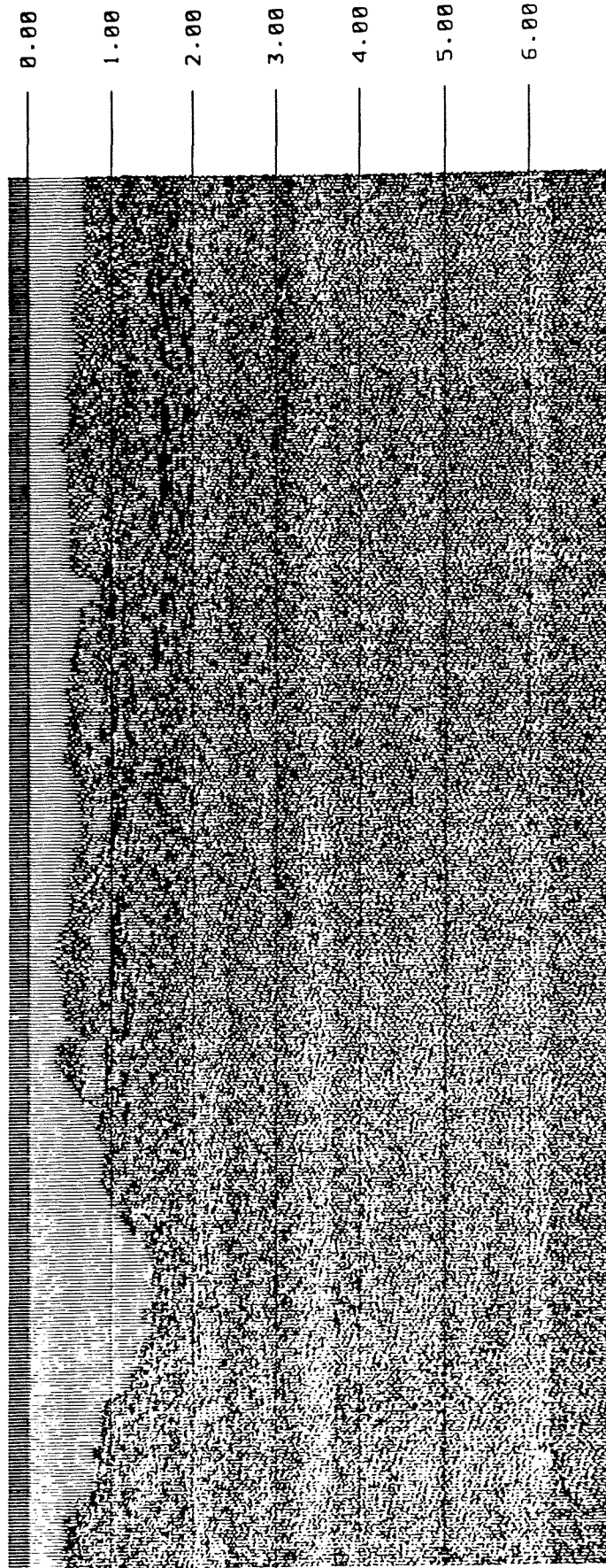
Figure 1. Mammoth Lakes 1984 CDP line with original processing.

CDP

0.00   1.00   2.00   3.00   4.00   5.00   6.00

878
868
858
848
838
828
818
808
798
788
778
768
758
748
738
728
718
708
698
688
678
668
658
648
638
628
618
608
598
588
578
568
558
548
538
528
518
508
498
488
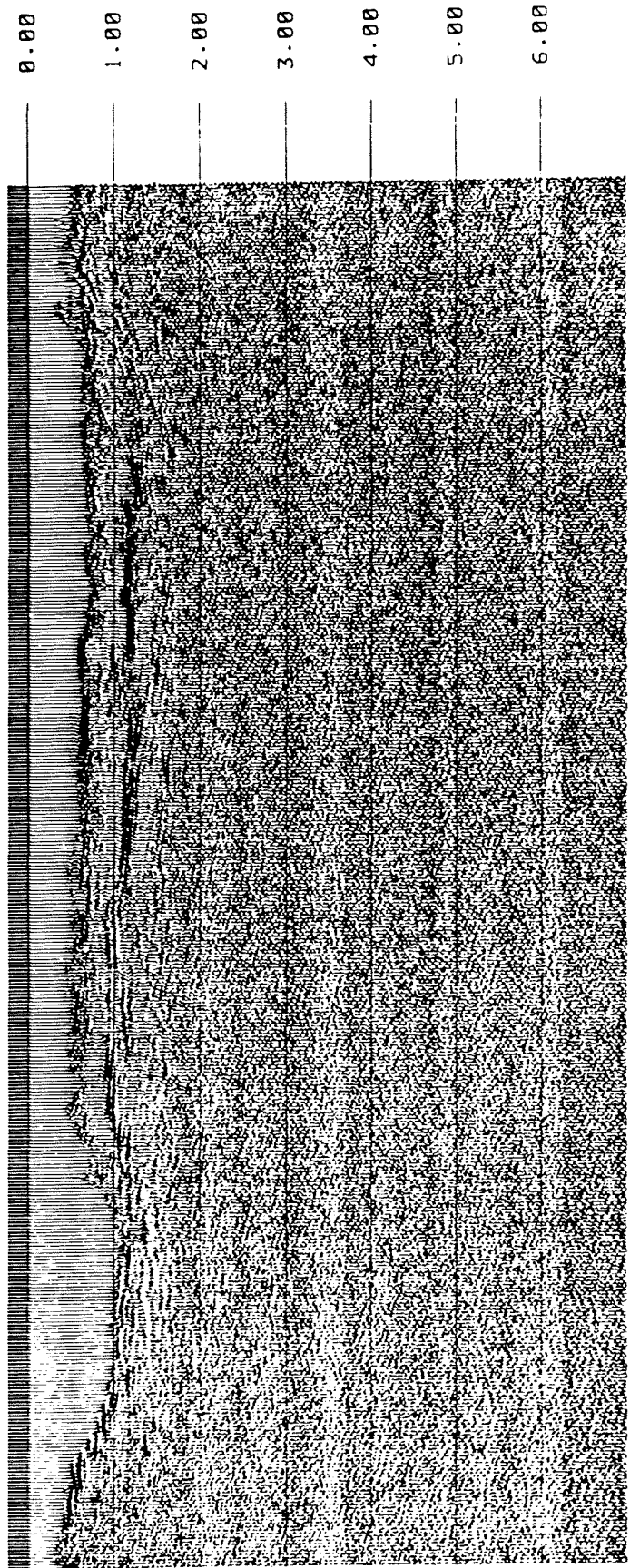
Figure 2. Reprocessed Mammoth Lakes 1984 CDP line.

68

CDP

878
868
858
848
838
828
818
808
798
788
778
768
758
748
738
728
718
708
698
688
678
668
658
648
638
628
618
608
598
588
578
568
558
548
538
528
518
508
498
488

0.00
1.00
2.00
3.00
4.00
5.00
6.00

TOP OF BISHOP TUFF

BASE OF BISHOP TUFF
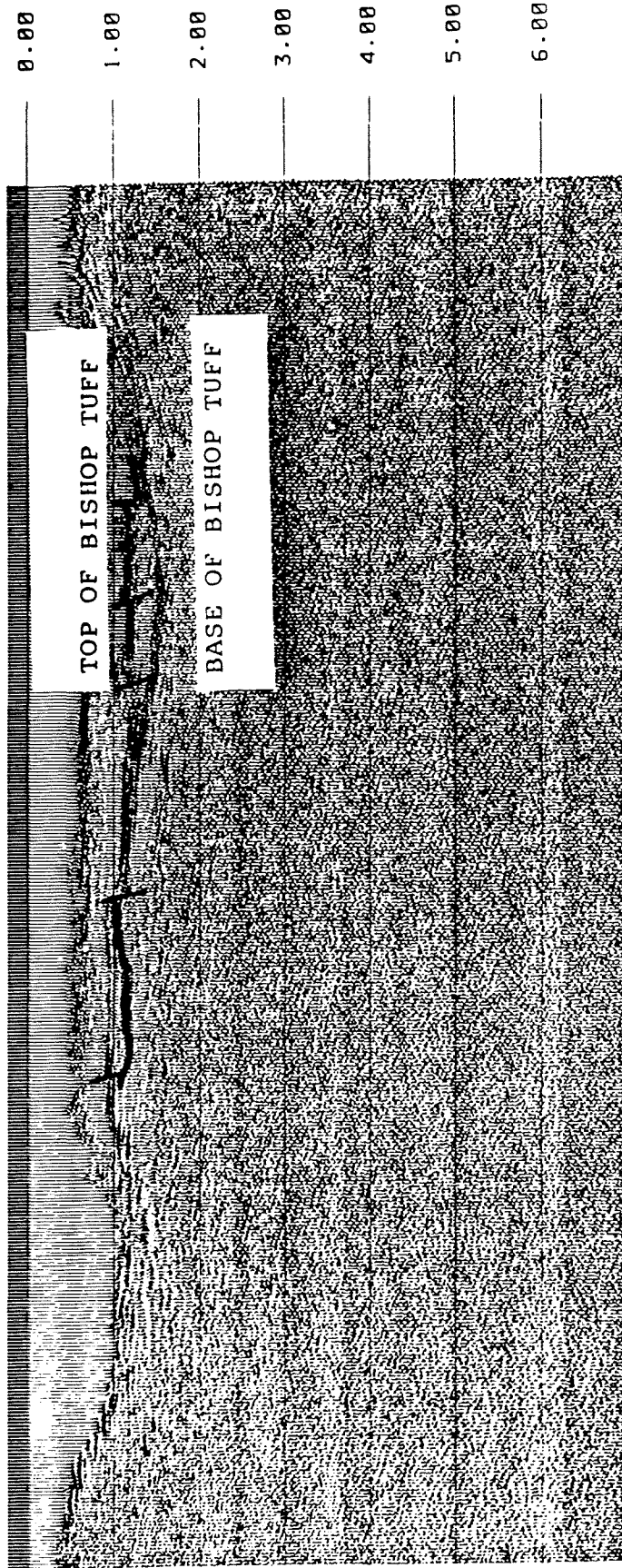
Figure 2a. Interpreted reprocessed section, Mammoth Lakes 1984 CDP line.

69

CDP
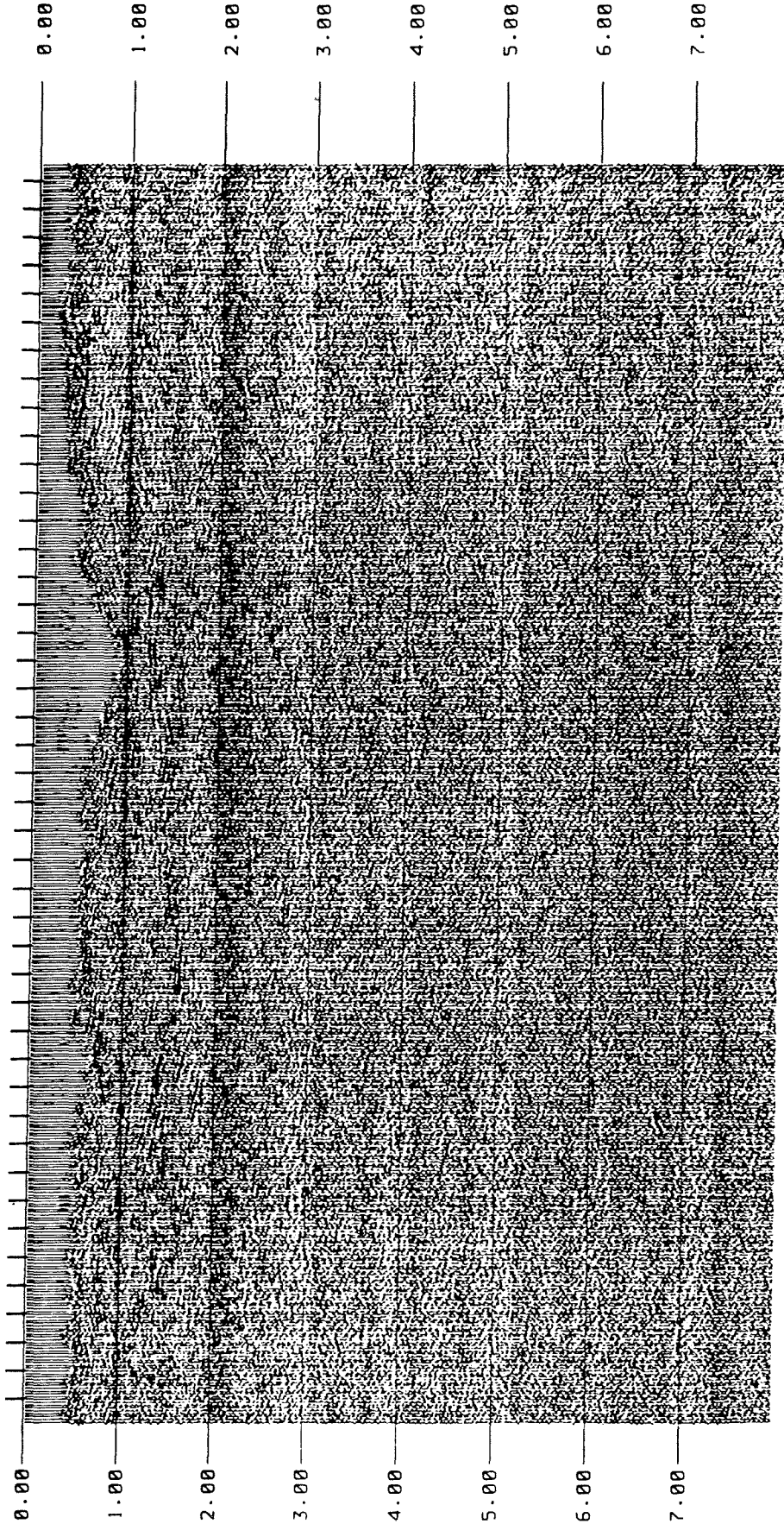
Figure 3.   Final stack 1985 Mammoth Lakes CDP line.

70

CDP

Figure 3.a Final stack 1985 Mammoth Lakes CDP line.
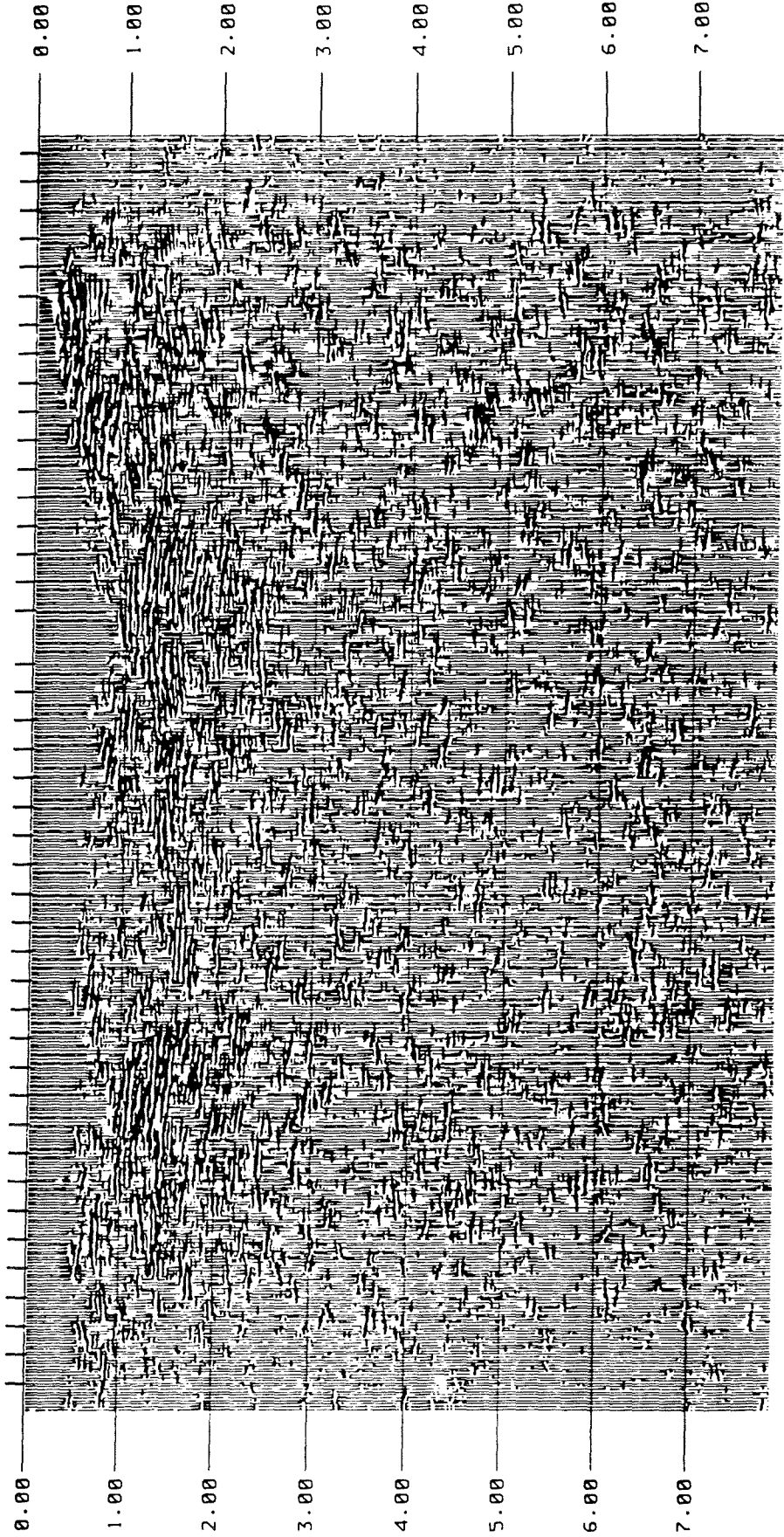
Figure 4. Coherency filtered final stack 1985 Mammoth Lakes CDP line.

THE MAMMOTH LAKES WIDE ANGLE SEISMIC REFLECTION EXPERIMENT

P.E.MALIN, H.L.TONO, AND W.J.MURPHY

INSTITUTE FOR CRUSTAL STUDIES
UNIVERSITY OF CALIFORNIA SANTA BARBARA
SANTA BARBARA, CA 93106

In the summer of 1985 we recorded 2 seismic reflection profiles in the resurgent dome area of Long Valley Caldera. The data recording was done as a "piggyback" experiment in wide angle reflection profiling to the more standard vibroseis CMP profiles that were being shot by the University of Wyoming. While the UW vibrators profiled a 9 km, northwest-southeast line across the dome from roughly Casa Diablo to Lookout Mountain, our 48 channel recording equipment was alternated between linear, 1.5 km long ground arrays several km north and south of the vibrator line. Despite heavy wind conditions, single sweeps of the 4 vibrator sources could be seen 60% of the time at the wide angle arrays. These data have been edited, divided into groups of nearby shots, and diversity stacked to give 35 northern and 38 southern wide angle shot gathers.

The shot gathers reveal a diversity of subsurface conditions and strong lateral changes. Static shifts in the first breaks of the gathers suggest that imaging deeper structures will depend critically on geometrically correct models and processing procedures for the shallow caldera fill and flows. A crude hand method of aligning first breaks from adjacent shots with overlapping traces was tested on the stacked data. The resulting travel time section shows several deeper arrivals, some of which can be interpreted in terms of known and inferred geological structures. The data in fact seem to image the Bishop Tuff at 0.5 and 2.0 km depth, and a much deeper horizon, below 10 km, the presence of which has been also suggest by studies of upcoming P-waves.

To improve the static corrections and better understand the caldera geometry, we have traced rays through a range of models. We have recently been helped in our modeling by a new gravity model along the profile line (S. Carle and N. Goldstein, LBL, personal communication, 3-87). We have also reduced and modeled some shot gun seismic data taken by Sandia Labs as part of the overall reflection study, which have helped with the shallow velocities along the profiles.

Our remaining work includes completion of the ray tracing, particularly using the models provided by the new gravity interpretation. This effort is intended to provide an accurate control over the static corrections that will applied in further processing of the wide angle data. Any resulting record section containing deep reflectors will require further modeling and testing to establish the image as real.

Introduction. In the summer of 1985 we joined the University of Wyoming in a seismic reflection profiling effort in Long Valley - Mammoth Lakes Caldera. This project was supported by Sandia National Laboratories. The University of Wyoming brought out 4 medium (14 ton) p-wave vibroseis units, 2 on buggy and 2 on truck mounts, and a 96 channel MDS 12 reflection seismograph. This equipment was used to shot a roughly 9 km narrow angle CMP line across the resurgent dome of the caldera (see CMP line location in Figure 1). The station and shot spacing were 33.5 m, the sweep was 10 to 30 hz over 20 sec, with a 8 sec listen.

In a passive piggyback experimental effort, UCSB laid out two 1.6 km spreads, with the same station spacing, a few km off the north and south ends of the UW profile (Figure 1). The ground array used in this experiment was tuned to enhance direct and reflected waves in the vertical plane containing the source and receivers, and to suppress out of plane signals. This tuning was accomplished by stringing the 12 phone geophone groups normal to the profile line (Figure 2). This unconventional field deployment makes use of the large offset between source and receiver, and the low velocity of the weathering layer in the caldera to suppress unwanted in line waves such as the ground roll.

As the UW vibrators profiled the central line, we alternately recorded the experimental spreads with our 48 channel DFS 4 reflection seismograph. Despite the necessity of working in a passive mode, and consequently with no control over recording during local heavy winds, we were able to observe the vibrator sweeps on over 60 % of the shot gathers we collected.

The resulting experimental "wide angle reflection" data set has plotted, edited, grouped into nearby shots, and diversity stacked. The sections of CMP line covered by the data include the south molt, Casa Diablo, Smokey Bear Flat, and the southwest flank of Lookout Mountain (see the stacking chart in Figure 3). Examples of the data from both the north and south spreads are shown in Figure 4.

The Data. The static shifts of the first arrivals seen in the shot gather data (the southern shot gather in particular) illustrate many of the difficulties encountered in seismic imagery of laterally complex areas such as Long Valley caldera. To begin with, the first arrivals show that directly under the southern spread the thickness of the shallow low velocity layer must change rapidly: the first breaks actually slow down at larger offsets (southern spread in Figure 4). This characteristic could be due to either abrupt faulting of the caldera wall, or rapid thickening of the caldera fill.

Deeper coherent horizons that underlie these shallower features are made difficult to image because the static shifts of the shallow layers apply to the seismic energy reflected off them as well. We have made several attempts to overcome this aspect of the data.

Traditionally, static corrections can be derived from time differences between nearby source-receiver pairs that should have identical travel times in flat laying, laterally homogeneous media. Using this idea, we have constructed a record section by overlaying time shifted shot gathers that have overlapping source and receiver pairs (Figures 5 and 6). The resulting section has several coherent secondary arrivals, the possible interpretation of which we discuss later.

It would seem, then, that a very detailed study of the local structure under the receiver arrays could yield the necessary information to achieve a dramatically improved image of the horizons beneath the dome. The most direct approach to this problem is to match the shot gather data with ray tracing models.

74

Ray Tracing. Initially, because of the presence of the Casa Diablo hot springs, and general interest in the southern molt, we have concentrated on the southern spread and its nearest shot points. As indicated in Figure 4c, there are several distinctive features to the subsurface of this site: (1) a relatively fast top layer, which either encounters (2) an abrupt faulted caldera wall, or, alternatively a thickening section of caldera fill, and (3) a deeper faster horizon, conceivably also of the wall rock.

Given this general statement as a starting point, we began our ray tracing by testing models of the sort shown in Figure 7. The distinctive features of this model are the disruption of first arrivals by a fault block of wall rock, which not only diffracts the direct waves but also includes back reflection from the side of the block. The model does seem to account for some of the confusion of arrivals in the near offset traces and backward moving energy. While the diffraction off the faulted block moves off more quickly than is the case for the data, its amplitude is small and could be buried in the noise. Finally the fast horizon at the base of the model, from which energy passes up along the fault block, does give a sense of the far offset first breaks seen in the data.

However, the incorrect moveout of the low amplitude section of the matching spread suggests that a very different model is needed. One possible type of model has been recently developed by S. Carle, using gravity data (S. Carle and N. Goldstein, LBL, personal communication, 3-87, see Figure 8). This model suggests a thickening and slowing basin would be a better fit for the first break data. We have also ray traced an example for this case and have found a satisfactory first cut fit to the data (Figure 9).

Interpretation to date. The interpretation we have to date comes from ray tracing of in models such as the one shown in Figure 8 and comparing to the crude static corrected data of Figures 5 and 6. From these comparisons, we have concluded that arrivals A and B are the top and bottoms of the welded Bishop tuff. They appear to be roughly .5 and 2.0 kms + .2 km below ground level.

Much deeper are two potential reflectors, one relatively continuous, the other very local and broken up. These are marked as C and D on the record sections. Ray tracing suggests that these events come from more than 10 km below the caldera floor. Corresponding horizons have been described by Prothero et al., using P-wave polarization conversions from up coming teleseism.
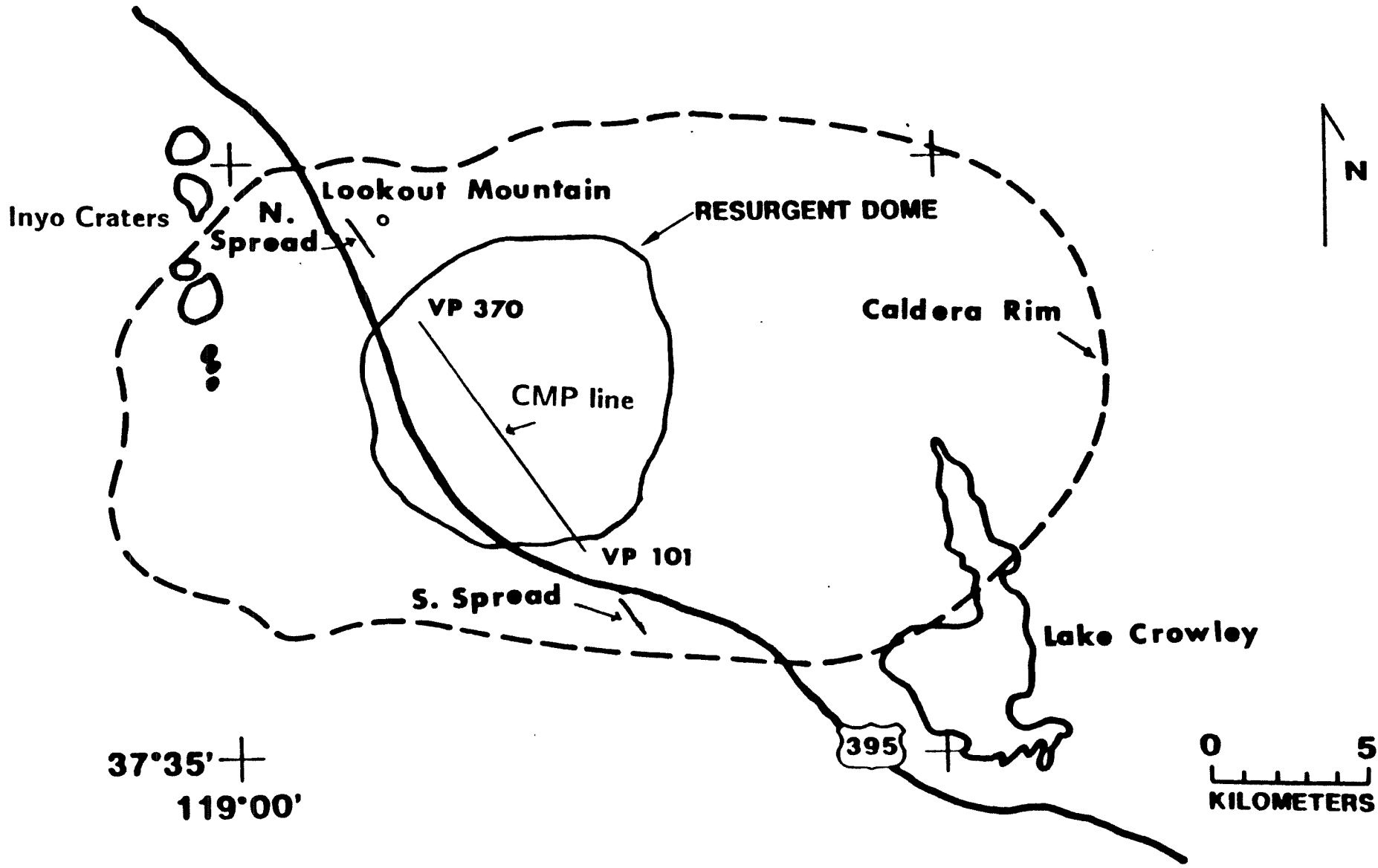
Figure 1

Figure 2

Southern wide angle ground array section

Geophone array

VP 101

2.5 m

3.7 km

S1

33 m

33.5 m

S2

S3

S4

N

Figure 3

STACKING CHART

North Spread	Wyoming CMP Line	South Spread

W.A. COVERAGE
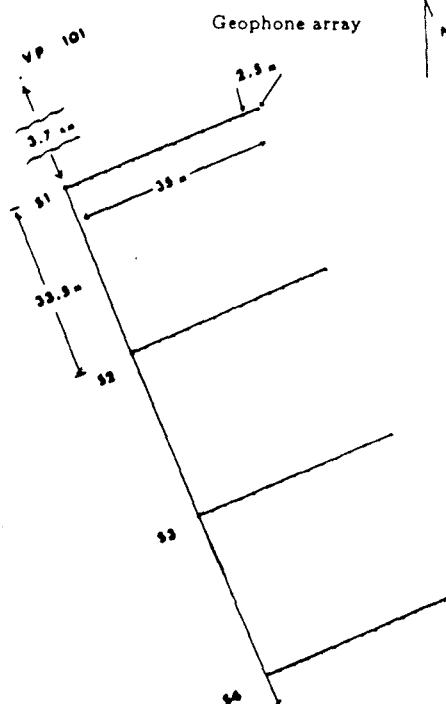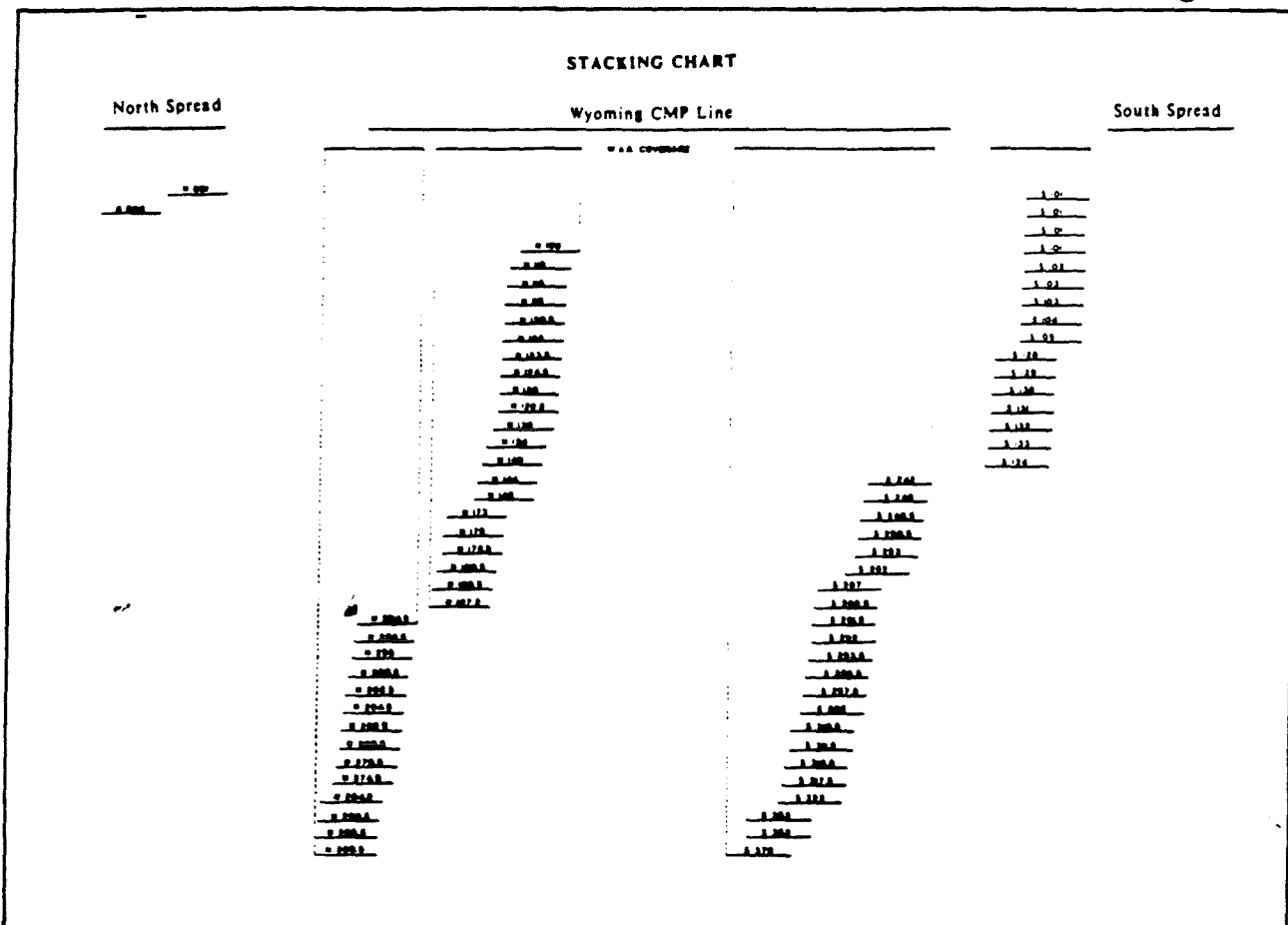
Figure 4A   Figure 4B   Figure 4C   Figure 4D

Southern spread

VP 101

Northern spread

VP 140

t (sec)

0

1

2

3

4

5

6

78
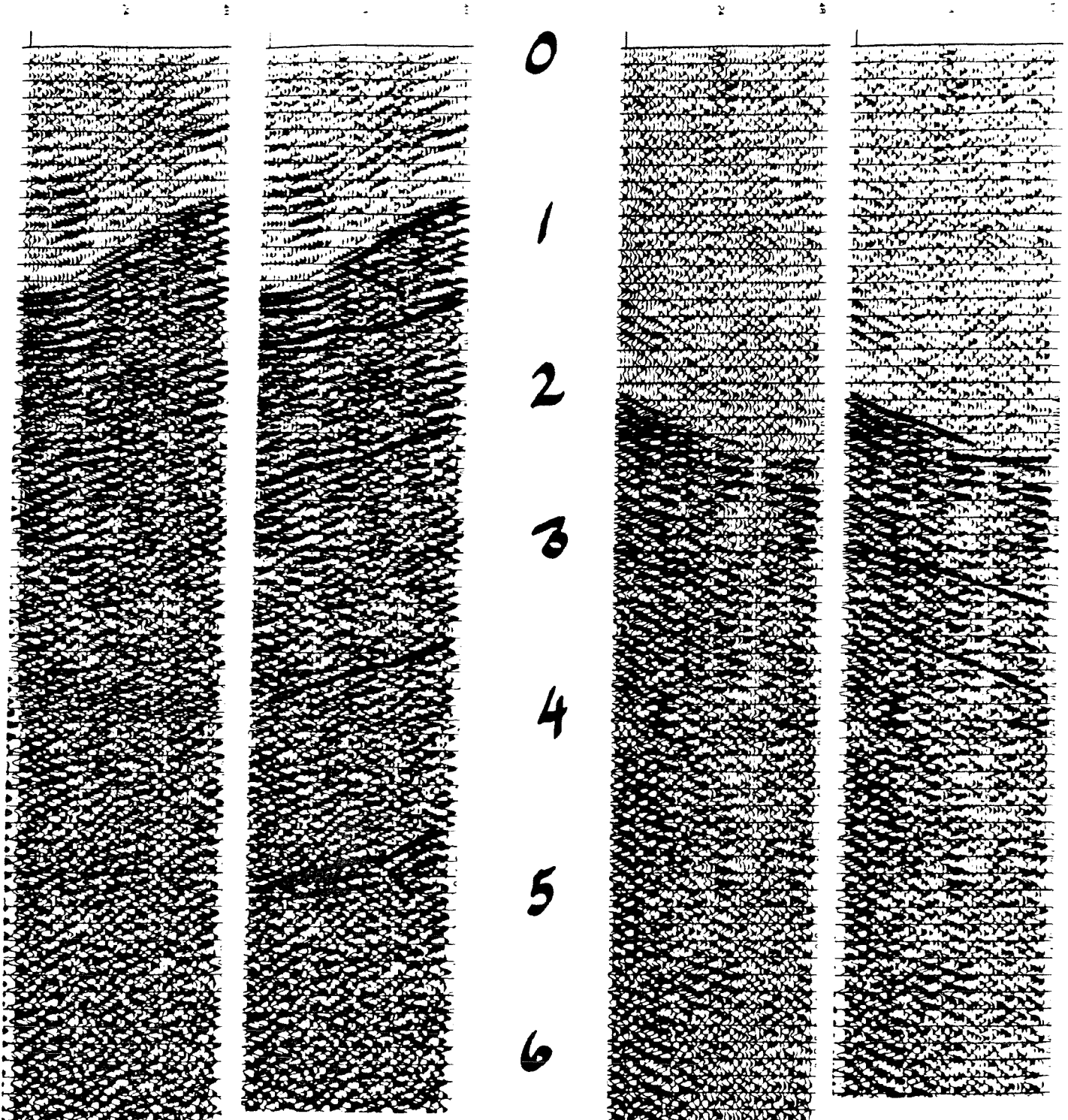
SOUTH SPREAD

interpretation

SOUTH SPREAD

SOUTH SPREAD

A

B

C

D

Figure 5

interpretation
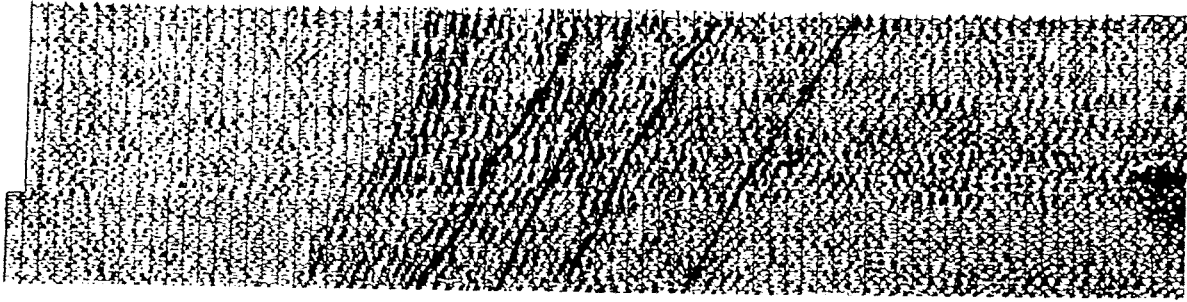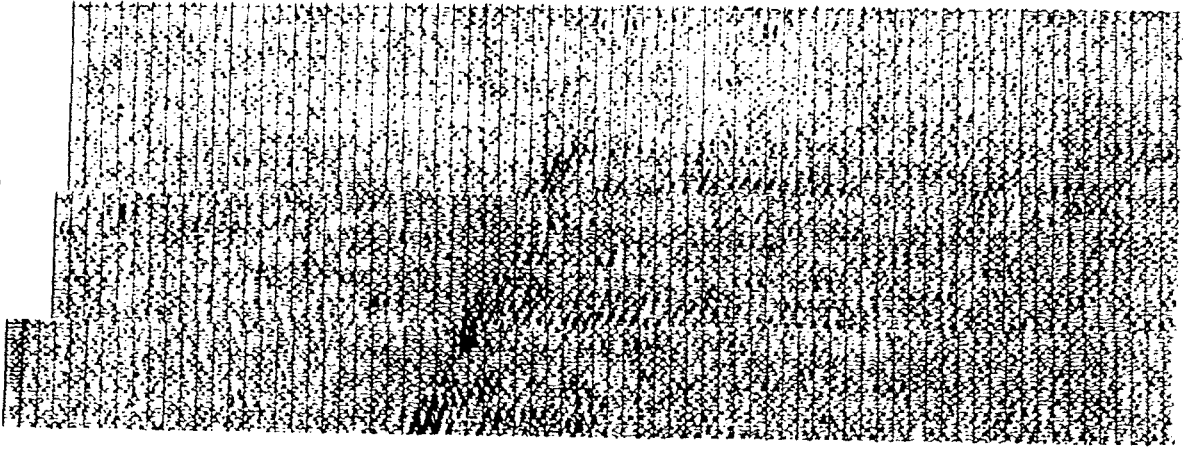
NORTH SPREAD

NORTH SPREAD

Figure 6

80

Figure 7

81
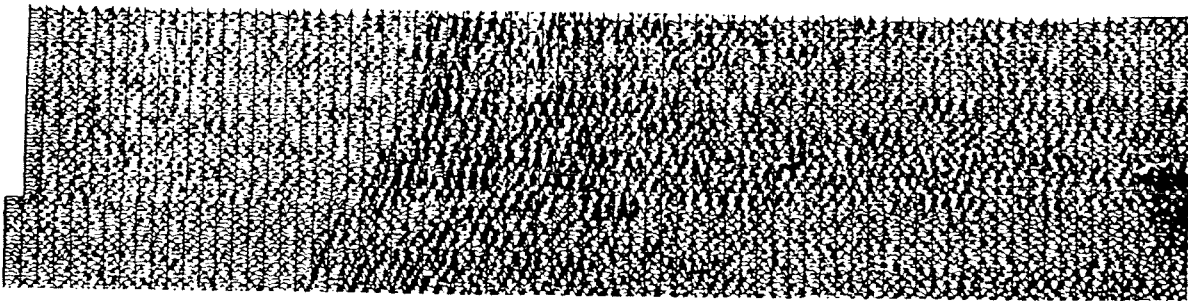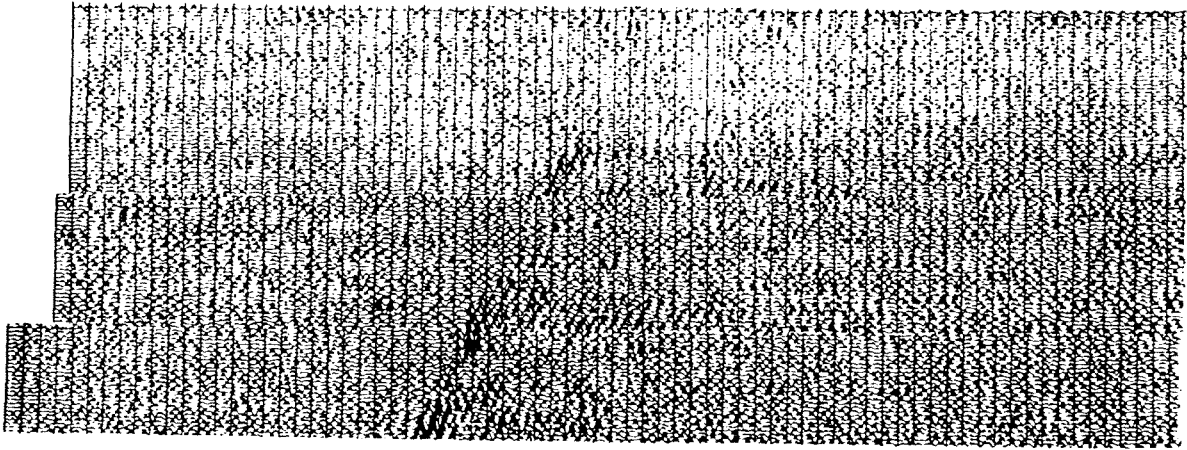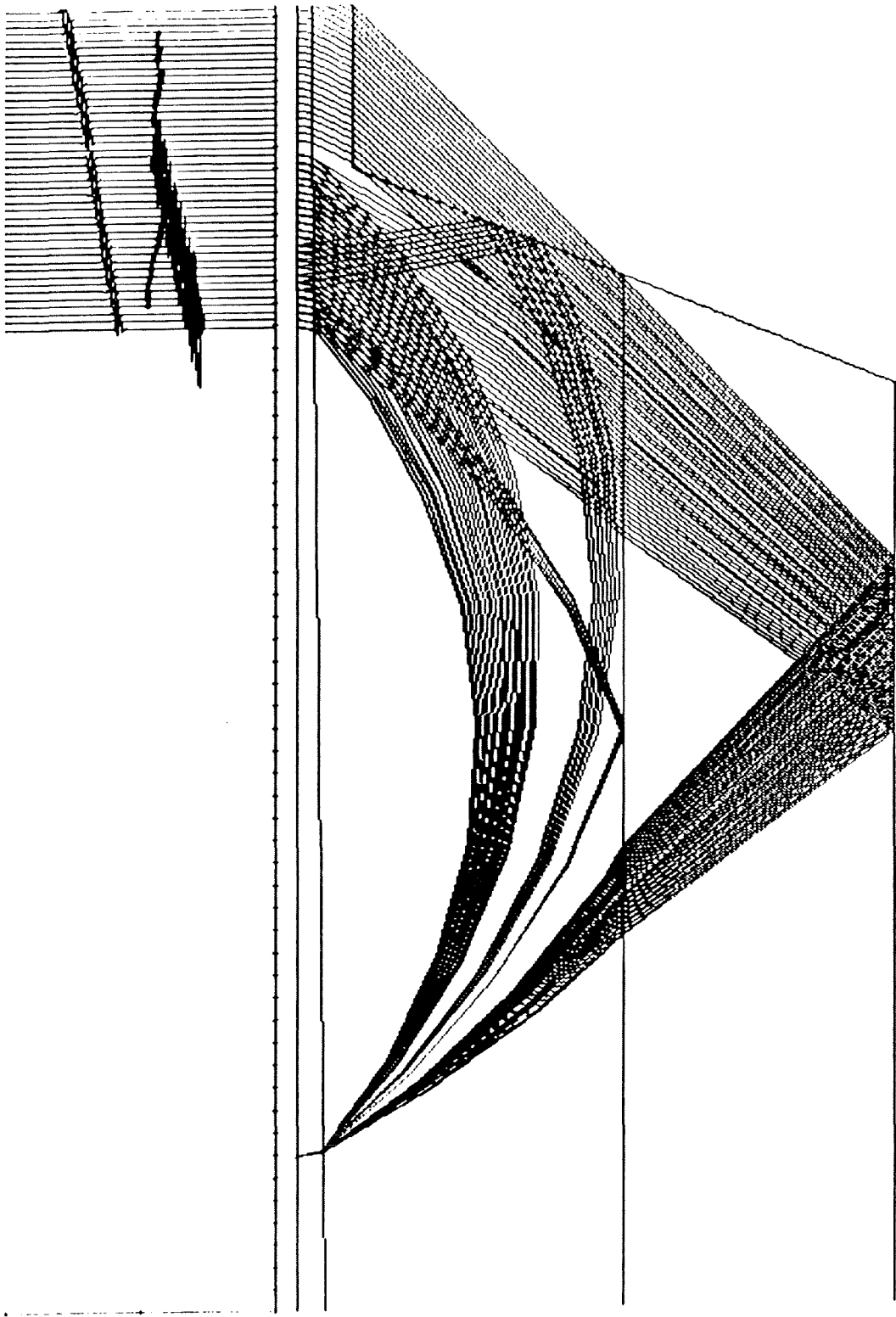
LONG VALLEY CALDERA

RESIDUAL GRAVITY ANOMALY

CALCULATED ....
OBSERVED —————————

UNIT	DENSITY
ALLUVIUM	2.00
PUMICE	1.70
TILL AND COLLUVIUM	1.80
RHYODACITE	2.44
BASALTS, ANDESITES	2.67
TILL	1.90
MOAT RHYOLITE	2.05
LAKE SEDIMENTS	1.70
EARLY RHYOLITE FLOWS	2.20
EARLY RHYOLITE TUFFS	1.75
UNWELDED BISHOP TUFF	2.05
WELDED BISHOP TUFF	2.35
GLASS MTN RHYOLITES	2.15
PRE-CALD RHYODACITE	2.45
PRE-CALD VOLCANICS	2.67
GRANITICS OR METASEDS	2.70
GRANITICS OR METASEDS	2.90
GRANITICS	2.60
GRANITICS OR METASEDS	2.90
GRANITICS OR METASEDS	2.90
GRANITICS?	2.80
DIKE?	2.50
BASEMENT	2.67

ELEVATION (KM)

5.0 X VERT EXAG

FIGURE BY S.CARLE

LOCATION

119° W

82
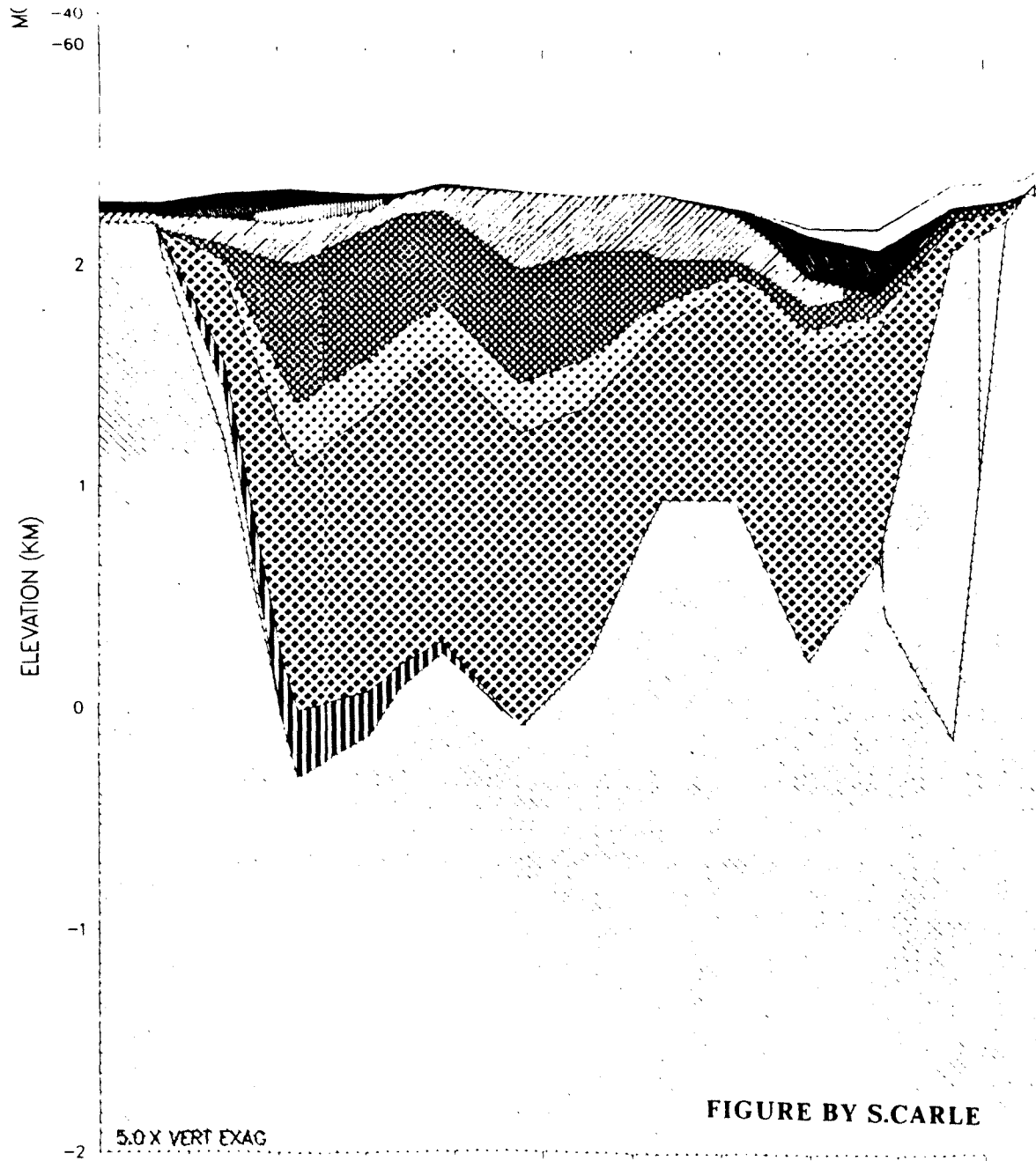
Figure 8

Figure 9

• VP101 Data
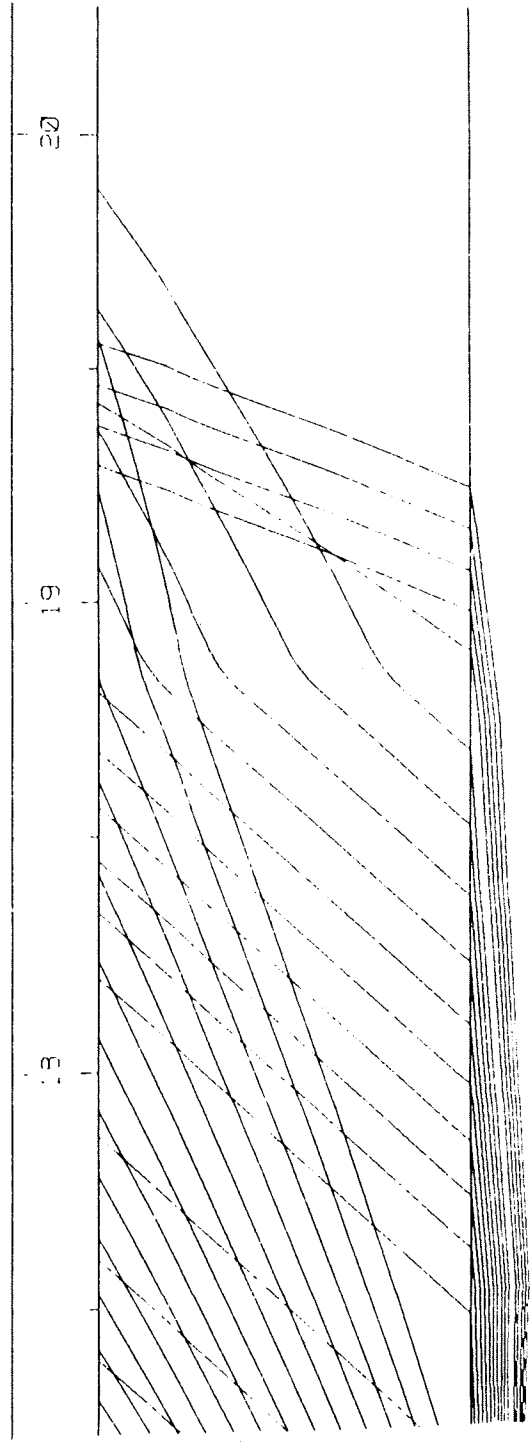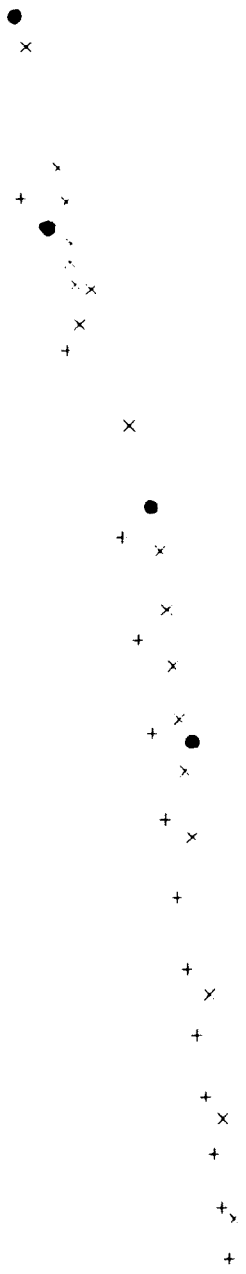
Southern spread Model after Carle.

83

Analysis of Long Valley Spectral Data Using
The NEWT System

by

S. McNutt
California Department of Conservation
Division of Mines & Geology
630 Bercut Drive
Sacramento, CA 95814

A NEWT seismic system is operated by the California Division of Mines and Geology to monitor earthquakes in the Long Valley region. The system is primarily used to evaluate spectral properties of earthquakes that may be of volcanic origin, in order to improve the State's emergency response capabilities. NEWT automatic processing includes determination of earthquake magnitudes and locations, computation of FFT spectra (depending on location), and plotting of spectra and seismograms. Figure 1 shows a seismic station location map. From July 1984 to March 1987, 8,500 events were recorded, and spectra have been obtained for about 30 percent of the total. Spectra are computed for all events between latitudes 37.4° and 37.8°N, and longitudes 118.5 and 119.1°W, including events both inside and outside Long Valley caldera. Spectra are corrected for instrument response and Q (Q = 500 for P-waves and 300 for S-waves), and are fitted with a theoretical curve based on Brune's source model. Examples of spectra are shown in Figure 2.

The purpose of this study is to present preliminary results of a systematic evaluation of NEWT S-wave spectra. The study consists of three parts: 1) comparison of spectra for earthquakes of different magnitudes but the same location; 2) comparison of spectra for earthquakes of similar magnitudes both inside and outside the caldera; and 3) comparison of spectra

for a low-frequency event to spectra for "normal" earthquakes with similar magnitudes and locations. Each part is treated separately below.

1. A swarm of 41 earthquakes occurred from February 26-March 6, 1987, in the Sierra block south of Long Valley caldera, near Red Slate Mountain. Magnitudes ranged from 0.9 to 4.2, and locations were within one minute of latitude 37° 31'N and longitude 118° 52'W, with a depth of 9 $\pm$ 2 km. Corner frequencies of these events range from 1.7 to 8.8 Hz, with larger events having systematically lower corner frequencies (Figure 3a). Events with magnitudes smaller than 2.4 have corner frequencies which fall into two groups: lower than 4.7 Hz and greater than 5.6 Hz (for station CNOC). The events with the lower corner frequencies fall on the same trend (Figure 3a) as the events with magnitude larger than 2.4. The others define a separate higher frequency group, suggesting higher stress drops. Alternatively, the larger numbers of smaller events may simply show more scatter in the data than is observed for the relatively few larger events.

2. Spectra from 24 earthquakes inside the caldera were compared to the spectra of Sierra block events. The caldera earthquakes range from magnitude 1.3 to 2.5, and are located in the south moat, at the northeast edge of the resurgent dome, and under the center of the resurgent dome. Corner frequencies for these events lie in a similar range (2.8-9.2 Hz for station CNOC) to those of the Sierra block events, and also fall into the same two groups (Figure 3b). Based on evaluation of corner frequencies alone, the caldera earthquakes cannot be distinguished from the Sierra block earthquakes, although visual inspection of the seismograms does reveal some subtle differences.

85

3. An apparent low-frequency event of magnitude 2.6 occurred at 10:26 on
    July 19, 1986 at 37° 29'N, 118° 54'W, with the depth poorly
    constrained but probably shallow ($<$3 km). S-wave spectra for this
    event show corner frequencies about 0.4 Hz lower than corner frequencies
    of other events with similar magnitudes and epicenters. In addition,
    coda spectra for the low-frequency event show corner frequencies 0.7 Hz
    lower than S-wave spectra, instead of the 0.2-0.4 Hz difference observed
    for most other events. The July 19, 1986 event is thus only marginally
    lower in corner frequency than other events, although its P-wave arrivals
    are more emergent and it lacks clear S-wave arrivals. The shallow depth
    ($<$3 km), which is poorly constrained, may be the reason for the
    anomalous seismogram appearance.

In summary, spectral analyses to date show mostly similarities between events
inside and outside Long Valley caldera. Earthquakes smaller than magnitude
2.4 have corner frequencies falling into two groups, which may reflect
differences in stress drop or scatter in the data. A previously identified
low-frequency event has only slightly lower corner frequencies than other
events, although its seismograms appear anomalous.

Figure 1

NEWT SEISMIC STATION LOCATION MAP   MARCH 1987
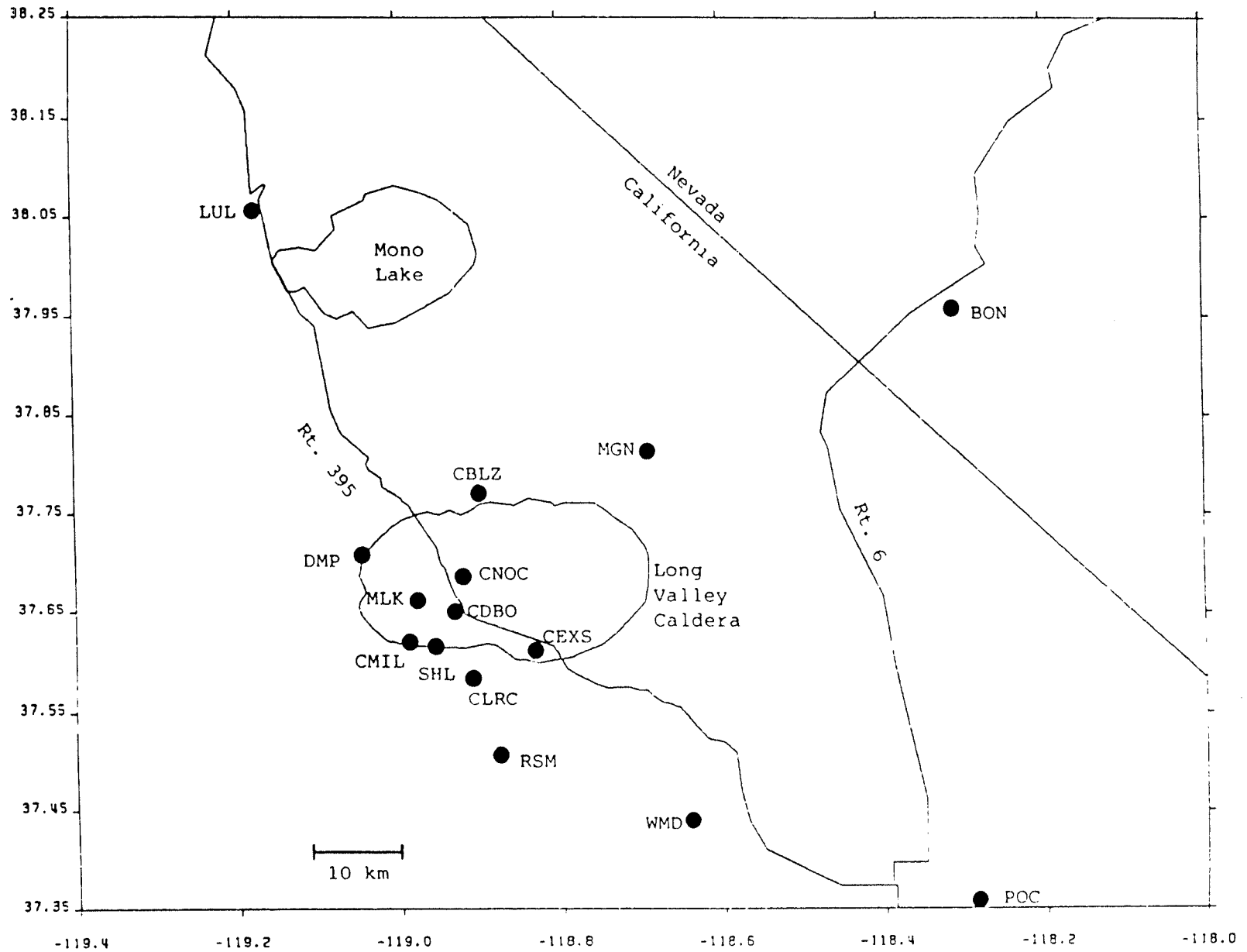
Figure 2

Examples of NEWT spectra for a M1.6 event 870226 14:22:34.81 37N31.52 118W52.05 9.6km

F00270.DAT

P   S   CODA   CALIB

CEXS

BAD OFFSET

27.06 START 39.6 LEN 5.1   43.16 START 39.6 LEN 20.0   CEXS

                    W= 21.27   W= 30.15
0:0   E: 0.02   0:1   E: 0.08   1X 1.00

S:2   S:2
F= 9.34   F= 3.25   D= 14.1

27.06   43.16

CNOC

1.17 START 39.1 LEN 2.8   5.68 START 41.8 LEN 5.1   9.07 START 41.8 LEN 20.0   CNOC

                W= 0.88   W= 4.10   W= 5.49
0:1   0.03   0:1   E: 0.04   0:1   E: 0.03   1X 1.00

S:3   S:3   S:2
F= 7.92   F= 7.08   F= 3.95   D= 23.9

1.17   5.68   9.07

WMD

3.24 START 39.6 LEN 3.1   11.75 START 42.6 LEN 5.1   20.19 START 42.6 LEN 20.0   WMD

                W= 2.16   W= 8.78   W= 12.34
0:0   E: 0.04   0:0   E: 0.02   0:1   E: 0.08   1X 1.00

S:2   S:2   S:2
F= 5.65   F= 3.28   F= 3.13   D= 24.3

3.24   11.75   20.19
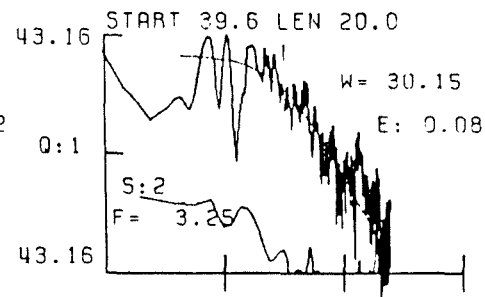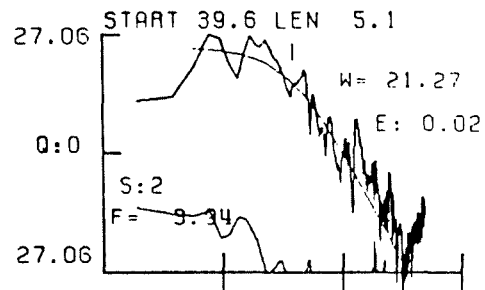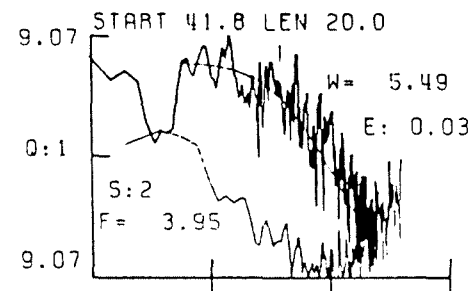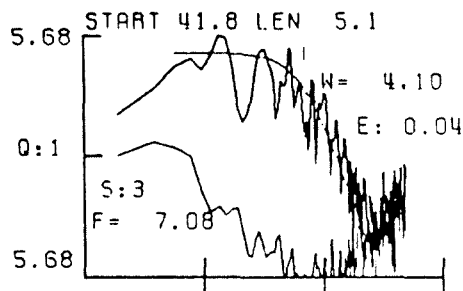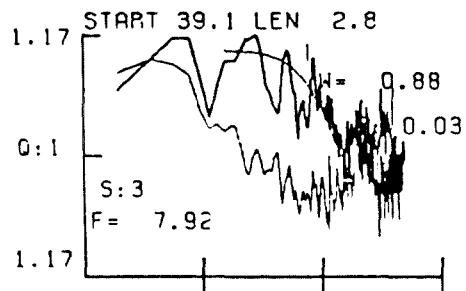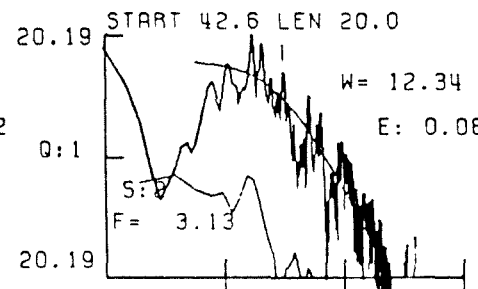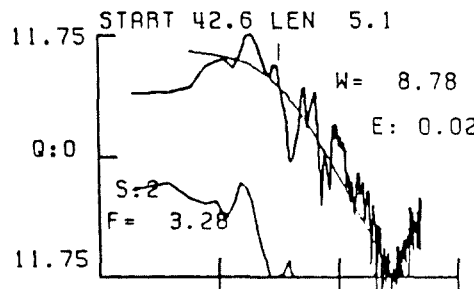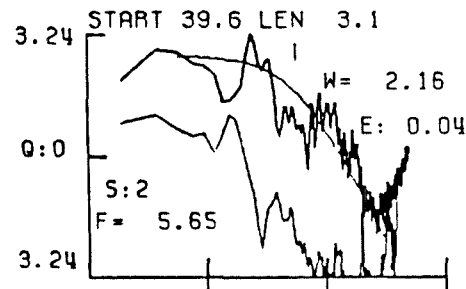
Figure 3. S-wave corner frequency vs. magnitude for earthquakes near and inside Long Valley caldera. Solid circles are NEWT-determined S-wave corner frequencies, the open circle is a value corrected from a coda corner frequency, and the triangles are Sierra block corner frequencies from events near the low-frequency event of July 19, 1986. "LF" indicates the low-frequency event.

Analysis of Borehole Seismograms from
Long Valley, California

G.J. Elbring and J.B. Rundle

Sandia National Laboratories
Alburquerque, New Mexico

In the fall of 1984, a three-component seismometer was emplaced in borehole OLV-1 (see Figure 1) at a depth of about 900 meters. Microearthquakes were recorded using this seismometer for a period of two months. Recording these events at a position beneath most of the caldera fill avoided much of the attenuation and multiples associated with such fill and provided much more interpretable records.

Concentrating on the region of greatest seismic activity and structural interest, we confined our analysis to events with azimuths between $130°$ and $180°$ from the well location. The events analyzed were then further restricted to provide a wide range of hypocentral depths. The positions of the events used are shown in Figures 1 and 5. Finally, the traces for both the vertical and two horizontal components were plotted as a function of depth versus time (Figure 2). Although these form unreversed "vertical hypocentral profiles" (VHP), interpretation of these sections should provide some information about the structure beneath the caldera.

Trial and error ray tracing was done to attempt to match both the compressional and shear wave arrival times. Example rays through the final P-wave velocity model and the travel times calculated for these rays plotted on the vertical component VHP section are shown in Figure 3. The abrupt delay in the P-wave first arrival at about 7 km depth is modeled as being a result of a low-velocity midcrustal body beneath the southern end of the resurgent dome. A secondary P-wave arrival about 0.3 s after the first arrival is explained by the model as a reflected phase from a dipping reflector beneath the northern end of the resurgent dome.

Modeling of the S-wave sections show similar features (Figure 4) with the addition of a secondary reflector to account for the small amplitude first arrival in the deeper parts of the VHP section. The final velocity model with both the P and S velocity structure is shown in Figure 5. Examinati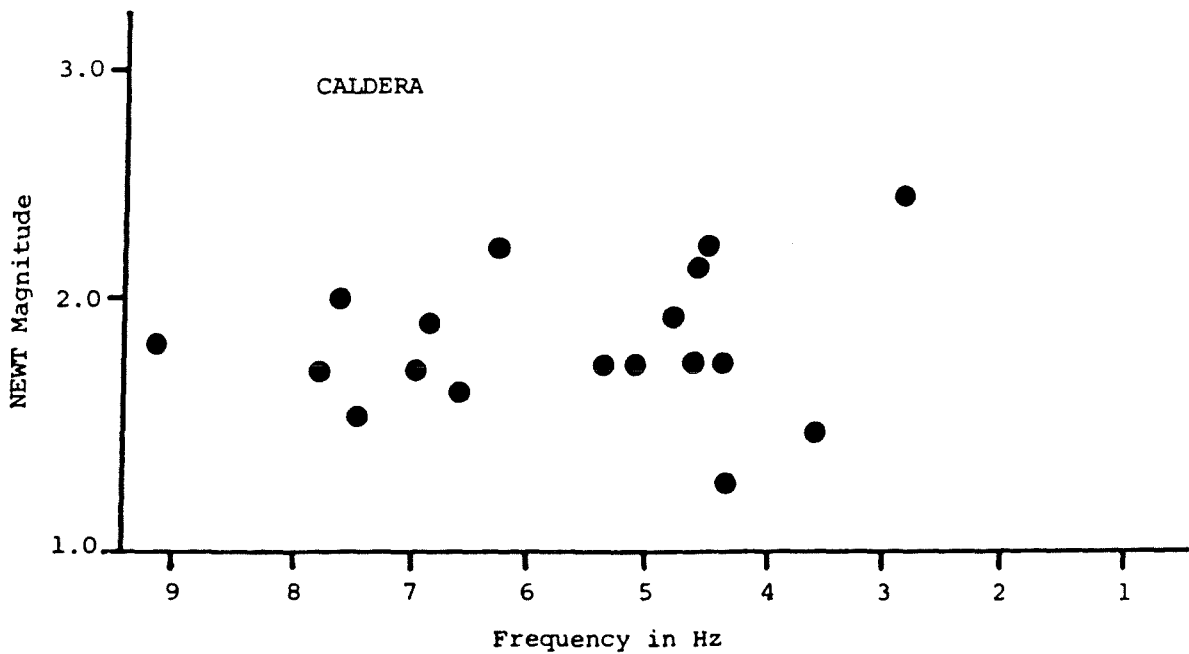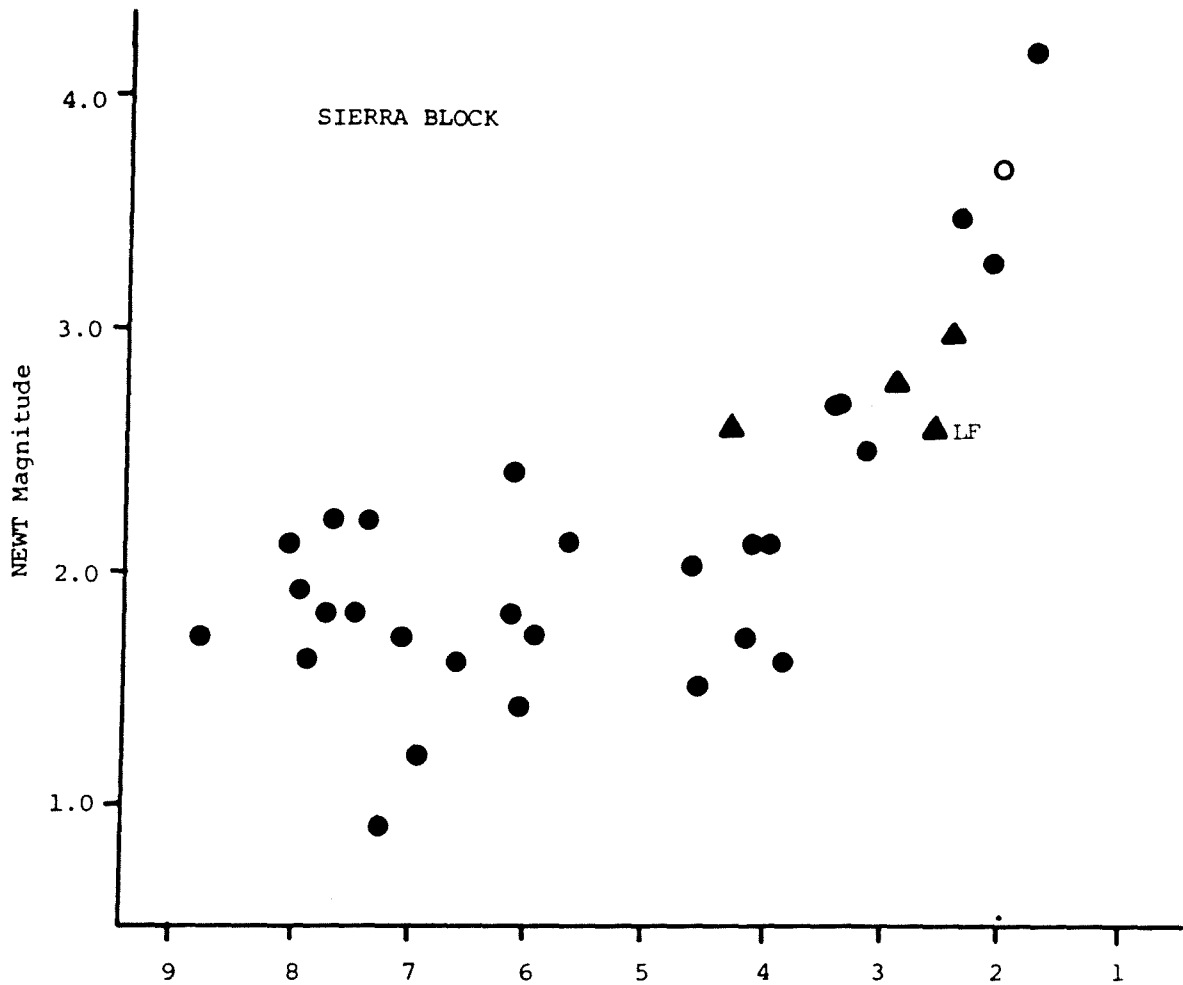on of the V_p/V_s ratio for different regions of the model shows a large increase in the ratio for the midcrustal low-velocity body. This would be expected if the zone were partial melt, normally characterized by a decrease in P-wave velocity accompanied by a greater decrease in the S-wave velocity resulting in an increase in the V_p/V_s ratio.

Based on these results, a final geologic interpretation is shown in Figure 6. The shallow structure is based on previous refraction work (Hill, 1985). The midcrustal low-velocity body is modeled as magma along with the region below the dipping reflector. The nature of the region below the reflector is only an assumption, however, since velocities are not defined for this area by this study. An altered zone is pictured surrounding this region to account for the secondary reflector seen in the S-wave data. Although this profile is not reversed and contains errors due to inaccuracies in the hypocentral locations, the model does agree well with previous studies of the area and provides a reasonable explanation of the observed travel times.

References

Hill, D. P, E. Kissling, J. H. Luetgert, and U. Kradolfer, Constraints on the upper crustal structure of the Long Valley-Mono Craters volcanic complex, eastern California, from seismic refraction measurements, J. Geophys. Res., 90, 11135-11150, 1985.

Luetgert, J. H., and W. D. Mooney, Crustal refraction profile of the Long Valley caldera, California, from the January 1983 Mammoth Lakes earthquake swarm, Bull. Seismol. Soc. Am., 75, 211-221, 1985.

Murphy, W. J., E. Renaker, M. Robertson, A. Martin, and P. Malin, The 1985 Mammoth wide-angle seismic reflection survey, EOS Trans. AGU, 66, 960, 1985.

Rundle, J. B., and J. H. Whitcomb, A model for deformation in Long Valley, California, 1980-1983, J. Geophys. Res., 89, 9371-9380, 1984.

Rundle, J. B., et al.; Seismic imaging in Long Valley, California, by surface and borehole techniques: An investigation of active tectonics, EOS Trans. AGU, 66, 194-200, 1985.

Sanders, C. O., Location and configuration of magma bodies beneath Long Valley, California, determined from anomalous earthquake signals, J. Geophys. Res., 89, 8287-8302, 1984.
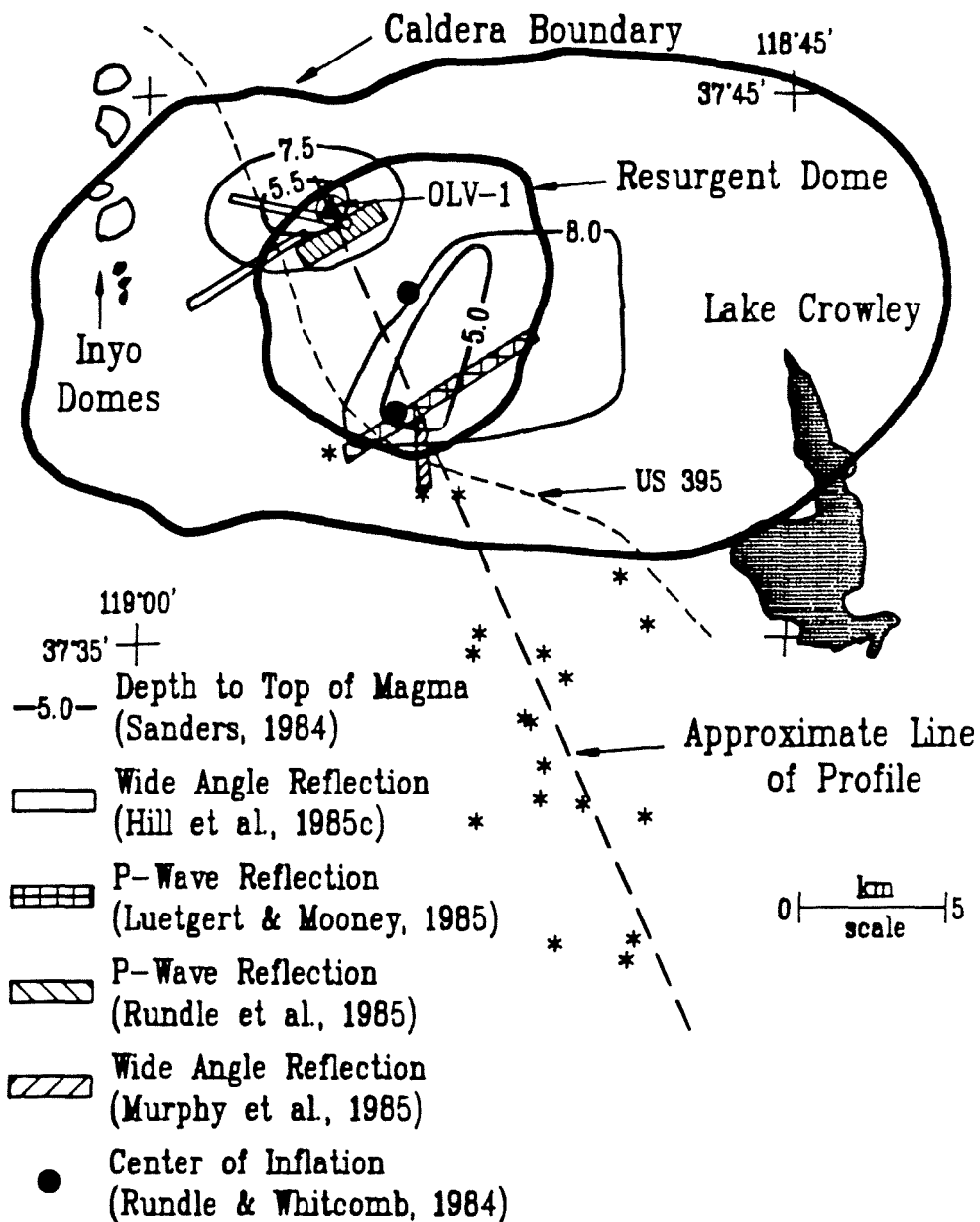
Fig. 1. Map of Long Valley region showing major physiographic features and subsurface features defined by several previous studies. Locations of well OLV-1 and earthquakes (asterisks) used in the present study are also indicated. Heavy dashed line shows orientation of cross section shown in following figures.
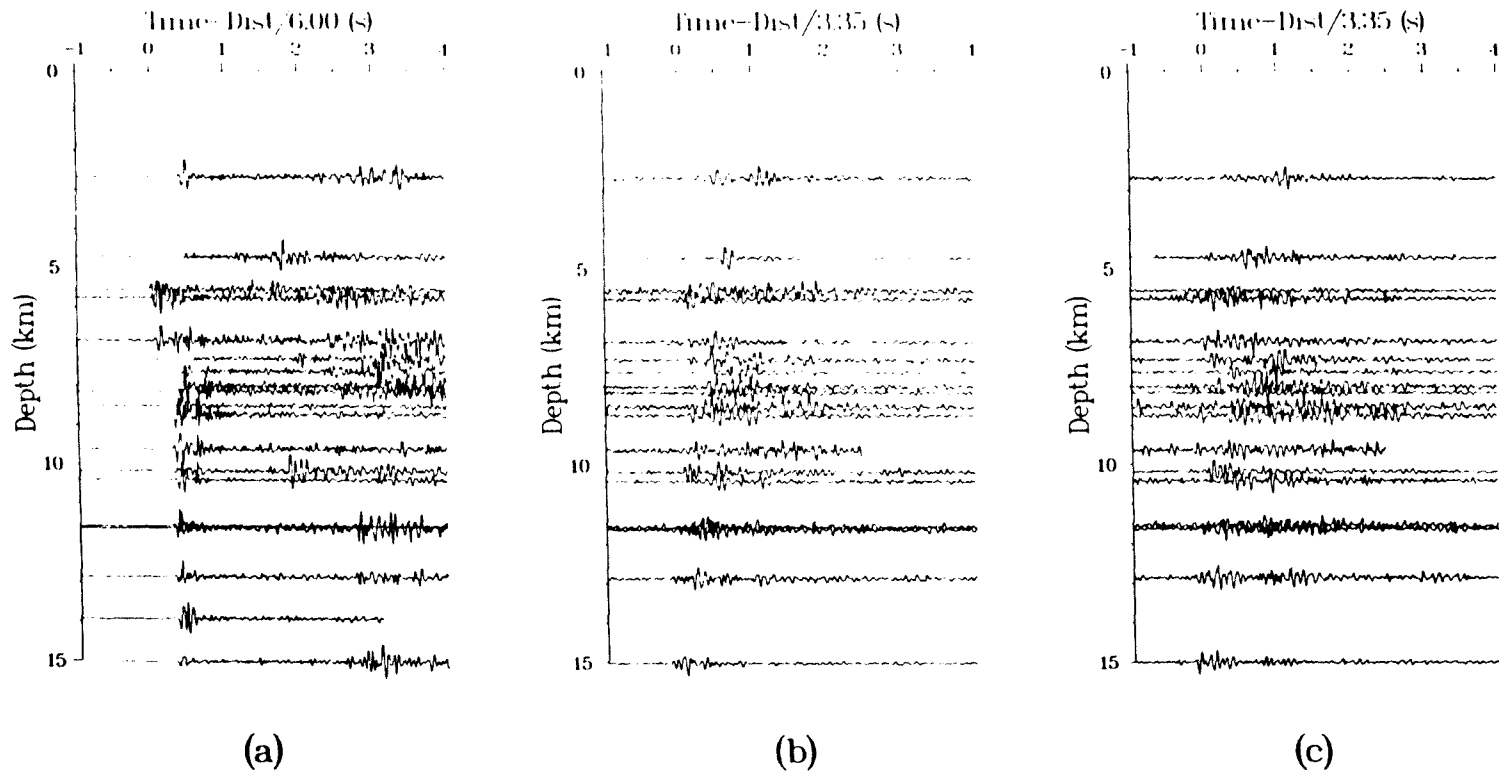
Fig. 2. Vertical hypocentral profiles for the (a) vertical and (b and c) two horizontal components of the borehole seismometer.
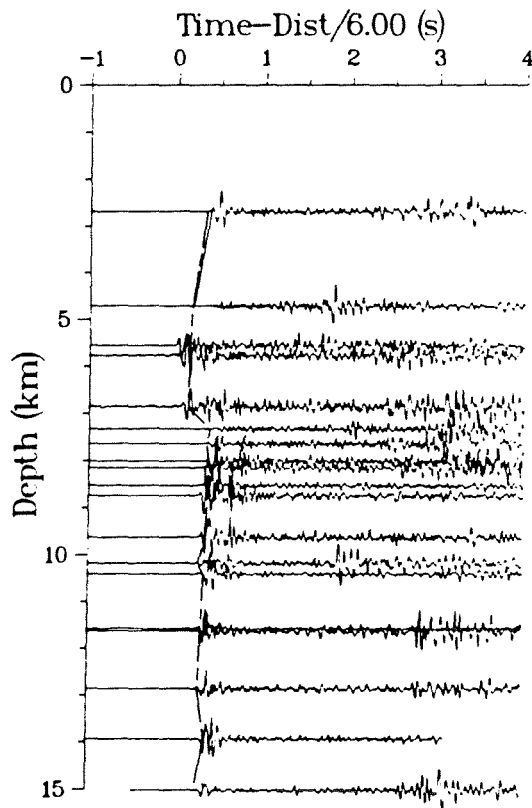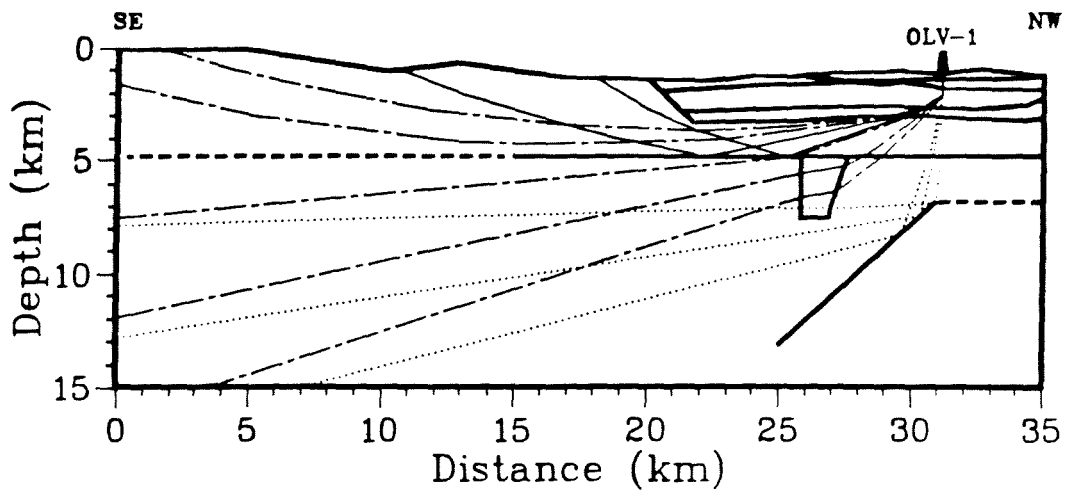
Fig. 3. Ray diagram and travel time curves for vertical component VHP. Phases shown in ray diagram and calculated travel times shown on VHP record section are direct P-wave (dashed), reflected off horizontal interface (solid), and reflected off dipping interface (dotted).
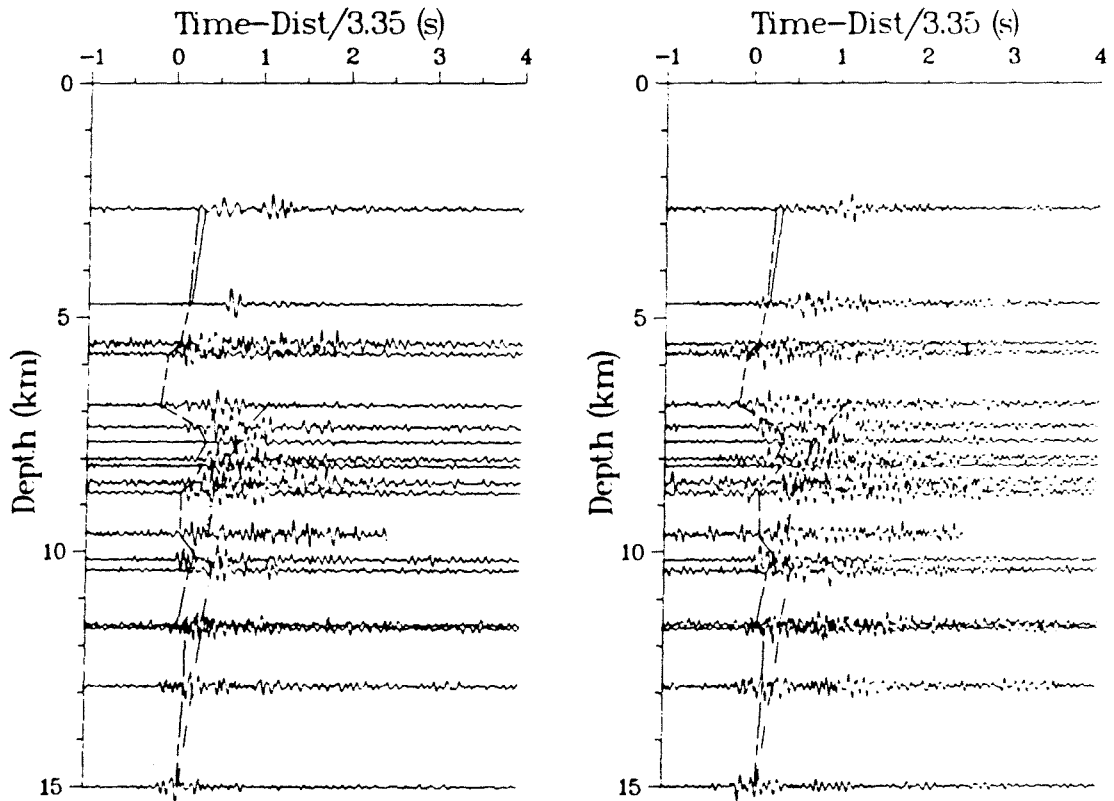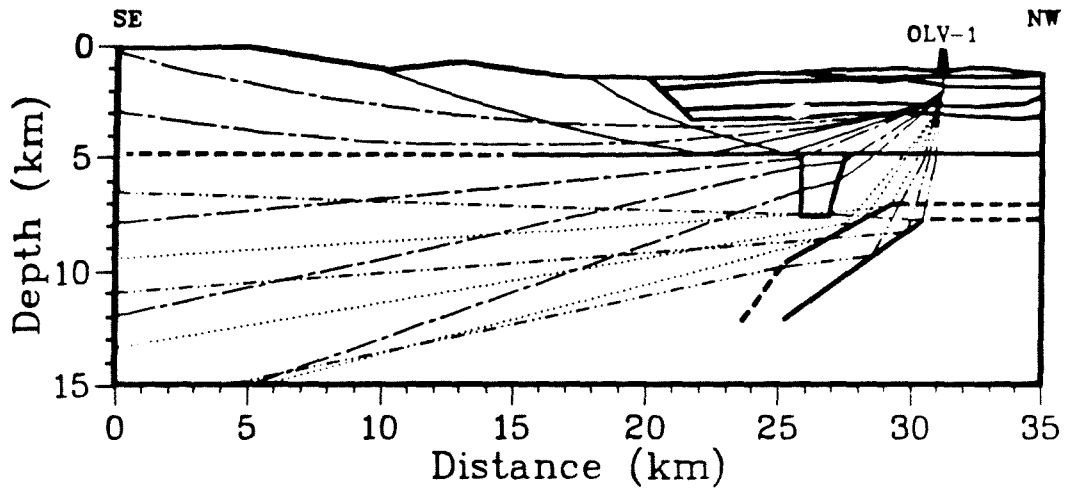
Fig. 4. Ray diagram and travel time curves for horizontal component VHPs. Phases shown in ray diagram and calculated travel times shown on VHP record sections are direct S-wave (dashed), reflected off horizontal interface (solid), reflected off upper dipping interface (dotted), and reflected off lower dipping interface (dash-dotted).
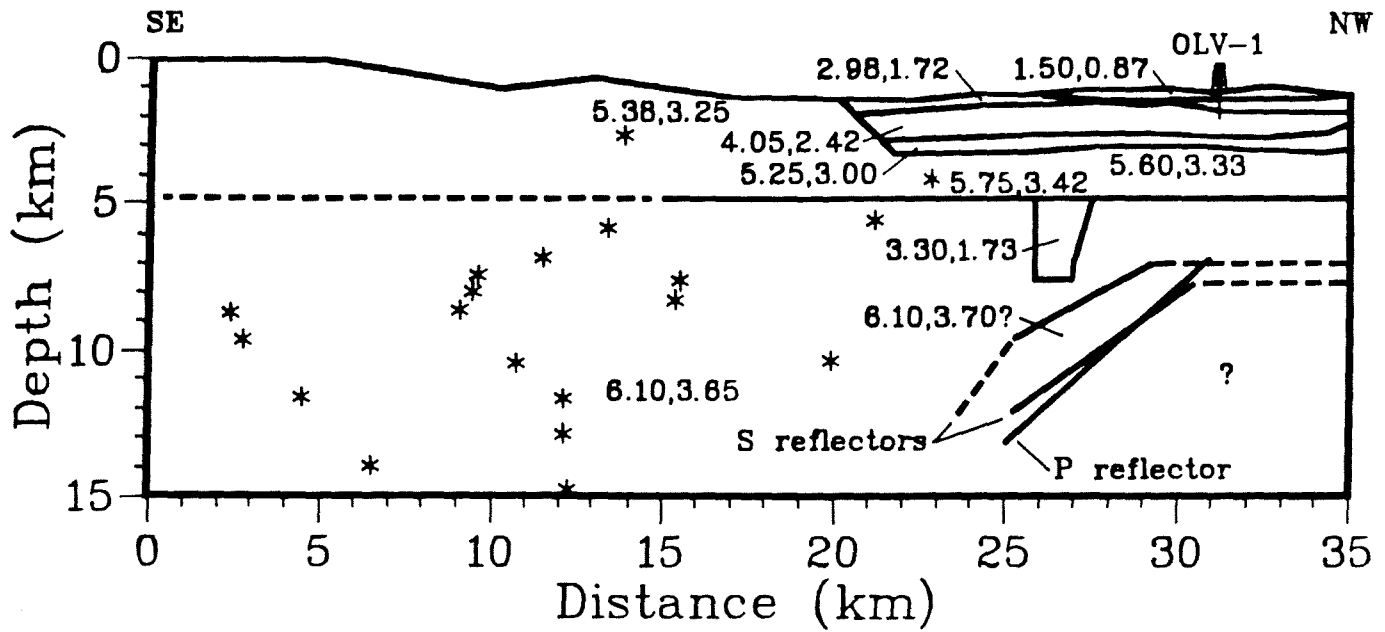
Fig. 5. Final velocity structure showing compressional (first) and shear (second) wave velocities in km/s. Earthquake hypocenters used in the study are again shown as asterisks.
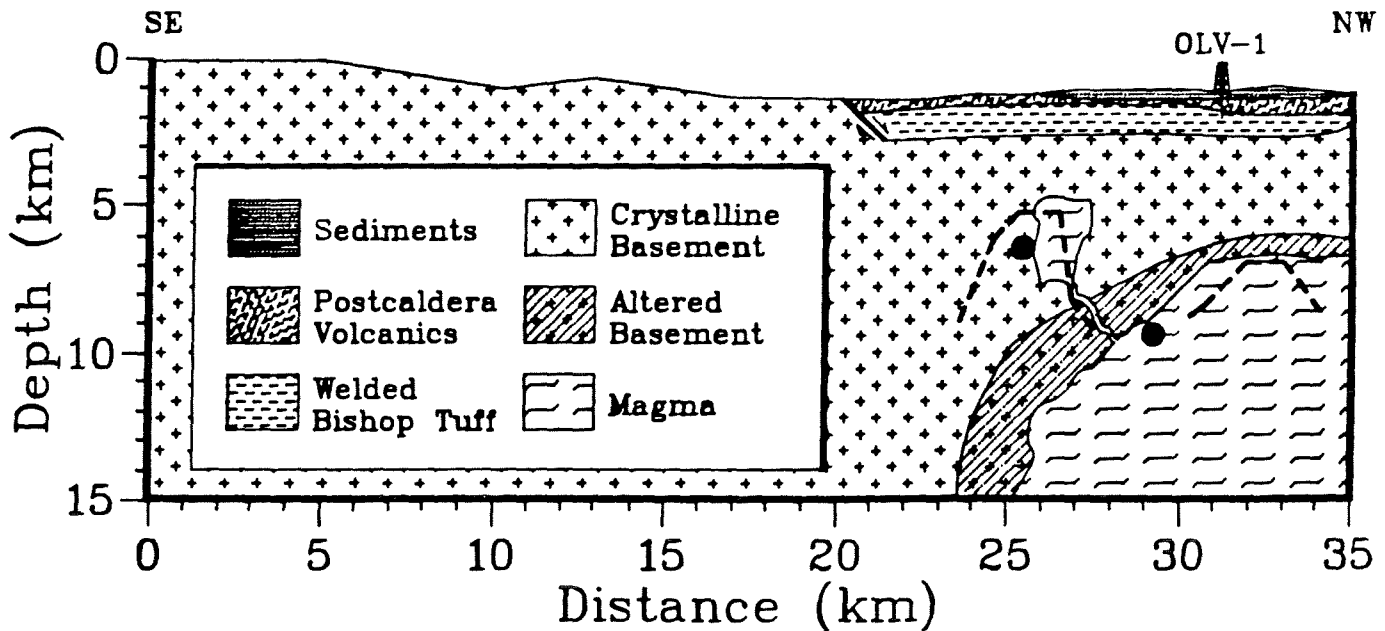
Fig. 6. Idealized geologic structure beneath Long Valley. Heavy dashed lines show outline of magma cupolas defined by Sanders (1984). Solid dots represent centers of inflation modeled by Rundle and Whitcomb (1984).

ABSENCE OF EVIDENCE FOR A MAGMA CHAMBER IN DOWNHOLE
AND SURFACE SEISMOGRAMS FROM LONG VALLEY
CALDERA, EASTERN CALIFORNIA

BY

EGILL HAUKSSON
University of Southern California
Department of Geological Sciences
Los Angeles, CA   90089-0741

From September 22 to October 9, 1984 14 digital recorders were deployed, each with a three-component seismometer, to record local earthquakes in Long Valley, California. The instruments were deployed in two separate clusters. The first cluster of nine instruments was located in the Casa Diablo region above a postulated magma chamber (Sanders, 1984). The second cluster of instruments located 7 km to the north of Casa Diablo and just south of Lookout Mountain, included a three-component seismometer deployed in a 900 m deep borehole OLV-1. (Figure 1). During the recording period 32 local earthquakes were detected by both the USGS seismic network in Long Valley and by the downhole as well as several surface instruments in the Casa Diablo area.

To show that travel time delays exist Elbring and Rundle (1986) used a subset of the downhole data analyzed in this study. They plotted a record section of reduced travel time (using a reduction velocity of 6.0 km/s and slant distance as reducing distance) as a function of hypocentral depth. They derived a crustal model with a low velocity wedge below the Casa Diablo area by fitting the first arrivals and some of the secondary arrivals in the record section. The low velocity wedge was derived from the following observation made by Elbring and Rundle (1986): "Below 7 km the first arrivals in the record section are consistently delayed by as much as 0.4 s when compared to first arrivals in the depth range between 5 and 7 km." Using forward modeling by trial and error they concluded that the low velocity wedge was needed to satify these first arrivals.

To evaluate the applicability of the Elbring and Rundle (1986) method to data recorded by both downhole and surface stations, several tests have been made. First, an evaluation of the appropriate reduction velocity was carried out. Second, the observed and the calculated travel times for a flat layered model are compared. Third, the epicentral distances between the borehole station and the hypocenters from Elbring and Rundle (1986) and recalculated distances from HYPOINVERSE are compared. Fourth, to test for possible variations in the Vp/Vs ratio from 1.67 to 1.9 (as suggested by Elbring and Rundle, 1986) the ts/tp ratio (where tp and ts are the observed P and S travel times, respectively) for each event was plotted as a function of depth. The results of these tests are discussed next.

The velocity model used routinely for earthquake locations in the Long Valley area by the U.S. Geological Survey (e.g., Cockerham and Pitt, 1984) can be used to determine the appropriate reduction velocity. The program HYPOINVERSE was used to calculate travel times through this model from three sets of hypothetical sources located 10, 20 and 30 km away from the borehole station (Figure 2). Each set consists of 29 sources spaced 0.5 km apart from 1.0 to 15.0 km depth. The travel times are plotted with three different reduction velocities (5.7, 6.0 and 6.3 km/s) in the top half of Figure 2. The results show that the 5.7 km/s reduction velocity is more appropriate for the Elbring and Rundle approach than the 6.0 km/s for the range of epicentral distances (10-30 km). Using the higher reduction velocity of 6.0 km/s, Elbring and Rundle (1986) introduce a focal depth dependent spread in the first arrivals of up to 0.25 s.

As an initial test for the presence of large P-wave travel time delays, the difference between observed and calculated travel times is plotted as a function of focal depth in Figure 3. The calculated travel times were obtained by using the flat layered velocity model for the Long Valley region (Cockerham and Pitt, 1984). The systematic bias of 0.2 s is caused by the 900 m elevation difference between the downhole and surface stations. The only significant variation in the travel time difference is the early arrival by 0.2 s from an earthquake at 5.9 km depth. No systematic delay in arrivals can be seen as a function of focal depth.

To obtain the reduced travel time curve in Figure 3 the slant distance between the downhole seismometer and the hypocenter has to be calculated. The slant distance is defined as $\sqrt{D^2+Z^2}$ where D is the epicentral distance and Z is the hypocentral depth. In this study HYPOINVERSE was used to calculate the epicentral distance using the fixed hypocentral parameters (including depth) published by Elbring and Rundle (1986) and initially provided by the U.S. Geological Survey (written comm. R. Cockerham, 1984). The travel times were determined as the difference between the picked P arrival time and the respective origin time published by Elbring and Rundle (1986). The reduced travel time versus depth profile from this study and from Elbring and Rundle (1986) are plotted in Figure 3 at a reduction velocity of 6.0 km/s. The same profile from this study is also plotted at reduction velocities of 5.7 and 6.3 km/s in Figure 3. The first arrivals below 7 km are not delayed with respect to the first arrivals above 7 km depth (as suggested by Elbring and Rundle, 1986). In addition, the reduction velocity of 5.7 km appears to provide a somewhat smoother curve in the depth range of 3 to 10 km. The effect of the choice of reduction velocity however appears to be small and does not explain the substantial difference betweeen the reduced travel time of Elbring and Rundle (1986) and this study.

In an attempt to explain this difference in reduced travel times, the epicentral distances used by Elbring and Rundle were redetermined from the following information: (1) the P arrival times in the reduced travel time curve from Elbring and Rundle (1986); (2) the travel times used in this study, which are the difference between the observed P arrival and the origin time published by Elbring and Rundle (1986) and; (3) hypocentral depth published by Elbring and Rundle (1986). The difference between the Elbring and Rundle epicentral distances and the epicentral distances calculated with

HYPOINVERSE (doing only one iteration step with the same fixed location) are plotted in Figure 4. This depth profile has a similar shape as the reduced travel time profile from Elbring and Rundle (1986) and provides a simple explanation for the shape of the travel time curve reported by Elbring and Rundle (1986) (Figure 3).

Elbring and Rundle (1986) constructed similar reduced travel time versus depth profiles for S-waves. They concluded from trial and error forward modeling of the S arrivals using ray tracing that the Vp/Vs ratio was 1.67 in the upper crust with the exception of the low velocity wedge where they found a Vp/Vs ratio of 1.9. To test their findings of possible variations in the Vp/Vs ratio, the observed ratio of S to P travel times for each earthquake are plotted as a function of depth in Figure 5. The uncertainty in determining P and S travel times is approximately 0.1 s and the uncertainty in depth determination is ±1 km in most cases. The data in Figure 5 illustrate the absence of significant variations of the Vp/Vs ratio with depth.

The values from the Elbring and Rundle (1986) study are also shown for comparison in Figure 5. Because the average total ray path may be 20 km long and only a 3 km long section of the ray path would be within the low velocity wedge, the average change in S travel time caused by the high Vp/Vs ratio within the wedge would be approximately 0.2 s. In the depth range 5-8 km the Vp/Vs ratio (averaged over a 20 km distance) therefore increases from 1.67 to 1.72 because of the high Vp/Vs within the low velocity wedge. It thus follows that the downhole data cannot easily resolve the variation in the Vp/Vs ratio in the low velocity wedge.

Initially, Elbring and Rundle (1986) analyzed a subset of the seismograms included in this study. They used forward modeling based on two dimensional ray tracing to locate two magma chambers beneath the caldera. The shallower chamber was located beneath Casa Diablo at a depth of 3.7 km and had dimensions of approximately 2 km by 6 km. The deeper, larger chamber was located at a depth of 5.5 km near the northern part of the resurgent dome. The results of this study, however, demonstrate that the reduced travel time depth profile for P-waves used by Elbring and Rundle (1986) although a valid procedure, was incorrectly determined. The reduced travel time depth profile determined from this study shows no systematic variation of travel time with depth, and hence does not support the magma chamber concept.

REFERENCES

Cockerham, R. S. and A. M. Pitt. Seismic activity in Long Valley caldera area, California: June 1982 through July 1984, U.S. Geological Survey, Open File Report 84-939, 493-526, 1984.

Elbring, G. J. and J. B. Rundle. Analysis of borehole seismograms from Long Valley, California: Implications for caldera structure, J. Geophys. Res., 91, 12651-12660, 1986.

Sanders, C. O. Location and configuration of magma bodies beneath Long Valley, California, determined from anomalous earthquake signals. J. Geophys. Res. 89, 8287-8302, 1984.

LONG VALLEY CALDERA
DOWNHOLE AND SURFACE STATIONS
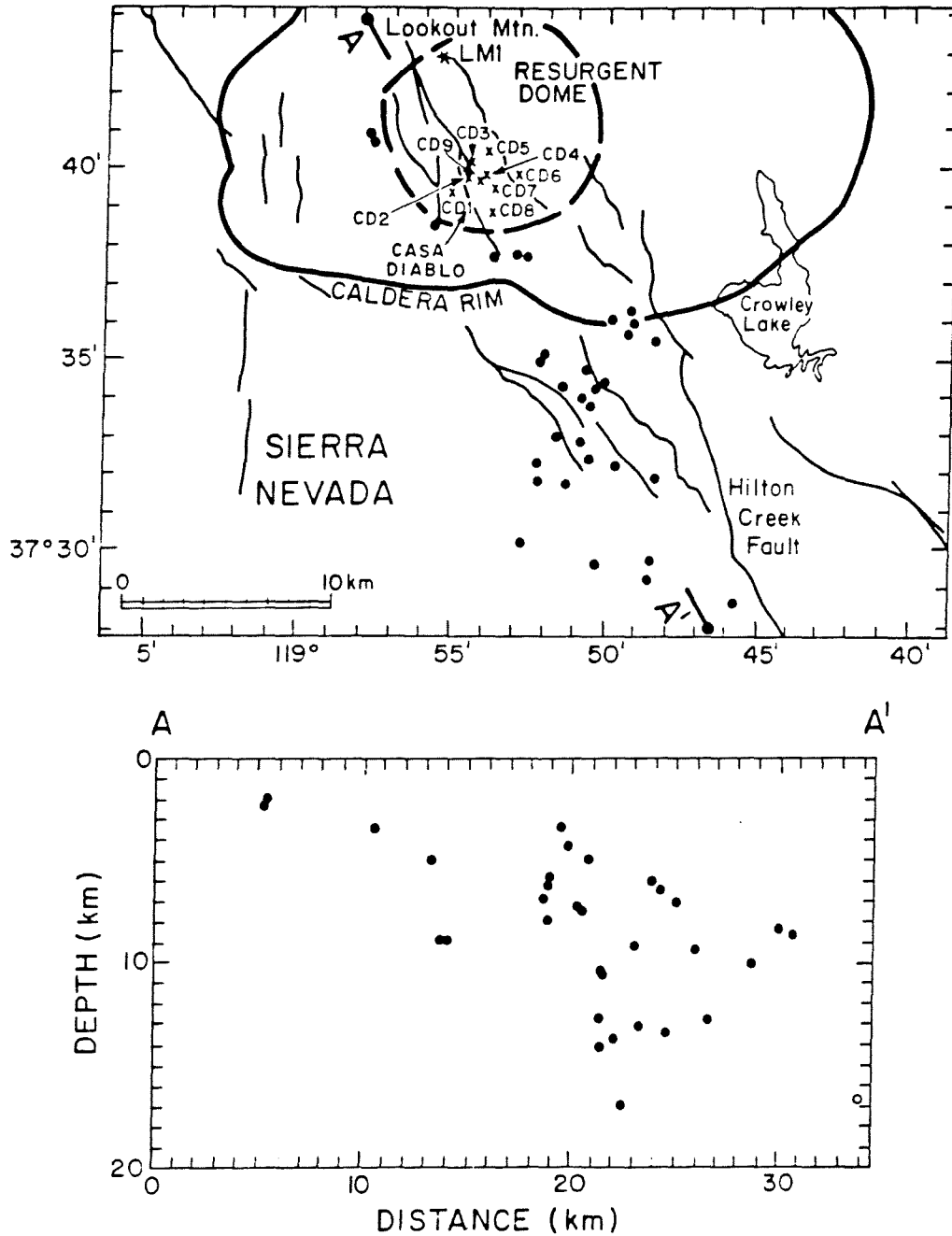
Figure 1. (Top) Map of the Long Valley caldera and surrounding region. The borehole station (LM1) was located just south of Lookout Mountain. Surface stations (CD1-CD9) were deployed in the Casa Diablo area above the proposed magna chamber identified by Sanders (1984). Earthquakes (relocated with HYPOINVERSE; see also Table 1) recorded by the downhole station and some of the surface stations are shown as closed circles. (Bottom) a north-northwest striking cross section showing depth distribution of hypocenters.
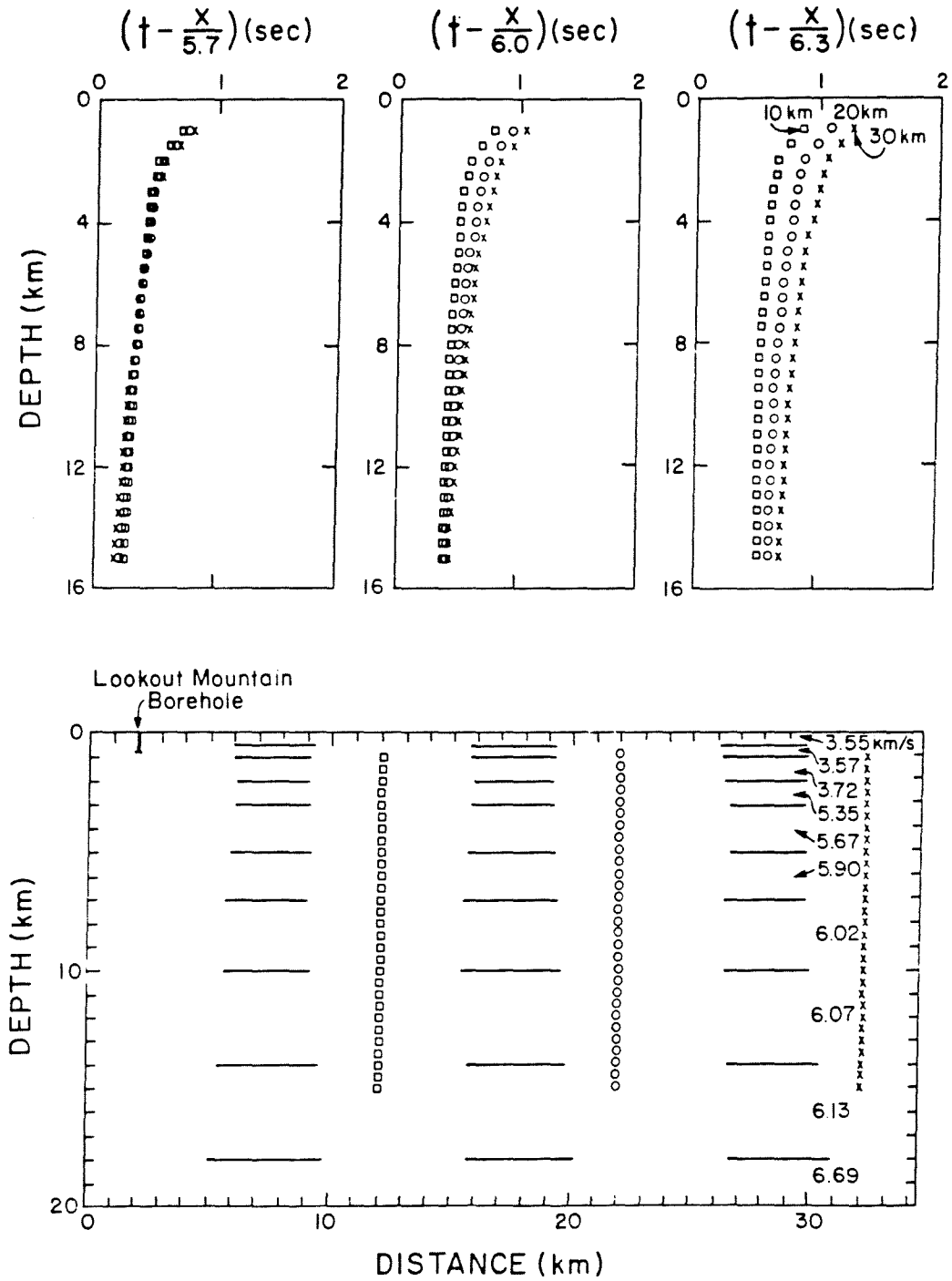
Figure 2. Calculated reduced travel time as a function of depth. Fixed sources are assumed at 10, 20, and 30 km distance away from the borehole site and HYPOINVERSE is used to calculate travel times and epicentral distances. Crustal velocity model is from Cockerham and Pitt (1984). Note how different reduction velocities affect the relative arrival times.
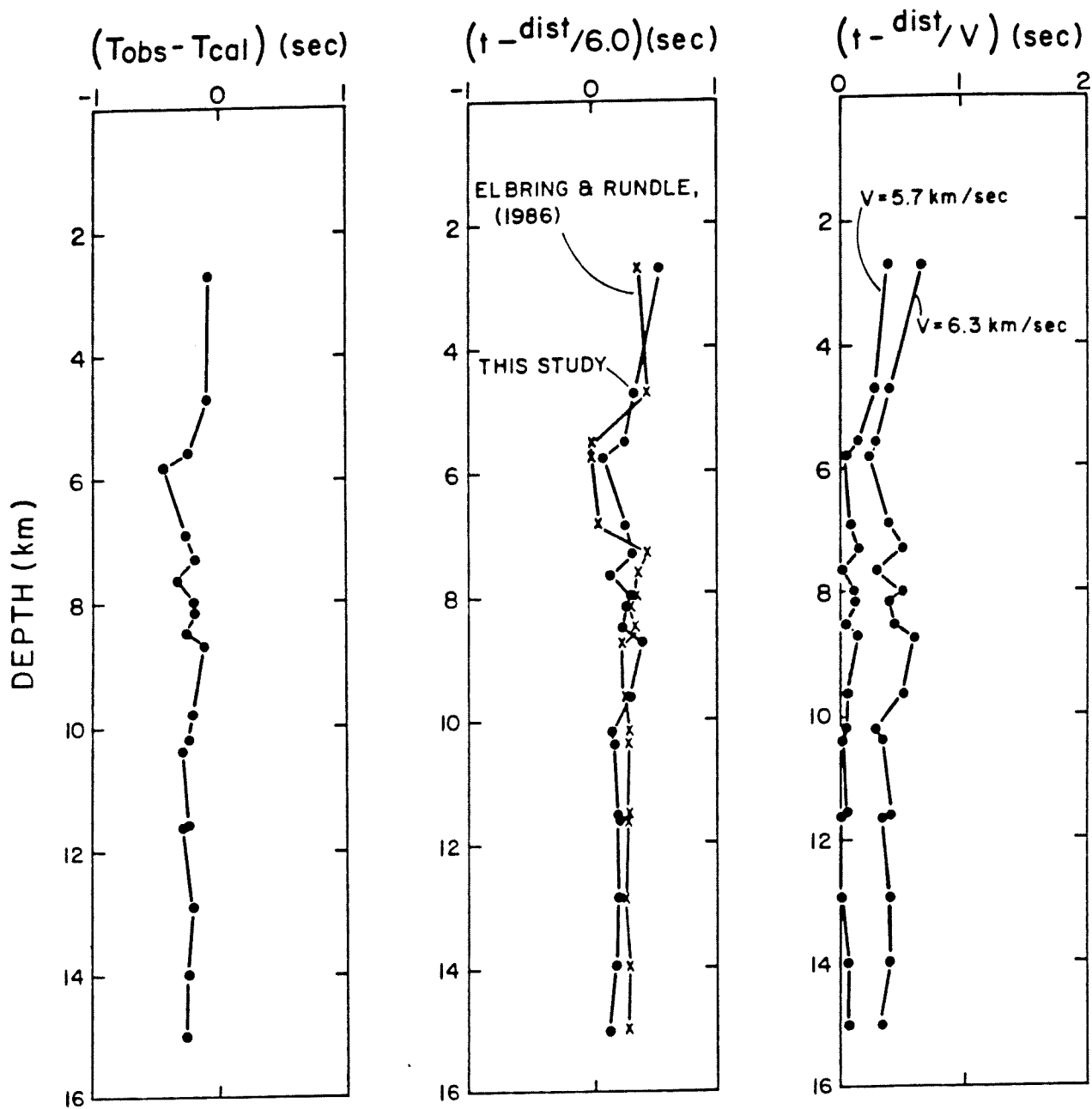
Figure 3. (Left) Difference between observed and calculated travel time plotted as a function of focal depth. (Center) A comparison of reduced travel time versus focal depth from Elbring and Rundle (1986) and from this study. Also shown (Right) are the data from this study plotted at different reduction velocities. Only data from the 19 events studied by Elbring and Rundle (1986) are included.
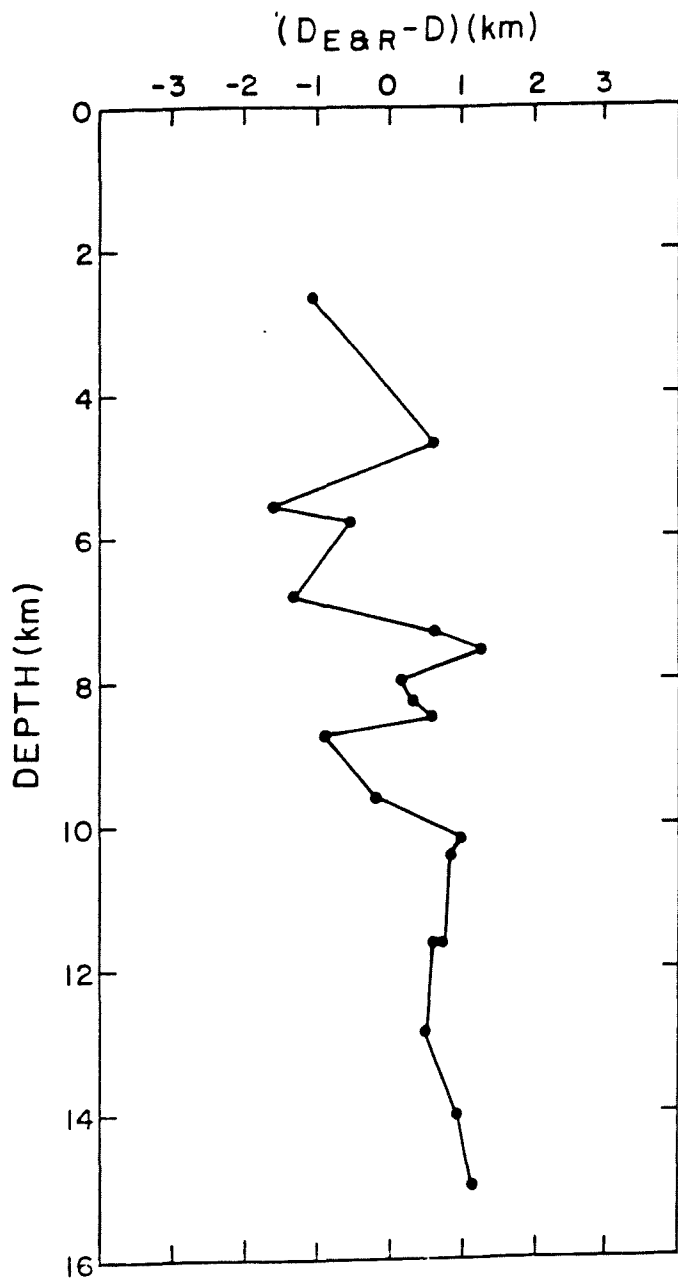
Figure 4. Difference in epicentral distance used by Elbring and Rundle (1986) and the epicentral distance calculated by HYPOINVERSE for the same hypocenters and the same borehole station location.
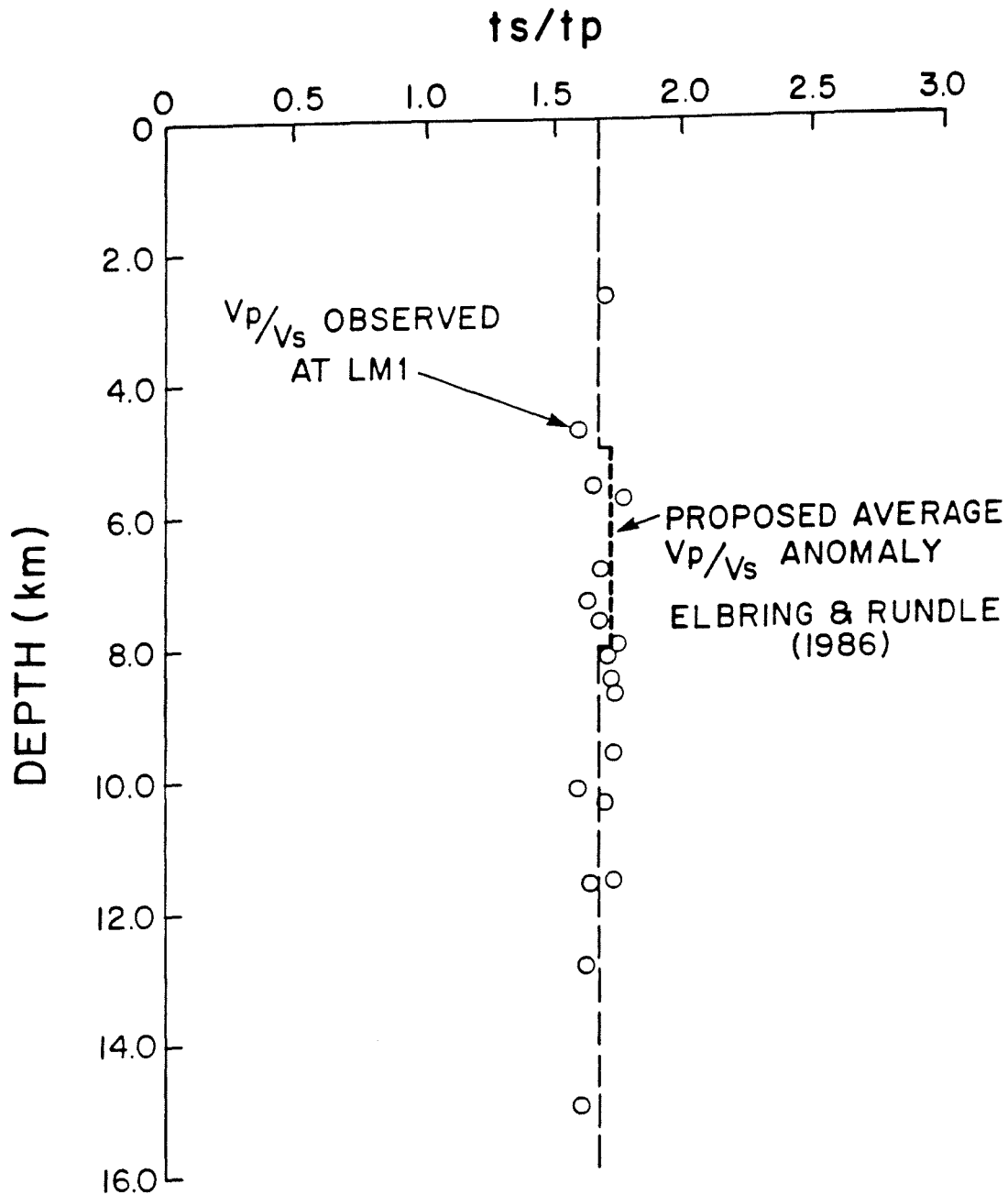
Figure 5. Observed S travel time divided by observed P travel time at the borehole station (LM1) plotted as a function of hypocentral depth. The Vp/Vs ratio found by Elbring and Rundle (1986) is also plotted for comparison. Only data from the 19 events studied by Elbring and Rundle (1986) are included.

Preliminary Analysis of 3-Component Seismograms for
S-Wave Attenuation in Long Valley Caldera

C. O. Sanders and W. L. Ellsworth

U. S. Geological Survey, Menlo Park, CA

Preliminary analysis of 3-component seismograms from earthquakes recorded by portable seismic stations (16) deployed in the Long Valley caldera region, eastern California, from June to November 1984 reveals complexities in the S-wave attenuation structure in the caldera. Seismograms from two 8-km-deep earthquakes located near Casa Diablo and recorded at seismic stations to the NW and E-SE are relatively simple, with clear P- and S-wave arrivals. Seismic stations located at azimuths from N to E-NE record complex seismograms with multiple secondary arrivals and extended coda. Interpretation at present is difficult, but S-wave energy traveling through the caldera seems to suggest that attenuating structures can not be large and continuous. Simple seismograms recorded at these stations from a shallow earthquake beneath Mammoth Mountain and from a deep earthquake southeast of the caldera confirm the anomalous nature of deeper travel paths through the central Long Valley caldera. Detailed study of digital data, including polarization, spectral, travel-time, and first motion analysis of S, P, and other phases will help illuminate the finer structure of the caldera above about 8 km depth.

Deep Structure of Long Valley, California, Based on Deep Reflections from Earthquakes.

John J. Zucca and Paul W. Kasameyer

Lawrence Livermore National Laboratory
P.O. Box 808,
Livermore, CA 9455u

Knowledge of the deep structure of Long Valley comes primarily from seismic studies. Most of these efforts have focussed on delimiting the top of the inferred magma chamber. We present evidence for the location of the bottom of the low velocity layer (LVL). Two other studies have provided similar information. Steeples and Iyer (1976) inferred from teleseismic P-wave delays that low-velocity material extends from 7 km depth to 25 to 40 km, depending on the velocities assumed. Luetgert and Mooney (1985) have examined seismic refraction data from earthquake sources and have identified a reflection that appears to be from the lower boundary of a magma chamber. They detected the reflection with a linear array of single component stations, and assuming it traveled in a vertical plane, matched the travel time and apparent velocity (6.3 km/sec) to deduce that it was a P-P reflection from within a LVL. We recorded a similar phase with a 2-dimensional array of three-component stations, and carried out a similar analysis, but utilized additional information about the travel path, particle motions and amplitudes to constrain our interpretation.

Our data comes from a passive seismic refraction experiment conducted during August 1982. Fourteen portable seismograph stations were deployed in a network with approximately 5 km station spacing in the Mono Craters region north of Long Valley (Figure 1). The network recorded earthquakes located south of Long Valley and in the south moat. Three components of motion were recorded at all sites. The data represent one of the few times that three-component data has been collected for raypaths through a magma chamber in the Long Valley area.

DATA The array operated in an individual station triggered mode. Although more than 100 events were recorded by elements of the array, only the three earthquakes shown in Figure 1 triggered a large portion of the array.

Figure 2 shows the vertical component record sections for one of the three events. The three record sections have different characters. All show the P arrival quite clearly, but only EQ1 and EQ3 show a clear S arrival. The horizontal component data mirror the vertical component data including the lack of a clear S arrival from EQ2. For EQ1 a very prominent arrival occurs between the P and S arrivals. We call this arrival the Pr arrival after the notation used in Luetgert and Mooney (1985). There is also a faint suggestion that the Pr arrival exists from EQ3. Note that the solid lines in Figure 2 show correlations only; they do not represent computed travel times from a model.

The relative amplitude relationships of the Pr phase are important. At the traces where Pr is observed, the P arrival is the smallest amplitude, the Pr arrival is the next largest, and the S arrival is the largest.

Our data and the Luetgert and Mooney (1985) data are similar in travel time and amplitude relationships, but they obtained more consistent recordings of Pr and observed it from at least seven events. Our Pr phase arrives much later than that of Luetgert and Mooney and has a 10% higher apparent velocity.

We used particle motions and array processing to answer two important questions about the data: First, does Pr arrive at the surface as a P or S wave? This is an important question since the earlier study of these reflected phases recorded vertical component data only, and it is not certain that the phases are P waves. On a vertical versus radial particle component plot, we saw that P and Pr exhibit similar behavior except that Pr arrives at a much steeper angle, indicating that Pr indeed arrives at the station as a P wave. Second, does Pr travel in the vertical plane between the network center and the event or has it been laterally refracted through the high-velocity Sierran basement to the west? Inspection of radial versus transverse component plots suggests that both P and Pr arrive off-axis from the west. This same result was obtained for most of the other stations recording EQ1. However, by treating the network as an array and fitting a plane wave to the Pg and Pr arrivals, we see that the energy traveled straight from the source to the stations. An explanation for this apparent contradiction is that particle motions can be severely effected by near surface structure, but the plane-wave analysis should reflect the overall travel of the wave. Combining the above observations, we conclude, as Luetgert and Mooney (1985) had done for their data, that the Pr phase arrives at the array as a P wave and has sampled deeper in the crust than P, beause of the steeper angle of incidence.

MODELING In the modeling which follows we attempt to explain four sets of observations for EQ1 discussed above. The first is the travel times of Pg, Pr, and Sg. The second is the angle of incidence data from the particle motion analysis. The third is the relative amplitudes of the Pg, Pr, and Sg arrivals and the fourth is the areal variability of the Pr arrival. To model the data we used the computer program SEIS81 (Cerveny and Psencik, 1981) which allows raytracing of both P and S waves through two-dimensional media. We fixed the structure above 5 km depth by using the Hill et al., (1985a) analysis of a USGS seismic refraction profile.

The simple assumption that the event was strike slip is all that is necessary for our amplitude ratio modeling. If the event were not strike slip, we would have to know the focal mechanism very well to do any amplitude modeling.

Two dimensional models, such as the one shown in Figure 3, appear to provide the best fit to the data. This model is based on a LVL centered under Long Valley and Mono Craters. A critical or post-critical reflection from a slightly tilted high velocity-contrast reflector at the base of the LVL produces the large amplitudes. For this model, several features were arbitrarily fixed. The top of the LVL was assumed to be horizontal and fixed at 7.5 km depth below the receivers. The southern boundary was held at the caldera boundary and set to be almost normal to the ray paths at that point. The thickness and velocity in the LVL trade off and are poorly constrained; for this model we set the velocity at 5.0 km/sec. With those assumptions, the depth and tilt of the reflector at the base of the LVL is determined from the average Pr travel time and angle of incidence for the Pr arrival. This feature also allows us to almost match the amplitude data.

DISCUSSION Given that our data set is incomplete and unreversed, we have to rely on other information to constrain the models. The model illustrates many of the features required to fit the available data. To produce the observed amplitudes we need to enhance Pr by including a low-velocity zone underlain by a high-contrast reflector, a Pr take-off angle near 45° from vertical and a reflector geometry that allows post-critical reflections and focuses many rays toward the reflector. The only free parameter in the amplitude calculation is the velocity at the base of the reflector. We require a velocity above 7.0 km/s to produce post-critical reflections that approach the correct amplitude. A velocity as high as 8.1 km/s still produces a reasonable result. To match the travel times with a realistic LVL velocity, the path length in the LVL must be about 35 km, or the overall path must be more convoluted than that shown in Figure 3. To match the incidence angles, either the reflector must tilt to the south or the surface of the LVL must tilt down away from the caldera.

Figure 3 also shows a simplified geologic cross section after Hill, et al. (1985b). The geologic cross-section summarizes knowledge about the size of the magma body. The major features of our data set are that it requires a much larger magma body than is suggested by Hill, et al., (1985b) and also requires a high velocity base to the LVL. The LVL that fits our data extends to near the base of the crust, and from the southern boundary of the caldera to the Mono Craters area. To make the LVL smaller would require a lower velocity.

Although the point of entry into and exit from the LVL are not well determined from our data, the large difference in Pr-P times requires the ray paths to pass through a thicker and wider low velocity zone than is indicated by the "present magma chamber" of Hill, et al (1985b). In our model, the LVL extends to 28 km depth, comparable to the depths of basaltic intrusions suggested by Bailey (1982), and consistent with conclusions of Steeples and Iyer (1976) who suggest that magma could exist down to 25 km.

In this model the LVL is wider than the caldera, a somewhat surprising result, but consistent with the recent work of Achauer, et al (1986), who suggest that the magma body extends north to the Mono Craters area. The unexpected large lateral extent is supported by the fact that to match the travel times we require more than 1 second delay (in two directions) in the LVL, much larger than the values of 0.35s (Steeples and Iyler, 1976) and 0.13 (Achauer et al., 1986) observed for one-way, nearly vertical paths. If the shallow high velocity material is only found directly beneath the magma body, then reflection paths may be more sensitive to delays in the magma than near-vertical teleseisms, which also pass through the anomalously fast material.

These data have several puzzling features, all indicating that the magma body has a complex shape. Why are our Pr-P times so different from those of Luetgert and Mooney? Rundle, (1985) et al, show the structure of the low velocity region beneath the caldera varies considerably. Luetgert and Mooney's reflection could have fortuitously bounced off a different part of the magma chamber. Why is there no Pr arrival observed from EQ2 and only the barest hint of it from EQ3? Two factors may contribute to this. First, since EQ3 is shallower and north of EQ1, its rays would strike the reflector at a steeper angle, and produce pre-critical reflections. Rays traced from EQ3 through the model shown in Figure 3 had Pr amplitudes reduced by a factor of 2 at the north end of the array and a factor of 10 at the south, compared to Pr from EQ1. Presumably, reflections from EQ2 would be even smaller since these rays would be even steeper. Second, the LVL may pinch

out west of the ray paths from EQ1 to the receivers. Figure 1 helps support this hypothesis. Thin solid lines connect EQ1 and EQ3 to stations where Pr is observed and thin dashed lines connect to stations that did not observe Pr. Note that in general the stations on the east side of the network observe Pr whereas the stations on the west side do not.

The interpretation of the high velocity material depends on what rock type can be reasonably assigned to a material with velocity greater than 7.0 km/s. From experimental studies rocks that have velocities greater than 7.0 km/s at lower crustal pressures (approximately 10 kilobars) have a high mafic mineral content. Candidates include gabbro, amphibolite, and gneiss at velocities approximately 7.0 km/s and dunite, eclogite, and peridotite at velocities approximately 8.0 km/s. One possible explanation, therefore, for the high velocity material is that it represents the upper mantle and that the reflector represents the crust-mantle boundary. This seems unlikely however, since that would require a crust much thinner than any of the estimates from regional seismic refraction surveys (Prodehl, 1979; Eaton, 1966). Another explanation is that the high velocity material represents rocks of basaltic (gabbroic) composition that have ponded in the mid-crust during their ascent from the mantle. The injection of basaltic magma into the crust melts the surrounding country rock and is the source for melts of rhyolitic composition (Hildreth, 1981).

Lachenbruch, et al., (1975) calculate that a minimum of 10 km of basaltic intrusions are required to maintain the Long Valley Caldera system for 2 m.y. Our rough estimates of the thickness of the underplating layer suggest it could be thicker. By combining observations of deep post-critical reflections and teleseismic delays, it may be possible to determine the relative amounts of rhyoltic melt and solidified basaltic magma beneath calderas.

REFERENCES

Achauer, U., L. Greene, J. R. Evans and H. M. Iyer (1986). Nature of the Magma Chamber Underlying the Mono Craters Area, Eastern California, as Determined from Teleseismic Travel Time Residuals, J. Geophys. Res., 91, B14, 13,873-13,891.

Bailey, R.A. (1982). Chemical evolution and current state of the Long Valley magma chamber, in Proceedings of Workshop XIX Active Tectonic and Magmatic Processes Beneath Long Valley Caldera, Eastern California, D.P. Hill, R.A. Bailey, A.S. Ryall (eds.), U.S. Geol. Survey Open File Report, 84-939, 25-40.

Cerveny, V., and I. Psencik, (1981). SEIS81, a 2-D seismic ray package, Charles Univ. Prague.

Eaton, J.P. (1966). Crustal structure in northern and central California from seismic evidence, in Geology of Northern California, E.H. Bailey, Ed., Calif. Div. Mines Geol. Bull., 190, 419-426.

Hildreth, W., (1981). Gradients in Silicic magma chambers: Implications for lithospheric magmatism, J. Geophys. Res., 86, 10153-10192.

Hill, D.P. (1976). Structure of Long Valley Caldera, California, from a Seismic Refraction Experiment, J. Geophys. Res., 81, 745-753.

Hill, D.P., E. Kissling, J.H. Luetgert, and U. Kradolfer (1985a). Constraints on the upper crustal structure of the Long Valley-Mono craters volcanic complex, Eastern California, from seismic refraction measurement, J. Geophys. Res., 90, 11135-11150.

Hill, D.P., R.A. Bailey, and A.S. Ryall (1985b). Active tectonic and magmatic processes beneath Long Valley caldera, Eastern California, an overview, J. Geophys. Res., 90, 11,111-11,120.

Lachenbruch, A. H., J. H. Sass, R. J. Munroe and T. H. Moses, Jr. (1976). Geothermal Setting and Simple Heat Conduction Models for the Long Valley Caldera, J. Geophysical Research, 81, No. 5.

Luetgert, J.H. and W.D. Mooney (1985). Crustal refraction profile of the Long Valley Caldera, California, from the January 1983 Mammoth Lakes earthquake swarm, Bull. Seis. Soc. Amer., 75, 211-221.

Prodehl, C. (1979). Crustal structure of the Western United States, U.S. Geol. Surv. Prof. Paper, 1034, 74pp.

Rundle, J.B., G.J. Elbring, R.P. Striker, J.T. Finger, C.C. Carson, M.C. Walck, W.L. Ellsworth, D.P. Hill, P. Malin, E. Tono, M. Robertson, S. Kuhlman, T. McEvilly, R. Clymer, S. B. Smithson, S. Deemer, R. Johnston, T. Henyey, E. Haukson, D. Leary, J. McCraney and E. Kissling (1985). Seismic Imaging in Long Valley, California by surface and borehole techniques: an investigation of active tectonics. EOS Trans Amer. Geophys. Un., vol. 66, no. 18, 194-201

Malin, E. Tono, M. Robertson, S. Kuhlman, T. McEvilly, R. Clymer, S.B. Smithson, S. Deemer, R. Johnson, T. Henyey, E. Hauksson, P. Leary, J. McCraney, and E. Kissling (1985). Seismic Imaging in Long Valley, California, by surface and borehole techniques: an investigation of active tectonics, EOS Amer. Geophys. Un. Trans., vol. 66, no 18, 194-201.

Steeples, D. W. and H. M. Iyer (1976). Low-Velocity Zone Under Long Valley as Determined from Teleseismic Events, J. Geophys. Res., 81, 849-860.
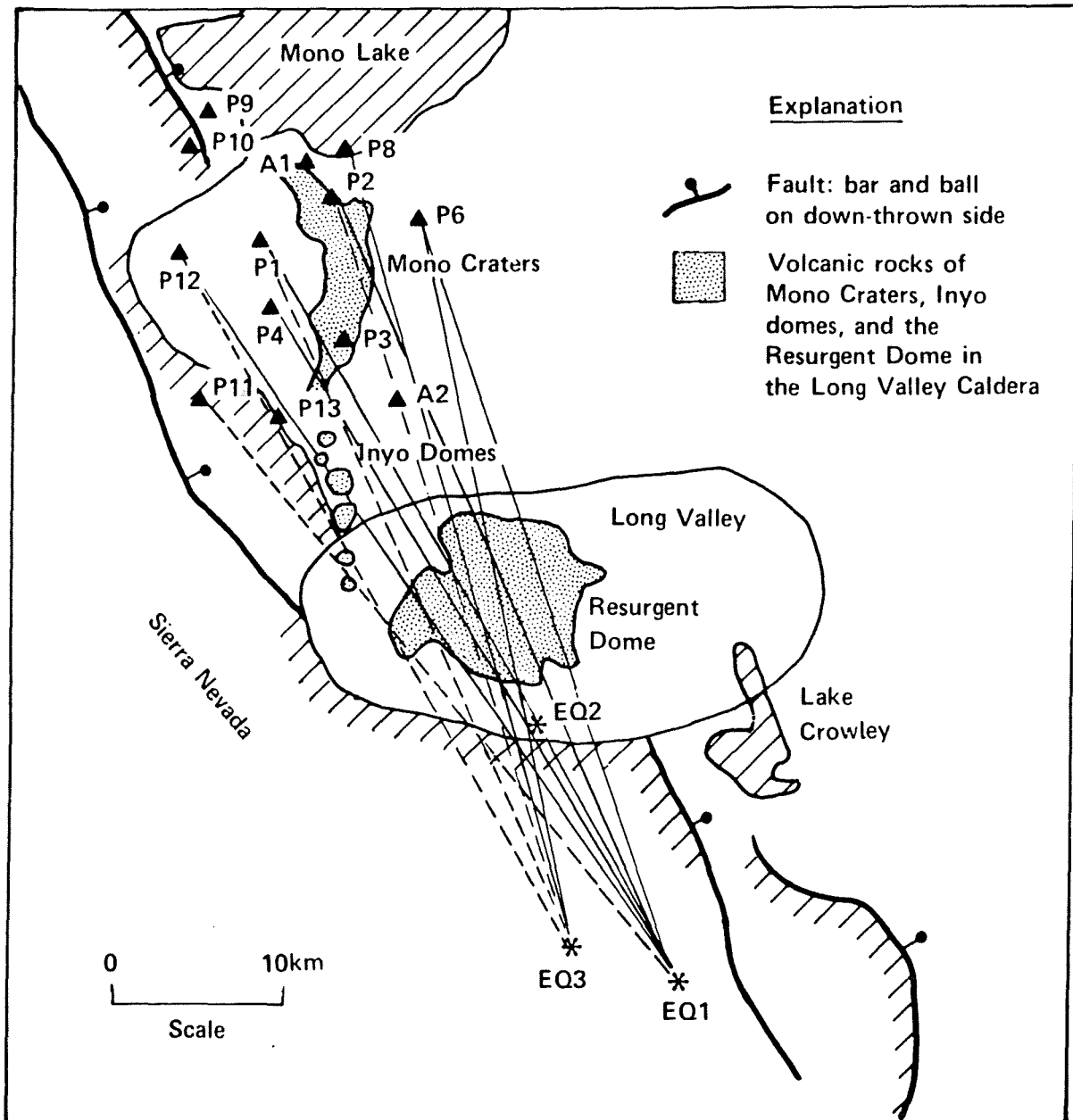
Figure 1. Regional geology and locations map for the LLNL 1982 passive seismic experiment. Solid and dashed lines radiating from EQ1 and EQ3 show along which path the Pr arrival is observed and not observed, respectively.
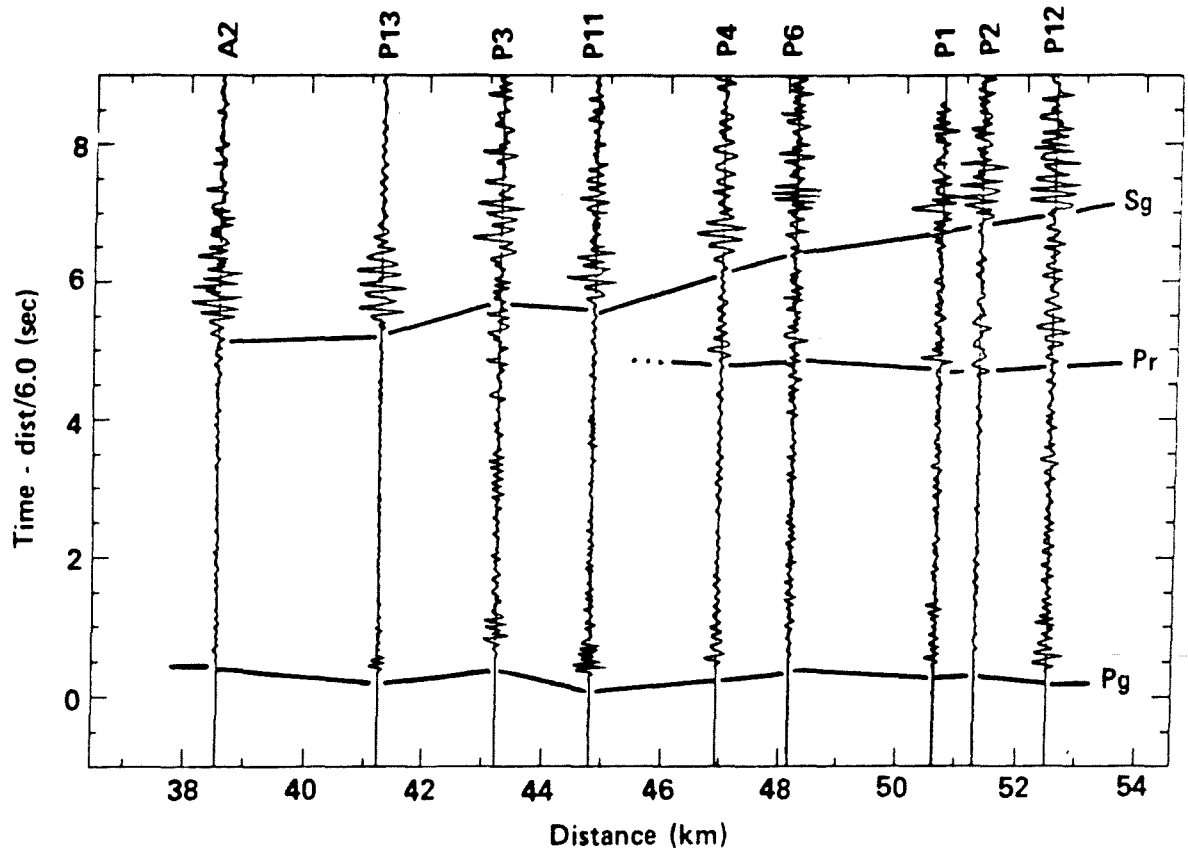
Figure 2. Record sections of vertical components for EQ1. The section
is plotted in a trace-normalized format and are reduced to
6 km/s.
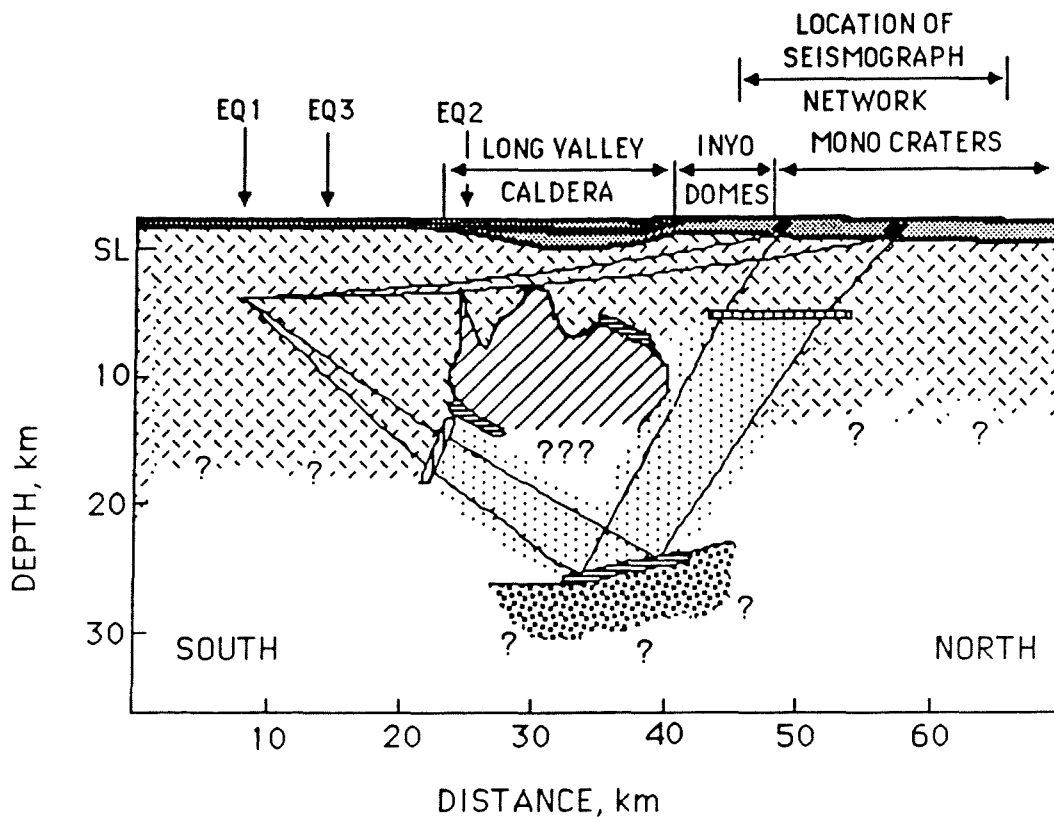
Figure 3. Geologic interpretation of calculated velocity structure. The low velocity zone from previous studies is adapted from Rundle et al. (1985). The reflector at 25 km distance and 12 km depth is from Luetgert and Mooney (1985). The reflector at 37 km distance and 7 km depth is from Hill (1976). The depth scale is referenced to sea level.

EXPLANATION

Post caldera rhyolite, sedimentary rocks, and Bishop Tuff

Sierran Basement

Low velocity zone (partial melt?) from previous studies

Low velocity zone from this study

High velocity reflector

Structure segments from which reflections are observed

Arbitrary boundaries between Sierran basement and the low velocity zone from this study

114

Pre-S Observations at Station SLK, NW of Long Valley, California

William A. Peppin and Thomas W. Delaplain

Seismological Laboratory
University of Nevada
Reno, NV 89557

We have studied 280 observations of a pre-S phase seen at (and only at) the single uncalibrated vertical station SLK, NW of Long Valley, California. Of the earthquakes giving rise to this phase, most occur within an elongated zone south of the caldera (the dashed area in **Figure 1**, which shows seismicity in the UNR catalog since May 1984). The reason why this phase is of particular interest can be seen in **Figure 2**, where observed travel times of P, S, and the SLK phase are shown. The lines give least-squares fit to the three sets of observations, and show that the pre-S phase is essentially parallel to S, but with a *negative* zero-distance intercept of 0.9029 ± 0.052 second.

It is not easy to find reasonable models which fit these observations: no model involving reflections or conversions on flat-lying interfaces will do because of the negative time intercept. Zucca and others (1987) described a similar phase, recorded on a mini-array in the vicinity of Station SLK for earthquakes within the dashed zone of Figure 1. Their interpretation, based on observations of apparent velocity and particle motion, was that their phase was a deep reflection from the bottom of a large magma chamber. Recent results from a mini-array placed at SLK show that the particle motion and apparent velocity of the SLK phase is similar to that found for the pre-S observations of Zucca and others. If the two phases are indeed identical, then their model predicts travel times approximately like the *dashed curves* in in Figure 2 (for foci with zero or 4 km focal depths). At the single distance range where they had observations (about 45 km), the observations fit the model, but this is clearly not the case for other distance ranges.

We propose a model which, we believe, fits not only the observations of Figure 2, but also those of Zucca and others (1987). It consists of modelling the SLK phase as an S to P conversion on an interface striking N45E and dipping 45 degrees SW. The surface trace of this trend is indicated in Figure 1. While this trend is correlable with no surface geologic feature (being well NW of the boundary of Long Valley caldera), the intersection of raypaths from the sources to SLK through this plane are near the Inyo Craters. Examples of seismograms and more details about this work appear in Peppin and Delaplain (1987).

References

Zucca, J.J., Kasamayer, P.W., and J.M. Mills, 1987. Observations of a reflection from the base of a magma chamber in Long Valley caldera, California, *Bull. Seism. Soc. Am.*, **77**, 1674-1687.

Peppin, W.A. and Delaplain, T.W., 1987. Pre-S observations at Station SLK, NW of Long Valley caldera, California, *Bull. Seism. Soc. Am.*, submitted.
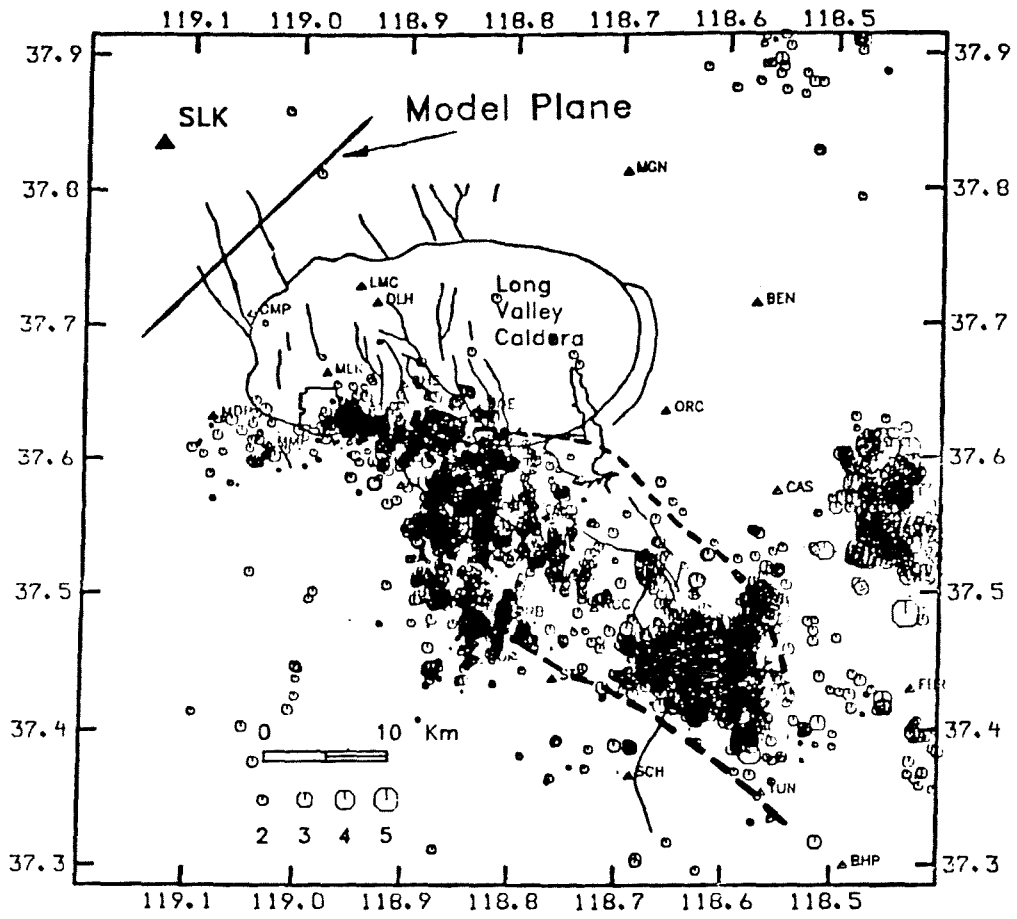
Figure 1
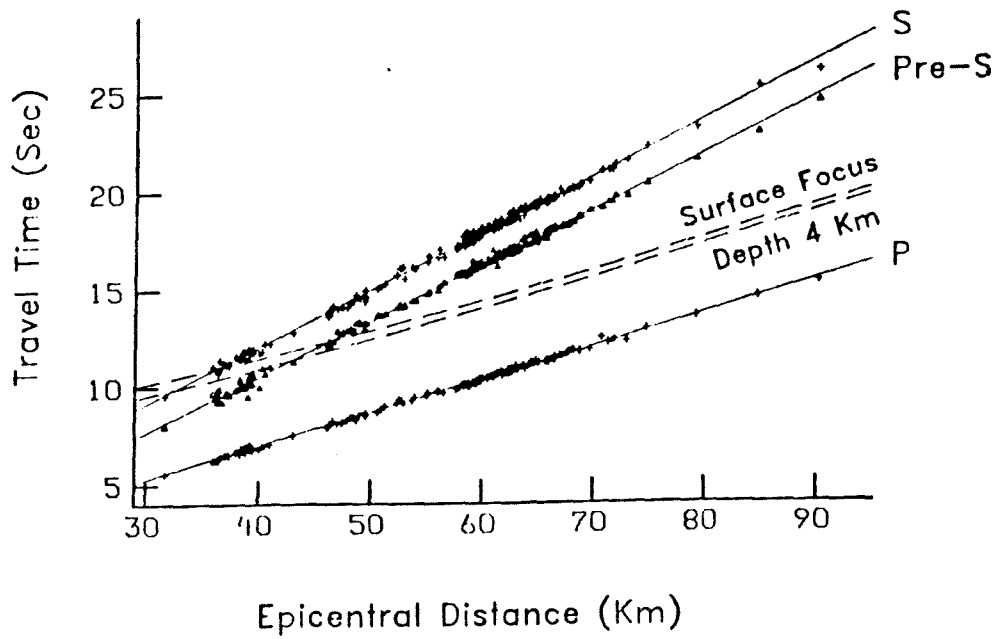
Figure 2

Potential Field and Electromagnetics

INTRODUCTION:
POTENTIAL FIELD AND ELECTROMAGNETIC STUDIES

Norman E. Goldstein

Lawrence Berkeley Laboratory

In this segment of the Symposium, the speakers will concentrate on three principal topics: gravity, electromagnetics, and deformation. Because of the limited time and the fact that the speakers who follow will delve into these topics with clarity and gusto, I will limit my introductory overview to two geophysical topics that are not covered elsewhere in the Symposium, but deserve at least a brief mention. For the sake of completeness and because of their direct relationship to caldera processes, I will try to summarize quickly key aspects of magnetics and self-potential.

Aeromagnetics

Several aeromagnetic surveys have been flown over Long Valley at different altitudes and line spacings. The one most often referred to was a high level (4 km or 13,200 feet above sea level barometric survey) flown by the USGS in 1973 along E-W lines spaced 1.7 km apart. Williams et al. (1977) attempted a quantitative interpretation of the data, and they suggested that extensive post-caldera hydrothermal activity may have drastically altered the composition of the titanomagnetites in the Bishop Tuff, causing the magnetic low in the area of the resurgent dome. Others have reported in informal conversations, as is now supported by holes M-1 and 44-16, that the low in the western part of the caldera is the result of lower magnetization of the post-caldera volcanics and a large wedge of Paleozoic metasediments that floor the caldera. The true nature of the magnetic high on the eastern flank of the resurgent dome has been revealed by recent paleomagnetic work (Mankinen et al., 1986) and from a detailed aeromagnetic survey flown 400 feet above terrain for the USGS in 1979 (Questor, 1980). In Figure 1 we have assembled some of these data along one of the NE-SW aeromagnetic profiles. The conductivity profile is the channel 6/channel 3 ratio from the INPUT survey conducted at the same time. What we show here is that the principal magnetic features can be accounted for by a combination of topographic effects and by the anomalously strong NRM (2 to 4×10^{-3} emu/cm^3) in some of the rhyolite domes and flows associated with early resurgence and later volcanism in the east moat. High remanence, high coercivity, high Konigsberger ratio (Q > 5), and the nature of the thermomagnetic heating curves for samples of these rhyolites indicate rapid cooling and the crystallization of a single low-Ti titanomagnetite species consisting of single-domain or pseudo-single-domain grains (Mankinen et al., 1986). This difference in magnetic rhyolites in the east compared to the nonmagnetic rhyolites in the west may be caused by compositional differences in the remelted crustal rocks and/or differences in the cooling histories.

117

As the low-level survey was designed to cover only the area of the hot water discharges on the east side of the resurgent dome (Fig. 2), the amount of information gained from the survey was limited. However, the combined aeromagnetic-INPUT data are useful for mapping the extent of the magnetic and resistive rhyolites of the east moat; parts of these flows are concealed by alluvium and lake sediments.

It should also be mentioned that Miyazaki (1985) completed a Ph.D. thesis at Stanford in which he estimated Curie isotherm depths beneath the caldera using the aforementioned high-level aeromagnetic data. Using several analysis methods: (a) a least-squares fit to prism models, (b) a least-squares fit to continuous models, and (c) spectral analysis, he found the Curie isotherm to be 4-5 km beneath the west moat, then deepening to 8 km beneath the eastern part of the caldera. Although these findings are consistent with what we now know of ages of volcanism and present subsurface temperatures, Miyazaki's findings may have been a bit fortuitous in light of what we believe to be the main causes of the aeromagnetic anomalies. That is, the calculated Curie isotherm depths could be influenced by strong near-surface magnetization contrasts.

Self-Potential

Since Anderson and Johnson (1976) reported their SP results over the central part of the caldera, we know of no other published work to extend the survey or to refine the interpretation. To summarize, Anderson and Johnson found a large (~1 volt) low associated with the caldera; they attributed this low to cold water inflow into the basin from the surrounding highlands. They also detected an equally large and very tantalizing (1 volt p-p) dipolar anomaly cutting through the west moat and the keystone graben of the resurgent dome. The anomaly axis strikes NNE and does not conform to the direction of previously mapped faults. On close examination, the SP anomaly in the western part of the caldera actually seems to have two principal components: (a) a high centered near Casa Diablo and striking northwesterly parallel to highway 395, and (b) the dipolar part centered over the resurgent dome. The Casa Diablo SP positive may be caused by the upflow of thermal fluids, which seems consistent, at this time, with current hydrogeological models. The dipolar anomaly is more difficult to explain. What makes it so interesting is that the anomaly shape can be generated by a heat source (i.e., a strong thermal gradient) across the contact between two regions of large contrast in electrical or thermal resistivity (e.g., a crystal-lized rock and its melt). The shape and location of the Long Valley SP anomaly indicate a possible heat source at ~4 km; this suggests that subsurface temperatures may be hotter beneath part of the resurgent dome than one would surmise from the amount of sensible heat detected in the Lookout Mountain (LM) drill holes. Mike Wilt, here at Berkeley, has run some numerical models using Sill's algorithm (Sill, 1983) to match the dipolar anomaly and has obtained some reasonable fits. However, because of the general nonuniqueness of the problem and the need to guess values for the voltage-coupling coefficients and thermal resistivity contrast, the numerical results provide only weakly permissive evidence for a heat source.

References

Anderson, L.A., and Johnson, G.R., 1976, Application of the self-potential method to geothermal exploration in Long Valley, California: J. Geophys. Res., v. 81, p. 1527–1532.

Mankinen, E.A., Grommé, C.S., Dalrymple, G.B., Lanphere, M.A., and Bailey, R.A., 1986, Paleomagnetism and K-Ar ages of volcanic rocks from Long Valley caldera, California: J. Geophys. Res., v. 91, p. 633–652.

Miyazaki, Y., 1985, Analysis of aeromagnetic anomalies: Mapping of Curie isothermal surfaces at Long Valley, California: Ph.D. thesis (unpublished), Stanford University, Stanford, California.

Questor, 1980, Airborne electromagnetic survey, United States Geological Survey: Survey blocks in California, Idaho and Nevada: Questor Surveys Ltd., Report, File No. 21056, Mississagua, Ontario L4V 1H3.

Sill, W.R., 1983, Self-potential modeling from primary flows: Geophysics, v. 48, p. 76-86.

Williams, D.L., Berkman, F., and Mankinen, E.A., 1977, Implications of a magnetic model of the Long Valley caldera, California: J. Geophys. Res., v. 82, p. 3030–3038.
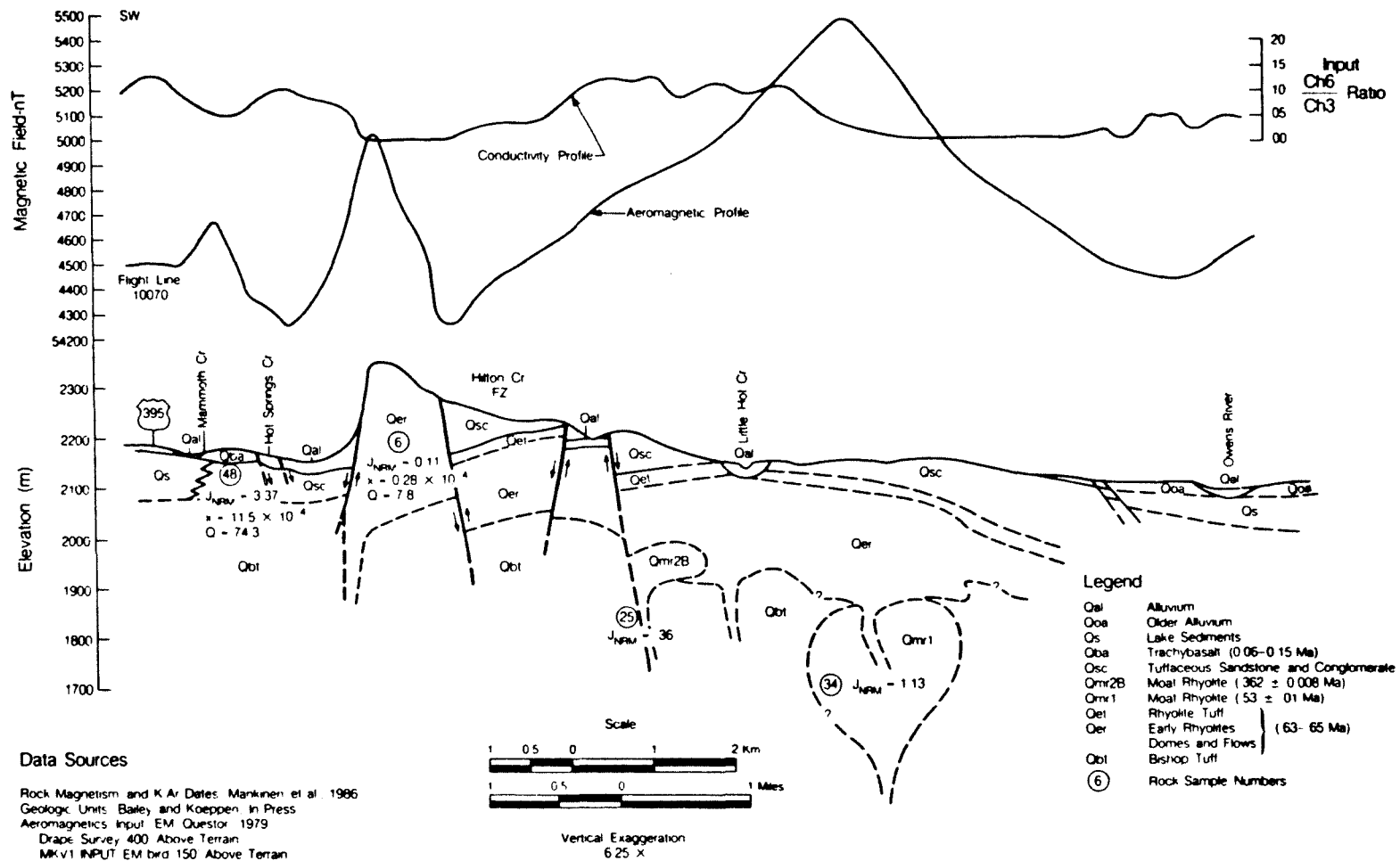
Figure 1. Aeromagnetic and relative conductivity profiles along a SW to NE flight line (Fig. 2) over the eastern side of the resurgent dome. The data were collected as part of a detailed low-level aeromagnetic-INPUT survey flown in 1979 for the USGS (unpublished data).
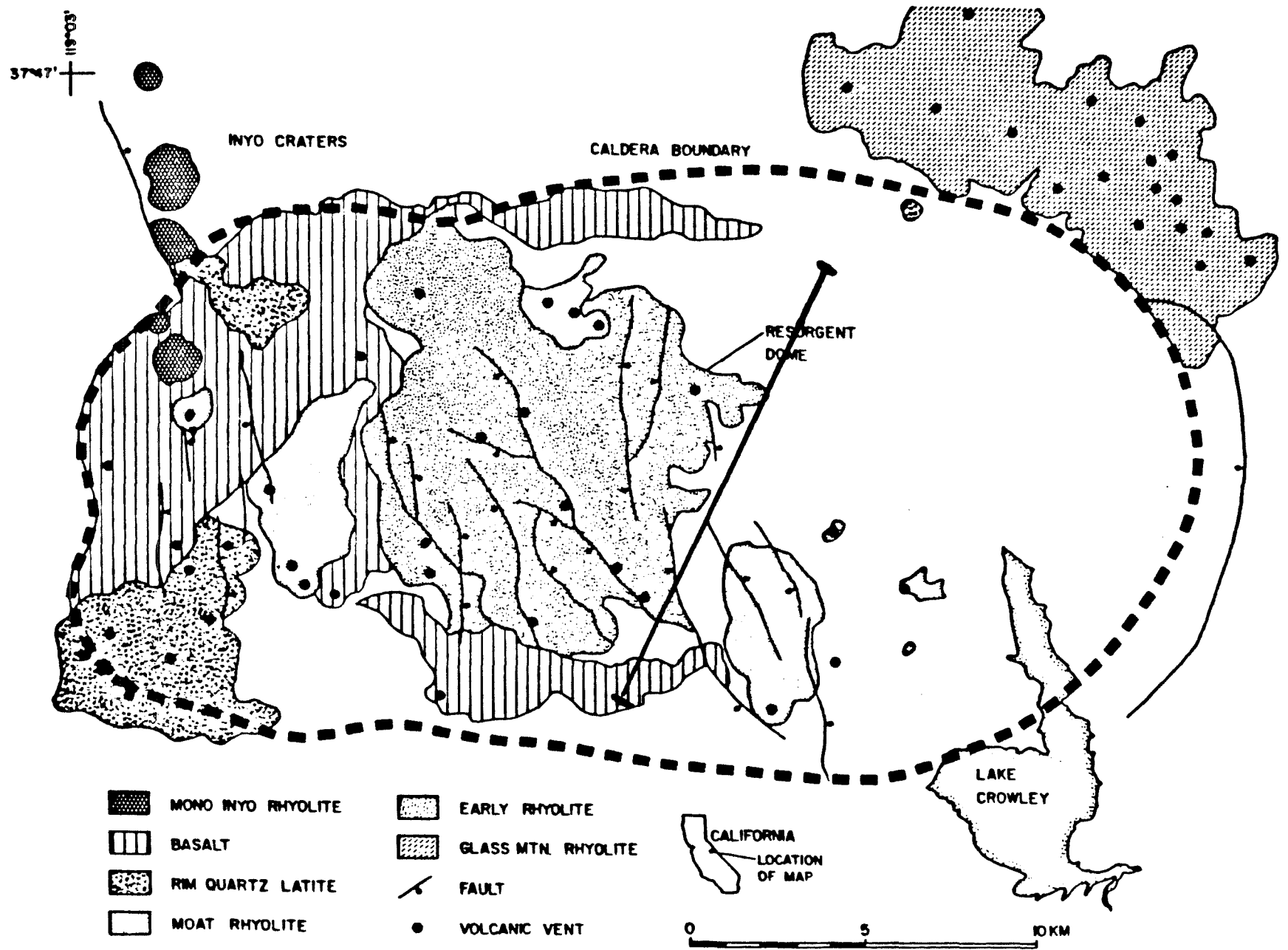
Figure 2. Generalized geology and location of the survey line from Fig. 1.

A Three-Dimensional Gravity Model
of the Geologic Structure
of Long Valley Caldera

Steven F. Carle
N. E. Goldstein

Earth Sciences Division, Lawrence Berkeley Laboratory
University of California, Berkeley, CA 94720

Introduction

Long Valley caldera originated around 0.73 Ma upon the eruption of the Bishop Tuff, an extensive ash-flow tuff (Bailey et al., 1976). Collapse of the roof over the magma chamber associated with the Bishop Tuff and subsequent volcanic resurgence have formed what is now an elliptical caldera measuring 29 km west-east by 15 km south-north, and having a maximum subsidence of 3.5 km. In addition to the Bishop Tuff, the caldera has been filled with the flows, dikes, and tuffs of resurgent volcanism, which has continued episodically up to recent time. Significant volumes of lake sediments, glacial till, alluvium, and reworked volcanics have been deposited in the caldera. The rocks of the caldera fill attain a maximum thickness of about 2.8 km, and because most of these rocks are less dense than the pre-caldera "basement" of granitics, metasediments, and metavolcanics, a gravity low of -50 mGal coincides with the caldera.

Several attempts to define and interpret this anomaly have been made in the past using 2-D and 3-D models (Kane et al., 1976; Abers, 1985). None of the previous interpretations have yielded definitive results, but in fairness, the interpretation here has benefited from a larger gravity data base and more subsurface control than available to previous workers. All published 3-D models simplistically assumed constant density of fill. All 2-D models suffered from the inherent three-dimensionality of the complicated density structure of Long Valley caldera. In addition, previous interpreters have lacked access to geological data, such as well lithologies (Benoit, 1984; Farrar et al., 1985; Smith and Rex; Suemnicht, 1986) and density logs, seismic refraction interpretations (Hill et al.,1985), surface geology (Bailey and Koeppen, 1977), and structural geology interpretations (Hill et al., 1985; Bailey et al., 1976). The purpose of this study is to use all available gravity data and geological information to constrain a multi-unit, 3-D density model based on the geology of Long Valley caldera and its vicinity. Insights on the geologic structure of the caldera fill can help other geophysical interpretations in determining near-surface effects so that deeper structure may be resolved. With adequate control on the structure of the caldera fill, we are able to examine the gravity data for the presence of deeper density anomalies in the crust.

Defining the Gravity Anomaly Associated with the Caldera

The gravity data set consists of 2026 stations from the U.S.G.S. and 473 stations contributed by Unocal Geothermal. All gravity measurements were reduced to Bouguer gravity (see Figure 1) using a terrain density of 2.67 g/cm^3, a good approximation of the average density of the crystalline

basement rocks in the region. About 900 of these stations are located within the model region, between 119° 9' W and 118° 35' W and between 37° 32.25' N and 37° 49.25' N, and the rest provide regional control. The regional gravity is strongly influenced by isostatic thickening of the crust associated with the Sierra Nevada mountains. The gravitational effect of a best fitting Airy isostatic model, having the parameters of sea level crustal thickness of 18 km and Moho density constrast of 0.55 g/cm^3, accounts for the regional gravity (see Figure 2). A range of Airy parameters were tried. The criteria for best fit was based on removal of the regional gravity trend correlated with regional topography and convergence of the residual gravity (see Figure 3) towards zero over outcropping basement rocks of density near 2.67 g/cm^3 (H. W. Oliver, written commumication, 1987; Blakely and McKee, 1985).

The Modelling Technique

All of the gravity modelling was done three-dimensionally because of the complex geological structure. The model consists of a grid of rectangular prisms with a horizontal cross section of about 1.4 km on a side and bounded vertically by the surface topography and the subsurface model structure. The model consists of 23 constant density units corresponding to the major geological units. Some geologic units defined by Bailey and Koeppen (1977) were combined for lack of resolution or simplicity. Each prism consists of a stack of the units with non-zero thickness. The vertical gravitational field at each grid point is computed using a cylindrical approximation to calculate the contribution of each prism (Kane, 1962). By comparing the observed and calculated residual gravity, the thickness of any number of the units may be iterated by a technique modified from the method of Cordell and Henderson (1968), so that the difference between observed and calculated gravity approaches zero. Also, the unit thicknesses may be adjusted manually (forward modelling).

The density constrasts chosen for the model units were based on well log information, laboratory analysis of core samples, and surface rock specimens (Abers, 1985; H. W. Oliver, written communication, 1987; S. J. Maione, written communication), and P-wave velocities (E. Kissling, written communication, 1986). Although the assumption of discrete density contrasts for individual geologic units is by no means exact, it is necessitated by the limited distribution of rock density measurements available, and it is far more realistic than the assumption of a constant density of fill. Because these units vary both in thickness and lateral extent, many of the features in the residual gravity can be accounted for by the distribution of units within the caldera fill, rather than by the total depth of fill, and hence the caldera structure.

The Interpretation

Most of the residual Bouguer gravity low can be accounted for by the Bishop Tuff, early rhyolite flows and tuffs, and lake sediments. Starting from an initial model, we interated the unit thicknesses by means of forward and inverse modelling until an agreeable fit between observed and calculated gravity and a priori information was attained. The other units are thin, or not extensive, near-surface layers whose distribution can largely be inferred on the basis of surface geology and well data. These units, including moat rhyolites, basaltic and andesitic flows, till, alluvium, and pumice, contribute to the residual gravity

and cannot be ignored. Some of the subtle features in the residual gravity were accounted for by modelling variations in the thicknesses of these units (see Figures 4,5, and 6).

By integrating the amount of vertical subsidence over the area of the model, obtaining the volume of subsidence in Long Valley caldera, we estimate that the volume of erupted magma associated with the Bishop Tuff and the resurgent volcanics is 900 km^3. Bailey et al. (1976) estimated a volume of subsidence of 800 km^3, of which 600 km^3 volume of magma was attributed to the Bishop Tuff eruption. We estimate that about 100 km^3 more Bishop Tuff is contained within the caldera than Bailey et al.'s (1976) estimate of 350 km^3. Because most of the intra-caldera Bishop Tuff is densely welded, we would add nearly 100 km^3 to Bailey et al.'s (1976) estimate of the volume of erupted magma associated with the Bishop Tuff, making our estimate of the order of 700 km^3. We can attribute most of the remaining 200 km^3 volume of subsidence to the resurgent volcanics, which we estimate corresponds to about 150 km^3 of erupted magma.

Basement Structure

In attempting to account for the residual gravity completely by caldera fill, it became apparent that part of the residual gravity is caused by anomalously low density rocks below the caldera fill, represented by a persistent misfit between observed and calculated gravity in and nearby the west side of the caldera. The required amount of fill rocks at all of the basement penetrating wells (M1, CP, 66-29, and 44-16) except for 66-29 would have to be greater then the well lithologies suggest. Over basement for several kilometers outside the caldera in the southwest and northwest, the observed gravity was consistently less than the calculated gravity, suggesting that the misfit is not due structural or density errors within the fill. Five explanations for this gravity misfit could be made, followed by arguments for or against:

1) A lack of stations outside the caldera. This analysis could benefit from better station coverage outside the caldera, however there appears to be enough data to justify the reality of the misfit. In a line of stations running up Laurel Canyon to the south of the caldera, the misfit persists (see Figure 5, upper). The Unocal data provides good control in the northwest.

2) Incorrect regional gravity. The regional gravity fits the geological data outside the caldera in three areas of geologic control: a region of granitic rocks of density near 2.67 g/cm^3 to the west and southwest of the caldera indicated by extensive surface sampling (H. W. Oliver, written communication, 1987), a region of anomalously high density basement rocks in the Benton Range to the east of the caldera indicated by high P-wave velocities in a 3-D geotomographic model (E. Kissling, written communication, 1986), and surface samples of granitics near 2.67 g/cm^3 collected in the Boundary Peak and Pellisier Flats plutons further to the east (Blakely and McKee, 1985). Within the caldera, the regional gravity is determined by the isostatic model which is consistent with the data outside the caldera. If the misfit were solely due to an error in the regional gravity correction, the crust below the caldera would appear to be isostatically overcompensated with respect to the regional control outside the caldera.

3) Density variations in the basement granitics or metasediments beneath the caldera. Density variations in basement rocks could account for the misfit (see Figure 6). Surface specimens to the immediate southwest of the caldera are consistently 2.55 to 2.65 g/cm^3 (Oliver, written communication, 1987). To explain the misfit completely by basement density variations, the basement

rocks to the south and northwest, which are downdropped within the caldera, would have to be, on the majority, less than 2.67 g/cm^3. Unfortunately, adequate sampling is not available there. Basement rocks further to the south appear to be highly variable above and below 2.67 g/cm^3. Evidence from a line of gravity stations up McGee Creek indicates anomalously dense basement rocks south of the caldera. The metasediments in this region are highly variable in composition, and could certainly be expected be highly variable in density. Thus, there is not overwhelming evidence that the basement rocks beneath Long Valley caldera are consistently less than 2.67 g/cm^3.

4) Presence of a low density silicic melt body beneath Long Valley caldera. Recent geophysical studies have implied that a silicic melt body exists beneath Long Valley caldera (Sanders, 1984; Ryall and Ryall, 1984; Hill et al. 1985; Savage and Cockerham, 1984; Rundle and Whitcomb, 1984; Denlinger and Riley, 1984). High pressure and temperature studies indicate that such a melt could have a density contrast of up to 10% with respect to its solid form (Hargraves, 1980). The computed gravitational effect of a melt body with a density contrast and configuration consistent with the above studies is not enough to account for the misfit.

5) Presence of a large low density pluton that may or may not contain residual melt. A large, silicic magma chamber existed before the eruption of the Bishop Tuff. Conceivably a large portion of this magma chamber remained after the Bishop Tuff eruption, providing the source for subsequent eruptions (Bailey et al., 1976), and may still remain, though extensively crystallized. If this crystallized magma is about 2.50 g/cm^3, a roundish, plutonic body of about 10 km width and 7 km thickness centered at -7 km elevation in the southwest-central part of the caldera can simply account for the misfit (see Figures 4,5 and 6). A residual gravity low centered near Devil's Postpile can similarly be accounted for by a low density (2.40 g/cm^3) plutonic body centered at about -5 km elevation (see Figure 4, lower).

Caldera Structure

Once the misfit was explained within the caldera, the caldera fill structure could be analyzed while maintaining lithological control at the wells and from other information. Although the cross sections (Figures 4,5 and 6) and the thickness of fill (post-caldera rocks including the Bishop Tuff) map (Figure 7) show much fine detail, more attention should be paid to the simpler, extensive features, which are most likely to be real.

Some structural features are very prominent in the thickness of fill map. The caldera area east of the extension of the Hilton Creek fault is the lowest part of the caldera floor, having a fairly uniform thickness of fill of 2-2.8 km, where the surface elevation is about 7000 feet. A trench-like feature surrounds the caldera floor to the west. The thickness of fill shallows in the south-central and southwest-central parts of the caldera.

A possible explanation of these structural features is that the pre-caldera Sierran range front extended within the caldera where the thickness of fill is now shallow. The trenches may have formed as a result of the eruption or northeastward drift of the downdropped block as it settled.

Another notable feature is the thickening of fill below the graben in the northwest near Highway 395, suggesting that the graben is associated with

deep, pre-caldera structure. The main caldera ring fractures are within the topographic boundary. In the northeast the ring fractures appear to step down over 2-3 km from the topographic boundary, consistent with ring fractures mapped on the surface (Bailey and Koeppen, 1977). The main ring fracture in the southwest is conincident with the strike of the Inyo Domes, suggesting that either the the Inyo domes chain lies on a pre-caldera fracture system, or that the Inyo domes fracture system propagated from the ring fracture.

References

Abers, G., 1985, The subsurface structure of Long Valley caldera, Mono County, California: A preliminary synthesis of gravity, seismic, and drilling information: *J. Geophys. Res.*, v. 90, n. B5, p. 3527-3636.

Bailey, R. A., Dalrymple, G. B., and Lanphere, M. A., 1976, Volcanism structure, and geochronology of Long Valley caldera, Mono County, California, *J. Geophys. Res.*, v. 81, n. 5, p. 725-744.

Bailey, R. A., and Koeppen, R. P., 1977, Preliminary geologic map of Long Valley caldera, Mono County, California, *U.S.G.S. Open-File Map 77-468*.

Benoit, W. R., 1984, Initial results from drillholes PLV-1 and PLV-2 in the western moat of Long Valley Caldera, Phillips Petroleum Company, unpublished report.

Blakely, R. J., and McKee, E. H., 1985, Subsurface structural features of the Saline Range and adjacent regions of eastern California as interpreted from isostatic residaul gravity anomalies, *Geology*, v. 13, p. 781-785.

Cordell, L., and Henderson, R. G., 1968, Iterative three-dimensional solution of gravity anomaly data using a digital computer, *Geophysics*, v. 33, n. 4, p. 596-601.

Denlinger, R. P., and Riley, F. S., 1984, Deformation of Long Valley caldera, Mono County, California, from 1975 to 1982, *J. Geophys. Res.*, v. 89, p. 8304-8314.

Hargraves, R. B., 1980, Physics of Magmatic Processes, Princeton University Press.

Hill, D. P., Bailey, R. A., and Ryall, A. S., 1985, Active tectonic and magmatic processes beneath Long Valley caldera, eastern california: an overview, *J. Geophys. Res.*, v. 90, n. B13, p. 11,111-11,120.

Hill, D. P., Kissling, E., Luetgert, J. H.,and Kradolfer, U., 1985, Constraints on the upper crustal structure of the Long Valley-Mono Craters volcanic complex, eastern California, from seismic refraction measurements, *J. Geophys. Res.*, V. 90, n. B13, p. 11,135-11,150.

Farrar, C. D., Sorey, M. L., Rojstaczer, S. A., Janik, C. J, Mariner, R. H., Winnet, T. L., and Clark, M. D., 1985, Hydrological and geochemical monitoring in Long Valley caldera, Mono County, California, 1982-1984, *U.S.G.S. Water-Resources Investigations Report 85-4183*.

Kane, M. F., 1962, A comprehensive system of terrain corrections using a digital computer, *Geophysics*, v. 27, n. 4, p. 455.

Kane, M. F., Mabey, D. R., and Brace, R., 1976, A gravity and magnetic investigation of the Long Valley caldera, Mono County, California, *J. Geophys. Res.*, v. 81., n. 5, p. 754-762.

Oliver, H. W., 1977, Gravity and magnetic investigations of the Sierra Nevada batholith, California, *Geol. Soc. Am. Bull.*, v. 88, p. 445-461.

Oliver, H. W., and Robbins, S. L., 1982, Bouguer gravity map of California, Mariposa sheet, California Division of Mines and Geology.

Ryall, A., and Ryall, F. D., 1984, Shallow magma bodies related to lithospheric extension in the western Great Basin, western Nevada and eastern California (abstract), *Earthquake Notes*, *55*, p. 11-12.

Sanders, C. O., 1984, Location and configuration of magma bodies beneath Long Valley, California, determined from anomalous earthquake signals, *J. Geophys. Res.*, v. 89, p. 8287-8302.

Savage, J. C., and Cockerham, R. S., 1984, Earthquake swarm in Long Valley caldera, California, January 1983: Evidence for dike injection, *J. Geophys. Res.*, v. 89, p. 8315-8324.

Smith, J. L., and Rex, R. W., Drilling results from the eastern Long Valley caldera, Republic Geothermal, Inc., unpublished report.

Suemnicht, G., 1986, Results of Deep Drilling in the western moat of Long Valley, California, preliminary version, Twelfth Annual Stanford Reservoir Engineering Workshop, Stanford, California.
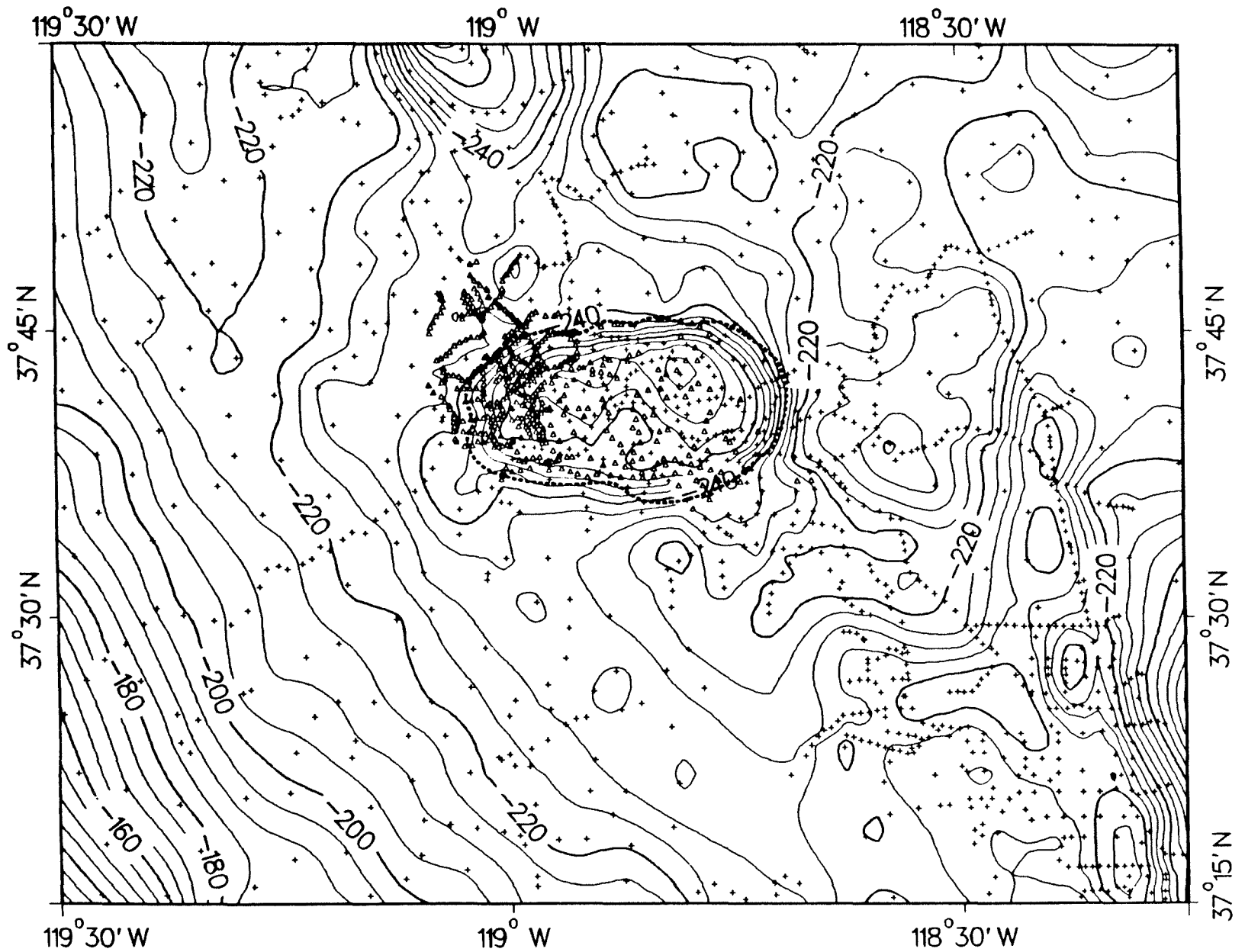
Fig. 1. Bouguer gravity map. The scale is 1:500,000. The contour interval is 5 mGals. Crosses denote U.S.G.S. gravity measurement stations. Triangles denote Unocal Geothermal gravity measurement stations. The dashed line is the topographic boundary of Long Valley caldera.

Fig. 2. Regional gravity map calculated from Airy model with sea level crustal thickness of 18 km and Moho density contrast of 0.55 g/cm . The scale is 1:500,000. The contour interval is 5 mGals. Crosses denote U.S.G.S. and Unocal Geothermal gravity measurement stations. The dashed line is the topographic boundary of Long Valley caldera.

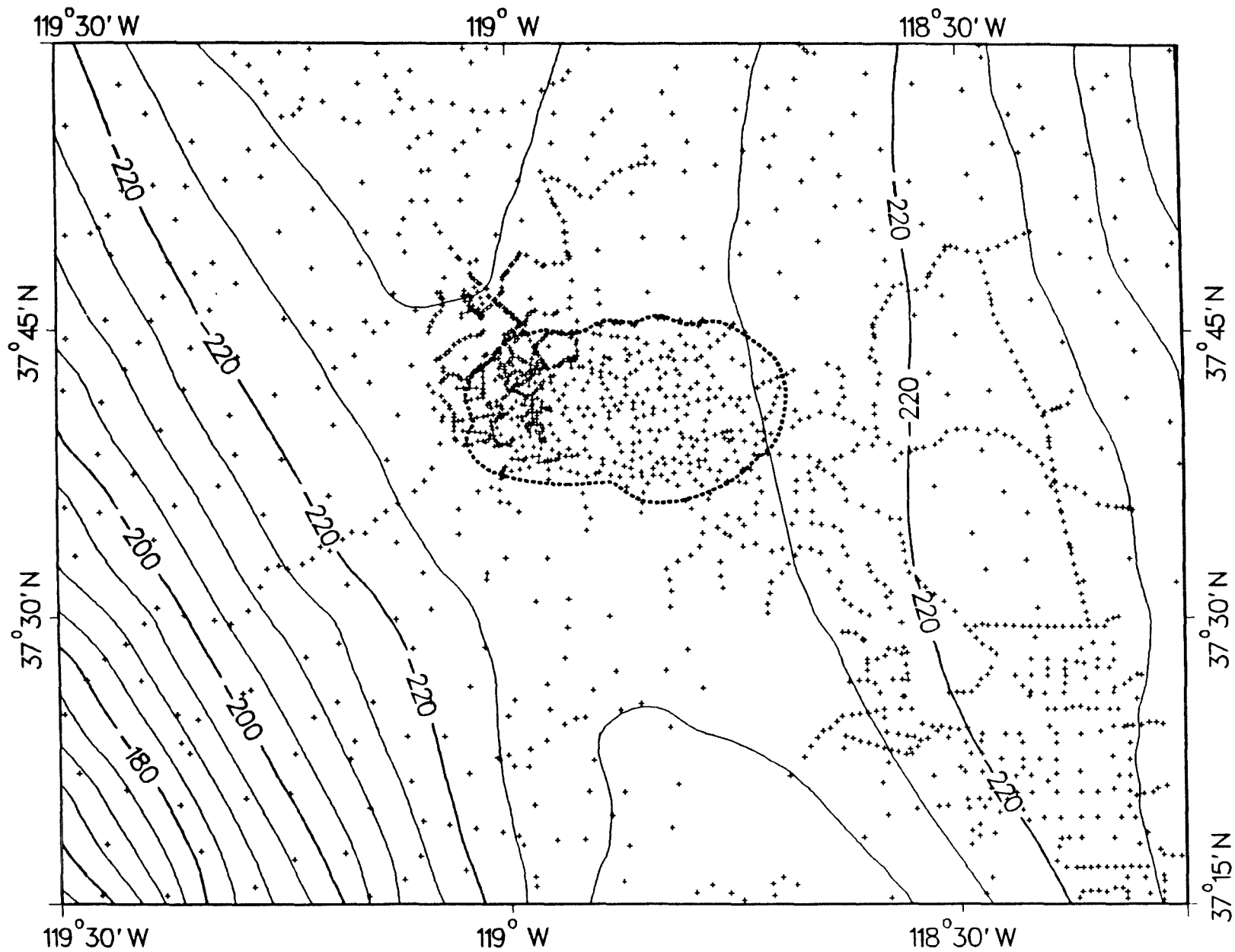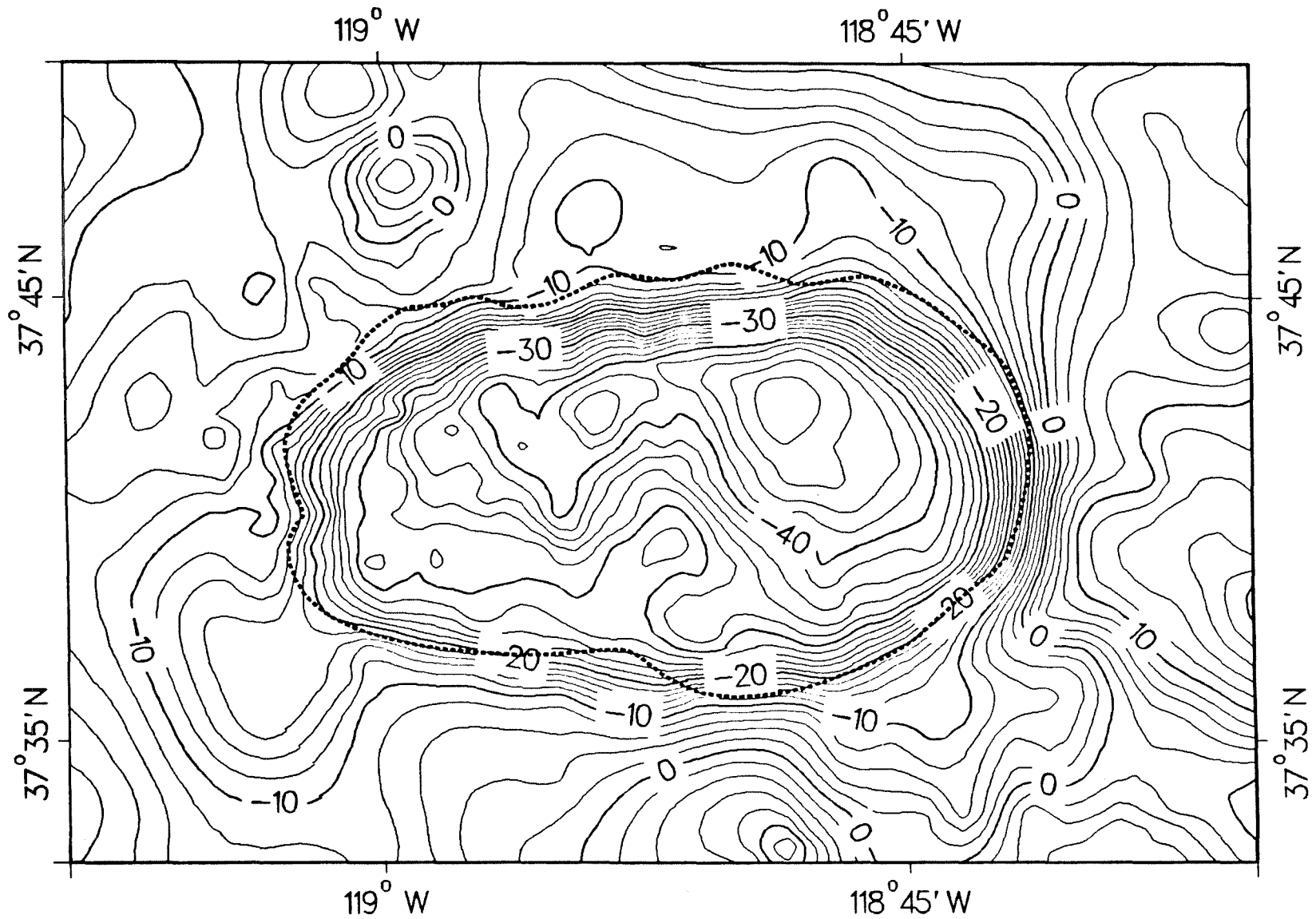Fig. 3. Residual gravity map in area of model. The scale is 1:250,000. The contour interval is 2 mGals. The dashed line is the topographic boundary of Long Valley caldera.

LONG VALLEY CALDERA

RESIDUAL GRAVITY ANOMALY

CALCULATED	o	o
OBSERVED	———	
NO PLUTONS	□	□

UNIT	DENSITY
ALLUVIUM	2.00
PUMICE	1.70
TILL AND COLLUVIUM	1.80
RHYODACITE	2.45
BASALTS, ANDESITES	2.67
TILL	1.90
MOAT RHYOLITE	2.05
LAKE SEDIMENTS	1.80
EARLY RHYOLITE FLOWS	2.20
EARLY RHYOLITE TUFFS	1.75
UNWELDED BISHOP TUFF	2.05
WELDED BISHOP TUFF	2.35
GLASS MTN RHYOLITES	2.15
PRE-CALD. RHYODACITE	2.45
PRE-CALD. VOLCANICS	2.67
GRANITICS OR METASEDS	2.70
GRANITICS OR METASEDS	2.90
GRANITICS OR METASEDS	2.60
GRANITICS OR METASEDS	2.90
GRANITICS OR METASEDS	2.90
GRANITICS OR METASEDS	2.80
LOW DENSITY PLUTON?	2.50
LOW DENSITY PLUTON?	2.40
BASEMENT	2.67

MGALS 0 -20 -40 -60

119 0.5 W

44-16

ELEVATION (KM) 4 3 2 1 0 -1 -2 -3 -4 -5 -6 -7 -8 -9 -10 -11 -12

2.0 X VERT EXAG

S   N

MGALS 0 -20 -40 -60

119 3.5 W

ELEVATION (KM) 4 3 2 1 0 -1 -2 -3 -4 -5 -6 -7 -8 -9 -10 -11 -12

2.0 X VERT EXAG

S   N

Fig. 4. Cross sections through the three-dimensional model along the indicated longitudes. The horizontal scale is 1:500,000. Cross-section orientation with respect to the topographic boundary of the caldera is shown in the lower right. "NO PLUTONS" indicates the calculated residual gravity if the low density plutons are removed from the model.

LONG VALLEY CALDERA

RESIDUAL GRAVITY ANOMALY

CALCULATED	o	o
OBSERVED	———————	
NO PLUTONS	□	□

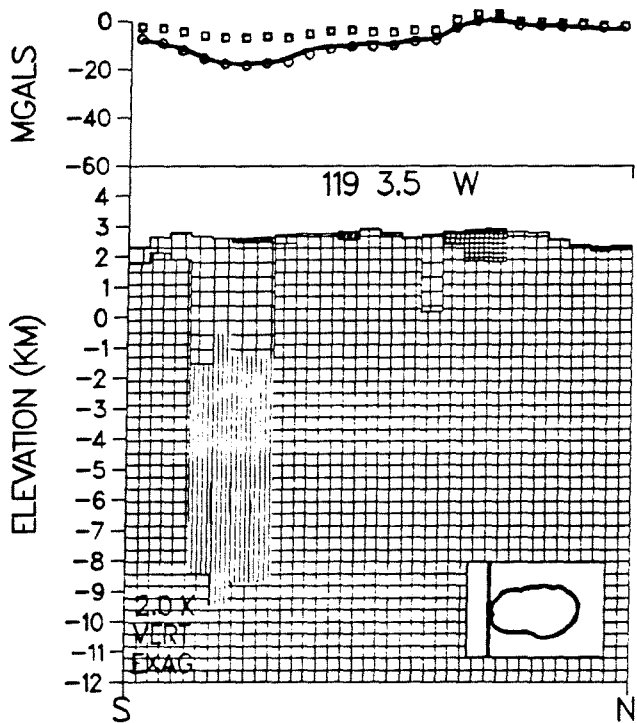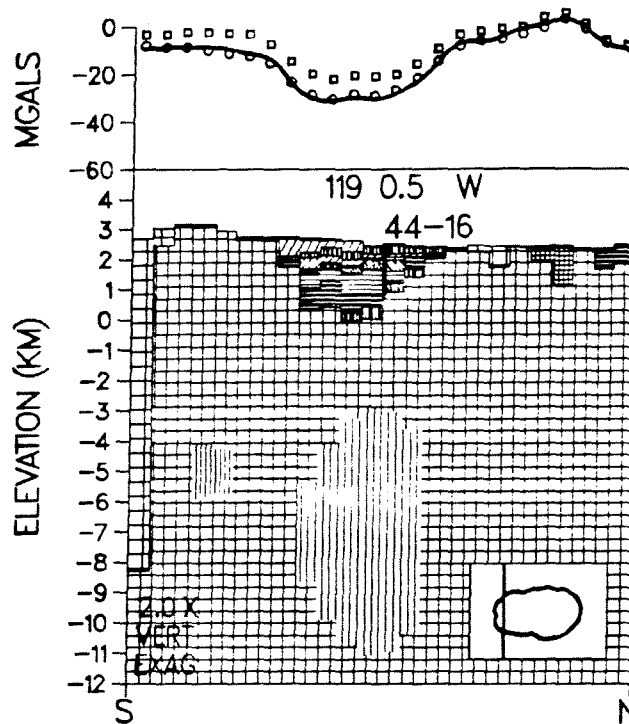| UNIT	DENSITY
ALLUVIUM	2.00
PUMICE	1.70
TILL AND COLLUVIUM	1.80
RHYODACITE	2.45
BASALTS, ANDESITES	2.67
TILL	1.90
MOAT RHYOLITE	2.05
LAKE SEDIMENTS	1.80
EARLY RHYOLITE FLOWS	2.20
EARLY RHYOLITE TUFFS	1.75
UNWELDED BISHOP TUFF	2.05
WELDED BISHOP TUFF	2.35
GLASS MTN RHYOLITES	2.15
PRE-CALD. RHYODACITE	2.45
PRE-CALD. VOLCANICS	2.67
GRANITICS OR METASEDS	2.70
GRANITICS OR METASEDS	2.90
GRANITICS OR METASEDS	2.60
GRANITICS OR METASEDS	2.90
GRANITICS OR METASEDS	2.90
GRANITICS OR METASEDS	2.80
LOW DENSITY PLUTON?	2.50
LOW DENSITY PLUTON?	2.40
BASEMENT	2.67

Fig. 5 Cross sections through the three-dimensional model along the indicated longi-
tudes. The horizontal scale is 1:500,000. Cross-section orientation with respect to the
topographic boundary of the caldera is shown in the lower right. "NO PLUTONS" indi-
cates the calculated residual gravity if the low density plutons are removed from the
model.

LONG VALLEY CALDERA

RESIDUAL GRAVITY ANOMALY

CALCULATED	o	o
OBSERVED	———	
NO PLUTONS	▫	▫

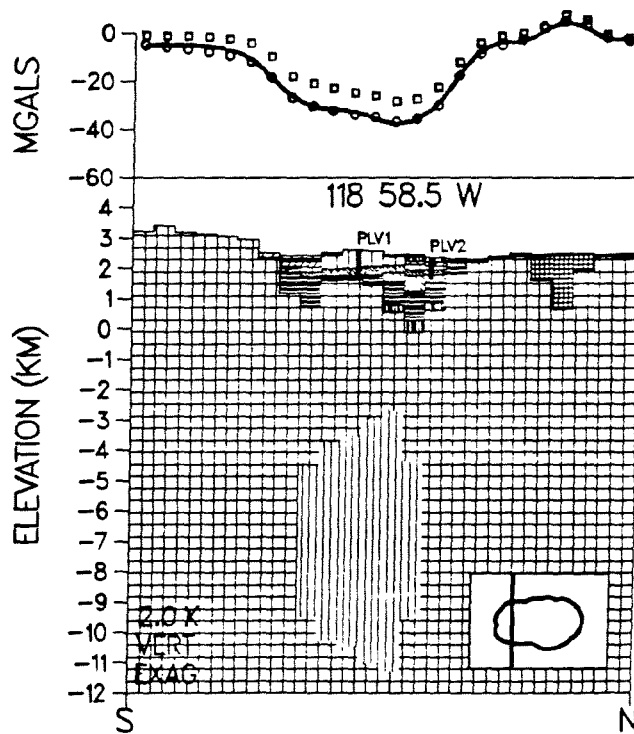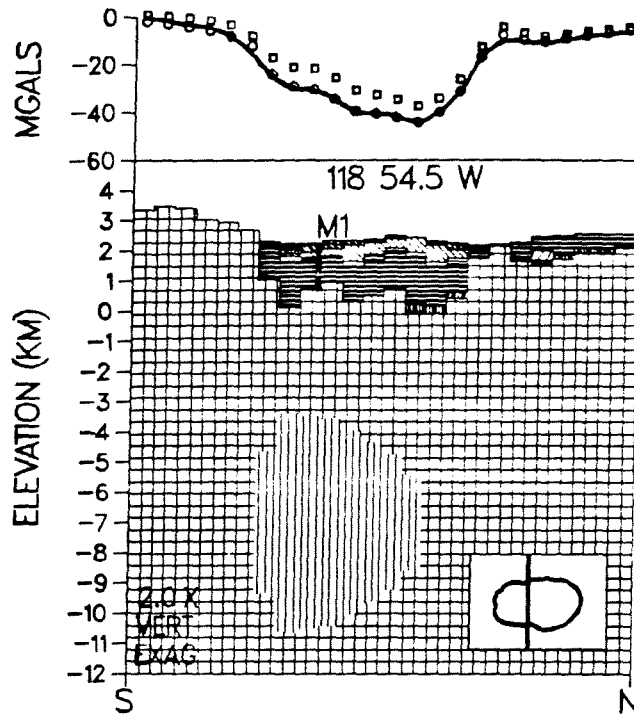| UNIT		DENSITY
ALLUVIUM		2.00
PUMICE		1.70
TILL AND COLLUVIUM		1.80
RHYODACITE		2.45
BASALTS, ANDESITES		2.67
TILL		1.90
MOAT RHYOLITE		2.05
LAKE SEDIMENTS		1.80
EARLY RHYOLITE FLOWS		2.20
EARLY RHYOLITE TUFFS		1.75
UNWELDED BISHOP TUFF		2.05
WELDED BISHOP TUFF		2.35
GLASS MTN RHYOLITES		2.15
PRE-CALD. RHYODACITE		2.45
PRE-CALD. VOLCANICS		2.67
GRANITICS OR METASEDS		2.70
GRANITICS OR METASEDS		2.90
GRANITICS OR METASEDS		2.60
GRANITICS OR METASEDS		2.90
GRANITICS OR METASEDS		2.90
GRANITICS OR METASEDS		2.80
LOW DENSITY PLUTON?		2.50
LOW DENSITY PLUTON?		2.40
BASEMENT		2.67

Fig. 6. Cross sections through the three-dimensional model along the indicated latitudes The horizontal scale is 1:500,000. Cross section orientation with respect to the topographic boundary of the caldera is shown in the lower right. "NO PLUTONS" indicates the calculated residual gravity if the low density plutons are removed from the model.

134

THICKNESS
OF FILL
(KM)

2.4
2.0
1.6
1.2
0.8
0.4
0.0

37°45'N
37°35'N

119°W
118°50'W
118°40'W
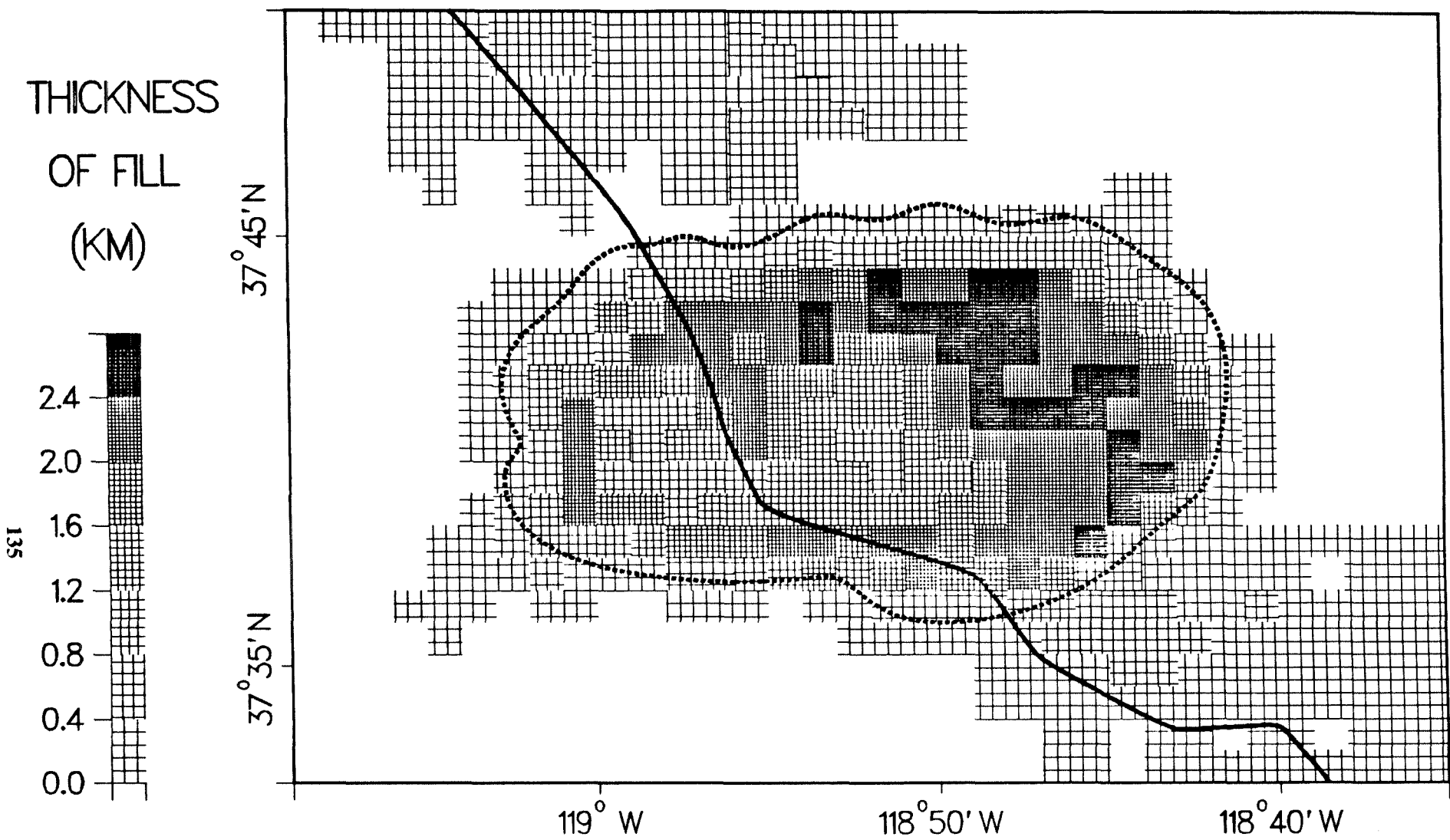
Fig. 7. Thickness of caldera fill, including all post caldera eruption rocks and the Bishop Tuff, according to the model. Scale is 1:250,000.

DELINEATING THE SUBSURFACE MEGA-STRUCTURE OF LONG VALLEY CALDERA; REGIONAL GRAVITY AND MAGNETOTELLURIC CONSTRAINTS

J.F. Hermance, G.A. Neumann and W. Slocum

Department of Geological Sciences
Geophysical/Electromagnetics Laboratory
Brown University
Providence, RI 02912

One of the principal tectonic elements in the Long Valley volcanic complex is the presence of a deep basin-like caldera bounded by steeply dipping normal faults having characteristic offsets of at least several kms. This paper reports a magnetotelluric interpretation which delineates the subsurface structure of this feature. As a preliminary step we have reinterpreted regional gravity data in terms of a simple 3-D model employing the inverse algorithm of Cordell and Henderson (1968). Our gravity model clearly defines the major subsurface features of the caldera walls. In addition, the basin fill and major boundary faults impose a strong imprint on regional magnetotelluric (MT) data as well. A strong similarity is seen between gravity model and telluric thin sheet interpretations; this underscores the fact that both types of data are largely influenced by the same geologic features: the caldera fill, basement topography, and the major boundary faults. Moreover as in the earlier, preliminary MT interpretation of Hermance et al. (1984), we see a conductive zone beneath the southwest moat as well. In addition, however, we now have evidence for a resistive "topographic high" cutting across the main body of the caldera from the northwest to the southeast. We assume that this horst block is the same feature described as a central platform by Kane et al. (1976) from gravity studies and that it has been a major element in the structural evolution of the resurgent dome. Such a structural "high" is quite compatible with limited drilling data.

BACKGROUND

One of the principal tectonic elements in the Long Valley volcanic complex is the presence of a deep basin-like caldera bounded by steeply dipping normal faults having characteristic offsets of at least several kms (Pakiser, 1961). There is increased interest in delineating the subsurface structure of this feature for a number of reasons (Hill, 1976; Kane et al., 1976; Bailey, 1982, 1983; Hermance et al., 1984; Abers, 1985; Hill et al., 1985; Jachens and Roberts, 1985). First, characterizing the location and maximum offset of these faults will lead to clearer models for the tectonic style of the evolution of this system. Second, there is strong evidence that recent sequences of seismicity and volcanism are structurally constrained by such boundary faults; thus there is a valuable predictive component in knowing the precise geometry of these features. Thirdly, the caldera basin forms the major hydrologic element in the region (Sorey, 1985; Blackwell, 1985). Its highly porous fill provides the major aquifer, and superimposed faults provide the vertical conduits for allowing water to enter or to exit the hydrologic system. Thus the detailed characterization of the subsurface geometry of Long Valley caldera continues to be an important objective of current geophysical studies (Hill et al., 1985; Jachens and Roberts, 1985). This paper reports the interpretation of gravity and magnetotelluric data from this area.

GEOLOGICAL AND GEOPHYSICAL CONSTRAINTS

A simplified geologic map for Long Valley caldera is shown in Figure 1. It is well-known that values of Bouguer gravity typically show strong negative values over the interior of the caldera caused by its low density fill (Pakiser, 1961; Kane et al., 1976; Abers, 1985; Jachens and Roberts, 1985). Of course there is some ambiguity in determining actual depth to bedrock from gravity data alone unless the density contrast is well-known. For example, because the density contrast between the basin fill and the surrounding country-rock was underestimated, early gravity interpretations of Long Valley caldera (e.g. Pakiser, 1961) significantly overestimated depth to basement. The interpretation measurably improved when Abers (1985) combined the interpretation of gravity data with Hill's (1976) seismic refraction interpretation. However Abers used a 2-D model which, while useful for characterizing local fault structures, is limited for the kind of regional study we are describing here.

Thus following Kane et al. (1976) we have reinterpreted the regional gravity data in terms of a 3-D model employing the inverse algorithm of Cordell and Henderson (1968). In keeping with Abers' results, however, we have increased the mean density contrast from the value of -450 kg/m^3 assumed by Kane et al. to a value of -625 kg/m^3. The results of our interpretation in Figure 2 largely confirm the earlier analysis of Kane et al. We have revised the average depth of caldera fill to smaller values (approx. 2 km) because of the larger density contrast that we feel is required by the seismic data. In particular, our gravity model clearly defines the major subsurface features of the caldera walls. Moreover the evidence persists for a high central platform separating the two basinal lows remarked upon by Kane et al.

The basin fill and major boundary faults impose a strong imprint on regional magnetotelluric (MT) data as well. The MT data base described by Hermance et al. (1984) has been augmented with measurements at a number of additional sites throughout the caldera and the adjacent area (Figure 3). In acquiring these new data, we particularly sought sites outside the rim of the caldera in order to better characterize the basin margins.

A REGIONAL ELECTRICAL MODEL FOR LONG VALLEY CALDERA

The thin-sheet modelling algorithm of Hermance (1982) was modified to account for conductivities which varied smoothly in the lateral direction. Starting with a model based on the average telluric field amplitudes at each site (the square root of the telluric ellipse area), the results were perturbed by hand over various sub-regions of the model until a reasonable agreement was achieved between the theoretical model and the observed telluric fields (Figure 4). Machine generated contours for the resulting model showed many sharp small-scale discontinuities which were artifacts of the computer contouring, therefore the model values were numerically smoothed (low pass filtered at a cut-off wavelength of 6 km, equivalent to our mean station spacing), and are replotted in Figure 5. The similarity between the gravity model in Figure 2 and the telluric thin sheet model in Figure 5 clearly underscores the fact that both types of data are largely influenced by the same geologic features: the caldera fill, topography on the underlying basement, and the major boundary faults.

As in the earlier, preliminary interpretation of Hermance et al. (1984), the telluric field data shows that a zone of enhanced conductivity appears to be present beneath the southwest moat. In addition, however, we now have

clear evidence for a resistive feature (the "topographic high" in Figure 5) cutting across the main body of the caldera from the northwest to the southeast. We tentatively assume that this is a horst block intimately associated with the structural evolution of the resurgent dome and is the same feature described as a central platform by Kane et al. (1976). The telluric data, however, show this feature to be much more continuous across the caldera than do the gravity data.

Such a structural "high" is quite compatible with the limited drilling data shown in Figure 6. In particular, the Mammoth-1 drillhole site on the south central flank of the resurgent dome encounters the metasedimentary basement at a much shallower depth than the two drillholes to the east (the granite porphyry encountered at the bottom of Clay Pit-1 is likely to be a post-caldera intrusive; see discussion in Hermance, 1983). Seismic refraction data (e.g. Hill et al., 1985) also suggest some sort of topographic relief beneath the resurgent dome, but have not yet been interpreted to reveal the kind of detail needed to confirm or to reject the intracaldera horst block shown in Figure 5.

REFERENCES

Abers, G., The subsurface structure of Long Valley caldera, Mono County, California: A preliminary synthesis of gravity, seismic, and drilling information, Jour. Geophys. Res., 90, 3627-3636, 1985.

Bailey, R.A., Mammoth Lakes earthquakes and ground uplift: Precursors to possible volcanic activity?, Earthquake Information Bulletin, 15, 88-102, 1983.

Bailey, R.A., Other potential eruption centers in California: Long Valley-Mono Lake, Coso, and Clear Lake volcanic fields, Status of Volcanic Prediction and Emergency Response Capabilities in Volcanic Hazard Zones of California, Special Publication No. 63, California Dept. of Conservation, Division of Mines and Geology, 17-28, 1982.

Bailey, R.A. and R.P. Koeppen, Preliminary geologic map of Long Valley caldera, Mono County, California; USGS Open File Map 77-468, 1977.

Blackwell, D.D., A transient model of the geothermal system of the Long Valley caldera, California, Jour. Geophys. Res., 90, 11,229-11,241, 1985.

Cordell, L. and R.G. Henderson, Iterative three-dimensional solution of gravity anomaly data using a digital computer, Geophysics, 33, 596-601, 1968.

Hermance, J.F., The Long Valley/Mono Basin volcanic complex in Eastern California: Status of present knowledge and future research needs, Rev. Geophys. Space Phys., 21, 1545-1565, 1983.

Hermance, J.F., The asymptotic response of three-dimensional basin offsets to magnetotelluric fields at long periods: The effects of current channeling, Geophysics, 47, 1562-1573, 1982.

Hermance, J.F., W.M. Slocum and G.A. Neumann, The Long Valley/Mono Basin volcanic complex: A preliminary magnetotelluric and magnetic variation interpretation, Jour. Geophys. Res., 89, 8325-8337, 1984.

Hill, D.P., Structure of Long Valley caldera, California, from a seismic refraction experiment, Jour. Geophys. Res., 81, 745-753, 1976.

Hill, D.P., E. Kissling, J.H. Luetgert and U. Kradolfer, Constraints on the upper crustal structure of the Long Valley-Mono Craters volcanic complex, Eastern California, from seismic refraction measurements, Jour. Geophys. Res., 90, 11,135-11,150, 1985.

Jachens, R.C. and C.W. Roberts, Temporal and areal gravity investigations at Long Valley caldera, California, Jour. Geophys. Res., 90, 11-210-11,218, 1985.

Kane, M.F., D.R. Mabey and R.-L. Brace, A gravity and magnetic investigation of the Long Valley caldera, Mono County, California, Jour. Geophys. Res., 81, 754-762, 1976.

Pakiser, L.C., Gravity, volcanism, and crustal deformation in Long Valley, California, U.S. Geol. Surv. Prof. Paper 424-B, B250-B253, 1961.

Sorey, M., Evolution and present state of the hydrothermal system in Long Valley caldera, Jour. Geophys. Res., 90, 11,219-11,228, 1985.

Figure Captions

Figure 1. Generalized geology of Long Valley caldera, after Bailey and Koeppen (1977).

Figure 2. A simple 3-D model for the depth of basin fill based on gravity data. We assume a mean density contrast of -625 kg/m^3 between the basin fill and the surrounding country rock.

Figure 3. Present magnetotelluric data set from Long Valley caldera shown as normalized telluric ellipses referenced at infinity to the unit electric field shown. The dashed line is the caldera boundary from Bailey and Koeppen (1977).

Figure 4. Comparison of the telluric field response of our preferred theoretical model to the observed data at 20 sec period.

Figure 5. A smoothed version of our final thin sheet model. Contours are in terms of conductance (depth-integrated conductivity) relative to a unit value at infinity. The relative conductance of our preferred model was low pass filtered using a 2-D numerical filter having a cutoff wavelength of 6 km. Increasing conductance is plotted downward to correspond to topography on resistive basement.

Figure 6.   Lithologies from deep boreholes in Long Valley caldera
(modified from Abers, 1985, to show true altitudes relative to
sea level).   Mammoth-1 is on the south central flank of
resurgent dome; Clay Pit-1 is at a lower altitude on the
eastern flank; Republic 66-29 is in the eastern moat (note
lake bed sediments at surface).

FIGURE 1

MONO INYO RHYOLITE

BASALT

RIM QUARTZ LATITE

MOAT RHYOLITE

EARLY RHYOLITE

GLASS MTN. RHYOLITE

FAULT

VOLCANIC VENT

CALIFORNIA

LOCATION OF MAP

INYO CRATERS

CALDERA BOUNDARY

RESURGENT DOME

LAKE CROWLEY

37°47'

119°03'

0   5   10 KM
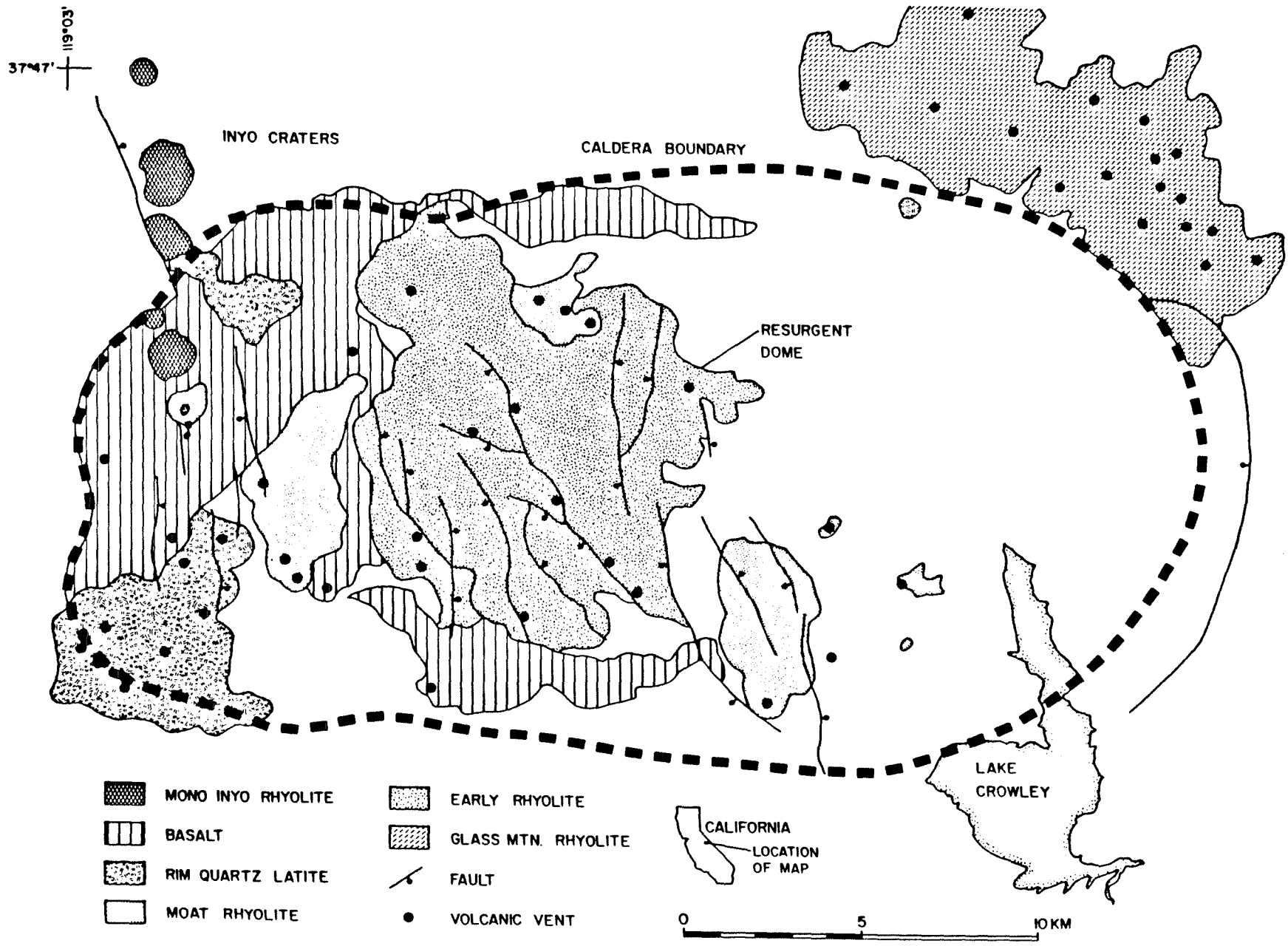
DEPTH OF BASIN FILL

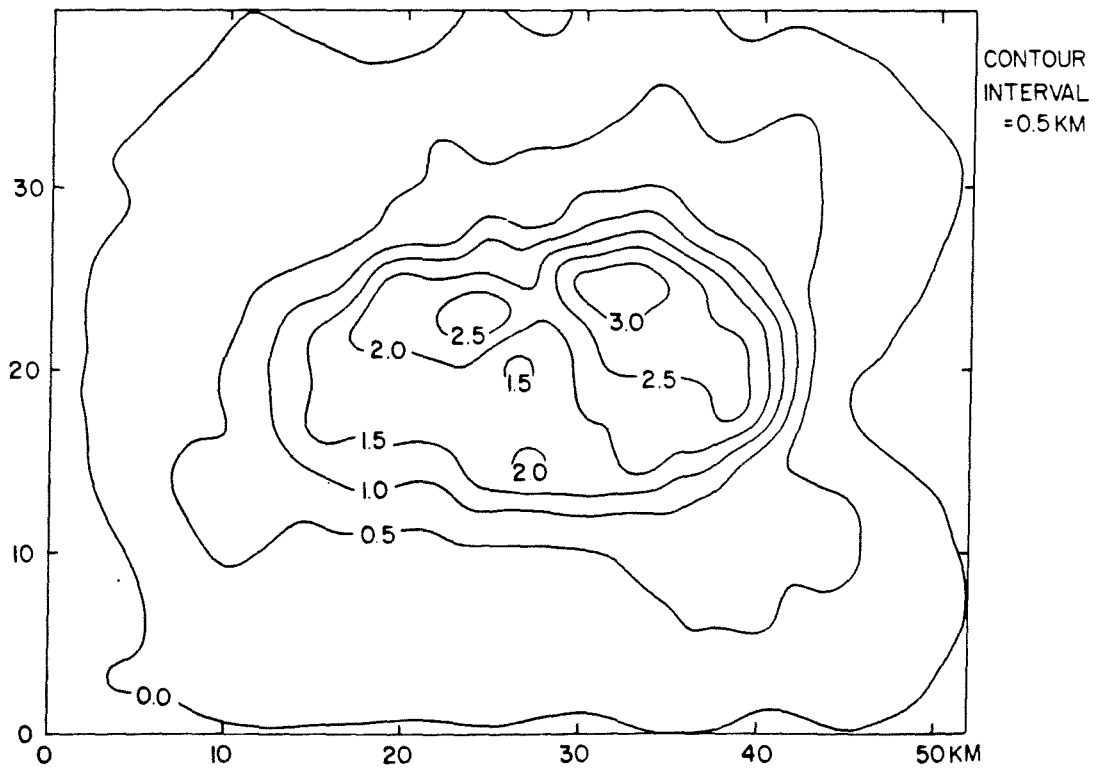## ($\Delta \rho$ = 625 KG/M^3)

FIGURE 2

PERIOD: 20.00
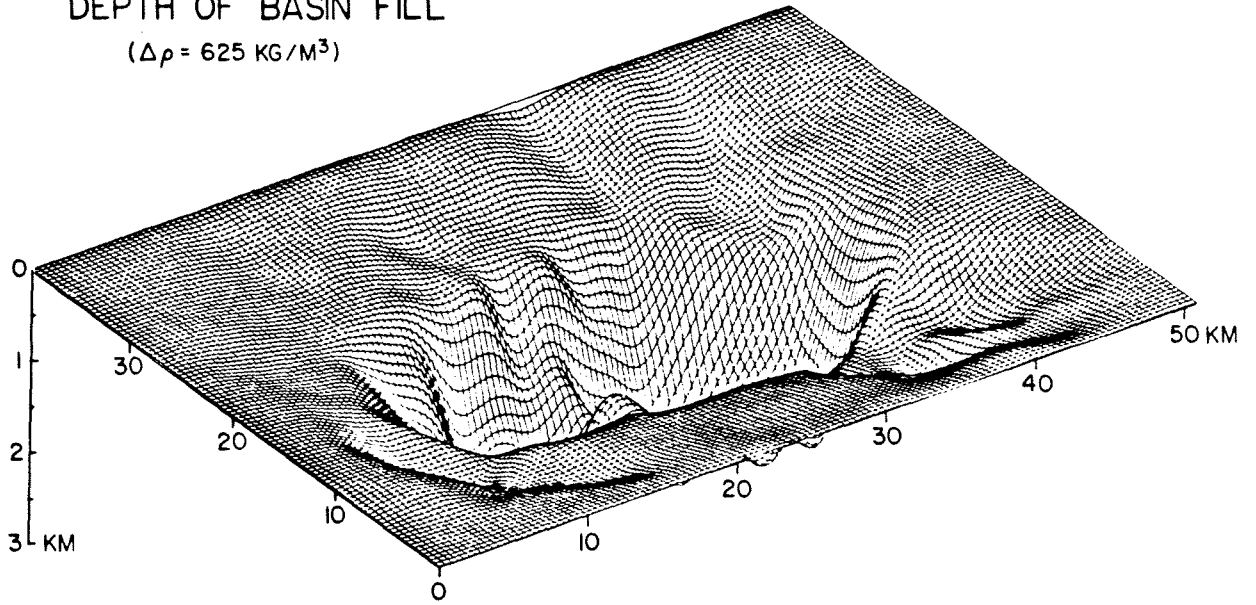
UNIT E-FIELD

MONO CRATERS

LAKE CROWLEY

395

146
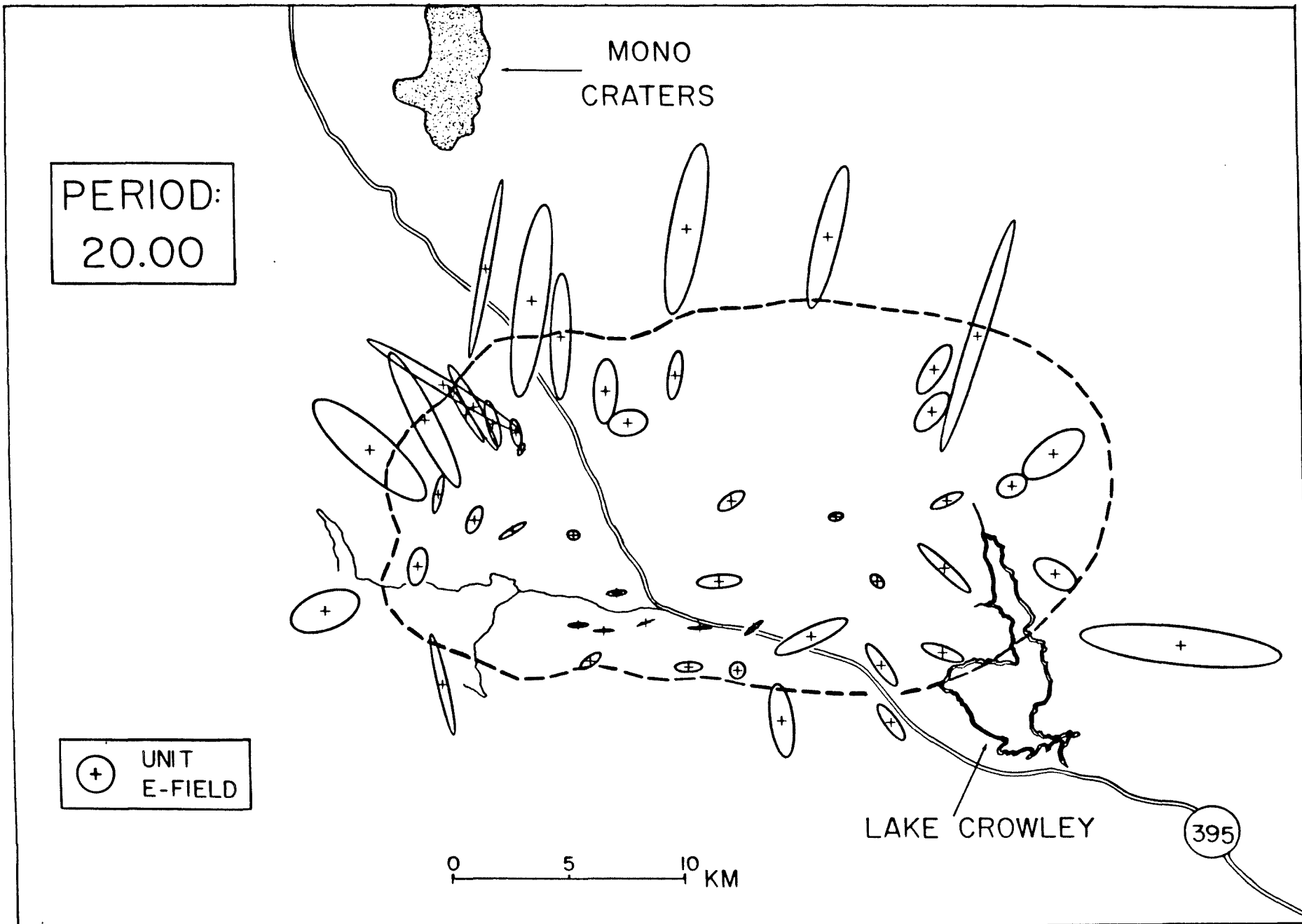
FIGURE 3

THEORETICAL TELLURIC ELLIPSES
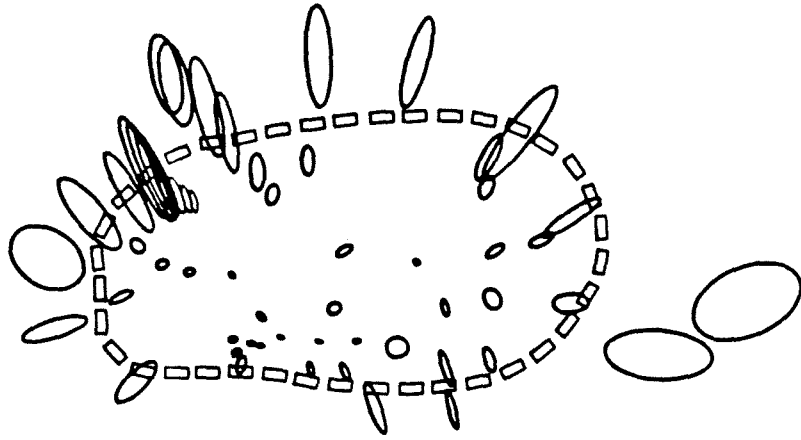
UNIT
E-FIELD

0   10   20 KM

OBSERVED TELLURIC ELLIPSES
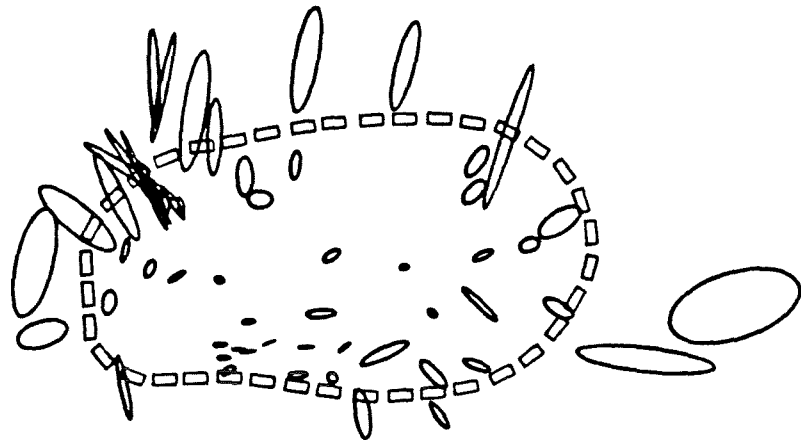
UNIT
E-FIELD

0   10   20 KM

FIGURE 4

147

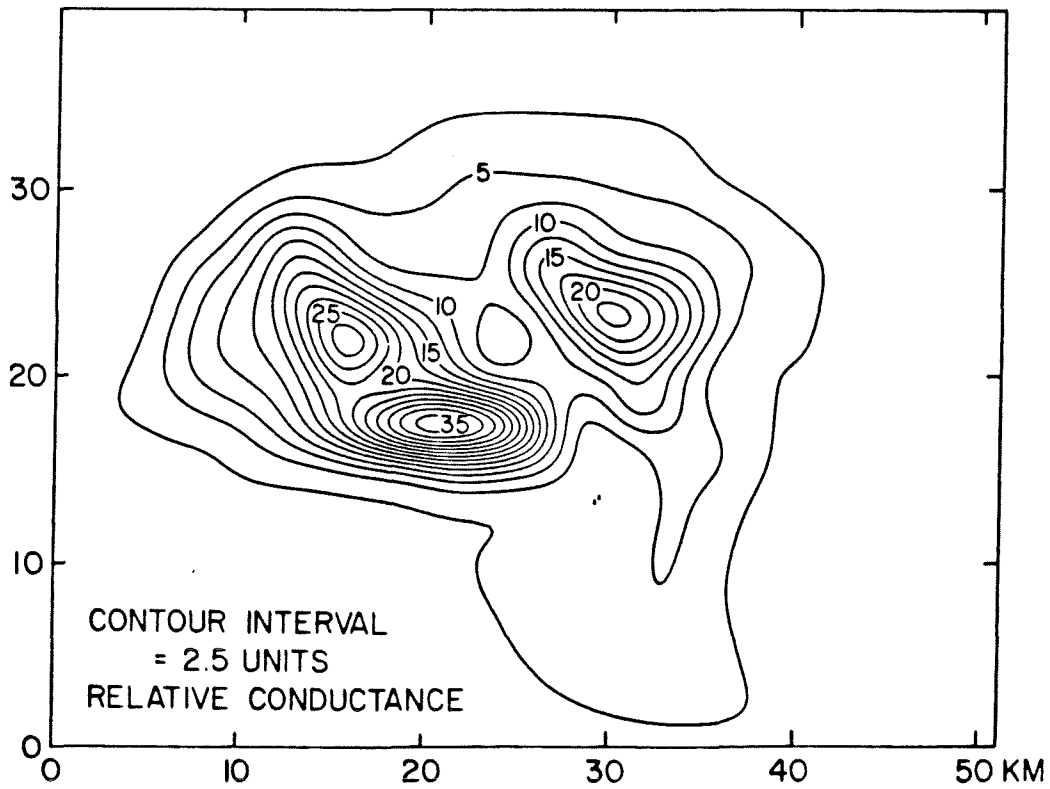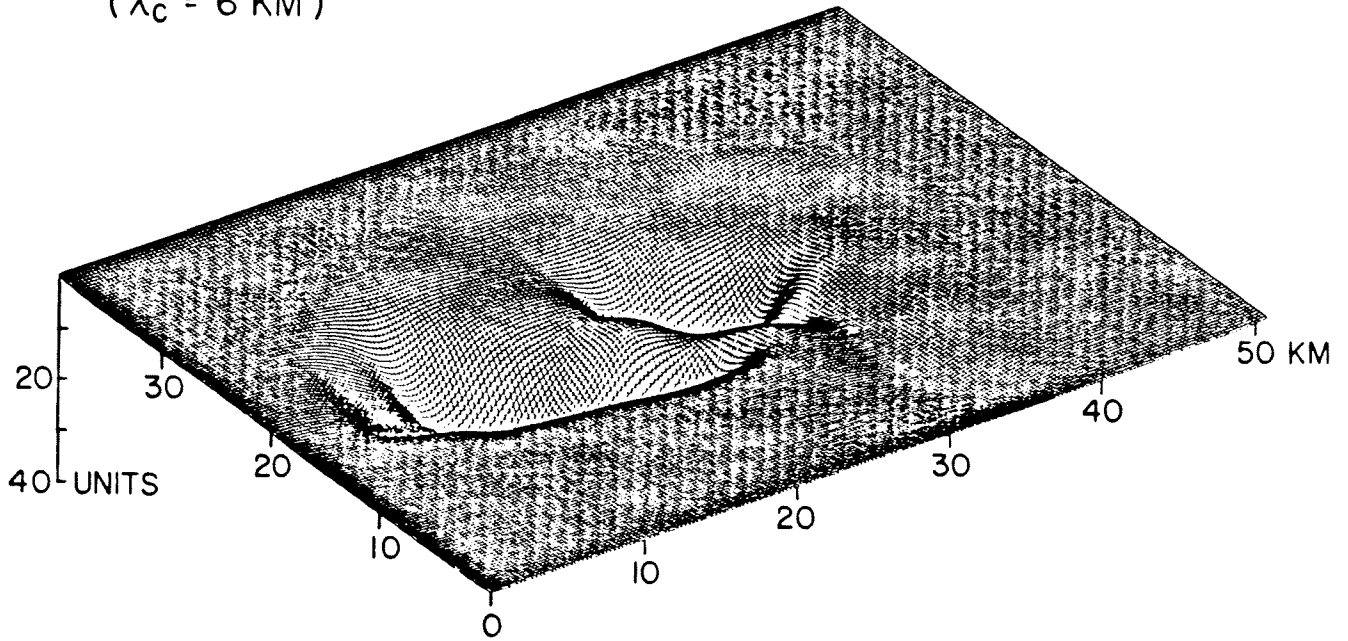# SMOOTHED VERSION OF FINAL MODEL
(λ_c = 6 KM)

FIGURE 5

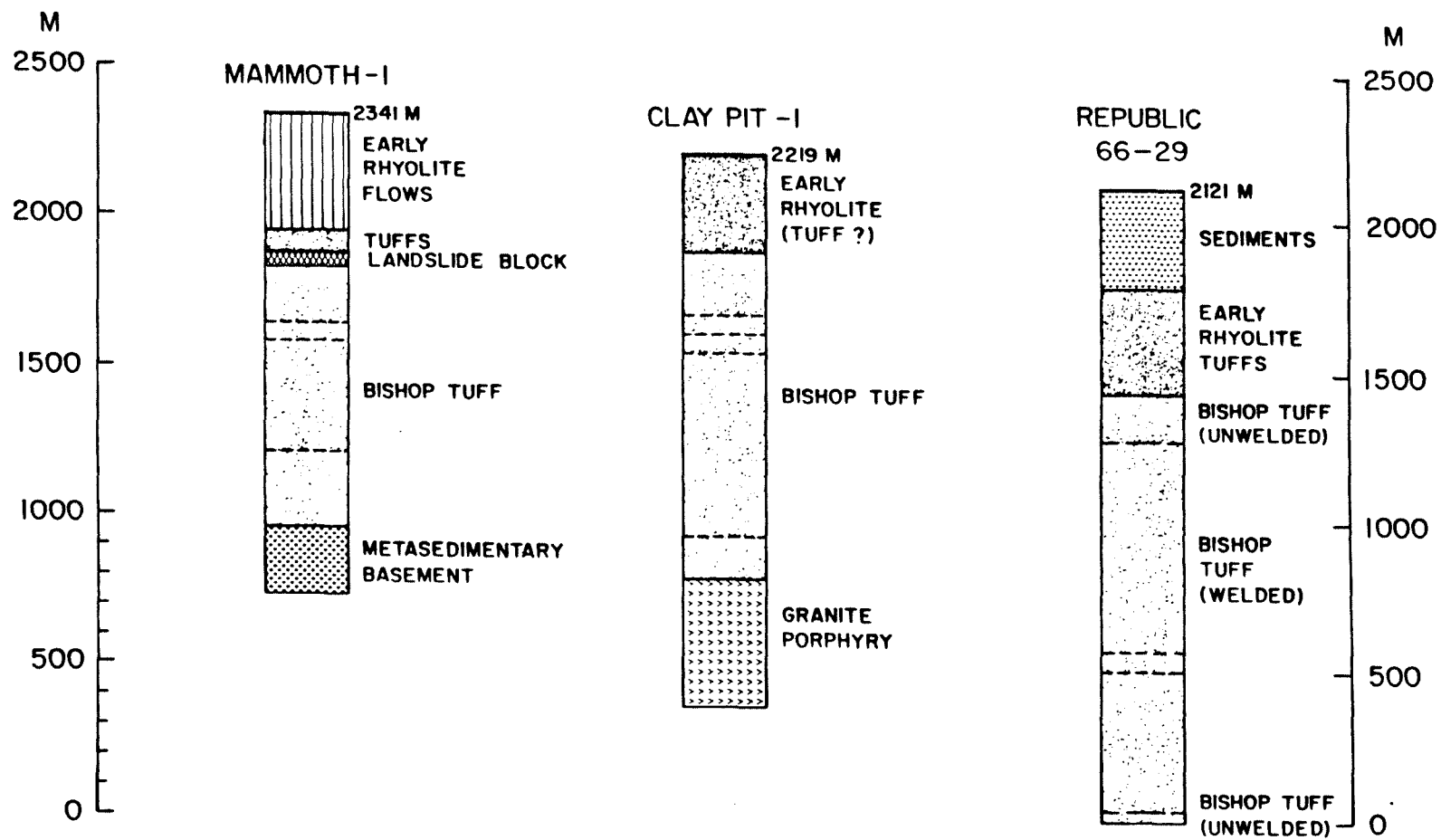FIGURE 6

Magnetotelluric Profiling Across Long Valley Caldera

Phil Wannamaker, UURI
Salt Lake City, Utah

From November 17 to December 16, 1986, UURI collected thirteen tensor magnetotelluric soundings across the eastern half of Long Valley caldera (Figure 1). The period range of measurement was from less than 0.01 to 300 s and the data quality overall is very good to excellent. The purpose of the survey is to gain control of upper crustal conductivity structure and to ascertain the presence of a deep hydrothermal or magmatic system. This work is supported by the DOE/Magma program.

Reconnaissance electrical geophysics together with gravity and refraction seismics suggest substantial upper crustal conductances especially in the east but also in the west and south moats (Figure 2). Bipole-bipole apparent resistivities, telluric ellipse orientations, faulting, and gravity all indicate a NNW structural trend on average beneath our MT profile. Thus, our soundings are presented and interpreted using a fixed N20°W x-axis.

Towards the eastern portion of the line, the soundings detect a conductive layer overlying or just within the Bishop Tuff (Figure 3). The layer deepens towards the east and persists beneath our eastern-most site. However, the layer comes to the surface and ends at site 2 about a mile SE of Clay Pit. This occurs approximately at the NW extension of the Hilton Creek fault zone as interpreted from previous USGS bipole-bipole work by D. Stanley.

To the west over the resurgent dome, near-surface resistivities increase with the presence of younger volcanics

(Figure 4). However, a deep conductive axis trending NNW is apparent especially in the impedance phase data at the middle and longer periods. The manifestation occurs exclusively in the TE mode data ($P_{xy} > \phi_{xy}$), verifying both the NNW trend and our selection of a fixed orientation for data interpretation. A simple 1-D inversion of P_{xy} and ϕ_{xy} gives a depth to the conductor of about 5 km.

The data we have collected is summarized in pseudosection form (Figures 5 and 6). The shallow conductive layer to the east and a very resistive basement especially in the west-central portion of the line are clear in both TE and TM modes. The very flat character of the TM phase ϕ_{yx} at long periods suggests uniform resistivity in the middle and lower crust, or at least inhomogeneities whose E-W extent is substantially less than their depths. Evidence for the NNW-trending deep conductor stated above lies in a high in ϕ_{xy} around 10 to 100 s beneath the resurgent dome, but extension of our profiling to the west is crucial to establish whether this represents an isolated axis.

151

FIGURES

1. Site location map for thirteen MT soundings taken in Long
    Valley caldera by UURI. SF denotes Santa Fe well pad.

2. Bipole-bipole apparent resistivity contour map (Stanley et
    al., 1976, JGR, 810-820) showing NNW structural and
    resistivity trends.

3. Station 10 near Cashbaugh Ranch in eastern portion of survey
    area. Note conductive layer apparent in both modes at
    periods around 0.3 s.

4. Station 1 about 1 km SW of Santa Fe well. Note the rapid
    decrease in P_{xy}, and the high values of ϕ_{xy}, relative to
    site 10 at middle to long periods. This is suggestive of a
    NNW-trending conductor beneath the resurgent dome.

5. Pseudosections of TM mode apparent resistivity P_{yx} along our
    profile. COntours are in Ω-m and degrees respectively.
    Observe the flat character of ϕ_{yx} at long periods.

6. Pseudosections of TE mode apparent resistivity P_{xy} and
    impedance phase ϕ_{xy} along our profile. Observe the
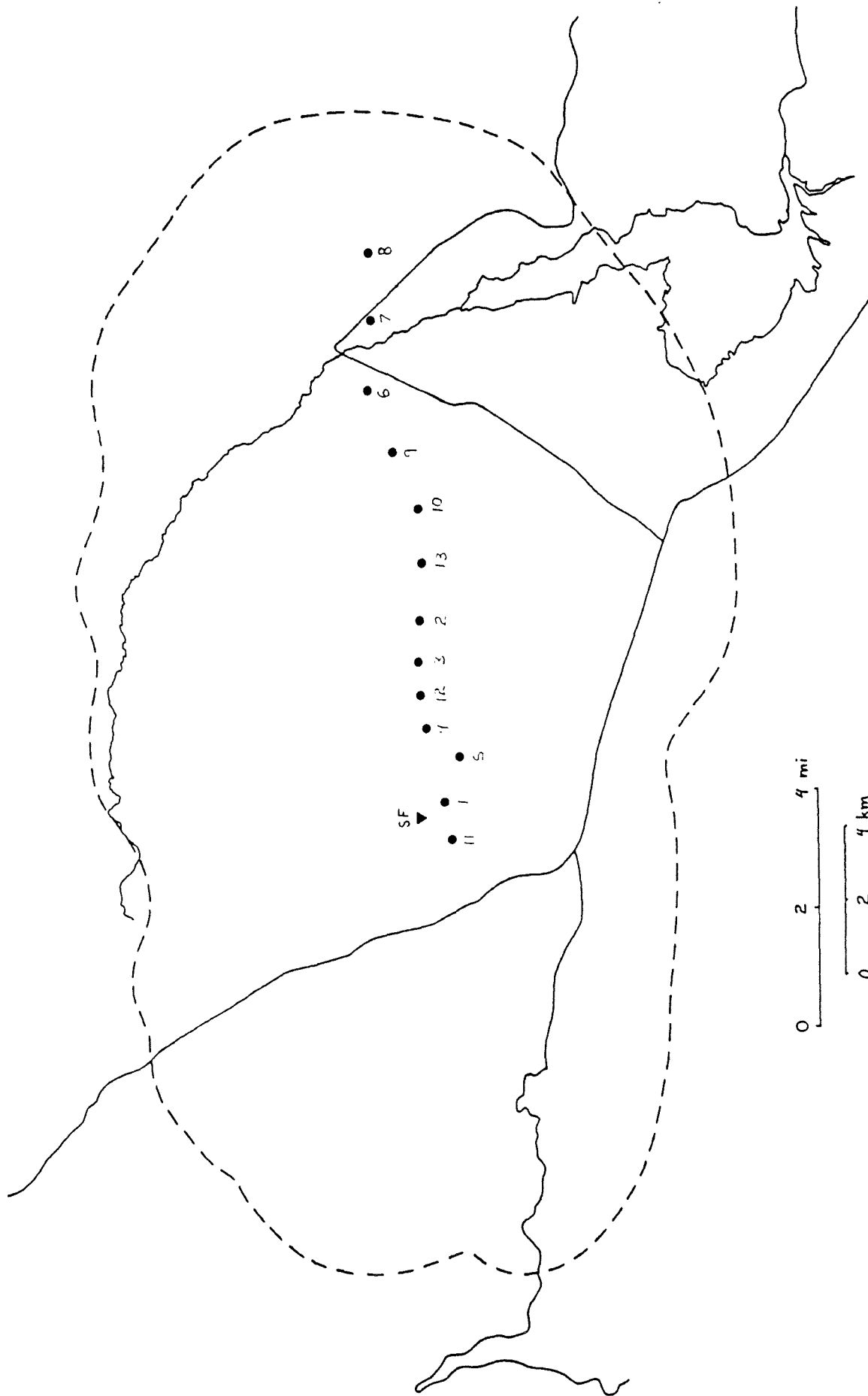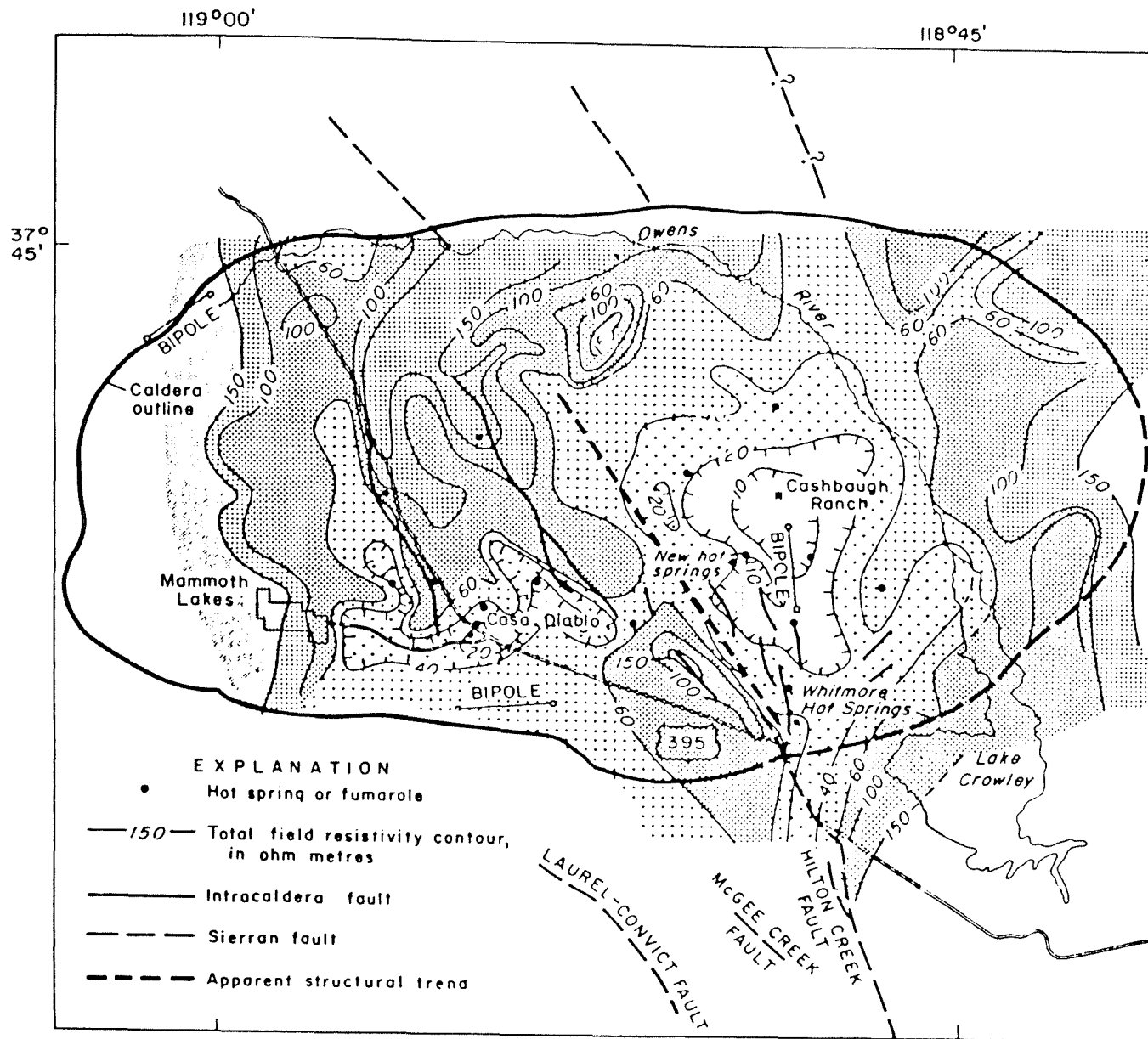   impedance phase high beneath the resurgent dome.

Fig. 1
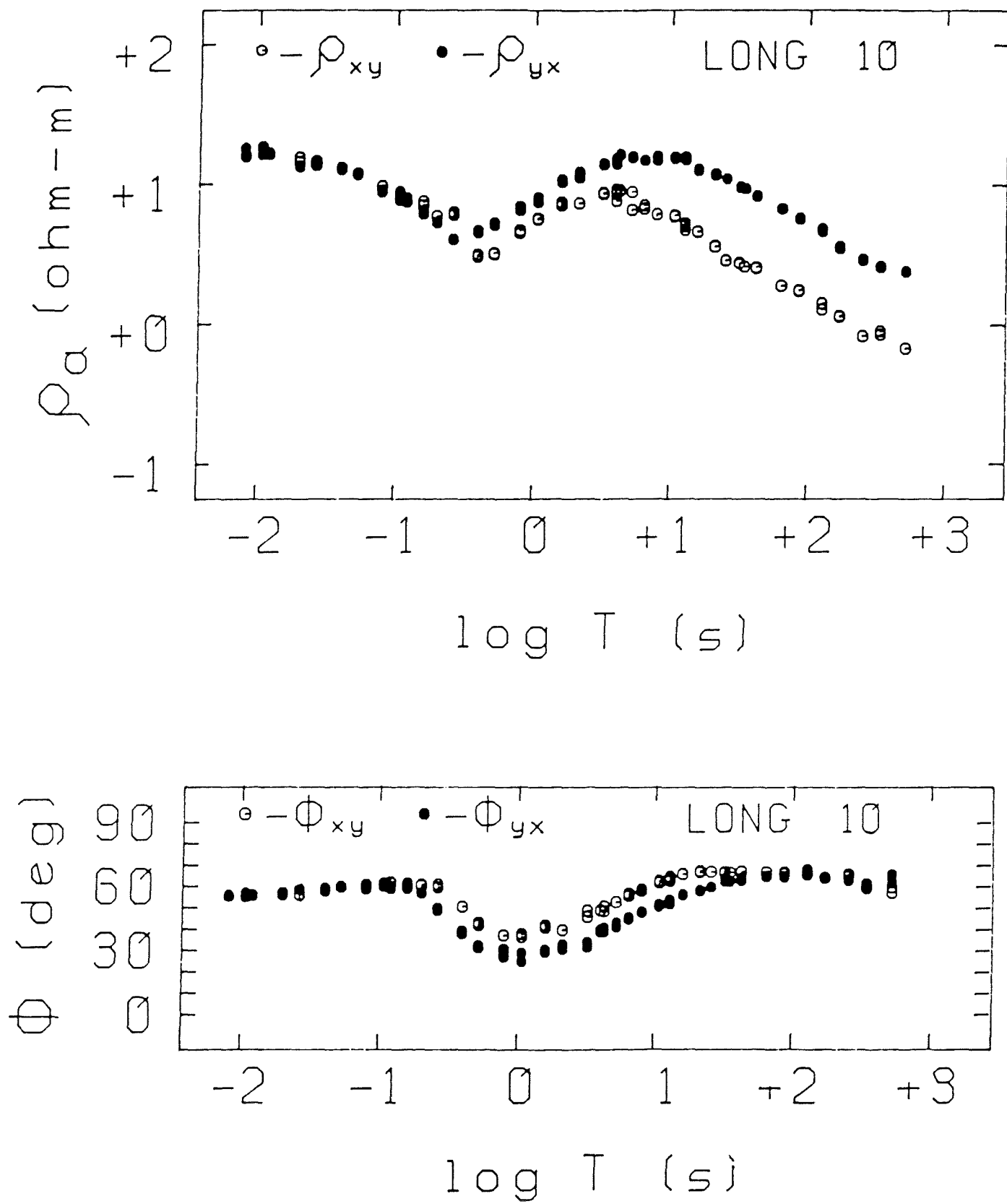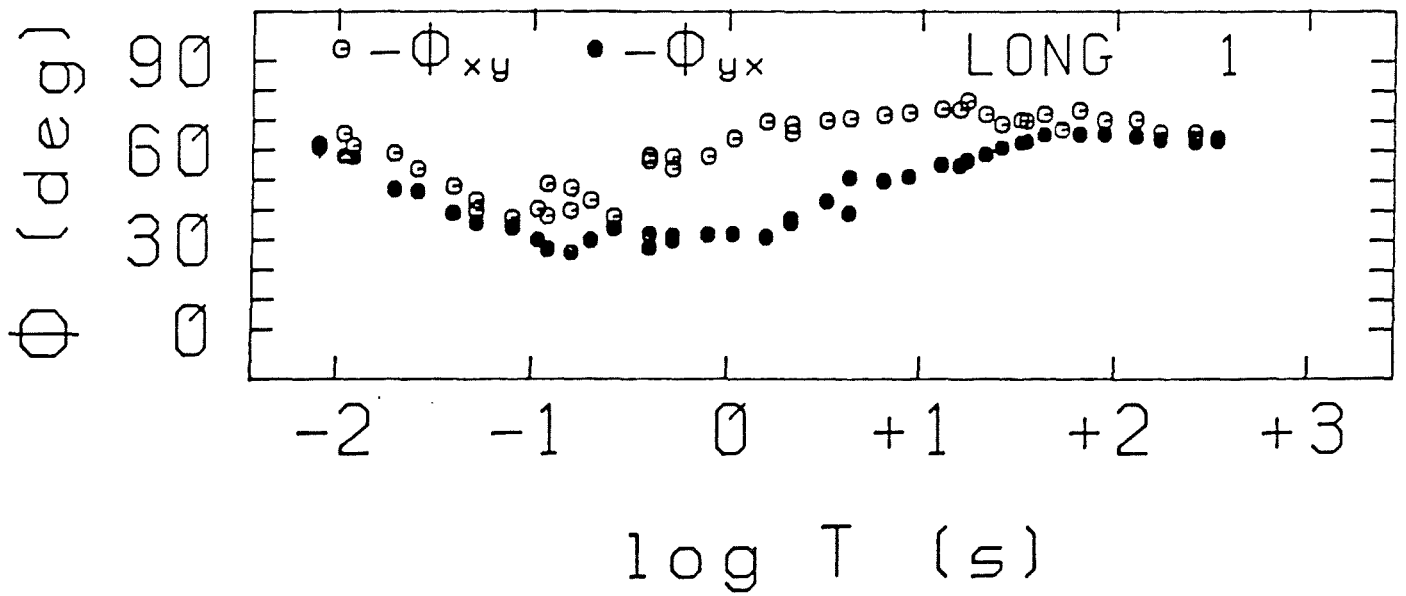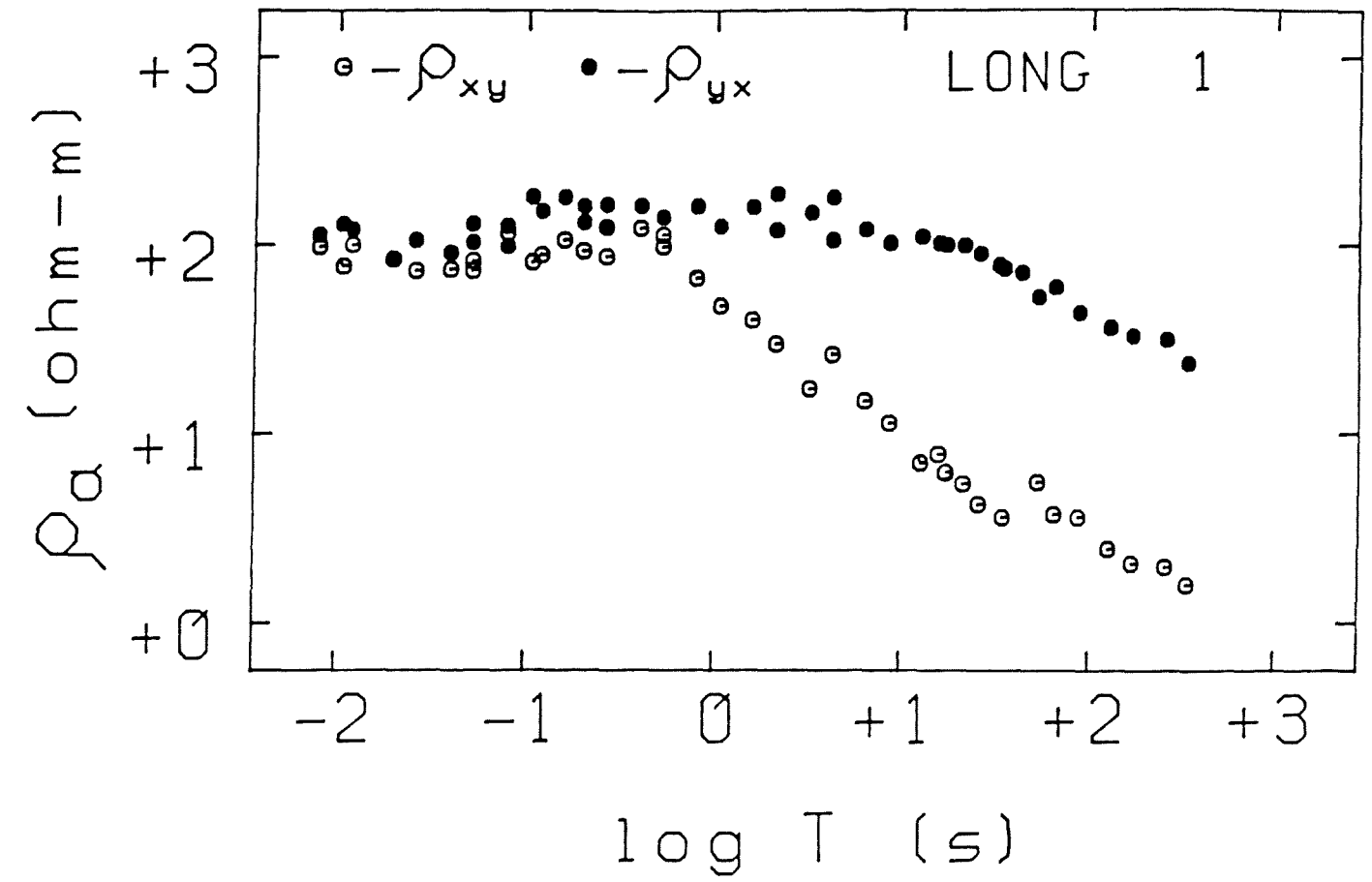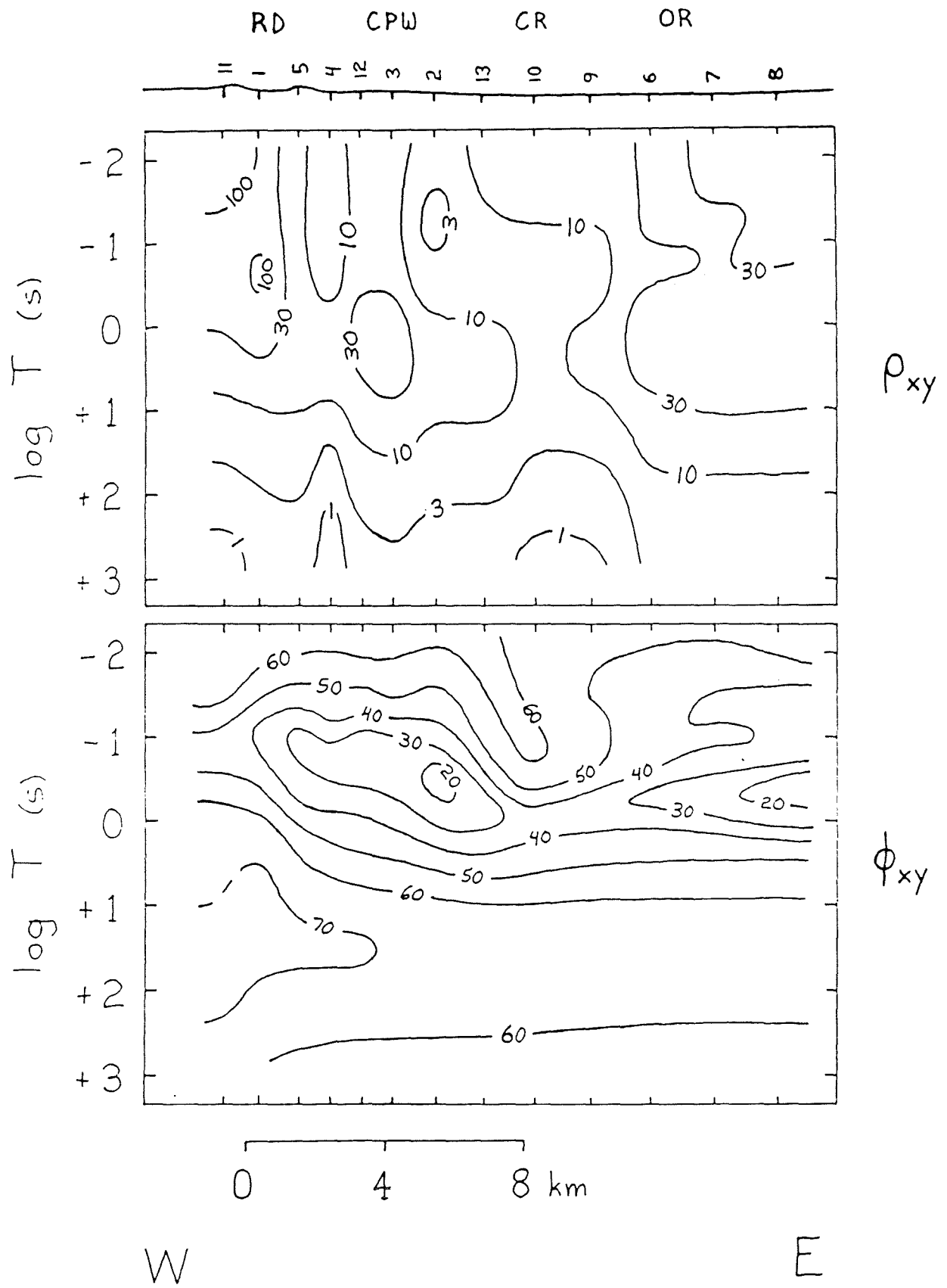
153

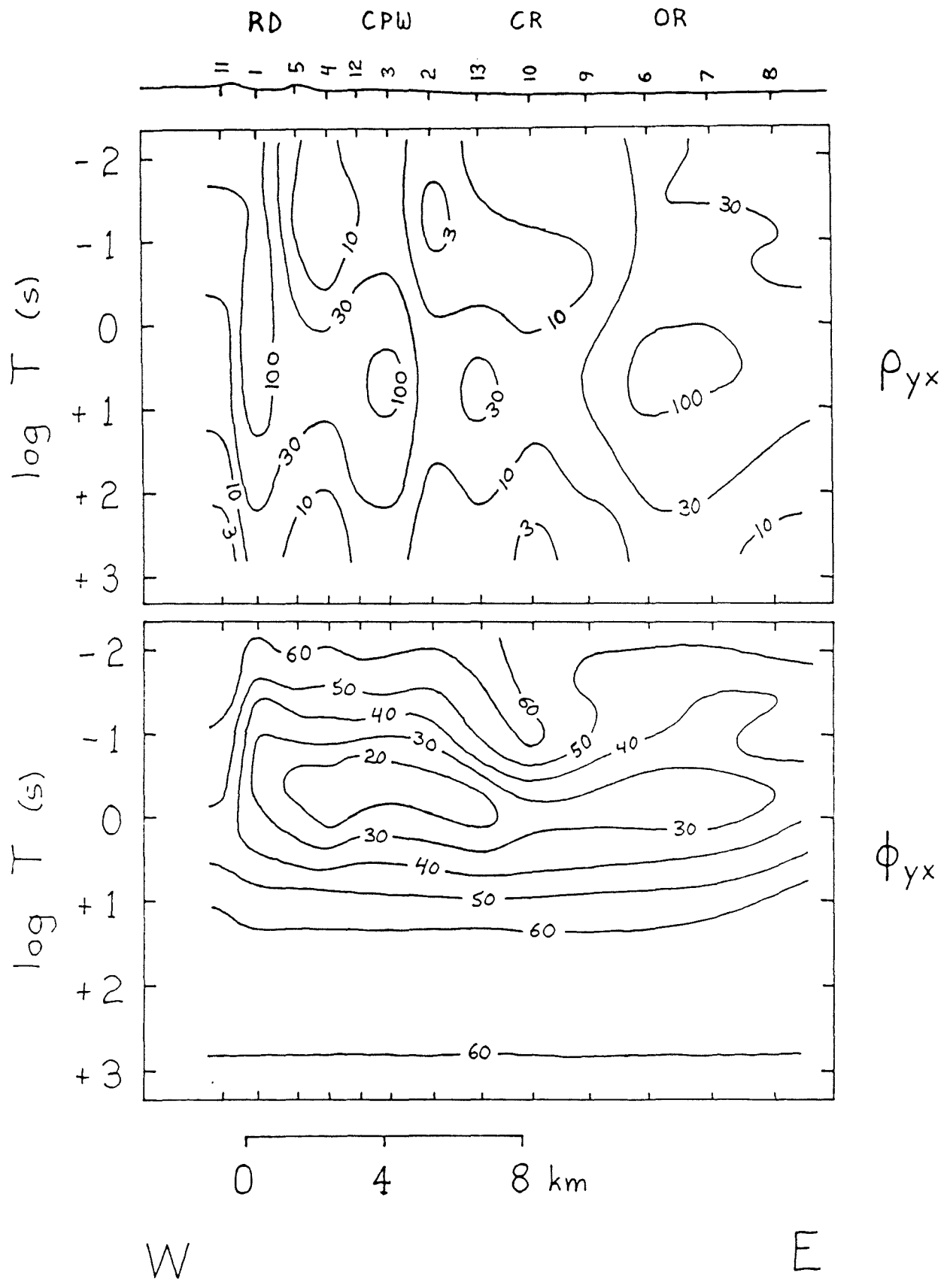Fig. 2

Fig. 3

Fig. 4

Fig. 5

Fig. 6

THREE-DIMENSIONAL INTERPRETATION OF
MAGNETOTELLURIC DATA IN LONG VALLEY, CALIFORNIA

Stephen K. Park
Institute of Geophysics and Planetary Physics
University of California, Riverside
Riverside, CA 92521

Carlos Torres-Verdin and H. Frank Morrison
Department of Engineering Geoscience
University of California, Berkeley
Berkeley, CA 94720

INTRODUCTION

The volcanic complex at Long Valley has been the subject of intensive study, as summarized by Hermance (1983). It is a silicic system which has exhibited recent activity, although the last major eruption was 700,000 years ago (Bailey et al., 1976). Long Valley is of great interest because of three major reasons: 1) its potential for an eruption; 2) its potential for containing shallow magma; and 3) its potential for geothermal resources.

Recent deformation was reported for the period of 1975-1982, and a spherical magma chamber located at a depth of 10 km was inferred to be the cause of the deformation (Savage and Clark, 1982). Intense seismic activity, including swarms of earthquakes in 1980 and 1982, accompanied this deformation (Ryall and Ryall, 1980, 1983). Long Valley has been monitored with a dense array of seismometers since then, and data from this array have been used to construct three-dimensional models of the caldera (Sanders, 1984). Sanders (1984) concludes that a body exists at depths of 4-13 km which has low velocity, and attenuates both compressional and shear waves. He suggests that this body may be composed of magma.

Several types of geophysical data have been cited as supportive of shallow magma in Long Valley (Rundle et al., 1986). Magma has been inferred in the previously mentioned interpretations of geodetic and seismic studies. Most of the electrical surveys have been for shallow (depths less than 2 km) targets, but Hermance et al. (1984) measured telluric fields and examined deeper structure. They concluded that their measurements were insensitive to the presence or absence of magma. However, Long Valley is the site of rich geothermal resources whether or not magma exists at depth.

Many geophysical surveys have been made of the geothermal resources in Long Valley. Lachenbruch et al. (1976) has developed thermal models for the distribution of heat in Long Valley Caldera. Hydrological investigations of the caldera provide lithological logs of many wells (Farrar et al., 1985). Stanley et al. (1976) conducted an extensive resistivity and electromagnetic survey which delineated several conductive anomalies. Chevron Resources Company and Unocal both have detailed studies of Long Valley which have been proprietary until recently. In 1986, Chevron and Unocal released 77 stations of magneto-telluric data from Long Valley to us.

Our goals were to develop interpretive methods in a complex volcanic environment and to confirm or deny the earlier assertion that the telluric data

were insensitive to the presence of magma (Hermance et al., 1984). We worked with many more MT sites (77 versus 23) and utilized a 3-D modeling program (Park, 1985). All possible pertinent geophysical information was incorporated into our electrical model.

The magnetotelluric response at frequencies from .001 Hz to 100 Hz is controlled almost completely by shallow structure in the caldera. The complex electrical structure in the first kilometer, coupled with a good conductor at a depth of 1,500 m, effectively screens any deeper structure beneath the caldera.

We present here an interpretation based principally upon phase. Static off-sets of the sounding curves are so severe that the apparent resistivities were only useful in constraining the shallow structure. The phase was particularly sensitive to the presence or absence of the conductor at 1,500 m.

CONSTRAINTS UPON THE MODEL

An interpretation of these data is impractical without external constraints. The electrical survey of Stanley et al. (1976) provided resistivities in the upper kilometer. These data were supplemented with 1-D inversions of the magne-totelluric responses at the higher frequencies for each station. The range of frequencies used at each site was variable, and depended upon the onset of significant anisotropy in the sounding curves. We used electrical logs from Lawrence Berkeley Laboratory (Goldstein, pers. comm., 1986) for three deep (1,600 m or more) wells in the caldera to establish the resistivity of several volcanic formations. Lithologic logs (Farrar et al., 1985) and seismic data (were compiled by Carle (1986) into isopac) maps for different formations and we incorporated his maps into our model. Carle's structural maps inferred from gravitational data also provided us with total thickness of the caldera.

The synthesized model is shown in Figure 1. The structure for the upper 1,000 m is based upon the above constraints with minor adjustments to fit the data. The structure from 1,000 m to 1,500 m is also based upon the above constraints, but modified to fit the observed phases. Principally, this modifi-cation consisted of placing the good conductor (1 ohm-m) where it was needed.

We attribute the high conductivity of the zone from 1,500 m to 1,700 m to metasediments and to fractured zones, based upon wells. The conductor is observed in a well approximately 5 km east of Mammoth Lakes at depths from 1,500 m to 1,700 m. This unit is a remnant of the roof pendant in the Sierra Nevada, and consists of metamorphosed sediments containing graphite (Goldstein, pers. comm., 1986). Measured resistivities from logs for this unit range from below 1 ohm-m to over 100 ohm-m, with approximately 80% of the unit below 1 ohm-m. Elsewhere, pervasive fractures are found in wells on the western side of the caldera (Goldstein, pers. comm., 1986).

The location of the conductor is consistent with the hypothesis that the metasediments were simply dropped down into the caldera as the magma chamber deflated during the eruption 700,000 years ago. These metasediments crop out to the north and south of the caldera, and the conductor matches nicely with these outcrops. However, the conductor is also located in close proximity to numerous faults and may be caused by fractures.

160

COMPARISON TO DATA

Chevron Resources Company released 54 stations of magnetotelluric data to us in 1986. Our original work was wholly with these data because the data from Unocal were not released until January, 1987. Hence, much of the interpretation is based upon Chevron's data, with Unocal's data used as an additional control.

We found that several patterns emerged upon examination of the phases at the 54 sites. Many sites were close to one another and exhibited similar behavior, in spite of severe problems with shallow, local heterogeneity. We clustered sites with similar behavior and present representative sites in Figure 2. Sites were clustered if they shared: 1) similar behavior of the phases; 2) common angles of rotation; 3) common strikes determined from tippers; and 4) similar anisotropy in the apparent resistivities. Clustering was necessary because of poor quality of the data and because of the complex, shallow structure. The data from Chevron were collected without remote referencing, so the quality of the soundings is variable. The later data from Unocal (23 sites) were collected with a remote reference, and the quality of these soundings is much better. However, we are still trying to resolve problems concerning the phases. The data exhibit phases which do not match those from the earlier data and do not match those calculated from any reasonable model.

The phases predicted using our model are shown in Figure 3. The overall agreement is good, although some minor discrepancies are seen. The quality of the data precludes a more detailed model than is shown in Figure 1. Note that no structure deeper than 1,600 m is needed to provide this good fit. The decrease in phase below 45° near 1 Hertz is associated with the absence of the good conductor at 1,500 m. The phase in the northeast quadrant of the caldera never dips below 45° and is almost monotonically decreasing with increasing frequency. This behavior could only be predicted if the good conductor was present beneath this region.

An extremely important conclusion from this study is that phase is not insensitive to lateral heterogeneity, but merely less sensitive to it. The differences in the phases of the maximum and minimum apparent resistivities (referred to hereafter as anisotropy in the phases) persist to frequencies at which the sounding is responsive to the electrical mantle (0.1 Hertz and lower). This anisotropy in phases is caused wholly by shallow (depth < 1,600 m) structure. We conclude from our work that there is simply no substitute for 3-D modeling in complex environments.

SENSITIVITY TO MAGMA

We have no results for this section yet, as that work is in progress. However, we can infer what our results will be from an analysis of the effects of the conductor at 1,500 m. Phases at sites directly over the conductor decrease by 30° at 1 Hz if the conductor is removed. Apparent resistivities increase by a factor of 5 if the conductor is absent. Sites more than 2 km from the edges of the conductor were not affected appreciably by the removal of the conductor (5° in phase and factors of 2 in apparent resistivities).

The placement of a larger, deeper (4-10 km) conductor representing magma is not possible without significantly modifying the responses. The presence of a

small body of magma is problematical, however. A small (2 km x 2 km x 500 m) conductor at a depth of 4 km or more would only affect data taken directly above it. Small changes in surrounding sites would be seen, but these changes could easily be interpreted as caused by shallower structure. The quality of data combined with the shallow complexity makes the identification of subtle changes impossible. The shallow structure in Figure 1 is constrained by a wealth of other geophysical data and cannot be modified greatly. We infer from our detailed analysis of the electrical data that any magma beneath Long Valley must be in small bodies, and that these small bodies are not detectable.

CONCLUSIONS

We have demonstrated that an interpretation principally using the phases is useful in complex, volcanic environments. While the problem of static offsets of sounding curves is alleviated using this method, the effects of shallow heterogeneity are still seen in the phases. There is no substitute for 3-D modeling of the structure. Patterns of the behavior of the phase were much clearer if we clustered similar sites.

The presence of a large body of magma beneath Long Valley is precluded, based upon interpretation of over 70 sites of MT data released by Chevron and Unocal. Small bodies of magma may be present, but the effects of these bodies are subtle except directly above them. These subtle effects are not noticeable in a survey with average quality of data and extremely complex, shallow structure.

ACKNOWLEDGEMENTS

REFERENCES

Carle, S. F., 1986, A three-dimensional gravity model of the geologic structure of Long Valley caldera, California: presented at American Geophysical Union Fall Meeting, San Francisco, Dec. 7-12, 1986.

Farrar, C. D., Storey, M. L., Rojstaczer, S. A., Janik, C. J., Mariner, R. H., and Winnett, T. L., 1985, Hydrologic and geochemical monitoring in Long Valley caldera, Mono County, California: U.S.G.S. Water-Resources Investigations Report 85-4183.

Hermance, J. F., 1983, The Long Valley/Mono basin volcanic complex in eastern California: status of present knowledge and future research needs: Rev. Geophys. and Space Phys. 21, p. 1545-1565.

Hermance, J. F., Slocum, W. M., and Neumann, G. A., The Long Valley/Mono basin volcanic complex: a preliminary magnetotelluric and magnetic variation interpretation: J. Geophys. Res. 89, p. 8325-8337.

Lachenbruch, A. H., Sass, J. H, Munroe, R. J., and Moses, T. H., Jr., 1976, Geothermal setting and simple heat conduction models for Long Valley caldera: J. Geophys. Res. 81, p. 769-784.

Park, S. K., 1985, Distortions of magnetotelluric sounding curves by three-dimensional structure: Geophysics 50, p. 785-797.

Rundle, J. B., Carrigan, C. R., Hardee, H. C., and Luth, W. C., 1986, Deep drilling to the magmatic environment in Long Valley caldera: EOS 67, p. 490-491.

Ryall, F. and Ryall, A., 1980, Spatial-temporal variations in seismicity preceding the May, 1980, Mammoth Lakes, California, earthquakes: Spec. Rept. Calif. Div. Mines Geol. 150, p. 27-39.

Ryall, F., and Ryall, A., 1983, Attenuation of P and S waves in a magma chamber in Long Valley caldera, California: Geophys. Res. Lttrs. 8, p. 557-560.

Sanders, C. O., 1984, Location and configuration of magma bodies beneath Long Valley, California, determined by anomalous earthquake signals: J. Geophys. Res. 89, p. 8287-8302.

Savage, J. C., and Clark, M. M., 1982, Magmatic resurgence in Long Valley caldera, eastern California: Science 219, p. 1432-1433.

Stanley, W. D., Jackson, D. B., and Zohdy, A. A. R., 1976, Deep electrical investigations in the Long Valley geothermal area, California: J. Geophys. Res. 81, p. 810-820.
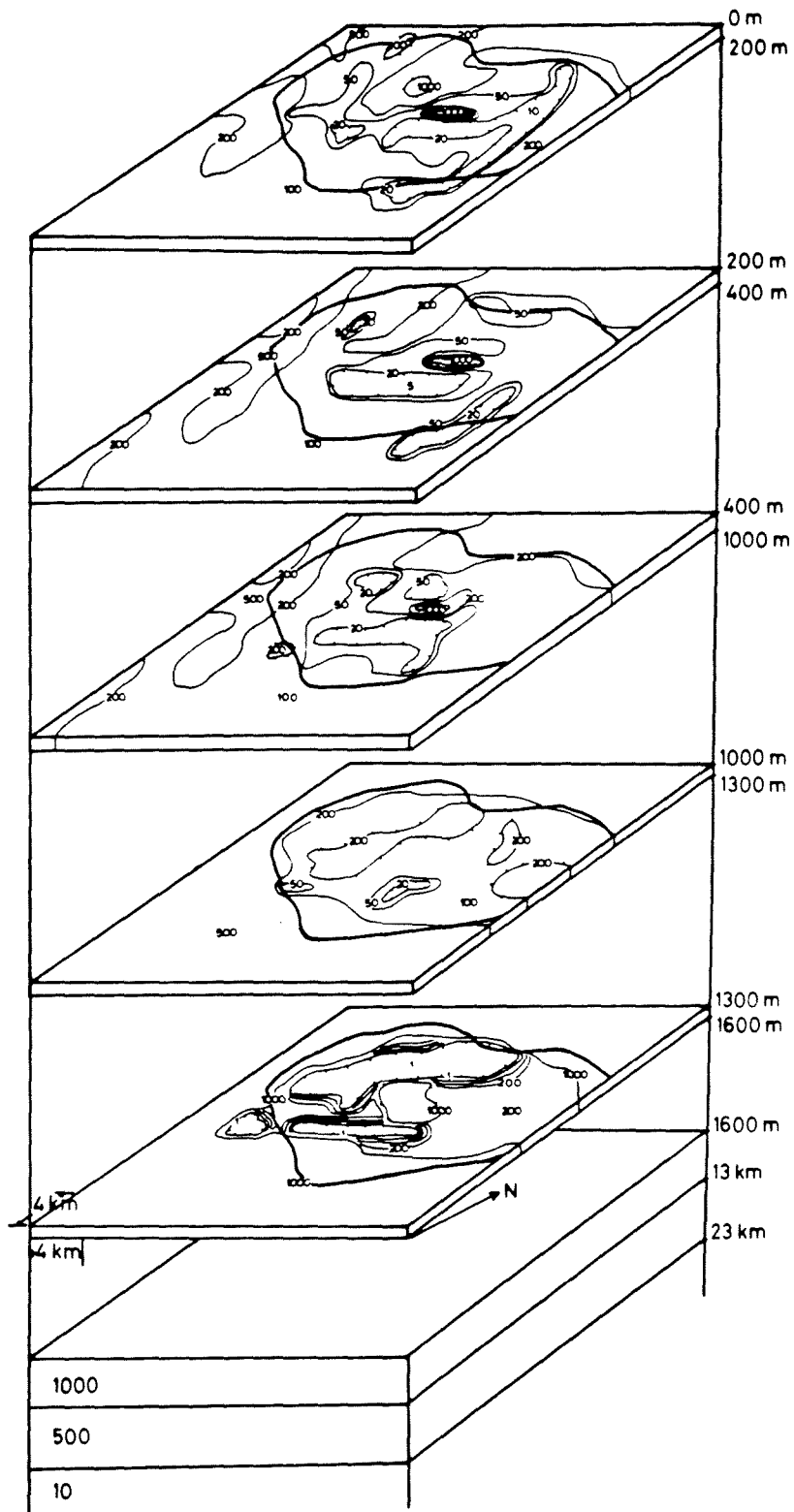
Figure 1- Isometric plot of electrical structure in and around Long Valley. Resistivities are contoured and are in ohm-m. Depths are shown on the right-hand side of plot. Outline of caldera is shown with heavy line on each slice. Note that heterogeneous structure is only 1600 m thick, and resistivities for the halfspace are in ohm-m.

164
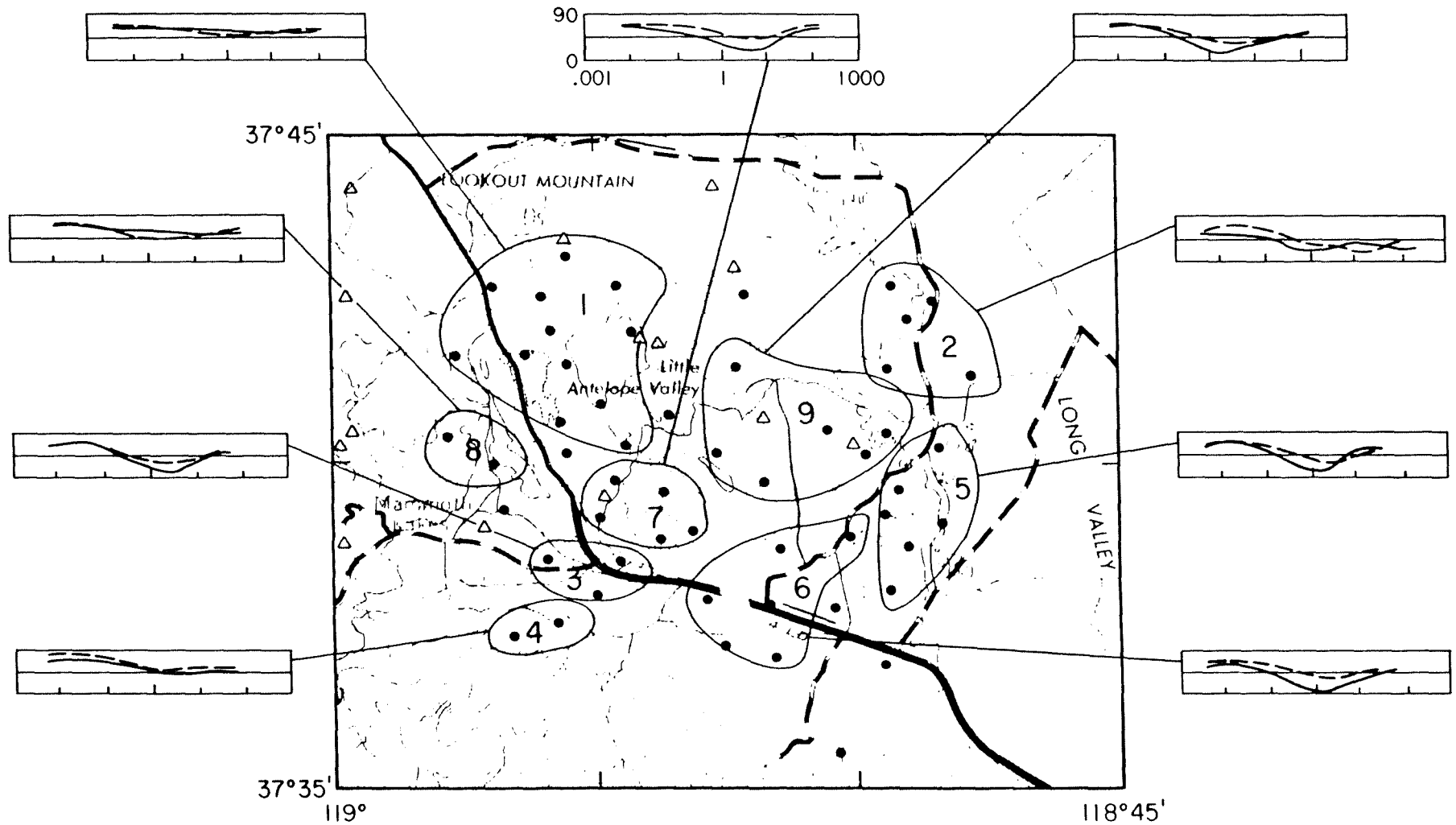
Figure 2 - Plots of the phases from clusters of sites in Long Valley with similar behavior. Chevron data are shown with solid dots and Unocal data are shown with open triangles. The phases are measured from 0° to 90° for frequencies from .001 Hertz to 100 Hertz.

165
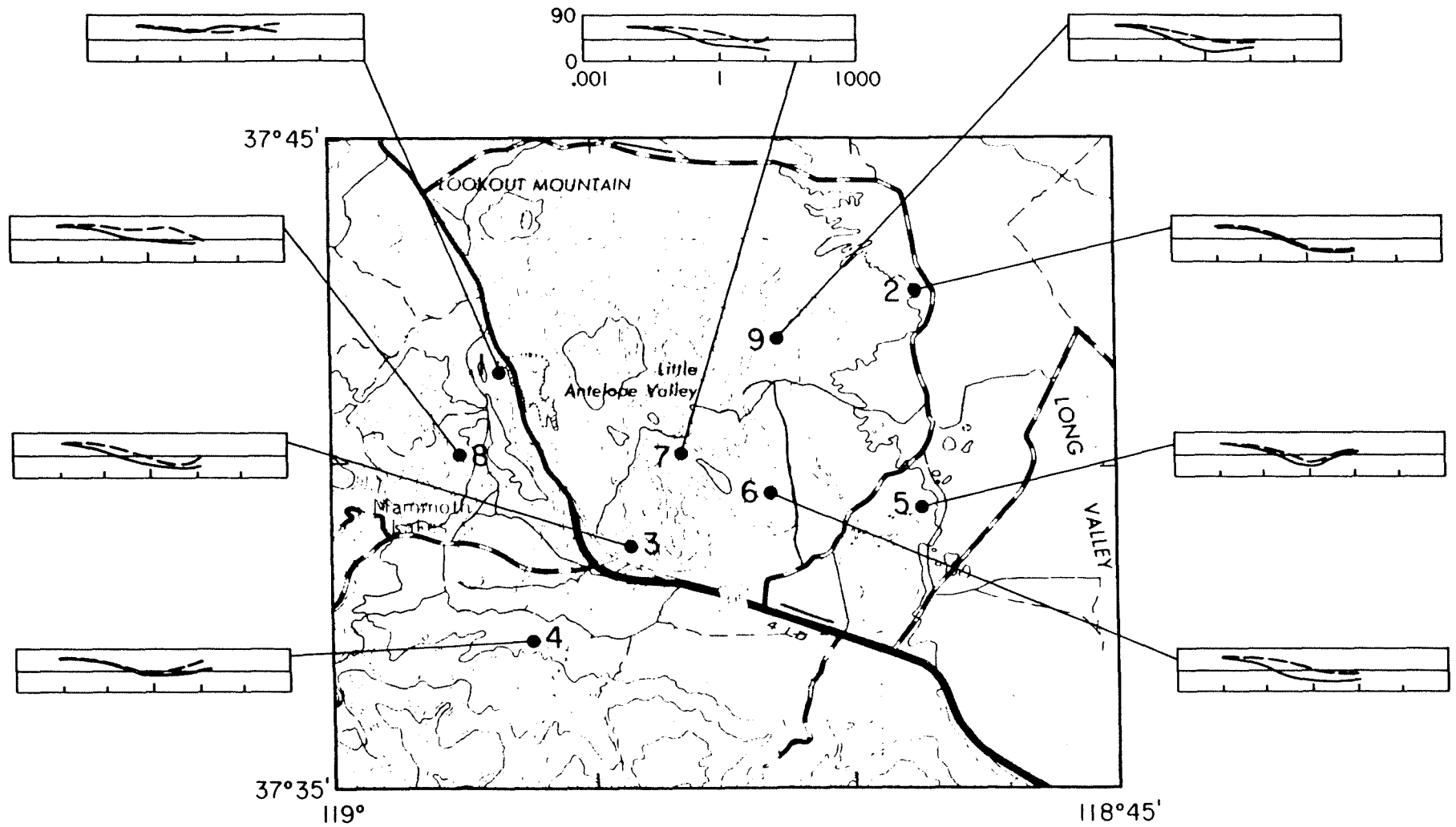
Figure 3 - Phases predicted from model shown in Figure 1. Scales and units are the same as in Figure 2. Numbering of sites corresponds to the numbering in Figure 2, but locations are taken from the grid for modeling. This grid is not shown.

166

GEODETIC MONITORING OF DEFORMATION WITHIN THE LONG VALLEY CALDERA, 1983.5–1987.1 DATA FROM THE TWO-COLOR GEODIMETER NETWORK

John Langbein
U.S. Geological Survey
345 Middlefield Road
Menlo Park, California 94025

Since June 1983, the U.S. Geological Survey has been frequently resurveying the lengths of several baselines within and near the Long Valley caldera. Measurements discussed here are made with a two-color geodimeter which has a precision characterized by $\sigma^2 = a^2 + b^2 l^2$, where a=0.5 mm, b=0.18 ppm and l is the baseline length, which for this network is between 2.0 and 10.5 km. The initial network consisted of 13 baselines located within the south moat and straddling the zone of seismicity defined by the January 1983 earthquake swarm. The network has since been expanded to 40 baselines. Some of the new baselines are in the south moat area, some span the resurgent dome near Lookout Mountain, and others straddle the Hilton Creek fault as it enters the caldera. Measurements of 7 to 11 baselines are made frequently, ranging from once per month to several times per week. Other baselines are only measured infrequently, approximately once or twice per year. In this mode of operation, both good temporal and spatial distribution of measurements are achieved.

Measurement procedures and data analysis for the two-color geodimeter network have been discussed elsewhere. The attached figures show the complete data through early March 1987 and a time series model that fits the data. The following discussion summarizes the data and their implications.

The initial measurements made from June 1983 through October 1984 have been discussed by *Linker et al.* (1986). The two-color measurements for that interval are characterized primarily by east-west extension. However, the strain field is not uniform. Furthermore, the data show that the rate of extension decreased during the 1-1/4 year interval. During the summer of 1983, extension rates on a couple of baselines averaged 5 ppm/yr, which is more than an order of magnitude greater than typical rates observed for geodetic baselines elsewhere in California. By mid-1984, the extension rates decreased by a factor of 2 to 3.

The discussion of the two-color geodimeter data is extended by *Langbein et al.* (1987a) using a longer record of observations, from June 1983 through October 1985. The additional measurements clearly define a decrease in rate of extension. In their paper, a model for deformation is proposed which satisfies the two-color geodimeter data and a set of length measurements made with a single-color geodolite (*Savage et al.*, 1987). In contrast to the two-color data, the geodolite measurements are made annually and on

longer baselines. The simple model consists of three sources of deformation. Included are two Mogi point sources of inflation, both representing inflation beneath the resurgent dome, and a rectangular dislocation with uniform dextral slip, representing the fault zone defined by the January 1983 earthquake swarm. One of the two point sources is located at 10 km depth and approximately 5 km due north of Casa Diablo Hot Springs. The second point source is located at a depth of 5 km approximately beneath the Hot Springs. The modeled fault in the south moat is 6 km wide and comes to within 0.5 km of the ground's surface.

The decrease in extension rate is modeled as a combination of decreasing rate of inflation beneath the resurgent dome plus decreasing rate of slip on the fault in the south moat. Although the statistical covariance between the shallow inflation and deep inflation is quite high (0.8), one calculation implies that the deep source inflated by 0.0138 ± 0.0008 km^3 from mid-1983 to mid-1984, and by 0.0052 ± 0.0008 km^3 from mid-1984 to mid-1985. Inferred slip in the south moat decreased from 33.3 ± 1.5 mm to 14.5 ± 1.5 mm during the same interval.

The inference of decrease in the rate of inflation is controversial when either the single-color geodolite and releveling data are examined for the interval 1983.5–1985.5. *Savage et al.* (1987) examined a set of geodolite baselines that are most sensitive to deep inflation and that are also least sensitive to sources of shallow deformation within the south moat. They argue that these baselines are best fit by linear-in-time trends and have no significant deceleration terms. However, *Langbein et al.* (1987) demonstrate that a factor-of-two decrease in the rate of deep inflation could have occurred, but would not be detected by these baselines. This is primarily due to the fact that these baselines are spatially too far from the deep source and do not have the necessary ratio of signal to noise to detect a factor-of-two rate decrease during the two-year interval. Although the three yearly releveling data would be ideal for detecting changes in the rate of inflation, the survey from the middle year, 1984, may be contaminated by a systematic error (*Savage et al.*, 1987).

The two-color geodimeter measurements between October 1985 through August 1986 are discussed in *Langbein et al.* (1986 and 1987b), and the length changes are dominated by the effect of the Chalfant Valley earthquake of 21 July 1986. The coseismic length changes are consistent with the magnitude 6.4 earthquake located approximately 40 km from the center of the network. The average strain change for the network is compressive 0.68 ± 0.05 ppm oriented N70°$\pm$ 3°W.Based upon the displacement data, the moment of this earthquake is 4.6×10^{25} dyne-cm. Since the network does not straddle the White Mountain frontal fault zone, the computed moment is dependent upon the position of the modeled fault plane.

REFERENCES

Langbein, J., M. F. Linker and D. L. Tupper, Coseismic strain changes observed within the Long Valley caldera due to 21 July 1986 Chalfant Valley earthquake, *EOS*, vol. 67, p. 1106, 1986 (abst.)

Langbein, J., M. Linker, and D. Tupper, Analysis of two-color geodimeter measurements of deformation within the Long Valley caldera: 1983.5–1985.8, submitted to *J. Geophys. Res.*, 1987a.

Langbein, J., D. Tupper, and M. Linker, Chalfant Valley earthquake of July 21, 1986; Measurement of coseismic deformation within the Long Valley caldera, Eastern California, unpublished manuscript, 1987b.

Linker, M. F., J. O. Langbein, and A. McGarr, Decrease in deformation rate observed by two-color ranging in Long Valley caldera, *Science*, vol. 232, p. 213, 1986.

Savage, J. C., R. S. Cockerham, J. E. Estrem, and L. R. Moore, Deformation near the Long Valley caldera, Eastern California, 1982–1985, submitted to *J. Geophys. Res.*, 1987.

Fig. 1.   Map showing the location of the two-color baselines in the region of Long Valley. The stations Casa, Miner, Whitmore, and Lookout are used as instrument set-up points. Measurements are frequently made from Casa to Krakatau, Hot, Shark, Taxi, Convict, Tilla, Miner, Sherwin, Knolls, Sewer, and Lomike. The outline of the caldera is shown with heavy dashed lines and the faults are shown by thin lines.

Fig. 2.   Line-length changes measured using the two-color geodimeter are shown for those baselines using Casa as a common end point. The vertical line during 1986 shows the time of the Chalfant Valley earthquake. The length changes, $L - L_o$, have been normalized by the average distance, L_o, and are plotted in parts per million (ppm). Furthermore, an arbitrary constant has been added to the strains for the convenience of plotting. The error bars correspond to +/- one standard deviation.

Fig. 3.   Location of the modeled sources of deformation within the two-color geodimeter network.

Fig. 4.   Results of time-dependent modeling of deformation sources within the Long Valley caldera. Details of the calculation are discussed by Langbein *et al.* (1987a). The four time-series represent the amount of inferred deformation of each source and they are also a best fit to a combined set of geodolite measurements from 1983.5 to 1985.5 (*Savage et al.*, 1987) and two-color geodimeter measurements through March 5, 1987. The location of these sources are shown in Figure 3. Two Mogi point sources, one at 10 km depth and a second at 5 km represent inflation of the resurgent dome. *The apparent decrease in rate of deep inflation may not be valid since the covariance between the two modeled point sources is high.* A third point source is used to model the fluid withdrawal at the Casa Diablo Geothermal Plant. The total amount of inferred withdrawl predicts that the ground subsided by 7 mm in the vicintity of the power plant which is nearly equivalent to to the observed subsidence of 10 mm (*Stein, personal commication*, 1987). The calculation of fluid withdrawl places a small, 1 mm, correction on the absolute displacement of the station Casa. The last source is right-lateral slip on a fault in the south moat. The model fault is within the seismic zone defined by the January 1983 swarm. Coseismic slip on the White Mountain frontal fault zone has been estimated simultaneously with the parameters of the 4 time series. Finally, the root mean square of the model misfits to the data normalized by the data error is equal to 1.05 which is quite good considering the simplicity of the model.

BALD

MICRO

LOOKOUT

SAGE

DEAD

KRAKATAU

KNOB

RODGER

MIKE

KNOLLS

HOT

GRATE

LOMIKE

CASA

SEWER

SHARK

WHITMORE

DUCK

GULL

SHERWIN

TAXI

TILLA

CONVICT

WALL

MINER

PILE

U911

D124

Fig. 1

Fig. 2

Fig. 3.

INFLATION at 10km

INFLATION at 5km

DEFLATION at 0.5km
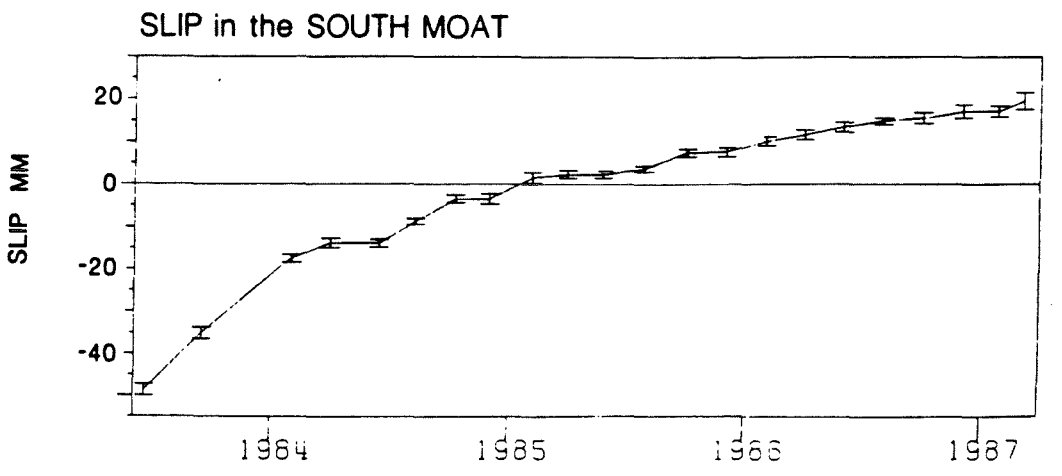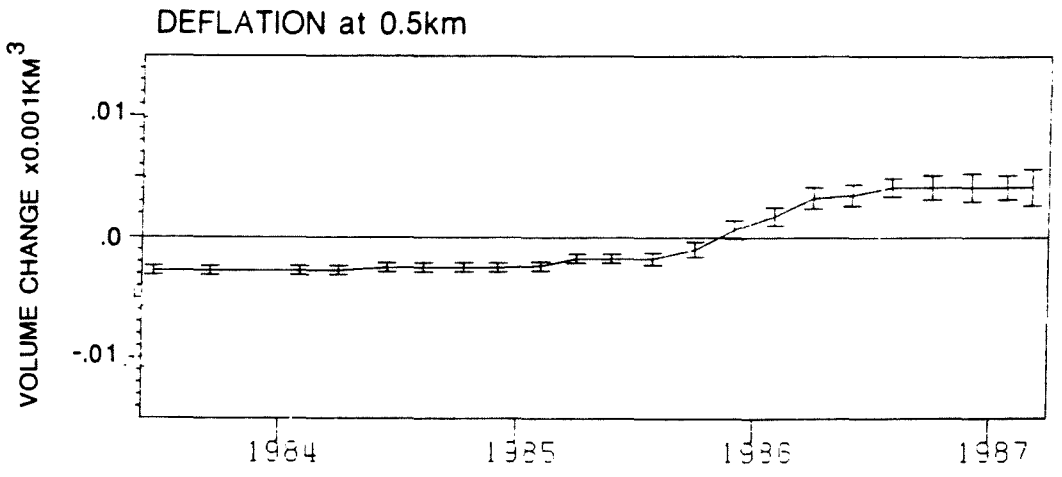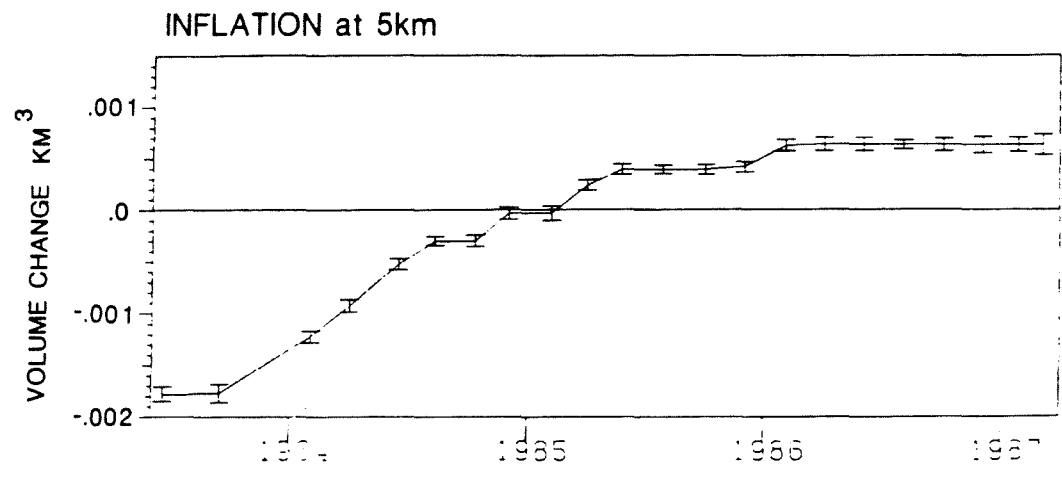
SLIP in the SOUTH MOAT
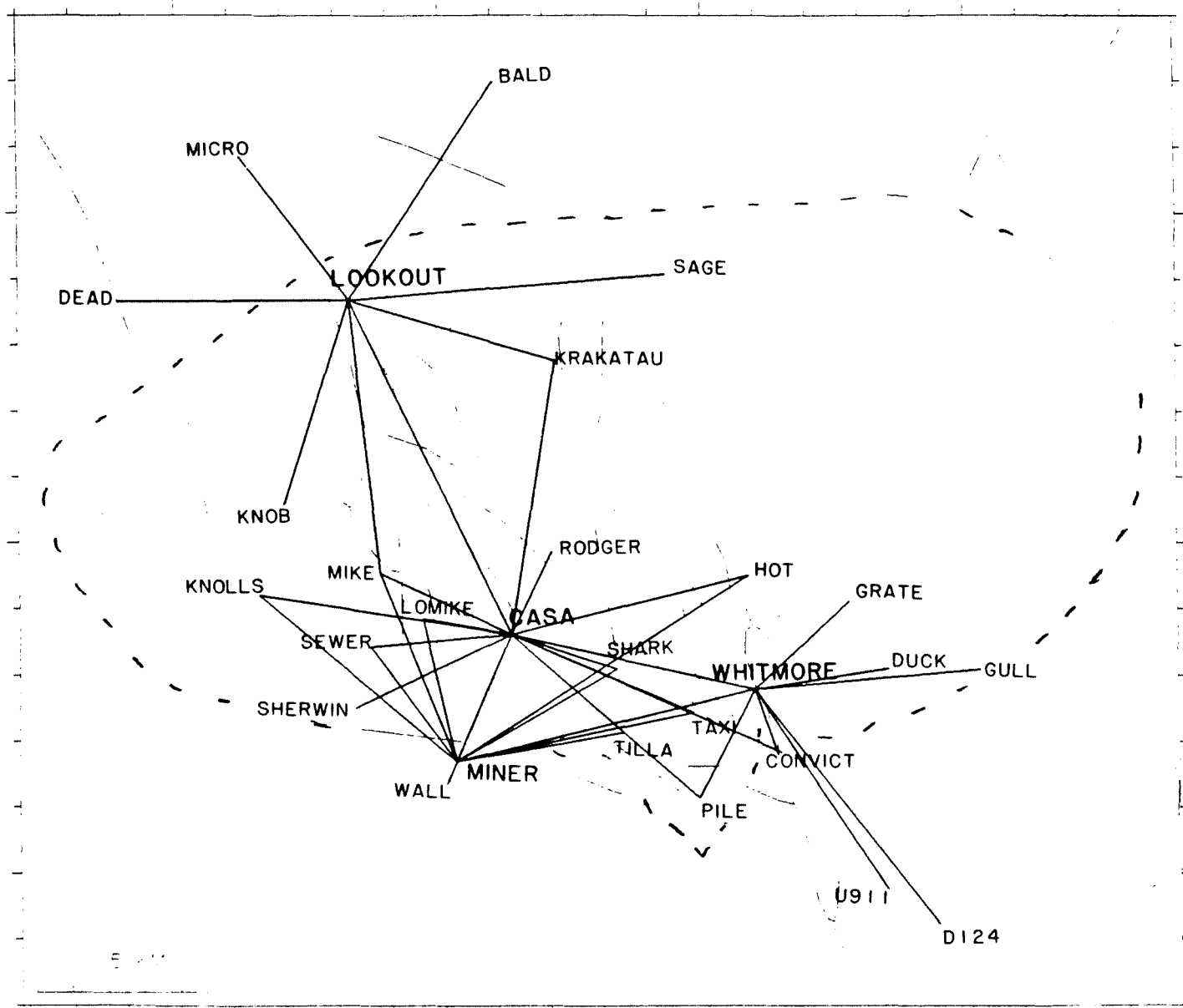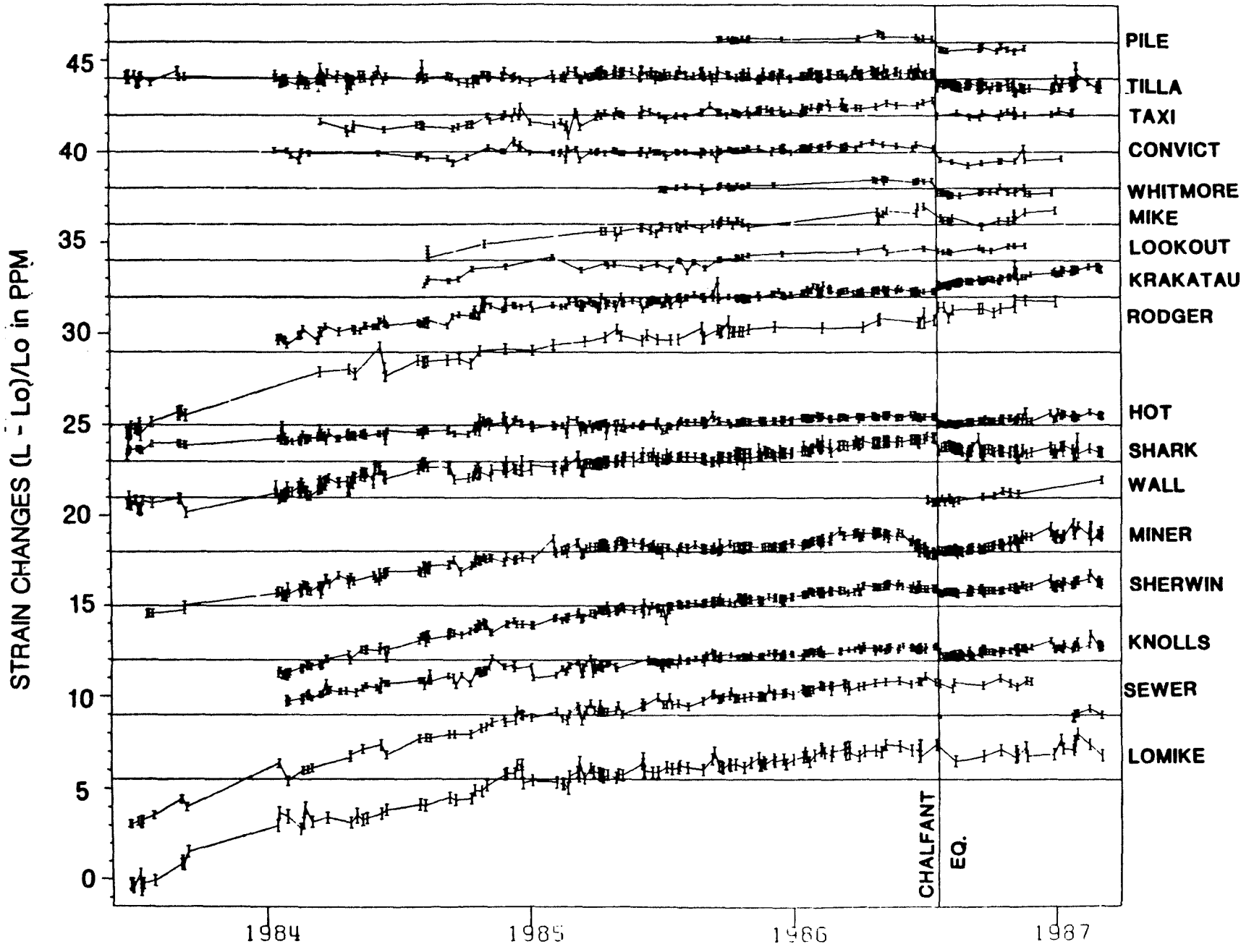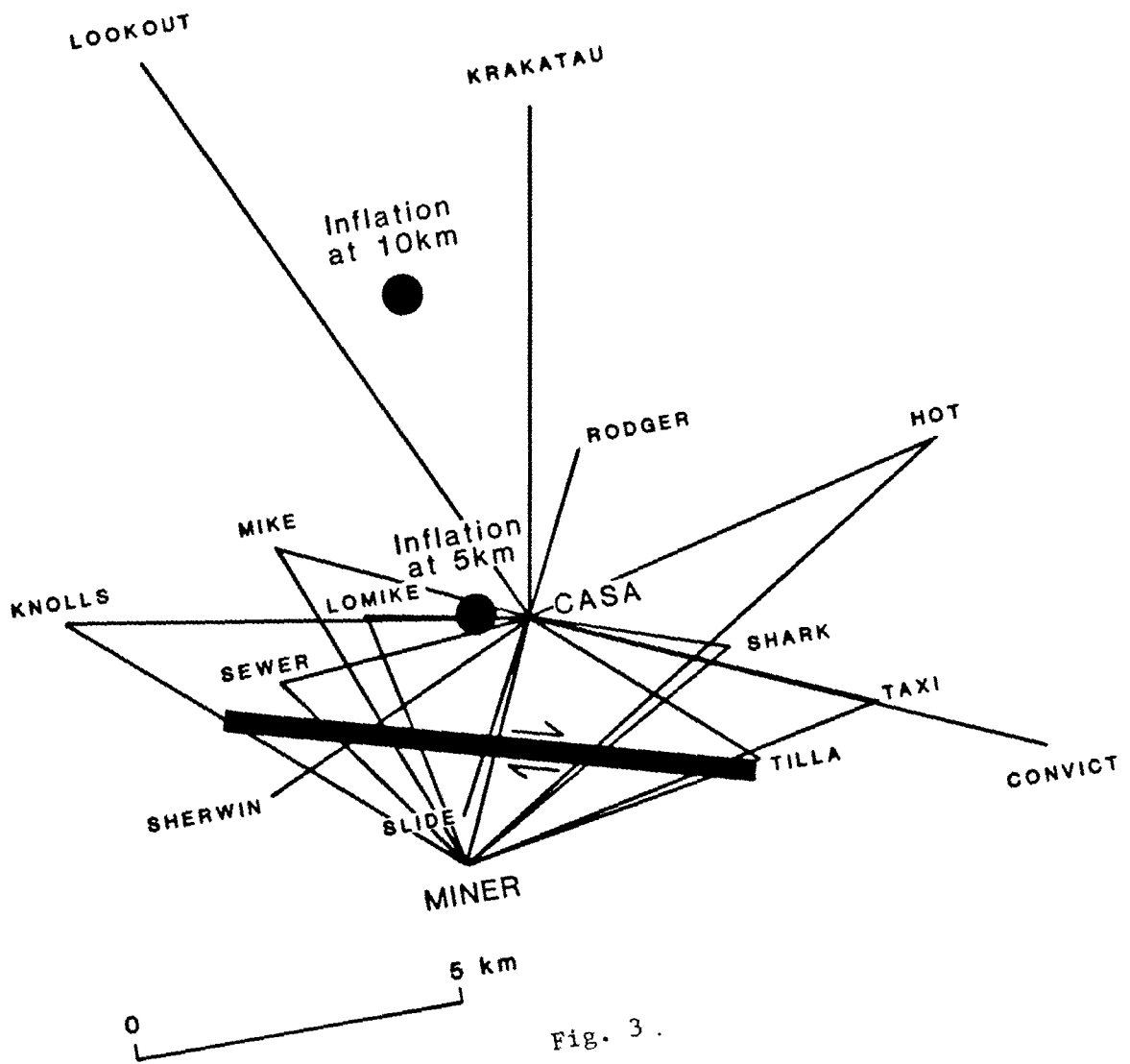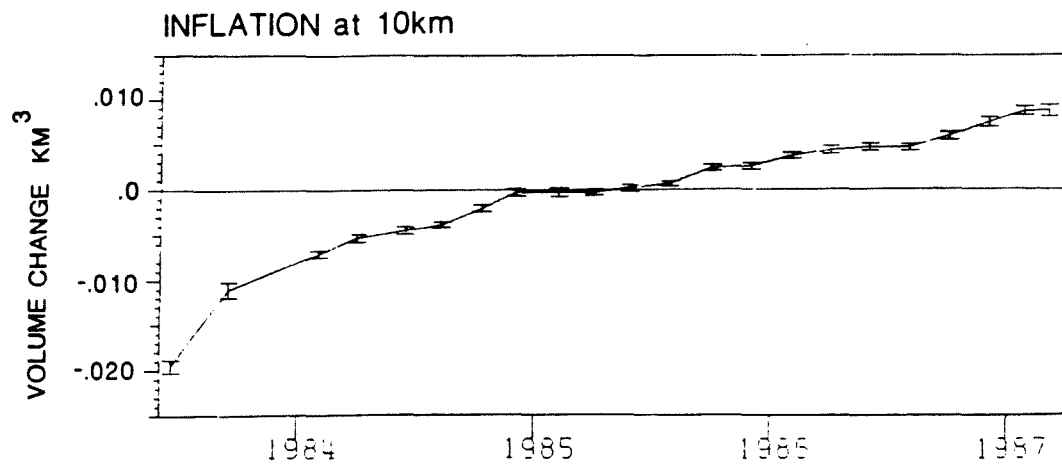
Fig. 4

174

STRUCTURAL IMPLICATIONS OF STRAIN AND

MAGNETIC MEASUREMENTS IN THE LONG

VALLEY/MONO CRATERS REGION

M. J. S. Johnston

U. S. Geological Survey

Menlo Park, CA, 94025

Repeated magnetic measurements have been made since 1972 with a 32-site array in upper Owens Valley. The array extends through Long Valley, around Mono Lake, across the Excelsior Mountains, and down Owens Valley. One or two sets of data have been obtained each year at each of the site pairs. Following the first Mammoth Lakes earthquakes in 1978, telemetered and portable recording magnetometers were also installed from Round Valley through the Long Valley Caldera. The primary feature in data from all sites between Round Valley and Mono Lake is a systematic and linear increase in field with time but with slightly different rates in different places. After correction for geomagnetic field secular variation, the rates peak to the north of Mono Craters at about 1 nT/a and fall off to the north and to the south through Long Valley. These data can be simple interpreted in terms of thermal remagnetization as a result of migration of the Curie point isotherm. A migration rate of about 1 m/a at a depth of 5 km

will satisfy the data. At shallower depths the rate will be correspondingly less. A minor change in rate may have occurred in the south moat region starting in 1978. Simple tectonomagnetic models which incorporate either a pressure source at a depth of about 5 km or pressure triggered shear stress release on the Hilton Creek could explain this change. Borehole strain measurements recorded at the Devil's Postpile during the Chalfant earthquake do not indicate attenuated strain expected if a large solid/liquid plexes existed beneath Long Valley.

DEFORMATIONS AND INFERRED STRESS FIELD

SENSITIVITY FOR ELLIPSOIDAL SOURCES

AT LONG VALLEY, CALIFORNIA, 1975-1982

M. Wu -- U. of Wisconsin

H. F. Wang -- LLNL

Ground deformation and seismicity observed from 1975 to the present support the existence of a major body of magma within the central part of the Long Valley caldera, California. Constraints on the source geometry are obtained from deformation modeling of uplift and trilateration data. The deformation data are analyzed with elasticity theory, which incorporates an ellipsoidal magma chamber, the Hilton Creek fault, and the South Moat fault (Fig. 1). The solution for surface displacements due to an ellipsoidally-shaped cavity under a normal, uniform pressure is approximated by a combination of inversions and forward searches. The models for which we apply a generalized linear inversion satisfy the boundary conditions exactly on the free surface of the half-space but approximately on the ellipsoid. The forward models employ a normal pressure boundary condition over the surface of the magma body in addition to satisfying the free surface condition. Although geodetic data indicating significant surface deformation have been collected from 1975 to the present, we use the data of 1975-1982 as this period is the only one which contains both: 1) significant uplift data (in excess of 0.4 m) and 2) sufficient horizontal displacement data throughout the caldera. The importance of having both vertical and horizontal data in the inversion modeling of magma sources is that even extremely different models can fit the same set of vertical displacement data, as has pointed out by a number of authors.

In our analysis of the 1975-1982 deformation data, the inversions from a point-ellipsoid model by Davis [1986] and a dilatational-strain ellipsoid model for which we have developed a theoretical solution are treated as initial results. Refinements are later made in a forward fashion to check the initial geometry and to calculate the related stress field. The mean error to the uplift data is not critically

sensitive on the source geometry, as expected. Considering the horizontal displacement data in the same time period, however, provides additional constraints. The best fit to the uplift plus horizontal deformation data indicates a nearly spherically-shaped source within the central part of the caldera at a depth about 9.5 km. However, significant deviations of some horizontal displacement data from the model suggest movements along structural faults are probably more complicated than the constant dislocations assumed.

Corresponding to the deformation data, the predicted perturbing stress field using a spherical model is mild, with a horizontal tensile stress changing from 1 MPa near the top area (Fig. 2a) to −1 MPa at a depth of 5 km on the vertical South Moat fault plane. It does not appear likely that such a perturbing stress could trigger slip movement along that fault. Stresses due to a narrow prolate ellipsoidal model, which produces about the same uplift as the spherical source model, leads to a horizontal tensile stress that is about one order of magnitude higher in the region directly above the source (Fig. 2b). For an assumed radius of 5 km in the spherical model, tangential stress at the surface of the magma chamber has a maximum tension near the bottom of the South Moat fault (Fig. 3a). It is possible that the 1983 earthquake swarms were triggered by the perturbing stress field plus shallow magma intrusions at the bottom of the South Moat fault. The crack opening location for magma injection is at the top of the source for the prolate ellipsoidal model (Fig. 3b). Hence we emphasize that stress is of importance as a means of discriminating between different magma source models. The stresses calculated from alternative deformation models may provide useful information for locating stress measurements in drill holes in Long Valley. Also, the stress field predicted by the best model may be useful for understanding seismicity and possible crack opening locations for magma injection.
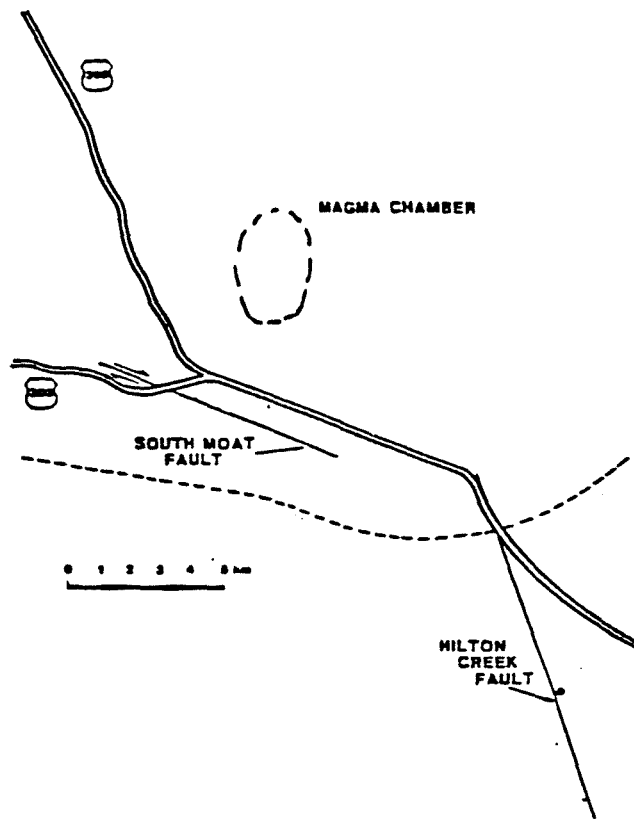
Figure 1. Surface view of southwest part of Long Valley modeled with an elastic half space
containing an inclined ellipsoidal magma chamber, a vertical strike slip fault and
an inclined dip slip fault (after Rundle and Whitcomb, 1984).

HORIZONTAL TENSILE STRESS, $\sigma_r(r)$ (MPa)

4

3

2

1

0

−1

−2

$z = 0$ km

$z = 1$ km

$z = 2$ km

0 2 4 6 8 10

DISTANCE FROM Z-AXIS, r (KM)

South Moat Fault

Υ

4.5

9.5

Z
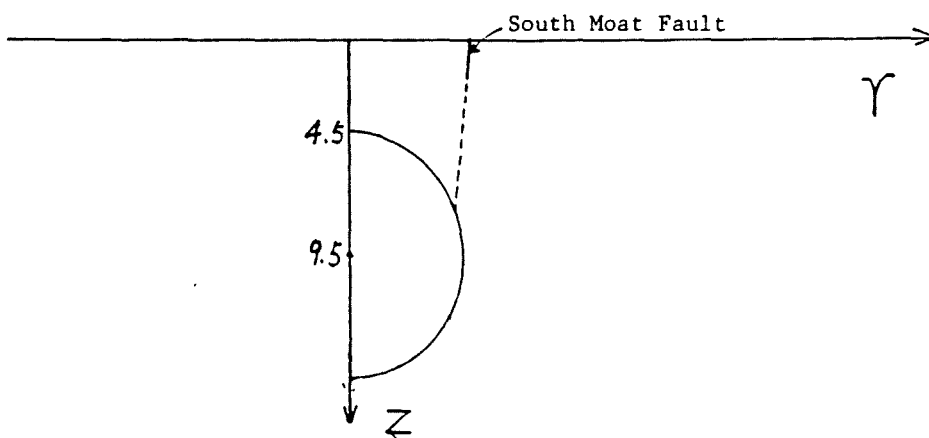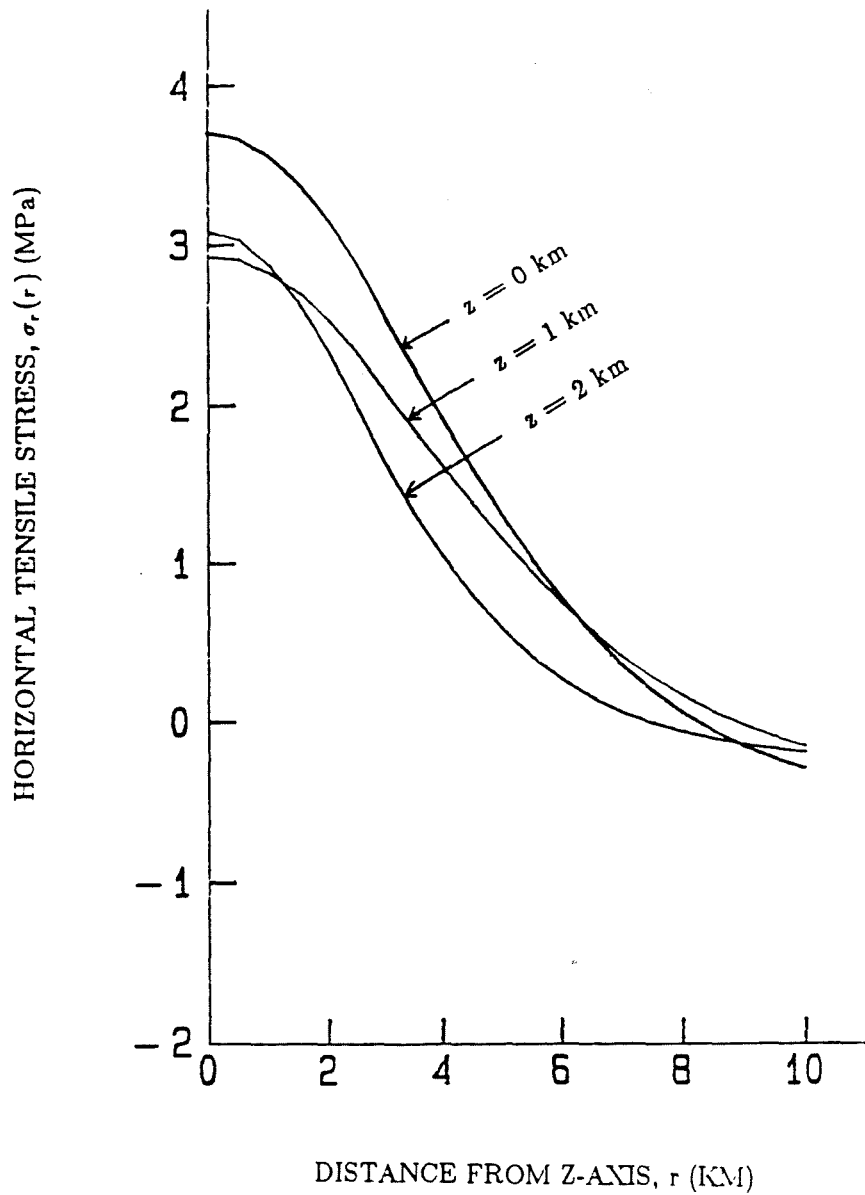
Figure 2a. Distribution of horizontal tensile stress σ_r. The tensile stress is plotted against distance r for the depths $z = 0$, $z = 1$ km, and $z = 2$ km, respectively. Stress distribution due to the spherical source with respect to the 1975–1982 surface deformation data.

180
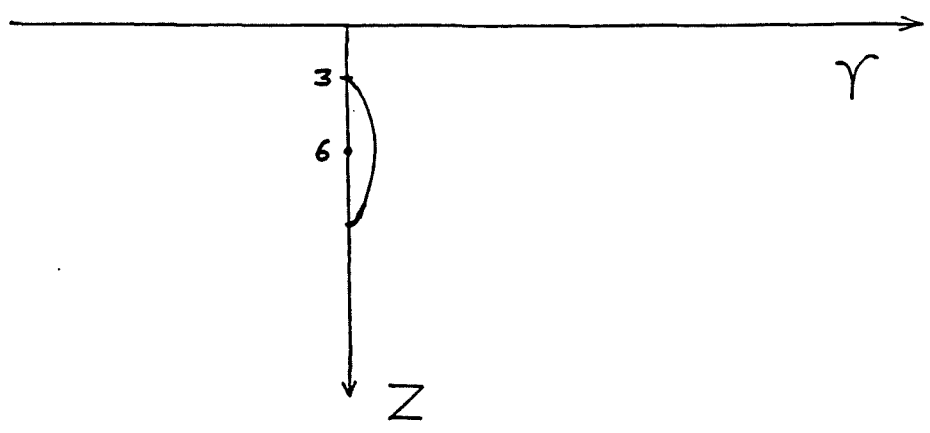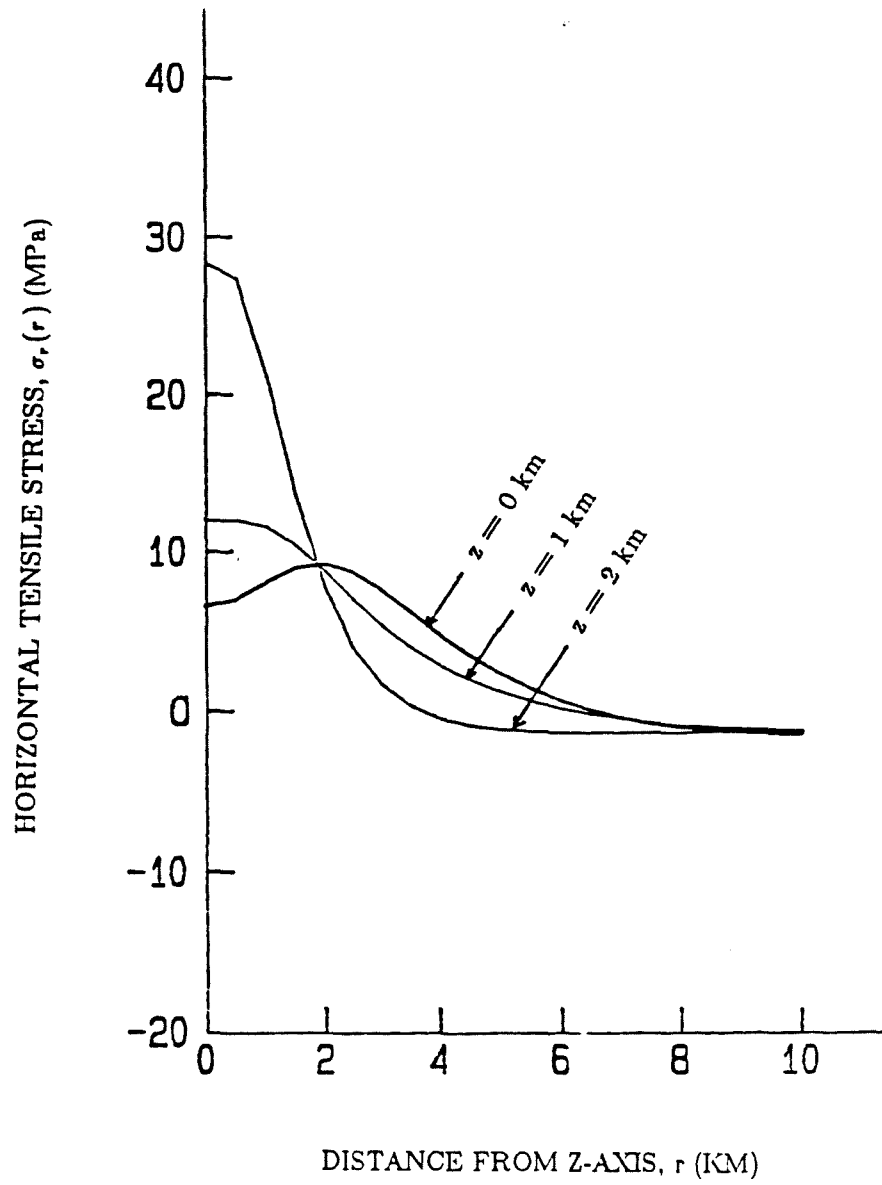
Figure 2b. Distribution of horizontal tensile stress σ_r. The tensile stress is plotted against distance r for the depths z = 0, z = 1 km, and z = 2 km, respectively. Stress distribution due to the narrow ellipsoid source with respect to the 1975–1982 uplift.
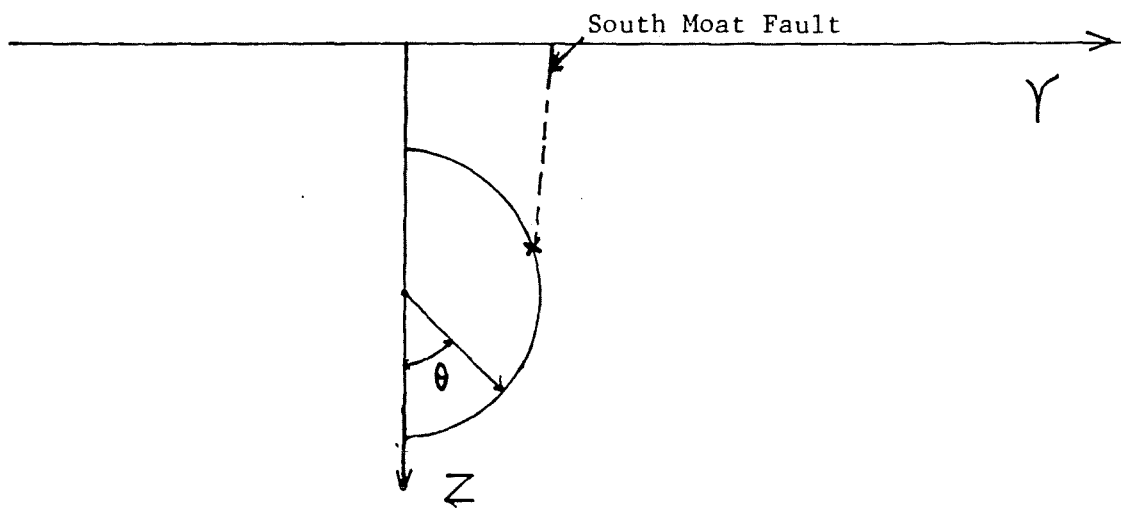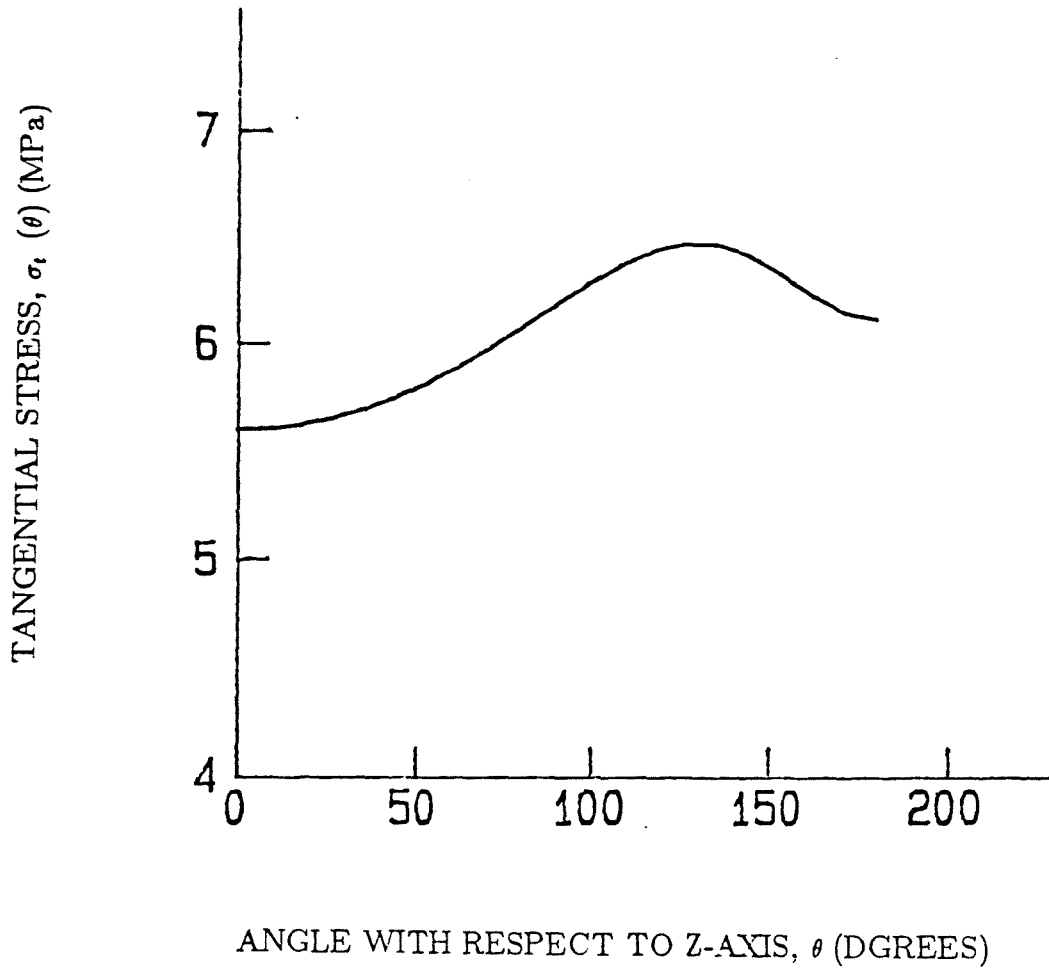
Figure 3a. Distribution of tangential stress σ_t at the surface the magma chamber. σ_t is plotted against the angle θ for the spherical source.

182
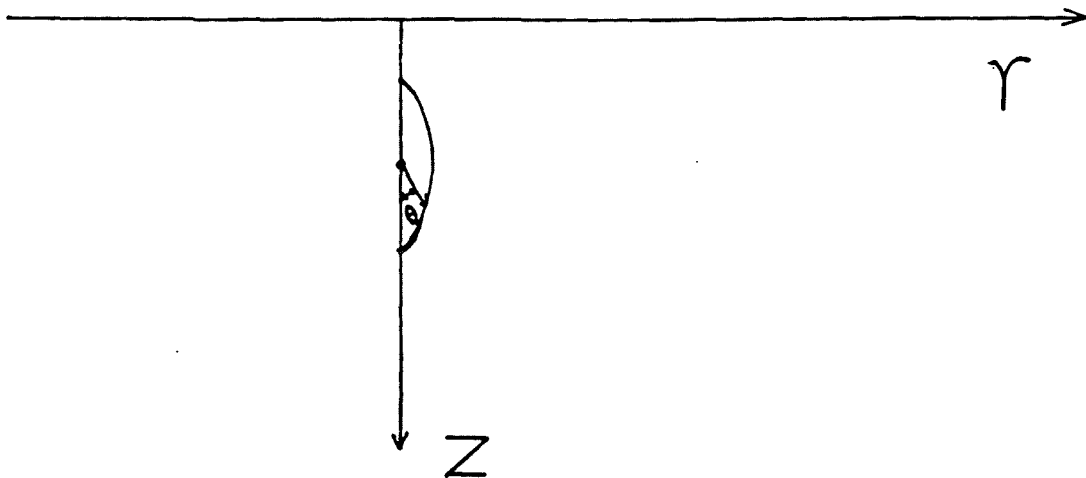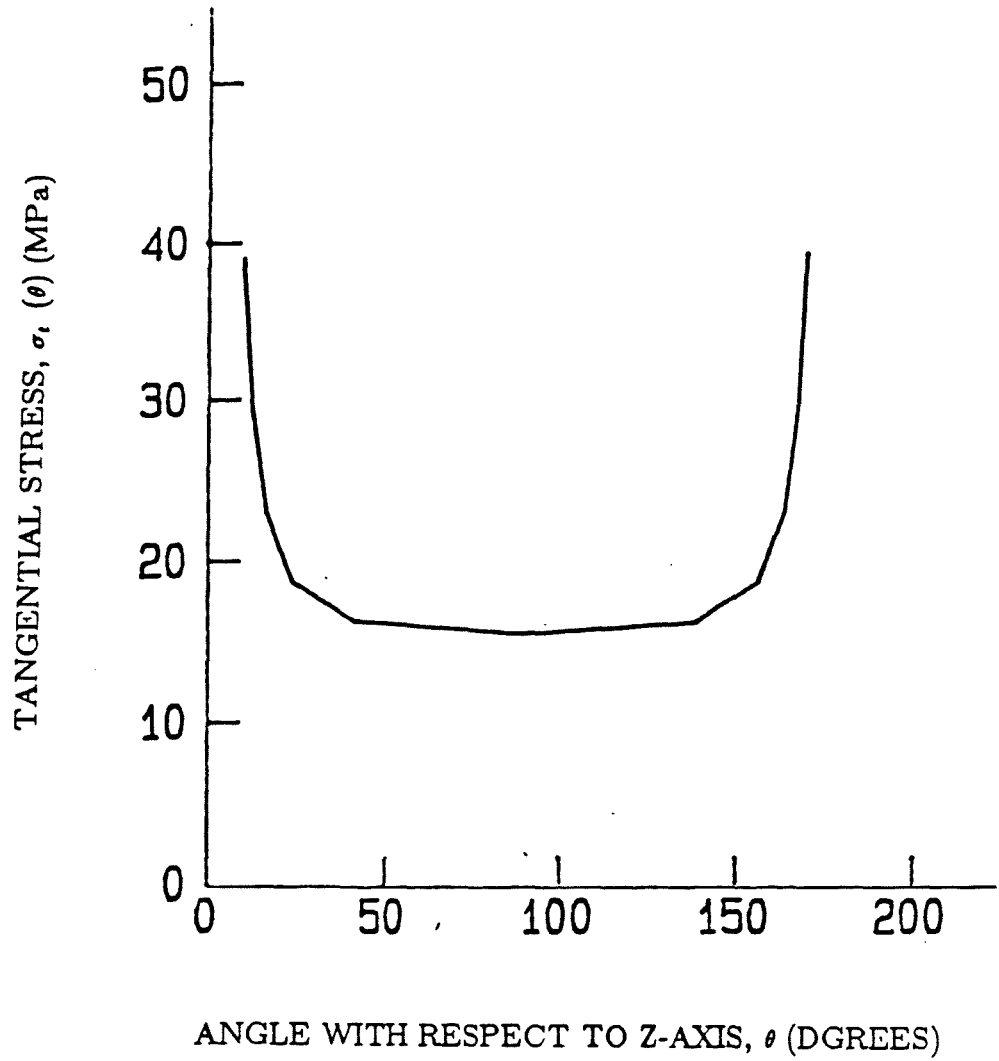
Figure 3b. Distribution of tangential stress σ_t at the surface the magma chamber. σ_t is plotted against the angle θ for the narrow ellipsoid souce.

183

Using Surface Displacement to Constrain Deformation at Long Valley Caldera, CA

D.W. Vasco[1,2]
L.R. Johnson[1,2]
N.E. Goldstein[1]

Center for Computational Seismology[1]
Earth Sciences Division
Lawrence Berkeley Laboratory
University of California
Berkeley, CA 94720

Department of Geology and Geophysics[2]
University of California
Berkeley, CA 94720

During the ten-year interval 1975–1985 up to 47 cm of vertical displacement has been measured within Long Valley caldera (Savage and Clark, 1982; Castle et al., 1984). Four surveys from this period, those made in 1982, 1983, 1984 and 1985, are examined relative to a survey from 1975. Because leveling prior to 1975 detected little or no displacement, this survey may serve as a base for subsequent measurements. The magnitude of the uplift from 1975 to the present and the occurrence of strong earthquake activity within the caldera has led to the suggestion that magma intrusion has taken place (Savage and Clark, 1982; Savage and Cockerham, 1984; Rundle and Whitcomb, 1984; Castle et al., 1984). Besides the observed deformation, the hypothesis of resurgent magmatic activity is supported by many lines of geophysical evidence, such as *P*-wave teleseismic delays (Steeples and Iyer, 1976; Ryall and Ryall, 1981), *S*-wave attenuation (Sanders, 1984; Sanders and Ryall, 1983), *P*-wave tomography (Kissling et al., 1984) and focal mechanisms (Julian, 1983).

To derive constraints on the possible magma intrusion in the region we assume that the uplift is only due to volume expansion. The effects of local faulting and regional tectonic forces were accounted for through modeling and the addition of error terms. Using the uplift data, we examined (a) the bounds on the depth to the top of any intrusion satisfying the data, (b) the total volume change associated with the intrusion satisfying the data, and (c) the incremental volume changes associated with the intrusion for the years 1982, 1983, 1984, and 1985. It was found that magma intrusion occurred above a depth of

13 km. Line 1 is the long northwest to southeast line of leveling stations that follows Highway 395 across Long Valley and over the western edge of the resurgent dome.

A generalized inverse was constructed. No assumptions of positivity were made in deriving this model. The noticeable elements in this solution are concentration of expansion in the second layer (4–8 km) and the lack of significant expansion below 12 km. The expansion is distributed within the second layer with little apparent concentration. The lowest region, below 12 km, contains contracting elements. This feature is attributed to elevation decreases outside the caldera and the discretized region of the model.

The result of minimizing the l^1 norm of the residuals, subject to the constraint that only expansion occur in the region, is presented. In detail this model differs from the generalized inverse, but both results share common elements. Again the bulk of the volume expansion, .20 km^3, occurs in the second layer. This time the changes are concentrated in the center block. No changes are found below this layer, and only diffuse expansion is found above it; most are less than .06 km^3.

We calculated a temporal estimate of the constraints on the possible intrusion at Long Valley caldera. No significant changes have occurred in the constraints on the depth of any magma body satisfying the data. Hence there is no suggestion that significant magma movement has occurred following the initial activity in the interval 1982–1975. Two models of volume change between 1983 and 1985 were derived, each using different assumptions. The models have certain features in common, such as predominant expansion between 4 and 8 km and very little expansion below 12 km. These features agree with the results from other inversions of displacement data, as shown in Table 1. They also support recent tomographic inversions (Kissling et al., 1984; Kissling, personal communication, 1986) in which the significant low P-velocity lies above 8 km.

TABLE 1

Model Comparisons				
Reference	Interval	Chamber Model	Depth to Center	Volume Change
Savage & Clark, 1982	1980-1975	point source	11	0.15
Savage & Cockerham, 1984	1983-1982	dipping dike	10	0.03
Rundle & Whitcomb, 1984	1983-1975	two spheres	5,8	0.0045,0.05
Castle et al., 1984	1983-1975	sphere	10	0.19
Denlinger & Riley, 1984	1982-1975	sill,sphere	7-8,<7	0.019,0.004
Wu & Wang, 1987	1983-1975	ellipsoid	10	0.18
This paper	1985-1982	l^1 inversion	4-8	0.20

References

Castle, R.O., Estrem, J.E. and Savage, J.C., 1984. Uplift across Long Valley caldera, California. J. Geophys. Res. 89, 11507–11515.

Denlinger, R.P., and Riley, F., 1984, Deformation of Long Valley caldera, Mono County, California, from 1975–1982. J. Geophys. Res. 89, 8303–8314.

Julian, B.R., 1983. Evidence for dyke intrusion earthquake mechanisms near Long Valley caldera, California. Nature 303, 323–324.

Kissling, E., and Ellsworth, W. and Cockerham, R.S., 1984. Three-dimensional structure of the Long Valley caldera, California, region by geotomography, 188–220, U.S. Geol. Surv. Open File Rept., 84–939.

Rundle, J.B. and Whitcomb, J.H., 1984. A model for deformation in Long Valley, California, 1980–1983. J. Geophys. Res. 89, 9371–9380.

Ryall, F. and A. Ryall, 1981. Attenuation of P and S waves in a magma chamber in Long Valley caldera, California. Geophys. Res. Lett. 8, 557–560.

Sanders, C.O., 1984. Location and configuration of magma bodies beneath Long Valley, California, determined from anomalous earthquake signals. J. Geophys. Res. 89, 8287–8302.

Sanders, C.O., Ryall, F., 1983. Geometry of magma bodies beneath Long Valley, determined from anomalous earthquake signals. Geophys. Res. Lett. 10, 690–692.

Savage, J.C., and Clark, M.M., 1982. Magmatic resurgence in Long Valley caldera, California: Possible cause of the 1980 Mammoth Lakes earthquakes. Science 217, 531–533.

Savage, J.C., and Cockerham, R.S., 1984. Earthquake swarm in Long Valley Caldera, California, January 1983: Evidence for dike inflation. J. Geophys. Res. 89, 8315–8324.

Steeples, D.W., and Iyer, H.M., 1976. Low-velocity zone under Long Valley as determined from teleseismic events. J. Geophys. Res. 81, 849–860.

Wu, M., and Wang. H.F., 1987, Deformations and inferred stress field sensitivity for ellipsoidal sources at Long Valley, California, 1975–1982, this volume.

Summary of Discussions

At the conclusion of the prepared talks, several scientists were asked to give their views regarding the scientific results presented at the symposium and in particular how these results are influencing the choice of drilling targets for the DOE programs such as Magma Energy Development and Thermal Regimes CSDP. The speakers were Roy Bailey (USGS), Jack Hermance (Brown University), Dave Hill (USGS), Gail Mahood (Stanford University), John Rundle (SNL), Ross Stein (USGS), and Gene Suemnicht (Unocal). Overall, their feeling was that significant progress seems to have been made in imaging the caldera structure and that we also have a much improved model for the hydrothermal system within the post-caldera rocks. However, there was no consensus among the speakers on the best place to drill to intersect a magma body. Gene Suemnicht, representing the interests of the Geology-Geohydrology-Geochemistry Study Group, favored a drilling program in the western moat area. John Rundle, on the other hand, showed that a plot of overlapping geophysical anomalies would dictate a deep drill hole on the resurgent dome. Jack Hermance made a strong argument for beginning a drilling program as soon as possible so as not to lose the momentum of the program and the interest of the scientific community, which has invested so much time and energy in the planning of a thermal regimes drilling program in Long Valley. He stated that we may never have enough information to pick the best site. Gail Mahood argued that it may be impossible to pick a best site in Long Valley because magma probably occurs in too small a volume to be clearly resolved by means of geophysics. She felt that if DOE were truly interested in a drillhole to magma, the only logical site is Yellowstone.

The results of drilling, geophysical studies, and geochemical analyses of soil gases and waters strongly support the long-held notion that the active upflow zone of the hydrothermal system and the heat sources driving the system are located in the west-southwest portion of the caldera. The following picture of the hydrothermal system has emerged. The principal recharge is from the west and northwest rims of the caldera; the cold waters invade selected volcanic units within the caldera fill or, guided by major Sierran frontal faults, penetrate the Paleozoic metasedimentary roof pendant rocks to depths of over 2 km, where they are heated to 220–230°C . The hot waters then ascend along a series of northwest-trending intra-caldera faults in the west and south moats and spread laterally into permeable units of the Bishop Tuff and Early Rhyolites. Most of the flow is west to east; a tongue may flow northeasterly through the resurgent dome. The cooled, mixed waters discharge at permeable fault zones on the south and east sides of the resurgent dome. Small ^{18}O shifts in the discharge waters indicate either a large water/rock ratio or rocks depleted in ^{18}O as a result of prolonged hydrochemical reactions. The increase in the $^{3}He/^{4}He$ ratio from west to east suggests the incremental addition of magmatic ^{3}He. The episodes of high seismicity in the period 1980–1983, when there was major swarm activity in the south moat, seemed to have a temporary effect on the hydrothermal system. The most notable changes were an increase in the temperature of thermal water discharges and co-seismic peaks in Rn, H, and other gases.

Electrical methods, mainly magnetotellurics and time-domain EM, essentially support the hydrogeological model and have aided in its development. Conductivity anomalies in the first 2 km are complex and are believed to be due mainly to an

increased concentration of hydrothermal clay minerals (smectites) but perhaps in part to increased temperature, matrix porosity, and fracturing.

Opinions varied on the nature of the heat sources driving the hydrothermal system. Although several geophysical papers presented at the symposium made specific reference to the possible effects of magma on the data, much of what was presented argued against the notion that a large, continuous magma chamber measuring 500 to 1000 km^3 exists today. Individual melt zones are likely to be small. Such zones would present both a challenge to detection by geophysics and to intersection by drilling.

The present limits of resolution using electromagnetic and seismic geotomography are not good enough to resolve individual bodies less than 2 km in linear dimension and deeper than 4 or 5 km. It is a real challenge to geophysicists to design experiments to improve on this. On the positive side, however, Roy Bailey was encouraged by the coincidence of the P-wave anomalies beneath the western part of the caldera and, in particular, their proximity to the extension of the Hartely Springs Fault, which has been a focus of magma eruption in post-caldera times. These anomalies may reflect the residual part of the main Long Valley chamber, now mostly crystallized but kept hot by continued injections of basaltic magma. Gail Mahood also pointed out that we cannot ignore the possible heating of waters by relatively shallow intrusives beneath the west moat and the composite rhyodacitic volcano known as Mammoth Mountain.

There also remain strong arguments, as expressed by Jack Hermance, John Rundle, and Ross Stein, for a major source of heat beneath the resurgent dome. Although holes in this area have encountered generally low temperatures, the resurgent dome area is roughly the center of many overlapping geophysical anomalies. Besides the seismic anomalies that several workers have reported, the main evidence for a deep heat source comes from the uplift data and an unexplained but possibly interesting SP anomaly. Ross Stein argued that even though the estimated 0.1 to 0.2 km^3 of magma injected beneath the resurgent dome is a small amount, the deformation and related seismicity in the south moat are among the strongest geophysical anomalies detected in the caldera. Therefore, they are among the best pieces of evidence that a major heat source exists beneath the affected areas.

John Hermance and John Rundle felt strongly about the need to formulate a drilling and science plan as quickly as possible and to begin drilling despite our current uncertainties. They argued that we already have enough testable geophysical targets so that a hole drilled from almost any location in the west-southwest part of the caldera or from the resurgent dome would prove to be not only of scientific value but would also provide a focus for future Long Valley activities. A hole intelligently located would serve several objectives: (1) a study of the deep parts of the hydrothermal system, (2) a means to calibrate present interpretations and models, and (3) an opportunity to conduct deep geophysical observations and experiments.

With regard to better defining the hydrothermal system, Mike Sorey, Gail Mahood, and Gene Suemnicht clearly favored a hole in the west moat, somewhere near the Shady Rest hole or toward Mammoth Mountain. Their principal objectives

are to drill and test the hottest part of the present-day hydrothermal system, to test for the contribution of heat from post-caldera intrusives, to study in detail the temperature-age relationships of multiple episodes of hydrothermal alteration, and to intersect fault zones that strongly influence fluid flow.

Seismologists at the symposium had the most divided views on the significant seismic anomalies and on the question of whether to drill a deep hole and what its target should be. The need for better and more carefully planned seismic experiments was evident in the opinions expressed by a few. Among the large number of unexplained phenomena the seismologists want to investigate in future experiments are the following: (1) the nature, distribution, and cause(s) of P- and S- wave attenuation, (2) the causes of site-dependent late P- phases, (3) the cause of the low-frequency earthquakes around Mammoth Mountain, and (4) the cause of the deep reflections and their relations to melt zones. Answers to all these questions might be obtained from a well-designed experiment involving long-term monitoring using a downhole array of 3-component geophones. The high-quality data possible from this array would allow seismologists to study local microseisms originating from within the caldera, larger regional earthquakes, and teleseisms.

On a regional scale, seismologists and geologists are still grappling with the causes for the recent episodic nature of major seismicity in relation to Sierran front tectonics and in relation to what may be the stirrings of possible related magmatic complexes near Long Valley, such as to the north at Mono Craters. Understanding the causes of the geophysical anomalies associated with the Long Valley caldera may hold the key to understanding the present-day tectonic and volcanic processes along the eastern front of the central Sierra Nevada.

Acknowledgements

Appendix: List of Attendees

Name	Affiliation
John F. Arestad	Santa Fe Minerals, Inc.
Roy Bailey	U.S. Geological Survey—Menlo Park
Desmond M. Bain	U.S. Dept. of Agriculture
Louis Bartel	Sandia National Laboratories
J. Beall	Geysers Geothermal
Phil Beilin	U.S. Geological Survey—Menlo Park
Richard Berg	University of Wyoming
Ross Black	University of Wyoming
Steve Carle	University of California—Berkeley
Rob Cockerham	U.S. Geological Survey—Menlo Park
Jim Combs	GEO Operator Co.—San Mateo
Phil Dawson	U.S. Geological Survey—Menlo Park
Dick Dondanville	Unocal
James Dunn	Sandia National Laboratories
John Eichelberger	Sandia National Laboratories
Greg Elbring	Sandia National Laboratories
Bill Ellsworth	U.S. Geological Survey—Menlo Park
Mel Erskine	Consultant
Chris Farrar	U.S. Geological Survey—Santa Rosa
Steve Flexser	Lawrence Berkeley Laboratory
Robert A. Fournier	U.S. Geological Survey—Menlo Park
Terry Gerlach	Sandia National Laboratories
Charles Gilbert	U.S. Department of Energy, Germantown
Norman E. Goldstein	Lawrence Berkeley Laboratory
Doug Goodwin	Consultant
Roger Greensfelder	Geothermex
Robert Habel	City of Sacramento
Sean E. Hagerty	California Bureau of Land Management
Egill Hauksson	University of Southern California
John F. Hermance	Brown University
Chris Higgins	California Division of Mines & Geology
Wes Hildreth	U.S. Geological Survey—Menlo Park
David P. Hill	U.S. Geological Survey—Menlo Park
Ken Holden	Bureau of Land Management
Joe Iovenitti	Thermal Power Company
William Isherwood	Geothermex
H.M. Iyer	U.S. Dept. of Interior
Malcolm Johnson	U.S. Geological Survey—Menlo Park
Paul Kasameyer	Lawrence Livermore National Laboratory
M. Kennedy	University of California—Berkeley
George A. Kolstad	U.S. Department of Energy—Germantown
John Langbein	U.S. Geological Survey—Menlo Park
Bret Leslie	University of Southern California
Daniel L. Lyster	Mona County, California

Ian MacGregor	National Science Foundation
Gail Mahood	Stanford University
Ernest Majer	Lawrence Berkeley Laboratory
Peter Malin	University of California—Santa Barbara
Don Mangold	Lawrence Berkeley Laboratory
Larry Mastin	Stanford University
Skip Matlick	Mesquite Group
Thomas V. McEvilly	Lawrence Berkeley Laboratory
Vernon R. McLean	Bishop, California
James McNitt	Geothermex
Stephen R. McNutt	California Division of Mines & Geology
Tsvi Mediav	Trans-Pacific Geothermal, Oakland
Richard J. Miller	Cascadia Pacific Corporation
Martin W. Molloy	U.S. Dept. of Energy (SAN)
H. Frank Morrison	University of California—Berkeley
L.J. Patrick Muffler	U.S. Geological Survey—Menlo Park
Gregg Nordquist	Unocal—Santa Rosa
Steve Park	University of California, Riverside
Bill Peppin	Mackay School of Mines—Reno
Colin Powers	University of California—Berkeley
William Prothero	University of California—Santa Barbara
Karsten Pruess	Lawrence Berkeley Laboratory
Peter Pyle	Berkeley Group, Inc.
Marshall Reed	U.S. Department of Energy—Washington, D.C.
John Rundle	Sandia National Laboratories
Chris Sanders	U.S. Geological Survey—Menlo Park
Alex Schreiner	Unocal
Ron Schroeder	Berkeley Group, Inc.
Lisa Shevenell	Los Alamos National Laboratory
Scott Smithson	University of Wyoming
Mike Sorey	U.S. Geological Survey—Menlo Park
Mitchell Stark	Unocal
Lee Steck	University of California—Santa Barbara
Ross Stein	U.S. Geological Survey—Menlo Park
Francis G. Stehli	DOSECC, Inc.
Gene Suemnicht	Unocal—Santa Rosa
Stanley Sun	California Bureau of Land Management
Chan Swanberg	GEO Operator Co.—San Mateo
Charles M. Swift	Chevron Resources
Richard Thomas	California Division of Oil and Gas
Carlos Torres	University of California—Berkeley
Dave Tralli	Jet Propulsion Laboratory
Chin-Fu Tsang	Lawrence Berkeley Laboratory
Bob Varga	Unocal
Don Vasco	Lawrence Berkeley Laboratory
Donald L. Vinson	Pacific Lightening Energy Systems
Herb Wang	Lawrence Livermore National Laboratory
Phillip Wannamaker	University of Utah
Mike Wilt	University of California, Berkeley

Harold Wollenberg   Lawrence Berkeley Laboratory
Mingdong Wu   University of Wisconsin
Lee Younker   Lawrence Livermore National Laboratory
Mark S. Ziegenbein   U.S. Bureau of Land Management